



UNIL | Université de Lausanne

Unicentre

CH-1015 Lausanne

<http://serval.unil.ch>

Year : 2011

Tumor sensitizing function and mechanism of action of a RasGAP derived peptide

ANNIBALDI Alessandro

ANNIBALDI Alessandro, 2012, Tumor sensitizing function and mechanism of action of a RasGAP derived peptide

Originally published at : Thesis, University of Lausanne

Posted at the University of Lausanne Open Archive.
<http://serval.unil.ch>

Droits d'auteur

L'Université de Lausanne attire expressément l'attention des utilisateurs sur le fait que tous les documents publiés dans l'Archive SERVAL sont protégés par le droit d'auteur, conformément à la loi fédérale sur le droit d'auteur et les droits voisins (LDA). A ce titre, il est indispensable d'obtenir le consentement préalable de l'auteur et/ou de l'éditeur avant toute utilisation d'une oeuvre ou d'une partie d'une oeuvre ne relevant pas d'une utilisation à des fins personnelles au sens de la LDA (art. 19, al. 1 lettre a). A défaut, tout contrevenant s'expose aux sanctions prévues par cette loi. Nous déclinons toute responsabilité en la matière.

Copyright

The University of Lausanne expressly draws the attention of users to the fact that all documents published in the SERVAL Archive are protected by copyright in accordance with federal law on copyright and similar rights (LDA). Accordingly it is indispensable to obtain prior consent from the author and/or publisher before any use of a work or part of a work for purposes other than personal use within the meaning of LDA (art. 19, para. 1 letter a). Failure to do so will expose offenders to the sanctions laid down by this law. We accept no liability in this respect.



UNIL | Université de Lausanne

Faculté de biologie
et de médecine

Département de Physiologie

**Tumor sensitizing function and mechanism of action of a
RasGAP derived peptide**

Thèse de doctorat ès sciences de la vie (PhD)

présentée à la

Faculté de biologie et de médecine
de l'Université de Lausanne

par

Alessandro ANNIBALDI

Master de Biologie de l'Università degli Studi di Roma 'La Sapienza'

Jury

Prof. Margot Thome-Miazza, Président
Prof. Christian Widmann, Directeur de thèse
Prof. Philippe Juin, expert
Prof. Tatiana Petrova, expert
Prof. Jean-Marc Joseph, expert

Lausanne 2012

Imprimatur

Vu le rapport présenté par le jury d'examen, composé de

<i>Président</i>	Monsieur Prof. Laurent Schild
<i>Directeur de thèse</i>	Monsieur Prof. Christian Widmann
<i>Experts</i>	Monsieur Dr Jean-Marc Joseph
	Madame Dr Tatiana Petrova
	Monsieur Dr Philippe Juin

le Conseil de Faculté autorise l'impression de la thèse de

Monsieur Alessandro Annibaldi

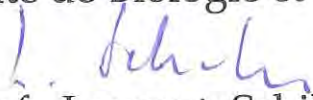
Master de l'Université "La Sapienza" Rome

intitulée

**Tumor sensitizing function and mechanism
of action of a RasGAP derived peptide**

Lausanne, le 23 mars 2012

pour Le Doyen
de la Faculté de Biologie et de Médecine


Prof. Laurent Schild

« Le libertà non si concedono, si prendono »

(Pëtr Kropotkin)

La mia piú profonda riconoscenza a tutte le persone che ho incontrato durante questi cinque anni e che hanno significativamente contribuito alla mia crescita come ricercatore ma soprattutto come persona; le mie parole non basterebbero ad esprimere la mia gratitudine.

TABLE OF CONTENTS

SUMMARY	1
RÉSUMÉ	3
INTRODUCTION	5
Cancer Hallmarks	7
Activated growth signaling	8
Overriding anti-cancer barrier	9
Angiogenesis	10
Metastasis	11
Alteration of glucose metabolism	12
Genomic instability	13
Mutator hypothesis or oncogenic stress?	14
Apoptosis	15
Direct model	18
Indirect model	19
Direct vs Indirect	20
A new way of activating Bax: the “Trap and Release” Mechanism	21
Caspases	23
Ras signaling	25
RasGAP	25
RasGAP not only as GTPase-activating protein	26
G3BP1	27
RasGAP as caspase substrate	28
Cancer treatment	29
TAT-RasGAP₃₁₇₋₃₂₆: a tumor sensitizer	30
Reference list	32

Review	44
OBJECTIVES	49
RESULTS	51
Part I	53
Introduction	55
Contribution	56
Research Article	57
Part II	69
Introduction	71
Contribution	72
Research Article	73
Part III	79
Introduction	81
Contribution	82
Research Article	83
Part IV	97
Introduction	99
Contribution	99
Introduction	100
Materials and methods	101
Results	108
Discussion	120
Reference list	124
Part IV	127
Introduction	129
Contribution	129
Introduction	130

Materials and methods	131
Results	133
Discussion	136
Reference list	137
DISCUSSION AND PERSPECTIVES	139
Reference list	146
Standard protocols from the Widmann's laboratory used during this thesis work	149

SUMMARY

Cancer is the second cause of death after cardio-vascular diseases in economically developed countries. Two of the most commonly used anti-cancer therapies are chemo and radiotherapy. Despite the remarkable advances made in term of delivery and specificity of these two anti-tumor regimens, their toxicity towards healthy tissue remains a limitation. A promising approach to overcome this obstacle would be the utilization of therapeutic peptides that specifically augment the sensitivity of tumoral cells to treatments. Lower therapeutical doses would then be required to kill malignant cells, limiting toxic effects on healthy tissues.

It was previously shown in our laboratory that the caspase-3 generated fragment N2 of RasGAP is able to potentiate the genotoxin-induced apoptosis selectively in cancer cells. In this work we show that fragment N2 strictly requires a cytoplasmic localization to deliver its pro-apoptotic effect in genotoxin-treated cancer cells.

The tumor sensitizing capacity of fragment N2 was found to reside within the 10 amino acid sequence 317-326. Our laboratory earlier demonstrated that a peptide corresponding to amino acids 317 to 326 of RasGAP fused to the TAT cell permeable moiety, called TAT-RasGAP₃₁₇₋₃₂₆, is able to sensitize cancer cells, but not normal cells, to genotoxin-induced apoptosis.

In the present study we describe the capacity of TAT-RasGAP₃₁₇₋₃₂₆ to sensitize tumors to both chemo and radiotherapy in an *in vivo* mouse model. The molecular mechanism underlying the TAT-RasGAP₃₁₇₋₃₂₆-mediated sensitization starts now to be elucidated. We demonstrate that G3BP1, an endoribonuclease binding to amino acids 317-326 of RasGAP, is not involved in the sensitization mechanism. We also provide evidence showing that TAT-RasGAP₃₁₇₋₃₂₆ potentiates the genotoxin-mediated activation of Bax in a tBid-dependent manner.

Altogether our results show that TAT-RasGAP₃₁₇₋₃₂₆ could be potentially used in cancer therapy as sensitizer, in order to improve the efficacy of chemo and radiotherapy and prolong the life expectancy of cancer patients. Moreover, the understanding of the TAT-RasGAP₃₁₇₋₃₂₆ mode of action might help to unravel the mechanisms by which cancer cells resist to chemo and radiotherapy and therefore to design more targeted and efficient anti-tumoral strategies.

RÉSUMÉ

Le cancer est la cause principale de mortalité dans les pays économiquement développés. Malgré la grande hétérogénéité qui existe au sein des différents cancers, le manque de contrôle de prolifération ainsi que l'impossibilité de mourir par apoptose représentent les prérequis essentiels pour l'établissement et le développement du cancer. Deux des thérapies anti-cancéreuses les plus utilisées sont la chimiothérapie et la radiothérapie. Malgré les progrès remarquables effectués en termes de spécificité et d'acheminement de ces deux stratégies, leur toxicité envers les tissus sains reste une limitation pour leur utilisation. Une stratégie prometteuse afin de surmonter cet obstacle serait d'utiliser des peptides thérapeutiques qui augmentent spécifiquement la sensibilité des cellules tumorales aux traitements, ce qui permettrait de diminuer les doses utilisées et réduirait ainsi les effets secondaires toxiques sur les tissus sains.

Notre laboratoire a démontré précédemment que le fragment N2, résultant du clivage de RasGAP par la caspase-3, avait la propriété de potentialiser l'apoptose induite par des génotoxines, et ceci spécifiquement dans les cellules cancéreuses. Dans cette étude, nous montrons que le fragment N2 requiert une localisation strictement cytoplasmique afin d'avoir une action pro-apoptotique dans les cellules cancéreuses traitées aux génotoxines.

L'effet de sensibilisateur tumoral que possède le fragment N2 est toujours conservé dans une séquence minimale de 10 acides aminés à l'intérieur du fragment N2, la séquence 317 à 326. Notre groupe de recherche a démontré précédemment qu'un peptide correspondant aux acides aminés 317 à 326 de la protéine RasGAP fusionné au peptide de perméabilisation TAT, appelé TAT-RasGAP₃₁₇₋₃₂₆, avait le pouvoir de sensibiliser les cellules cancéreuses, mais pas les cellules saines, à la mort induite par les génotoxines.

Dans cette étude, nous décrivons le pouvoir du peptide TAT-RasGAP₃₁₇₋₃₂₆ à sensibiliser les tumeurs à la chimio- et à la radiothérapie *in vivo* à l'aide d'un modèle murin. Les mécanismes moléculaires à la base de cette sensibilisation commencent désormais à être élucidés. Nous avons démontrés que G3BP1, une endoribonucléase connue pour se lier aux acides aminés 317-326 de RasGAP, n'était pas impliquée dans cette sensibilisation. Nous avons aussi amené la preuve que TAT-RasGAP₃₁₇₋₃₂₆ potentialise l'activation de Bax induite par des génotoxines dépendamment de la protéine tBid.

Pris ensemble, nos résultats montrent que TAT-RasGAP₃₁₇₋₃₂₆ pourrait potentiellement être utilisé dans un contexte de chimio- ou radiothérapie comme sensibilisateur. Ceci dans le but d'améliorer l'efficacité des traitements utilisés actuellement et de prolonger l'espérance de vie de patients atteints du cancer. De plus, la compréhension du mode d'action de TAT-RasGAP₃₁₇₋₃₂₆ pourrait aider à définir les mécanismes par

lesquels les cellules cancéreuses acquièrent une résistance aux chimio- et radiothérapies, et ainsi inventer des stratégies anti-tumorales plus efficaces et ciblées.

Introduction

INTRODUCTION

Cancer hallmarks

Cancer is a class of genetic diseases that, in spite of their high heterogeneity, share some common traits. Ten years ago six features common to most cancers were pointed out by Hanahan and Weinberg in the renowned review entitled ‘The Hallmarks of Cancer’: self-sufficiency in growth signal, insensitivity to anti-growth signal, evasion of apoptosis, unlimited replicative potential, angiogenesis and metastasis [1] (Figure 1). During the last decade two new hallmarks were associated to cancers: reprogramming of the cellular metabolism and immune destruction evasion. All these cellular alterations, arising from genetic mutational events occurring for example in oncogenes or tumor-suppressor genes, are accumulated stepwise during the neoplastic transformation and each of them confers to tumor cells a selective growth or survival advantage. [2-4].

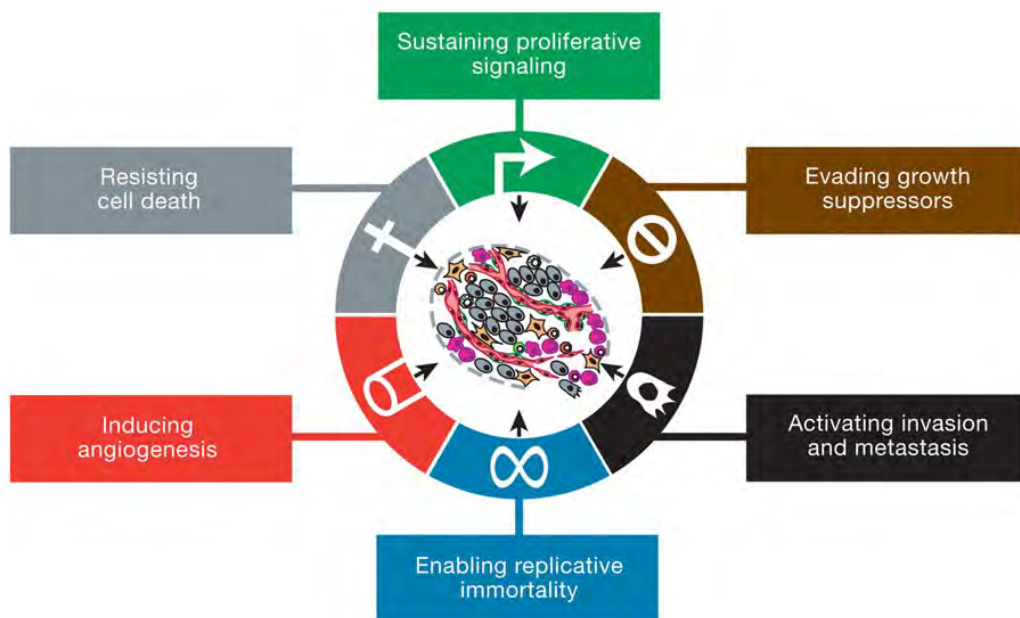


Figure1. The Hallmarks of cancer. Illustration of the six hallmark capabilities originally proposed by Hanahan and Weinberg. Adapted from *Hanahan D. and Winberg, R.A., Cell, 2011.*

Activated growth signaling

Proliferation of normal cells is tightly regulated by the growth factor availability within tissues. Cancer cells have developed different strategies to evade this strict control ensuring tissue homeostasis and therefore to reduce their dependence or to render themselves independent of growth signals. One is represented by the over-expression of growth factor receptors that allows cancer cells to become sensitive to the basal growth factor levels present in the tissue that normally would not stimulate proliferation [5-7]. Another mechanism allowing cancer cells to provide themselves with proliferating signals is the acquired ability to produce growth factors for which they express the cognate receptors, generating in this way a positive feedback often denominated autocrine stimulation [8-10]. Growth factor receptors can also be mutated in their cytoplasmic portion generating persistent proliferation signals without the need of their engagement by the respective ligands. One representative example is the EGFR (Epidermal Growth Factor Receptor), a receptor tyrosine kinase often bearing mutations in the kinase domain that result in an increased kinase activity and therefore in a hyperactivation of downstream proliferative pathways [11]. Alternatively, growth receptor-activated signaling pathways are often misregulated in cancer, leading to a constitutive activation of the proliferative signals downstream of the receptors. Ras and c-Myc oncoproteins are two of the most know examples of mutated/deregulated factors operating within the growth receptor-activated proliferative circuits [12-17].

Normal tissue proliferation is regulated both by proliferative signals that allow the cell population within the tissue to expand and by growth arrest signals that re-establish steady-state conditions. Therefore if transformed cells acquire independence of proliferation, on the other hand they

should also be able to ignore anti-proliferative signals. One of the most common anti-proliferative factors is TGF- β , a soluble factor that, by the binding to its cognate receptor on the cell surface, starts an anti-proliferative program [18;19]. Cancers are often able to elude this TGF- β -mediated anti-growth signal by mutating either its specific receptor or components of the intra-cellular circuitry that translates its anti-proliferative signals [20]. At the molecular level the irresponsiveness to growth arrest signals that characterizes tumor cells is often due to the inactivation of tumor suppressor genes such as retinoblastoma protein (Rb) [21-23], a protein controlling the cell cycle entry, or PTEN, a phosphatase that counteracts the PI3-kinase-mediated proliferative signals [24].

Overriding anti-cancer barriers

After acquiring the proliferative independence, cancer cells must win immortality in order to generate macroscopic tumors. Indeed normal cells undergo a limited number of replication cycles after which they irreversibly enter a quiescent but viable phase called senescence [25]. The main cellular event leading to the entrance to this non-proliferative state is the progressive telomere shortening, taking place at each cycle of cell division, as a direct consequence of the lack of telomerase in normal somatic cells. Telomerase is the enzyme that counteracts telomere erosion by adding new TTAGGG repeats to the 3' ends of chromosomes [26], however it is only active in cells during the embryonic development and in cells belonging to the germination line [27;28]. Interestingly about 90% of human cancers express telomerase that enable transformed cells to overcome the telomere shortening process and the activation of the senescence program, therefore allowing them to become immortal [29]. Senescence is by now considered as one of the two cell-imposed barriers against carcinogenesis by virtue of the fact that it restrains the replicative potential of normal cells [30].

The second anti-cancer barrier normal cells raise against tumoral transformation is represented by the apoptotic cell death process [31]. Apoptosis is a physiological process of programmed cell death aimed at the elimination of damaged and harmful cells [32;33]. The genetic damages cancer cells accumulate during carcinogenesis activate the apoptotic cell death program with the final goal of eliminating damaged cells before they become dangerous for the organism. In order to counteract the DNA-damage induced cell death signals, cancer cells resort to apoptosis elusion to secure their own viability and clonal expansion.

Angiogenesis

Tumor expansion requires continuous supplies of oxygen and nutrient to support the high proliferation rate of cancer cells that therefore must acquire the ability to promote the synthesis of vasculature during the macroscopic tumoral mass formation [34]. Angiogenesis is a physiological process that consists in the growth of new blood vessels from pre-existing vessels. This process is normally active during embryogenesis whereas in the adult it only takes place under particular physiological or pathological conditions (e.g. during wound healing) [35]. Conversely, during tumor progression an angiogenic program, called angiogenesis switch, is constitutively on, sustaining the tumor expansion [36;37]. Well know angiogenic inducers are the members of the vascular endothelial growth factors family (VEGFs) [38]. The mechanism underlying the angiogenic switch can vary from tumor to tumor. Indeed some reports indicate that the oncogenes expressed within the tumor cells can up-regulate the expression of angiogenic factors [39;40] while other reports show that tumor surrounding or tumor infiltrated cells, such as mast cells and macrophages, are instructed by tumoral cells to promote the angiogenic switch [41;42].

Metastasis

The leading cause of death in cancer suffering patients has to be attributed to metastasis [43]. Metastasizing refers to the ability of cancer cells to leave the primary tumor mass and to invade new sites within the body. The metastatic process consists of different phases. In the initial phase malignant cells acquire the ability to invade the surrounding tissue towards blood and lymphatic vessels where they intravasate to enter the circulation (intravasation) and disseminate throughout the body. The following step, called extravasation, allows cancer cells to exit the circulation, reach the new colonization site and form small nodules (micrometastasis) that finally grow into new macroscopic tumoral masses [43] (Figure 2).

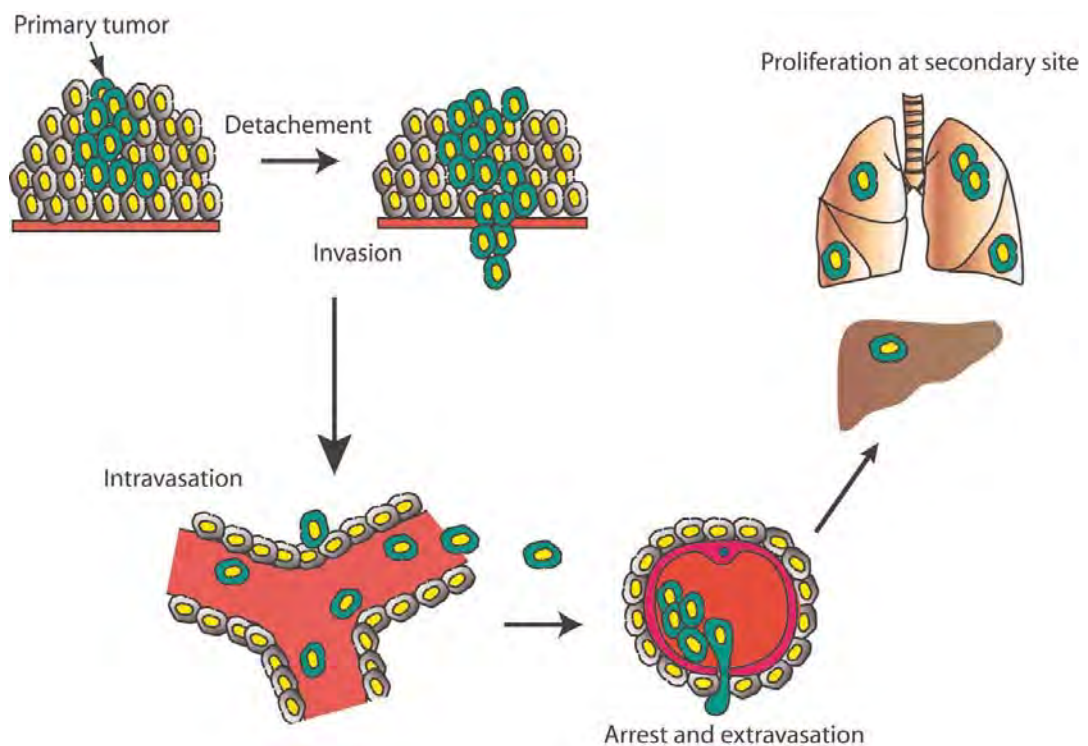


Figure 2. The metastatic process. Illustration of the multistep process of metastasis formation. Adapted from Hunter et al., *Breast Cancer Research*, 2008.

The main molecular events leading to the cancer cell reprogramming that underlies this multistep process start now to be understood, and it seems that the initial cellular change driving metastasis is the so called ‘epithelial-mesenchymal transition’ (EMT). The EMT is characterized by the loss of surface molecules that mediate cell to cell adhesion (e.g. E-cadherin) that promotes the capacity of tumor cells to escape the primary tumor site. There are reports indicating that, once disseminated to distal organs, malignant cells undergo the reverse program, the mesenchymal-epithelial transition (MET) allowing them to form new tumor colonies [44;45].

Alteration of glucose metabolism

Cellular energy metabolism is one of the main processes that are affected during the transition from normal to cancer cells. In particular, glucose metabolism is very often altered in tumor cells. Glycolysis is a catabolic process that converts one molecule of glucose into two pyruvates with the production of two ATP and two reduced nicotinamide adenine dinucleotide (NADH) molecules. Pyruvate in the presence of oxygen undergoes oxidation to CO₂ and H₂O in the oxidative phosphorylation pathway, resulting in the production of approximately 36 molecules of ATP. Alternatively, in the absence of oxygen, pyruvate is transformed into lactic acid in the anaerobic glycolysis pathway. However, conversion of glucose to lactic acid can occur in the presence of oxygen and this is known as the Warburg effect or aerobic glycolysis. Interestingly, most cancer cells produce large amounts of lactate regardless of the availability of oxygen. The altered glucose metabolism characterizing malignant cells was the subject of a review I wrote and that was published in *Current Opinion in Clinical Nutrition and Metabolic Care*. This review can be found at the end of the introduction.

Genomic instability

The genetic and molecular mechanisms allowing the sequential acquisition of mutations during carcinogenesis, and therefore the onset of the above described hallmarks, have been intensively studied in the last two decades. It is now clear that cancer cells exhibit a marked genomic instability that explains the higher mutational rate of malignant cells compared to normal cells [46;47]. Therefore genomic instability has been recently defined as a cancer enabling characteristic that would increase the chances of spontaneous mutational events, whose fixation in the genome is translated into the acquisition of the aforementioned tumor hallmarks [2]. The question the scientific community raised long time ago was: where does this genomic instability peculiar to malignant cells originate from?

Mutator hypothesis or oncogenic stress?

There are two different theories potentially explaining why cancer cells exhibit high mutation rate. The first is the so called 'mutator hypothesis' stating that the genomic instability in pre-cancerous lesions is to be attributed to defects in the 'caretaker genes', that are the genes responsible for DNA repair and mitotic checkpoint [3;48-51]. Indeed improper DNA damage repair or uncontrolled progression through the cell cycle can increase the basal mutation rate in pre-cancerous cells, thus generating this characteristic genomic instability that then drives tumor development. To support this theory is the evidence that some hereditary cancers, such as HNPCC (hereditary non-polyposis colon cancer), show mutation in the DNA repair genes and that inherited mutations within caretaker genes, such as BRCA1/2, predispose to the development of breast cancer [52;53]. However recent high-throughput analysis of human cancer genomes failed to identify caretaker genes that were frequently mutated in sporadic cancers. Genes

emerging as the most frequently mutated were known oncogenes, such as *Ras* and *EGFR*, and tumor suppressor genes, *PTEN*, *NF1*, *p16INK4A* and *p53* [54-59].

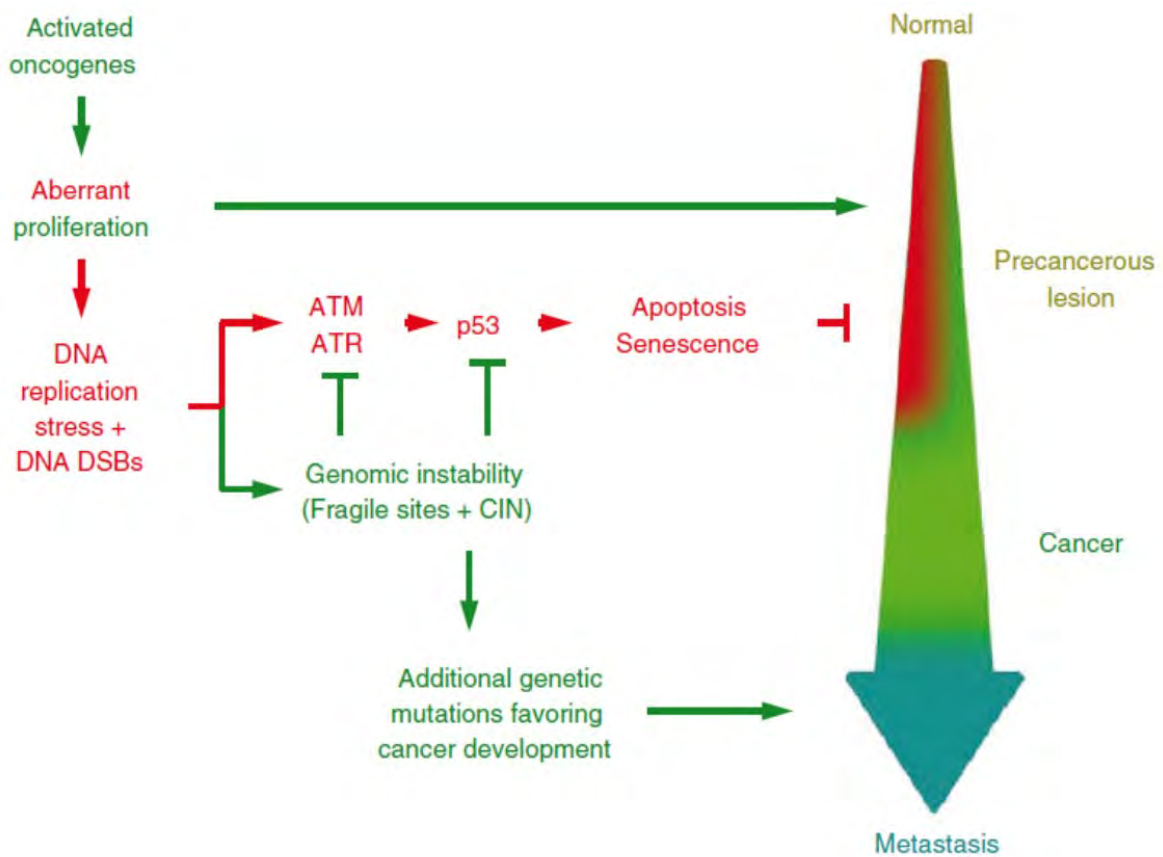


Figure 3. Oncogenic stress model. DNA replication stress causes genomic instability that drives the progression from pre-malignant lesion to cancer. Adapted from Halazonetis T., et al., *Science*, 2008.

The high mutation rate of p53 and the fact that it could also be considered a caretaker gene, because it serves as DNA damage checkpoint protein, seems to be in favor of the mutator hypothesis. Nevertheless it has been demonstrated, both in mouse and human models, that p53 deletion does not cause genomic instability and that genomic instability is present in pre-malignant cells before the onset of p53 mutations [60;61]. In addition the finding that the over-

expression of oncogenes generates DNA replication stress led to the ‘oncogenic stress’ model formulation [31;62]. This model states that in pre-cancerous lesion the gain of function mutation of an oncogene or the loss of function mutation of a tumor suppressor generates the replication stress. This is defined as the condition in which DNA undergo a replicative overload triggering replication forks collapse. DNA replication stress, and so the collapse of replicative forks was shown to be the cause of DNA double strands breaks (DBS) and DNA-damage induced activation of p53, triggering in turn either senescence or apoptosis [31;62]. Therefore, in sporadic cancer, the sustained DNA replication stress associated with oncogene activation increases the rate of DBS, provoking genomic instability, which in turn generates a selective pressure for p53 mutation, required for the breaching of the two anti-cancer barriers represented by senescence and apoptosis (Figure 3). This selective pressure would therefore explain the high

p53 mutation rate found in malignant cells. Additionally the replicative stress also favors the accumulation of additional mutations required for cancer progression.

Apoptosis

Apoptosis, or programmed cell death, is a physiological process required to remove damaged or redundant cells during development and for the maintenance of tissues homeostasis [33].

Cells can undergo apoptosis through the extrinsic pathway, initiated by death receptors exposed on the cell surface or the intrinsic pathway, activated as result of exposition to cellular insults (e.g. genotoxins, radiation, UV and growth factor deprivation) (Figure 4).

The extrinsic pathway involves the engagement of membrane death receptors, such as TNFR1 or Fas, by their cognate binding factors (TNF, FasL/CD95L), leading to the trimerization of the receptors and to the assembly at their intracellular domains of a caspase activation platform

called DISC. The DISC (death-inducing signalling complex) mediates the activation of initiator caspases 8 and 10 that in turn activate effector caspases (caspase 3/6/7) [63;64]. Effector caspases then cleave a number of different nuclear and cytoplasmic substrates determining the cellular demise.

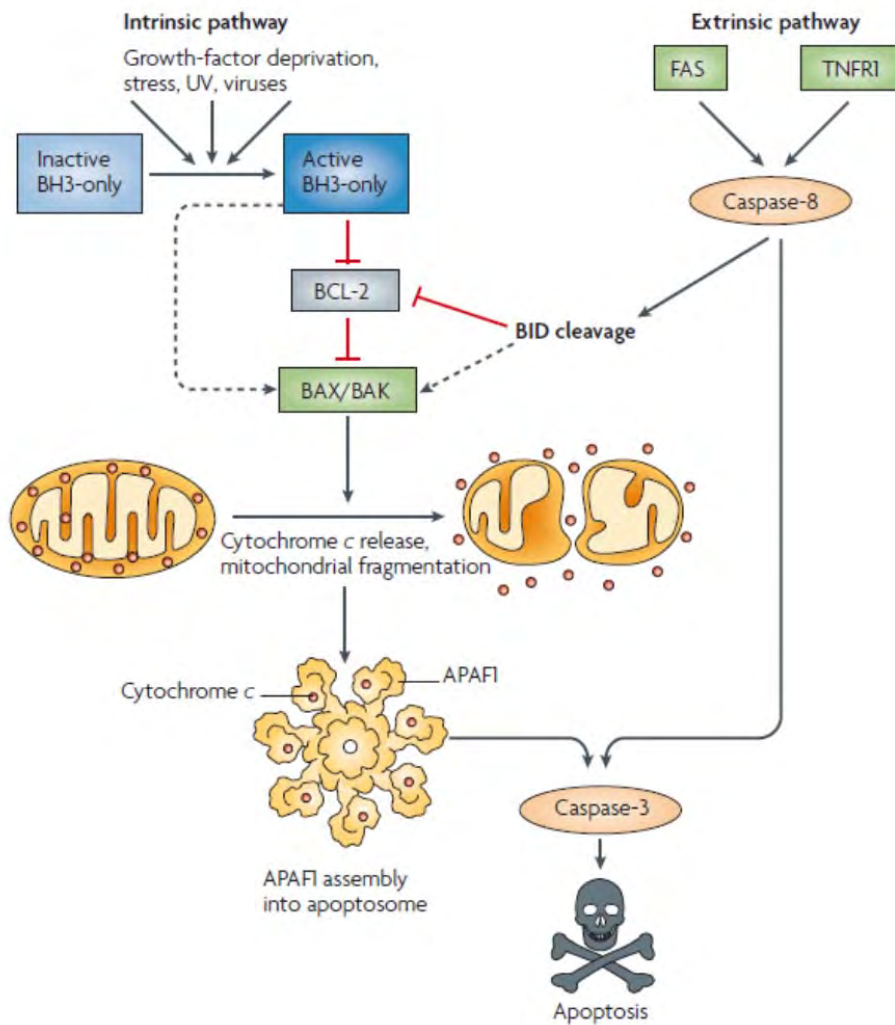


Figure 4. Intrinsic and extrinsic apoptosis. Schematic illustration of the death receptor- mediated and mitochondrial-mediated apoptotic pathways. Adapted from Youle R., J. and Strasser A., *Nature Reviews*, 2008.

The intrinsic pathway is characterized by the disruption of the mitochondrial membrane integrity [65]. The loss of mitochondrial integrity causes the release in the cytoplasm of apoptogenic factors such as cytochrome *c*, AIF (apoptosis inducing factors) and Smac (second-mediated activator of caspase) [66]. Cytochrome *c*, once released, promotes the formation of a complex called apoptosome. The apoptosome, formed by cytochrome *c*, the protein Apaf-1 and the caspase 9, triggers the activation of the caspase 9 that in turn activates, by proteolytic cleavage, executioner caspases (caspase 3/6/7) [67].

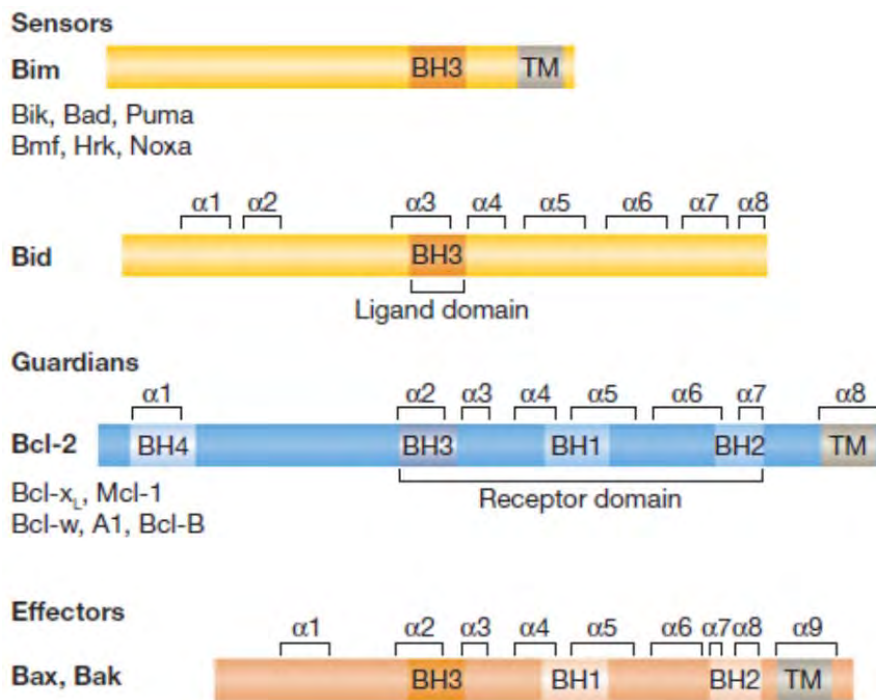


Figure 5. The three functional subgroups of the Bcl-2 family members. Sensors: BH3-only proteins in the text; Guardians: pro-survival proteins in the text. BH: Bcl-2 homology; TM region: *trans*-membrane region. Adapted from Strasser A., et al., *EMBO J.*, 2011

The mitochondrial integrity is tightly controlled by proteins belonging to the Bcl-2 family. All the Bcl-2 family members share a close homology in up to four domains called BH (Bcl-2 Homology) and they can be divided on the basis of their pro-survival and pro-apoptotic function.

The pro-survival proteins are Bcl-2, Bcl-w, Bcl-X_L, Mcl-1 and A1. The pro-apoptotic proteins consist of two sub-classes of proteins: the first includes Bax and Bak, that are able to directly induce cytochrome *c* release, and the second includes the so called BH3-only proteins that are Bad, Bim, Bid, Bik, Bmf, Hrk, Noxa and Puma [65;68](Figure 5). However the mechanisms by which Bax and Bak get activated and induce the MOMP (mitochondrial outer membrane permeabilization), required for the cytochrome *c* release, are still a matter of controversy. Two main models, known as the 'direct model' and the 'indirect model' of activation of Bax and Bak, have been proposed.

Direct model

The direct model classifies the BH3-only proteins into two sub-groups: activators and sensitizers. The activators are Bim, Bid and probably Puma, the sensitizers are the other members of the BH3 group (e.g. Bik and Noxa). The activators have the ability to bind to and directly activate Bax and Bak, whereas sensitizers are envisaged to displace the activators from the pro-survival proteins (Figure 6). The first evidence in favour of the direct model is that Bax and Bak, under normal conditions, are not thought to be complexed to anti-apoptotic proteins. In fact it has been shown that both Bax and Bak BH3 domain, responsible for the binding to the Bcl-2 family pro-apoptotic members, is buried in absence of stress. This observation implies that in healthy cells, Bax and Bak are not complexed to the pro-survival proteins [69;70]; in particular, Bax is a cytoplasmic monomer whereas Bak is constitutively localized at the mitochondrial membrane. Evidence supporting the direct model was also provided by Martinou's laboratory that showed that truncated Bid was able to induce Bax conformational changes and activation [71] with the consequent release of cytochrome *c* from mitochondria. Many reports confirmed and extended these observations to Bim and Puma, whereas other BH3-only proteins (e.g. Bik and Noxa) were

shown not to trigger Bax and Bak activation and mitochondrial membrane integrity disruption [72-77]. Another observation supporting the direct model is that mutations on Bax and Bak preventing them from binding to Bcl-2, Bcl-X_L and Mcl-1, do not result in their constitutive activation, suggesting that mechanisms other than the pro-survival protein-mediated repression are required for Bax and Bak activation [78]. Finally an NMR study characterized, for the first time, the interaction between a Bim BH3-derived peptide and Bax [79]. This study not only described the interaction site for the direct Bax activation mediated by BH3-only protein activators, but also helped to unravel the multistep mechanism of Bax activation [76;79;80]

Indirect model

The indirect model postulates that the Bax and Bak are kept in check by the anti-apoptotic members of the Bcl-2 family in order to prevent them from triggering the apoptotic program. Upon an apoptotic stimulus, the BH3 only members neutralize the anti-apoptotic proteins to favour the release of Bax and Bak[81] (Figure 6).

The indirect model excludes any kind of Bim/Bid-mediated Bax and Bak direct activation. The first evidence in favour of the indirect model comes from David Huang's group that showed no direct binding of the BH3 activators to Bak and Bax. By contrast the binding of BH3-only members with the anti-apoptotic proteins of the Bcl-2 family has been widely reported [82;83].

Moreover some BH3-only proteins, such as Bim and Puma, are more potent than other at binding the anti-apoptotic members. Indeed Bim, Puma and Bid have been shown as able to bind with the same affinity to all the anti-apoptotic players, explaining why they are the most effective apoptosis inducers among the BH3 only members [82].

Direct vs Indirect

The direct model, as mentioned, theorize that Bim and Bid directly activate Bax and Bak. If this model is correct, mice lacking Bim and Bid should have a phenotype similar to the phenotype of mice lacking Bax and Bak that die *in utero*. By contrast mice $Bim^{-/-} Bid^{-/-}$ appear largely normal. Moreover fibroblast derived from $Bim^{-/-} Bid^{-/-}$ mice remained sensitive to apoptotic stimuli and Bax activation normally occurs. According to the direct model Bad and Noxa are ‘sensitizers’, i.e. they cannot directly activate Bax and Bak, but together have the capacity to neutralize all the anti-apoptotic members. When they are over-expressed in fibroblast lacking Bim and Bid, Bax activation and cytochrome c release normally occur [83]. This shows that Bid and Bim are dispensable for the induction of apoptosis and that only neutralizing the anti-apoptotic players it is possible to trigger the activation of Bax. Additionally it has been observed that when Bid was mutated in order to abrogate its ability to bind Bak and Bax but not the anti-apoptotic proteins, cells were still able to undergo apoptosis [83]. At this point it might be argue that despite the absence of Bid and Bim there is still Puma that could directly activates Bax, even if the role of Puma as direct Bax activator is still controversial, explaining why $Bim^{-/-} Bid^{-/-}$ KO cells remain sensitive to apoptotic stimuli. Recently, a triple Bim/Bid/Puma KO mouse was generated, that phenocopied the Bax/Bak KO mouse [84]: the dispute on direct or indirect model is then solved in favour of the direct model? Not really! A consistent part of the scientific community does think that there are still substantial differences of phenotype between the Bax/Bak knock-out mice and the Bim/Bid/Puma KO mice [85]

To conclude there is strong evidence in favour of both models, even if neither the indirect nor the direct model can fully explain all the described results. It might be argued that that these two mechanisms are both valid, they might even coexist in the cell and be complementary as

proposed by David Andrews and collaborators in the so called ‘embedding together model’ which tries to fuse elements from both the direct and indirect model [86;87].

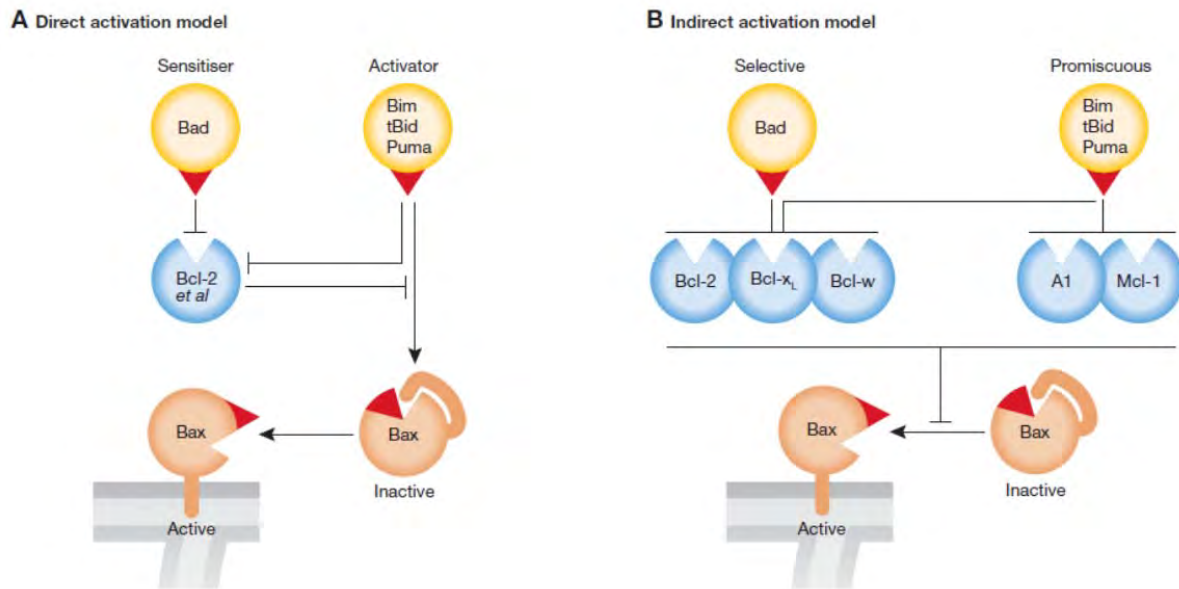


Figure 6. Direct and Indirect models of Bax/Bak activation. In the direct activation model, the activator BH3-only proteins (Bim, tBid and probably Puma), via their BH3 domain (red triangle), can directly engage and activate Bax (or Bak). In healthy cells the pro-survival family members (referred to as ‘Bcl-2 et al’) prevent this by sequestering the BH3-only activators. After an apoptotic signal, the sensitizer BH3-only proteins (e.g. Bad, Noxa, Bik) displace the activators from the anti-apoptotic proteins to activate Bax or Bak. (B) In the indirect activation model, the BH3-only proteins displace Bax and Bak from the inhibitory binding to the Bcl-2 family anti-apoptotic proteins, triggering their activation. Adapted from *Strasser A., et al., EMBO J., 2011.*

A new way of activating Bax: the ‘Trap and Release’ Mechanism

Recently, Philippe Juin and collaborators showed that the anti-apoptotic protein Bcl-X_L is able by itself, without the participation of the BH3-only proteins, to prime Bax and maintain it in an active conformation. The displacement of Bax from Bcl-X_L is then translated into Bax-mediated mitochondrial membrane disruption, cytochrome *c* release and apoptosis (Figure 7). The exact molecular mechanisms underlying this Bcl-X_L-mediated Bax activation, referred to as ‘Trap and Release’ model, are not fully understood. It has been speculated that Bcl-X_L facilitates the

exposure of the Bax BH3 domain that is then neutralized by the BH3-binding hydrophobic groove of Bcl-X_L. The exposure of the BH3 domain might be then accompanied by a general conformational change of the Bax molecule that, once Bax is displaced from Bcl-X_L, leads to its insertion into the outer mitochondrial membrane and oligomerization. Alternatively, Bcl-X_L binds to Bax molecules that spontaneously underwent conformational change and maintains activated Bax molecules in a safety status. These data are of particular interest because they unravel a new and revolutionary level of regulation of the Bcl-2 family members and might facilitate the understanding of how Bcl-X_L prevents cell death [88].

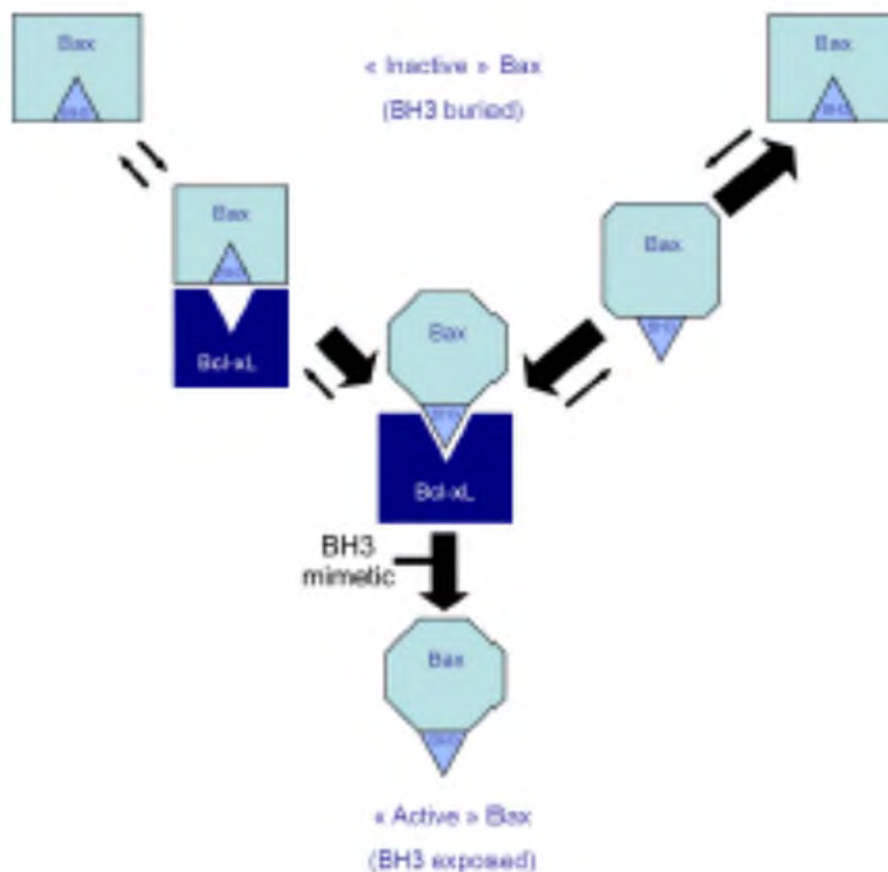


Figure 7. 'Trap and Release' Bax activation mechanism. Model for Bax activation via its interaction with and then release by Bcl-X_L. Adapted from *Gautier F., et al., Molecular and Cellular Biology, 2011.*

Caspases

Caspases (cysteine-dependent **aspartate-specific protease**) are proteases that cleave aspartic acid-containing polypeptides using their cysteine side chain, playing a central role in apoptosis [89;90]. For long time since their discovery, caspases were believed to participate only in the apoptotic cell death process, with the exception of caspase 1, known to be a pro-inflammatory effector.

In the last decade mounting observations seemed to invalidate the paradigm of caspases only being cell death mediators and the scientific community has now accepted that caspases are also involved in life-maintaining processes, namely cell differentiation and survival [91-94]. Indeed, to all the conventionally considered pro-apoptotic caspases has been attributed at least one non-apoptotic function [95]. Anyway, the initial distinction between pro-apoptotic and inflammatory caspases can be still useful for a general classification (Figure 8). The pro-apoptotic caspases are divided into two groups: initiators and effectors. Initiator caspases (8 and 10 for the extrinsic pathway and 9 for the intrinsic pathway) are also called apical caspases because they initiate the apoptotic cascade. They exist as inactive monomers; they are characterized by a long prodomain and activated by the dimerization stimulated by their recruitment to the respective activation platform: DISC for caspase 8-10 and apoptosome for caspase 9. Using these classification parameters, also the caspase 2 could be considered an initiator caspase as it bears a long prodomain and it is activated by a molecular platform called PIDDosome; however the activation mechanism and the exact function of caspase 2 still remain to be fully elucidated.

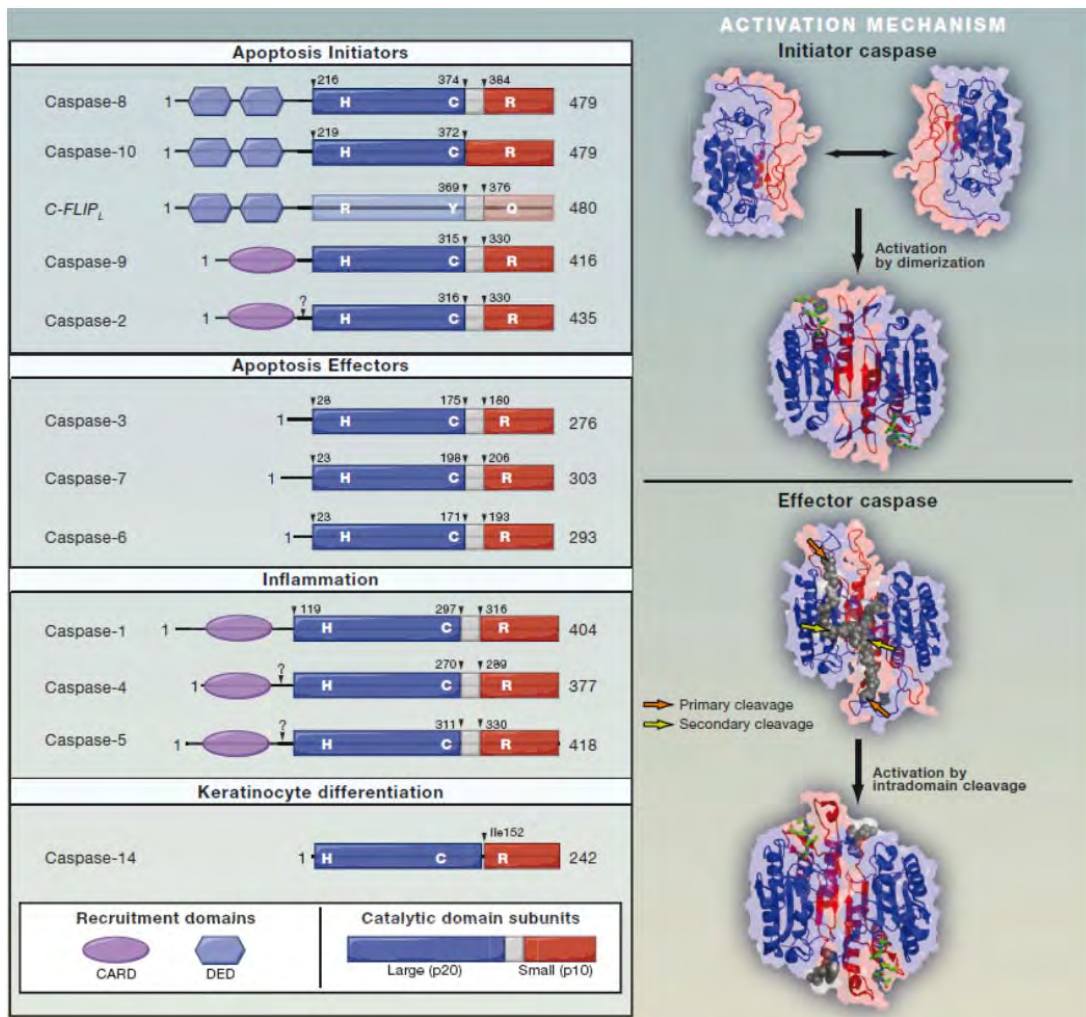


Figure 8. Caspases classification. Caspases can be classified in pro-apoptotic and inflammatory caspases. Pro-apoptotic caspases are further divided into initiator caspases (8-10 and probably 2), activated by dimerization, and effector caspases (3-6-7), activated by intra-domain cleavage. Inflammatory caspases are caspase 1/4/5. Adapted from Salvesen G., S., et al. *Cell*, 2011.

Executioner caspases, caspase 3, 6 and 7, are so called by virtue of the fact that they execute the apoptotic process by integrating the apoptotic signalling into cell dismantling. They exist as inactive dimers that are activated by initiator caspase-mediated proteolytic cleavage [96-99]. All the knowledge about the mechanism of activation of executioner caspases comes from the crystal structure of caspase 7, where it was possible to observe a conformational change of the active site

after such a proteolytic cleavage [100]. Finally, inflammatory caspases (caspase1-4-5), whose role is to mediate the maturation of specific cytokines required by the immune system, are probably activated in a fashion similar to the initiator caspases [101].

Ras signaling

The Ras protein was identified as the transforming gene of the Harvey and Kirsten strains of rat sarcoma viruses [102;103]. Ras is a protein belonging to the small GTPase family that is involved in the cellular signal transduction downstream of growth factor associated receptors that controls distinct cellular processes such as proliferation, migration and apoptosis [104]. Ras cycles between an active state, when bound to GTP, and an inactive state, when bound to GDP [105], and its cycling is tightly controlled by two classes of proteins: GEFs and GAPs. GEFs (guanine exchange factor) enhance the rate of GDP dissociation [106], whereas GAPs (GTPase activating protein), like p120-RasGAP (from now on referred to as RasGAP), accelerate the intrinsic GTPase activity of the small GTPases to promote their inactivation [107].

RasGAP

RasGAP is a well-known GAP protein that functions as a negative regulator of Ras signaling [108;109]. It is a 120-kDa cytosolic protein ubiquitously expressed and highly conserved across species [108;110] (Figure 9). The N-terminal region contains a Src Homology 3 domain (SH3) flanked by two Src Homology 2 domains (SH2), followed by a pleckstrin homology (PH) and by a calcium-dependent phospholipid-binding domain (CaLB/C2) [111;112]. SH2 domain binds phosphorylated tyrosines containing sequences, such as the cytoplasmic portion of tyrosine kinase-associated receptors, the PH domain binds to the cytoplasmic membrane phospholipids such as phosphatidylinositol 4-5 biphosphate and the CaLB/C2 is responsible for protein-protein

interactions. SH3 domains are known to bind proline-rich motifs (PxxP). Interestingly the RasGAP SH3 was proposed not to bind proline-rich motif, suggesting that RasGAP may interact with its binding partners through unconventional SH3 domain interactions [110;113]. The catalytic domain GAP that stimulates the hydrolysis of Ras-bound GTP is localized in the C-terminal region [107;114].



Figure 9. RasGAP structure. PPP:proline-rich region; SH2: Src homology domain 2; SH3: Src homology domain 3; PH: pleckstrin homology domain; C2: calcium-dependent lipid domain and GAP:GTPase activating protein domain.

RasGAP not only as GTP-ase activating protein

RasGAP was also described to act as Ras effector in functions related to proliferation, differentiation and apoptosis, independently of its GAP activity.

Several reports support this role for RasGAP. For example, Ras oncogenic mutants do not respond to RasGAP, but when they were mutated in the effector binding site (aa 30-40), known to be also the RasGAP binding site [115], they lost their transforming activity. Moreover a mutation within the RasGAP binding domain of Ras that does not affect their reciprocal interaction (Ala 39) does not result in the loss of Ras transforming activity [116]. Hence this report provides evidence in favour of RasGAP being a component of the Ras signalling pathway. This hypothesis was corroborated by a study showing that the N-terminal domain of RasGAP (nGAP, residues 1-666) was able to abolish oncogenic Ras activity but not normal Ras therefore acting as a competitive antagonist for the endogenous Ras/RasGAP complex and so preventing

the Ras signalling [117]. Another study, showing that the opening of the muscarin receptor-activated potassium channel can be inhibited by the Ras/RasGAP complex, demonstrated that the SH2-SH3 region of RasGAP, residing in its N-terminal part, mediates this inhibition [118]. It is also important to mention that disruption of the RasGAP gene (*Rasa1*) leads to embryonic lethality at day 10.5 due to aberrant cardiovascular development [119]. In conclusion, all this piece of evidence support a role for the N-terminal portion of RasGAP in some of the Ras-mediated biological response.

G3BP1

In 1996, the laboratory of Bruno Tocque, in search of RasGAP interacting proteins potentially acting as Ras effectors, discovered a new protein binding to its SH3 domain that was called G3BP1 (**GAP SH3 Binding Protein 1**) (Figure 10). G3BP1 is a 68 kDa cytosolic protein whose binding site on the RasGAP SH3 domain encompasses residues 317-326 [120]. Interestingly, this binding, mediated by the NTF2-like domain of G3BP1 [113], only takes place in serum-stimulated cells, whereas, in quiescent cells, G3BP1 re-localizes into the nucleus showing hyperphosphorylation on serine residues. Furthermore, in the absence of RasGAP, G3BP1 phosphorylation was abrogated. After the cloning it turned evident that G3BP1 was related to RNA-binding proteins, indeed, it bears two ribonucleoprotein (RNP) motifs, RNP1 and RNP2, forming the RNA consensus recognition motif (RRM) [121]. Consistently with this observation, it has been proved later that G3BP1 harbours an intrinsic endoribonuclease activity, in particular, it is able to cleave the 3'-untranslated region (3'-UTR) of the human c-myc RNA transcript [122] negatively regulating its stability. Moreover the G3BP1 ability to cleave mRNA was found to be positively regulated by its phosphorylation status. Conceivably, G3BP1 was believed to enable the accumulation of c-myc mRNA in proliferating cells, where it is associated to RasGAP and

dephosphorylated, and to mediate c-myc degradation in resting cells, where it is hyperphosphorylated and its endoribonuclease activity is on. Therefore G3BP1 seems to couple extracellular proliferative stimuli to c-myc mRNA metabolism through its binding to RasGAP, reinforcing the notion of RasGAP as a Ras effector.



Figure 10. G3BP1 Structure. Schematic representation of the G3BP1 protein structure. NTF2-like: nuclear transport factor 2-like domain; RRM: RNA recognition motif and RGG: arginine-glycine rich box.

RasGAP as caspase substrate

The RasGAP N-terminal part plays also a role in apoptosis (Figure 11). Indeed RasGAP was discovered to bear two caspase 3 consensus cleavage sites that are sequentially targeted, during the apoptotic process, as caspase 3 activity increases [123;124]. When caspase 3 activity is very low, RasGAP is cleaved at position 455 to generate an N-terminal fragment (called fragment N) and a C-terminal fragment (called fragment C) [125]. Interestingly fragment N protects cells from several different apoptotic stimuli when over-expressed in cells, through a pathway engaging the Ras/PI3K/AKT signalling arm [126]. It is pertinent to mention that caspase-3 is the only caspase able to cleave RasGAP, as demonstrated using caspase-3 knock-out mouse embryonic fibroblasts [127]. When caspase-3 activity augments, fragment N is further cleaved at position 157, leading to the generation of two distinct fragment that were called fragment N1 and N2, the latter containing the SH2-SH3-SH2 motif [125]. Importantly, this second cleavage at position 157 was shown to abolish the anti-apoptotic properties of the fragment N [125]. Intriguingly fragment N2

has pro-apoptotic functions in cancer cells, but not in normal cells, by sensitizing them to genotoxin-induced apoptosis, while having no effect by itself [128].

Cancer Treatment

The most commonly used anti-cancer treatments are surgery, chemotherapy, based on the utilization of drugs that kill cancer cells, and radiotherapy, which uses high energy radiation to kill malignant cells. Surgery is the oldest modality of cancer treatment. The earliest report of a surgical treatment of cancer was written in Egypt circa 1600 B.C. Nowadays surgery is the most currently used kind of therapy of solid tumors while chemo and radiotherapy are rarely used as primary therapies but rather as adjuvant or neoadjuvant therapies. Adjuvant therapy is any treatment given after primary therapy, whereas neoadjuvant is any treatment given before the primary therapy. Adjuvant therapies, introduced during 1970s, are mainly represented by systemic therapies, i.e. therapies that use substances that travel through the bloodstream reaching and killing cancer cells all over the body, such as chemotherapy. They are aimed at the elimination of residual cancer cells that were not removed by surgery within the primary tumor site or that might have spread to colonize new tumor sites, causing recurrence of the tumor. To this respect, a recent report showed that adjuvant chemotherapy for early-stage breast cancer reduces the rate of tumor recurrence and the mortality of patients [129].

Neo-adjuvant therapies, experimented for the first time by Bonadonna and collaborators in 1975 [130], rely on the utilization of chemo and/or radiotherapy to shrink tumors that are inoperable at their current state, to render them resectable. There are reports showing that in breast cancer the utilization of neoadjuvant therapy allows breast-conserving surgery instead of mastectomy (surgical removal of the breast) [131] and that neo-adjuvant radiotherapy improves the survival in

patients with resectable pancreatic cancer [132;133]. Finally, the mortality of cancer has been declining since 1990, due both to prevention and early diagnosis and to the advances made by the modern medicine in cancer treatment [134].

TAT-RasGAP₃₁₇₋₃₂₆: a tumor sensitizer

Cancer treatment is limited by two major concerns: intrinsic or acquired resistance to therapies, particularly to radio and chemo-therapy, and side effects, generated when the therapeutical dose exceeds the toxic dose. The development of therapeutical strategies aimed at restoring the normal sensitivity of malignant cells or at increasing their responsiveness to treatments, would allow the reduction of the effective doses with a consequent limitation of side effects. One promising approach is represented by the utilization of therapeutic peptides acting as sensitizers selectively in tumor cells.

The RasGAP caspase 3-generated fragment N2 favours the genotoxin-induced apoptotic cell death selectively in cancer cells. In order to make fragment N2 a therapeutical tool for cancer treatment, its shortest amino acid sequence still bearing sensitizing activity, found out to reside in the amino acids 317-326, was fused to a cell penetration sequence from the TAT protein of HIV virus. The resulting TAT-RasGAP₃₁₇₋₃₂₆ peptide efficiently enters tumor cells *in vitro* and sensitizes several cancer cell lines to genotoxic compounds towards apoptosis [135]. Relatively little is known on its mode of action and on its selectivity for tumoral cells. The first mechanistic study showed that TAT-RasGAP₃₁₇₋₃₂₆-mediated sensitization to apoptosis requires an intact p53/Puma axis to occur, and that the increased apoptotic response has to be attributed to an increased mitochondrial membrane depolarization and caspase 3 activation [136].

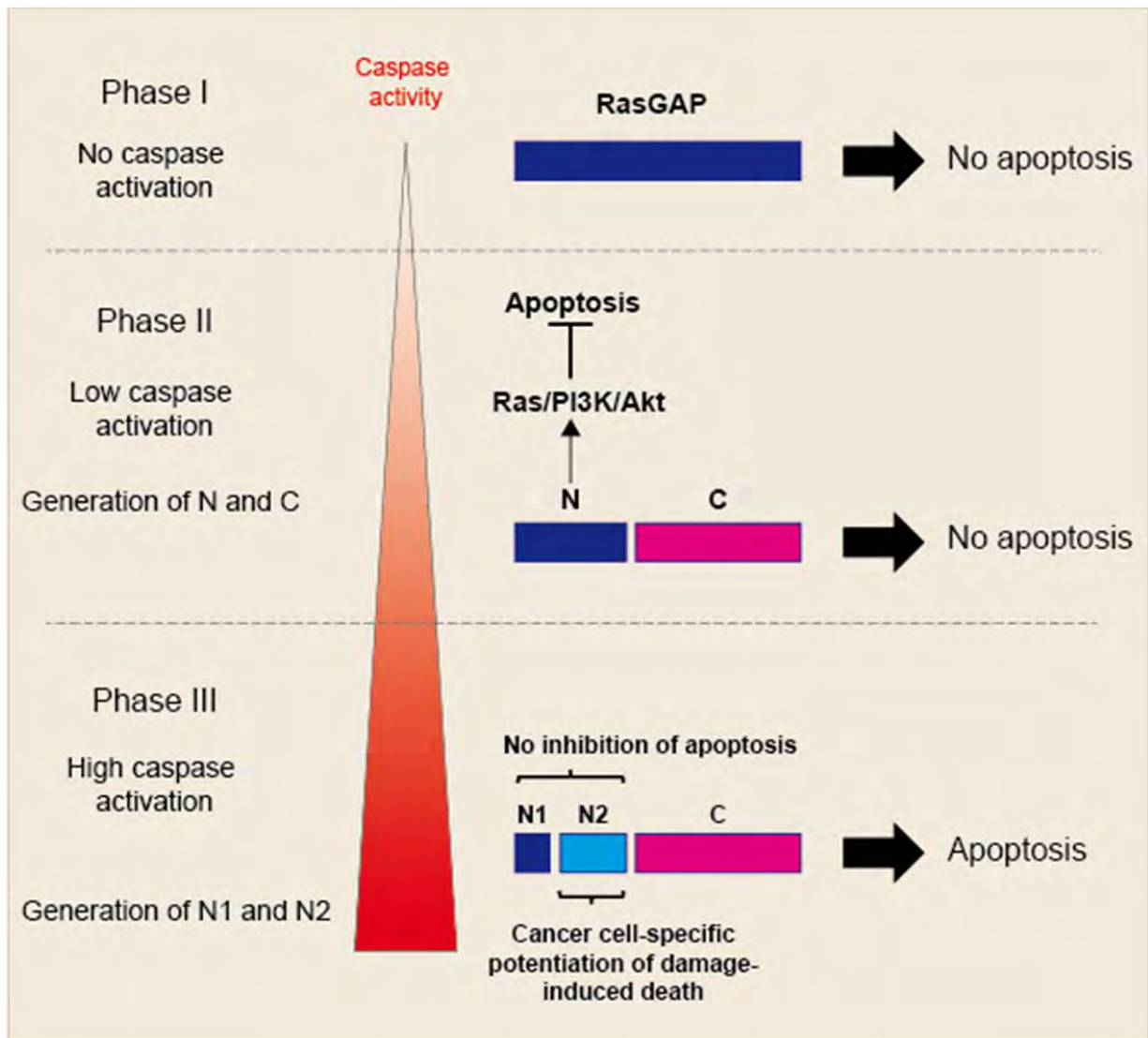


Figure 11. Model for the role of RasGAP cleavage fragments in the regulation of apoptosis.

Reference list

- [1] D. Hanahan, R.A. Weinberg, The Hallmarks of Cancer. *Cell* 100 (2000) 57-70.
- [2] D. Hanahan, R.A. Weinberg, Hallmarks of cancer: the next generation. *Cell* 144 (2011) 646-674.
- [3] P.C. Nowell, The clonal evolution of tumor cell populations. *Science* 194 (1976) 23-28.
- [4] A. Compagni, G. Christofori, Recent advances in research on multistage tumorigenesis. *Br.J.Cancer* 83 (2000) 1-5.
- [5] M. Korc, B. Chandrasekar, Y. Yamanaka, H. Friess, M. Buchler, H.G. Beger, Overexpression of the epidermal growth factor receptor in human pancreatic cancer is associated with concomitant increases in the levels of epidermal growth factor and transforming growth factor alpha. *J.Clin.Invest* 90 (1992) 1352-1360.
- [6] M. Schrevel, A. Gorter, S.M. Kolkman-Uljee, J.B. Trimbos, G.J. Fleuren, E.S. Jordanova, Molecular mechanisms of epidermal growth factor receptor overexpression in patients with cervical cancer. *Mod.Pathol.* 24 (2011) 720-728.
- [7] G. Selvaggi, S. Novello, V. Torri, E. Leonardo, G.P. De, P. Borasio, C. Mossetti, F. Ardisson, P. Lausi, G.V. Scagliotti, Epidermal growth factor receptor overexpression correlates with a poor prognosis in completely resected non-small-cell lung cancer. *Ann.Oncol.* 15 (2004) 28-32.
- [8] D. Wang, S. Patil, W. Li, L.E. Humphrey, M.G. Brattain, G.M. Howell, Activation of the TGFalpha autocrine loop is downstream of IGF-I receptor activation during mitogenesis in growth factor dependent human colon carcinoma cells. *Oncogene* 21 (2002) 2785-2796.
- [9] M.B. Sporn, A.B. Roberts, Autocrine growth factors and cancer. *Nature* 313 (1985) 745-747.
- [10] M.B. Sporn, G.J. Todaro, Autocrine secretion and malignant transformation of cells. *N.Engl.J.Med.* 303 (1980) 878-880.
- [11] S.V. Sharma, D.W. Bell, J. Settleman, D.A. Haber, Epidermal growth factor receptor mutations in lung cancer. *Nat.Rev.Cancer* 7 (2007) 169-181.
- [12] L. Soucek, J. Whitfield, C.P. Martins, A.J. Finch, D.J. Murphy, N.M. Sodikin, A.N. Karnezis, L.B. Swigart, S. Nasi, G.I. Evan, Modelling Myc inhibition as a cancer therapy. *Nature* 2008).
- [13] R.J. Shaw, L.C. Cantley, Ras, PI(3)K and mTOR signalling controls tumour cell growth. *Nature* 441 (2006) 424-430.

- [14] S. Schubert, K. Shannon, G. Bollag, Hyperactive Ras in developmental disorders and cancer. *Nat.Rev.Cancer* 7 (2007) 295-308.
- [15] L. Soucek, G.I. Evan, The ups and downs of Myc biology. *Curr.Opin.Genet.Dev.* 20 (2010) 91-95.
- [16] K.W. Kinzler, B. Vogelstein, Lessons from hereditary colorectal cancer. *Cell* 87 (1996) 159-170.
- [17] Y. Pylayeva-Gupta, E. Grabocka, D. Bar-Sagi, RAS oncogenes: weaving a tumorigenic web. *Nat.Rev.Cancer* 11 (2011) 761-774.
- [18] X.H. Feng, R. Derynck, Specificity and versatility in tgf-beta signaling through Smads. *Annu.Rev.Cell Dev.Biol.* 21 (2005) 659-693.
- [19] I.W. Taylor, J.L. Wrana, SnapShot: The TGFbeta pathway interactome. *Cell* 133 (2008) 378.
- [20] J. Massague, TGFbeta in Cancer. *Cell* 134 (2008) 215-230.
- [21] C.J. Sherr, Cancer cell cycles. *Science* 274 (1996) 1672-1677.
- [22] C.J. Sherr, F. McCormick, The RB and p53 pathways in cancer. *Cancer Cell* 2 (2002) 103-112.
- [23] D.L. Burkhardt, J. Sage, Cellular mechanisms of tumour suppression by the retinoblastoma gene. *Nat.Rev.Cancer* 8 (2008) 671-682.
- [24] T.L. Yuan, L.C. Cantley, PI3K pathway alterations in cancer: variations on a theme. *Oncogene* 27 (2008) 5497-5510.
- [25] L. HAYFLICK, P.S. MOORHEAD, The serial cultivation of human diploid cell strains. *Exp.Cell Res.* 25 (1961) 585-621.
- [26] E.H. Blackburn, Telomere states and cell fates. *Nature* 408 (2000) 53-56.
- [27] S.E. Artandi, R.A. DePinho, Telomeres and telomerase in cancer. *Carcinogenesis* 31 (2010) 9-18.
- [28] N.W. Kim, M.A. Piatyszek, K.R. Prowse, C.B. Harley, M.D. West, P.L. Ho, G.M. Coviello, W.E. Wright, S.L. Weinrich, J.W. Shay, Specific association of human telomerase activity with immortal cells and cancer. *Science* 266 (1994) 2011-2015.
- [29] C.M. Counter, A.A. Avilion, C.E. LeFeuvre, N.G. Stewart, C.W. Greider, C.B. Harley, S. Bacchetti, Telomere shortening associated with chromosome instability is arrested in immortal cells which express telomerase activity. *EMBO J.* 11 (1992) 1921-1929.
- [30] Y. Deng, S.S. Chan, S. Chang, Telomere dysfunction and tumour suppression: the senescence connection. *Nat.Rev.Cancer* 8 (2008) 450-458.

- [31] T.D. Halazonetis, V.G. Gorgoulis, J. Bartek, An Oncogene-Induced DNA Damage Model for Cancer Development. *Science* 319 (2008) 1352-1355.
- [32] N.N. Danial, S.J. Korsmeyer, Cell death: critical control points. *Cell* 116 (2004) 205-219.
- [33] R.C. Taylor, S.P. Cullen, S.J. Martin, Apoptosis: controlled demolition at the cellular level. *Nat.Rev.Mol.Cell Biol.* 9 (2008) 231-241.
- [34] J. Folkman, K. Watson, D. Ingber, D. Hanahan, Induction of angiogenesis during the transition from hyperplasia to neoplasia. *Nature* 339 (1989) 58-61.
- [35] M. Potente, H. Gerhardt, P. Carmeliet, Basic and therapeutic aspects of angiogenesis. *Cell* 146 (2011) 873-887.
- [36] D. Hanahan, J. Folkman, Patterns and emerging mechanisms of the angiogenic switch during tumorigenesis. *Cell* 86 (1996) 353-364.
- [37] V. Baeriswyl, G. Christofori, The angiogenic switch in carcinogenesis. *Semin.Cancer Biol.* 19 (2009) 329-337.
- [38] A.K. Olsson, A. Dimberg, J. Kreuger, L. Claesson-Welsh, VEGF receptor signalling - in control of vascular function. *Nat.Rev.Mol.Cell Biol.* 7 (2006) 359-371.
- [39] F. Okada, J.W. Rak, B.S. Croix, B. Lieubeau, M. Kaya, L. Roncari, S. Shirasawa, T. Sasazuki, R.S. Kerbel, Impact of oncogenes in tumor angiogenesis: mutant K-ras up-regulation of vascular endothelial growth factor/vascular permeability factor is necessary, but not sufficient for tumorigenicity of human colorectal carcinoma cells. *Proc.Natl.Acad.Sci.U.S.A* 95 (1998) 3609-3614.
- [40] J.L. Arbiser, M.A. Moses, C.A. Fernandez, N. Ghiso, Y. Cao, N. Klauber, D. Frank, M. Brownlee, E. Flynn, S. Parangi, H.R. Byers, J. Folkman, Oncogenic H-ras stimulates tumor angiogenesis by two distinct pathways. *Proc.Natl.Acad.Sci.U.S.A* 94 (1997) 861-866.
- [41] L. Soucek, E.R. Lawlor, D. Soto, K. Shchors, L.B. Swigart, G.I. Evan, Mast cells are required for angiogenesis and macroscopic expansion of Myc-induced pancreatic islet tumors. *Nat.Med.* 13 (2007) 1211-1218.
- [42] R. Kalluri, M. Zeisberg, Fibroblasts in cancer. *Nat.Rev.Cancer* 6 (2006) 392-401.
- [43] C.L. Chaffer, R.A. Weinberg, A perspective on cancer cell metastasis. *Science* 331 (2011) 1559-1564.
- [44] K.W. Hunter, N.P. Crawford, J. Alsarraj, Mechanisms of metastasis. *Breast Cancer Res.* 10 Suppl 1 (2008) S2.
- [45] A.C. Chiang, J. Massague, Molecular basis of metastasis. *N.Engl.J.Med.* 359 (2008) 2814-2823.

- [46] A. Aguilera, B. Gomez-Gonzalez, Genome instability: a mechanistic view of its causes and consequences. *Nat.Rev.Genet.* 9 (2008) 204-217.
- [47] B.A. Weaver, D.W. Cleveland, Does aneuploidy cause cancer? *Curr.Opin.Cell Biol.* 18 (2006) 658-667.
- [48] L.A. Loeb, Mutator phenotype may be required for multistage carcinogenesis. *Cancer Res.* 51 (1991) 3075-3079.
- [49] T.L. Orr-Weaver, R.A. Weinberg, A checkpoint on the road to cancer. *Nature* 392 (1998) 223-224.
- [50] D.P. Cahill, C. Lengauer, J. Yu, G.J. Riggins, J.K. Willson, S.D. Markowitz, K.W. Kinzler, B. Vogelstein, Mutations of mitotic checkpoint genes in human cancers. *Nature* 392 (1998) 300-303.
- [51] C.J. Lord, A. Ashworth, The DNA damage response and cancer therapy. *Nature* 481 (2012) 287-294.
- [52] R. Fishel, M.K. Lescoe, M.R. Rao, N.G. Copeland, N.A. Jenkins, J. Garber, M. Kane, R. Kolodner, The human mutator gene homolog MSH2 and its association with hereditary nonpolyposis colon cancer. *Cell* 75 (1993) 1027-1038.
- [53] F.S. Leach, N.C. Nicolaides, N. Papadopoulos, B. Liu, J. Jen, R. Parsons, P. Peltomaki, P. Sistonen, L.A. Aaltonen, M. Nystrom-Lahti, ., Mutations of a mutS homolog in hereditary nonpolyposis colorectal cancer. *Cell* 75 (1993) 1215-1225.
- [54] T. Sjoblom, S. Jones, L.D. Wood, D.W. Parsons, J. Lin, T.D. Barber, D. Mandelker, R.J. Leary, J. Ptak, N. Silliman, S. Szabo, P. Buckhaults, C. Farrell, P. Meeh, S.D. Markowitz, J. Willis, D. Dawson, J.K. Willson, A.F. Gazdar, J. Hartigan, L. Wu, C. Liu, G. Parmigiani, B.H. Park, K.E. Bachman, N. Papadopoulos, B. Vogelstein, K.W. Kinzler, V.E. Velculescu, The consensus coding sequences of human breast and colorectal cancers. *Science* 314 (2006) 268-274.
- [55] L.D. Wood, D.W. Parsons, S. Jones, J. Lin, T. Sjoblom, R.J. Leary, D. Shen, S.M. Boca, T. Barber, J. Ptak, N. Silliman, S. Szabo, Z. Dezso, V. Ustyanksky, T. Nikolskaya, Y. Nikolsky, R. Karchin, P.A. Wilson, J.S. Kaminker, Z. Zhang, R. Croshaw, J. Willis, D. Dawson, M. Shipitsin, J.K. Willson, S. Sukumar, K. Polyak, B.H. Park, C.L. Pethiyagoda, P.V. Pant, D.G. Ballinger, A.B. Sparks, J. Hartigan, D.R. Smith, E. Suh, N. Papadopoulos, P. Buckhaults, S.D. Markowitz, G. Parmigiani, K.W. Kinzler, V.E. Velculescu, B. Vogelstein, The genomic landscapes of human breast and colorectal cancers. *Science* 318 (2007) 1108-1113.
- [56] S. Jones, X. Zhang, D.W. Parsons, J.C. Lin, R.J. Leary, P. Angenendt, P. Mankoo, H. Carter, H. Kamiyama, A. Jimeno, S.M. Hong, B. Fu, M.T. Lin, E.S. Calhoun, M. Kamiyama, K. Walter, T. Nikolskaya, Y. Nikolsky, J. Hartigan, D.R. Smith, M. Hidalgo, S.D. Leach, A.P. Klein, E.M. Jaffee, M. Goggins, A. Maitra, C. Iacobuzio-Donahue, J.R. Eshleman, S.E. Kern, R.H. Hruban, R. Karchin, N. Papadopoulos, G. Parmigiani, B.

- Vogelstein, V.E. Velculescu, K.W. Kinzler, Core signaling pathways in human pancreatic cancers revealed by global genomic analyses. *Science* 321 (2008) 1801-1806.
- [57] D.W. Parsons, S. Jones, X. Zhang, J.C. Lin, R.J. Leary, P. Angenendt, P. Mankoo, H. Carter, I.M. Siu, G.L. Gallia, A. Olivi, R. McLendon, B.A. Rasheed, S. Keir, T. Nikolskaya, Y. Nikolsky, D.A. Busam, H. Tekleab, L.A. Diaz, Jr., J. Hartigan, D.R. Smith, R.L. Strausberg, S.K. Marie, S.M. Shinjo, H. Yan, G.J. Riggins, D.D. Bigner, R. Karchin, N. Papadopoulos, G. Parmigiani, B. Vogelstein, V.E. Velculescu, K.W. Kinzler, An integrated genomic analysis of human glioblastoma multiforme. *Science* 321 (2008) 1807-1812.
- [58] The Cancer Genome Atlas Research Network, Comprehensive genomic characterization defines human glioblastoma genes and core pathways. *Nature* 455 (2008) 1061-1068.
- [59] L. Ding, G. Getz, D.A. Wheeler, E.R. Mardis, M.D. McLellan, K. Cibulskis, C. Sougnez, H. Greulich, D.M. Muzny, M.B. Morgan, L. Fulton, R.S. Fulton, Q. Zhang, M.C. Wendl, M.S. Lawrence, D.E. Larson, K. Chen, D.J. Dooling, A. Sabo, A.C. Hawes, H. Shen, S.N. Jhangiani, L.R. Lewis, O. Hall, Y. Zhu, T. Mathew, Y. Ren, J. Yao, S.E. Scherer, K. Clerc, G.A. Metcalf, B. Ng, A. Milosavljevic, M.L. Gonzalez-Garay, J.R. Osborne, R. Meyer, X. Shi, Y. Tang, D.C. Koboldt, L. Lin, R. Abbott, T.L. Miner, C. Pohl, G. Fewell, C. Haipek, H. Schmidt, B.H. Dunford-Shore, A. Kraja, S.D. Crosby, C.S. Sawyer, T. Vickery, S. Sander, J. Robinson, W. Winckler, J. Baldwin, L.R. Chirieac, A. Dutt, T. Fennell, M. Hanna, B.E. Johnson, R.C. Onofrio, R.K. Thomas, G. Tonon, B.A. Weir, X. Zhao, L. Ziaugra, M.C. Zody, T. Giordano, M.B. Orringer, J.A. Roth, M.R. Spitz, I.I. Wistuba, B. Ozenberger, P.J. Good, A.C. Chang, D.G. Beer, M.A. Watson, M. Ladanyi, S. Broderick, A. Yoshizawa, W.D. Travis, W. Pao, M.A. Province, G.M. Weinstock, H.E. Varmus, S.B. Gabriel, E.S. Lander, R.A. Gibbs, M. Meyerson, R.K. Wilson, Somatic mutations affect key pathways in lung adenocarcinoma. *Nature* 455 (2008) 1069-1075.
- [60] J. Bartkova, Z. Horejsi, K. Koed, A. Kramer, F. Tort, K. Zieger, P. Guldborg, M. Sehested, J.M. Nesland, C. Lukas, T. Orntoft, J. Lukas, J. Bartek, DNA damage response as a candidate anti-cancer barrier in early human tumorigenesis. *Nature* 434 (2005) 864-870.
- [61] V.G. Gorgoulis, L.V. Vassiliou, P. Karakaidos, P. Zacharatos, A. Kotsinas, T. Liloglou, M. Venere, R.A. Dittullo, Jr., N.G. Kastrinakis, B. Levy, D. Kletsas, A. Yoneta, M. Herlyn, C. Kittas, T.D. Halazonetis, Activation of the DNA damage checkpoint and genomic instability in human precancerous lesions. *Nature* 434 (2005) 907-913.
- [62] J. Bartkova, N. Rezaei, M. Liontos, P. Karakaidos, D. Kletsas, N. Issaeva, L.V. Vassiliou, E. Kolettas, K. Niforou, V.C. Zoumpourlis, M. Takaoka, H. Nakagawa, F. Tort, K. Fugger, F. Johansson, M. Sehested, C.L. Andersen, L. Dyrskjot, T. Orntoft, J. Lukas, C. Kittas, T. Helleday, T.D. Halazonetis, J. Bartek, V.G. Gorgoulis, Oncogene-induced senescence is part of the tumorigenesis barrier imposed by DNA damage checkpoints. *Nature* 444 (2006) 633-637.
- [63] M.O. Hengartner, The biochemistry of apoptosis. *Nature* 407 (2000) 770-776.

- [64] H. Walczak, P.H. Krammer, The CD95 (APO-1/Fas) and the TRAIL (APO-2L) apoptosis systems. *Exp.Cell Res.* 256 (2000) 58-66.
- [65] R.J. Youle, A. Strasser, The BCL-2 protein family: opposing activities that mediate cell death. *Nat Rev Mol Cell Biol* 9 (2008) 47-59.
- [66] S. Fulda, K.M. Debatin, Extrinsic versus intrinsic apoptosis pathways in anticancer chemotherapy. *Oncogene* 25 (2006) 4798-4811.
- [67] S.B. Bratton, G.S. Salvesen, Regulation of the Apaf-1-caspase-9 apoptosome. *J.Cell Sci.* 123 (2010) 3209-3214.
- [68] J.C. Martinou, R.J. Youle, Mitochondria in apoptosis: bcl-2 family members and mitochondrial dynamics. *Dev.Cell* 21 (2011) 92-101.
- [69] M. Suzuki, R.J. Youle, N. Tjandra. Structure of Bax: Coregulation of Dimer Formation and Intracellular Localization. *Cell* 103[4], 645-654. 10-11-2000.
- [70] Y.T. Hsu, K.G. Wolter, R.J. Youle, Cytosol-to-membrane redistribution of Bax and Bcl-X(L) during apoptosis. *Proc Natl Acad Sci U S A* 94 (1997) 3668-3672.
- [71] S. Desagher, A. Osen-Sand, A. Nichols, R. Eskes, S. Montessuit, S. Lauper, K. Maundrell, B. Antonsson, J.C. Martinou, Bid-induced Conformational Change of Bax Is Responsible for Mitochondrial Cytochrome c Release during Apoptosis. *J.Cell Biol.* 144 (1999) 891-901.
- [72] A. Letai, M.C. Bassik, L.D. Walensky, Sorcinelli M.D., S. Weiler, and Stanley J, Distinct BH3 domains either sensitize or activate mitochondrial apoptosis, serving as prototype cancer therapeutics. *Cancer Cell*2008).
- [73] T. Kuwana, L. Bouchier-Hayes, J.E. Chipuk, C. Bonzon, B.A. Sullivan, D.R. Green, D.D. Newmeyer. BH3 Domains of BH3-Only Proteins Differentially Regulate Bax-Mediated Mitochondrial Membrane Permeabilization Both Directly and Indirectly. *Molecular Cell* 17[4], 525-535. 18-2-2005.
- [74] T. Kuwana, M.R. Mackey, G. Perkins, M.H. Ellisman, M. Latterich, R. Schneiter, D.R. Green, D.D. Newmeyer. Bid, Bax, and Lipids Cooperate to Form Supramolecular Openings in the Outer Mitochondrial Membrane. *Cell* 111[3], 331-342. 1-11-2002.
- [75] M.C.L.T.M.V.K.W.S.G.A.A.M.T.C.B.K.S.J. Wei, tBID, a membrane-targeted death ligand, oligomerizes BAK to release cytochrome c. *Genes & Development* 14 (2000) 2060-2071.
- [76] P.F. Cartron, T. Gallenne, G. Bougras, F. Gautier, F. Manero, P. Vusio, K. Meflah, F.M. Vallette, P. Juin, The first alpha helix of Bax plays a necessary role in its ligand-induced activation by the BH3-only proteins Bid and PUMA. *Mol Cell* 16 (2004) 807-818.

- [77] T. Gallenne, F. Gautier, L. Oliver, E. Hervouet, B. Noel, J.A. Hickman, O. Geneste, P.F. Cartron, F.M. Vallette, S. Manon, P. Juin, Bax activation by the BH3-only protein Puma promotes cell dependence on antiapoptotic Bcl-2 family members. *J.Cell Biol.* 185 (2009) 279-290.
- [78] H. Kim, M. Rafiuddin-Shah, H.C. Tu, J.R. Jeffers, G.P. Zambetti, J.J. Hsieh, E.H. Cheng, Hierarchical regulation of mitochondrion-dependent apoptosis by BCL-2 subfamilies. *Nat.Cell Biol.* 8 (2006) 1348-1358.
- [79] E. Gavathiotis, M. Suzuki, M.L. Davis, K. Pitter, G.H. Bird, S.G. Katz, H.C. Tu, H. Kim, E.H.Y. Cheng, N. Tjandra, L.D. Walensky, BAX activation is initiated at a novel interaction site. *Nature* 455 (2008) 1076-1081.
- [80] H. Kim, H.C. Tu, D. Ren, O. Takeuchi, J.R. Jeffers, G.P. Zambetti, J.J. Hsieh, E.H. Cheng, Stepwise activation of BAX and BAK by tBID, BIM, and PUMA initiates mitochondrial apoptosis. *Mol.Cell* 36 (2009) 487-499.
- [81] S.N. Willis, J.M. Adams, Life in the balance: how BH3-only proteins induce apoptosis. *Current Opinion in Cell Biology* 17 (2005) 617-625.
- [82] L. Chen, S.N. Willis, A. Wei, B.J. Smith, J.I. Fletcher, M.G. Hinds, P.M. Colman, C.L. Day, J.M. Adams, D.C.S. HUANG. Differential Targeting of Prosurvival Bcl-2 Proteins by Their BH3-Only Ligands Allows Complementary Apoptotic Function. *Molecular Cell* 17[3], 393-403. 4-2-2005.
- [83] S.N. Willis, J.I. Fletcher, T. Kaufmann, M.F. van Delft, L. Chen, P.E. Czabotar, H. Ierino, E.F. Lee, W.D. Fairlie, P. Bouillet, A. Strasser, R.M. Kluck, J.M. Adams, D.C.S. HUANG, Apoptosis Initiated When BH3 Ligands Engage Multiple Bcl-2 Homologs, Not Bax or Bak. *Science* 315 (2007) 856-859.
- [84] D. Ren, H.C. Tu, H. Kim, G.X. Wang, G.R. Bean, O. Takeuchi, J.R. Jeffers, G.P. Zambetti, J.J. Hsieh, E.H. Cheng, BID, BIM, and PUMA are essential for activation of the BAX- and BAK-dependent cell death program. *Science* 330 (2010) 1390-1393.
- [85] A. Villunger, V. Labi, P. Bouillet, J. Adams, A. Strasser, Can the analysis of BH3-only protein knockout mice clarify the issue of 'direct versus indirect' activation of Bax and Bak? *Cell Death.Differ.* 18 (2011) 1545-1546.
- [86] J.F. Lovell, L.P. Billen, S. Bindner, A. Shamas-Din, C. Fradin, B. Leber, D.W. Andrews, Membrane binding by tBid initiates an ordered series of events culminating in membrane permeabilization by Bax. *Cell* 135 (2008) 1074-1084.
- [87] B. Leber, J. Lin, D.W. Andrews, Embedded together: the life and death consequences of interaction of the Bcl-2 family with membranes. *Apoptosis.* 12 (2007) 897-911.

- [88] F. Gautier, Y. Guillemain, P.F. Cartron, T. Gallenne, N. Cauquil, D.T. Le, P. Casara, F.M. Vallette, S. Manon, J.A. Hickman, O. Geneste, P. Juin, Bax Activation by Engagement, Then Release From the BH3 Binding Site of Bcl-xL. *Mol.Cell Biol.*2010).
- [89] E.S. Alnemri, D.J. Livingston, D.W. Nicholson, G. Salvesen, N.A. Thornberry, W.W. Wong, J. Yuan, Human ICE/CED-3 protease nomenclature. *Cell* 87 (1996) 171.
- [90] P. Fuentes-Prior, G.S. Salvesen, The protein structures that shape caspase activity, specificity, activation and inhibition. *Biochem.J.* 384 (2004) 201-232.
- [91] J.Y. Yang, D. Michod, J. Walicki, C. Widmann, Surviving the kiss of death. *Biochemical Pharmacology* 68 (2004) 1027-1031.
- [92] L. Galluzzi, N. Joza, E. Tasdemir, M.C. Maiuri, M. Hengartner, J.M. Abrams, N. Tavernarakis, J. Penninger, F. Madeo, G. Kroemer, No death without life: vital functions of apoptotic effectors. *Cell Death.Differ.* 15 (2008) 1113-1123.
- [93] S. Launay, O. Hermine, M. Fontenay, G. Kroemer, E. Solary, C. Garrido, Vital functions for lethal caspases. *Oncogene* 24 (2005) 5137-5148.
- [94] M. Lamkanfi, N. Festjens, W. Declercq, T. Vanden Berghe, P. Vandenaebelle, Caspases in cell survival, proliferation and differentiation. *Cell Death.Differ.* 14 (2007) 44-55.
- [95] D.E. Bredesen, Programmed cell death mechanisms in neurological disease. *Curr.Mol.Med.* 8 (2008) 173-186.
- [96] C. Pop, G.S. Salvesen, Human caspases: activation, specificity, and regulation. *J.Biol.Chem.* 284 (2009) 21777-21781.
- [97] G.S. Salvesen, A. Ashkenazi, SnapShot: Caspases. *Cell* 147 (2011) 476.
- [98] S.J. Riedl, G.S. Salvesen, The apoptosome: signalling platform of cell death. *Nat.Rev.Mol.Cell Biol.* 8 (2007) 405-413.
- [99] E.M. Ribe, E. Serrano-Saiz, N. Akpan, C.M. Troy, Mechanisms of neuronal death in disease: defining the models and the players. *Biochem.J.* 415 (2008) 165-182.
- [100] J. Chai, Q. Wu, E. Shiozaki, S.M. Srinivasula, E.S. Alnemri, Y. Shi, Crystal structure of a procaspase-7 zymogen: mechanisms of activation and substrate binding. *Cell* 107 (2001) 399-407.
- [101] F. Martinon, K. Burns, J. Tschopp. The Inflammasome: A Molecular Platform Triggering Activation of Inflammatory Caspases and Processing of proIL-1 β . *Molecular Cell* 10[2], 417-426. 1-8-2002.
- [102] J.J. Harvey, An unidentified virus which causes the rapid production of tumours in mice. *Nature* 204 (1964) 1104-1105.

- [103] W.H. Kirsten, L.A. Mayer, Morphologic responses to a murine erythroblastosis virus. *J.Natl.Cancer Inst.* 39 (1967) 311-335.
- [104] J.F. Hancock, Ras proteins: different signals from different locations. *Nat.Rev.Mol.Cell Biol.* 4 (2003) 373-384.
- [105] M. Barbacid, ras genes. *Annu.Rev.Biochem.* 56 (1987) 779-827.
- [106] M. West, H.F. Kung, T. Kamata, A novel membrane factor stimulates guanine nucleotide exchange reaction of ras proteins. *FEBS Lett.* 259 (1990) 245-248.
- [107] M.S. Marshall, W.S. Hill, A.S. Ng, U.S. Vogel, M.D. Schaber, E.M. Scolnick, R.A. Dixon, I.S. Sigal, J.B. Gibbs, A C-terminal domain of GAP is sufficient to stimulate ras p21 GTPase activity. *EMBO J.* 8 (1989) 1105-1110.
- [108] M. Trahey, F. McCormick, A cytoplasmic protein stimulates normal N-ras p21 GTPase, but does not affect oncogenic mutants. *Science* 238 (1987) 542-545.
- [109] J.B. Gibbs, I.S. Sigal, M. Poe, E.M. Scolnick, Intrinsic GTPase activity distinguishes normal and oncogenic ras p21 molecules. *Proc.Natl.Acad.Sci.U.S.A* 81 (1984) 5704-5708.
- [110] B. Ross, O. Kristensen, D. Favre, J. Walicki, J.S. Kastrup, C. Widmann, M. Gajhede, High resolution crystal structures of the p120 RasGAP SH3 domain. *Biochemical and Biophysical Research Communications* 353 (2007) 463-468.
- [111] B. Tocque, I. Delumeau, F. Parker, F. Maurier, M.C. Multon, F. Schweighoffer, Ras-GTPase activating protein (GAP): a putative effector for Ras. *Cell Signal.* 9 (1997) 153-158.
- [112] P. Pamonsinlapatham, R. Hadj-Slimane, Y. Lepelletier, B. Allain, M. Toccafondi, C. Garbay, F. Raynaud, p120-Ras GTPase activating protein (RasGAP): a multi-interacting protein in downstream signaling. *Biochimie* 91 (2009) 320-328.
- [113] D. Kennedy, J. French, E. Guitard, K. Ru, B. Tocque, J. Mattick, Characterization of G3BPs: Tissue specific expression, chromosomal localisation and rasGAP120 binding studies. *Journal of Cellular Biochemistry* 84 (2009) 173-187.
- [114] P. Gideon, J. John, M. Frech, A. Lautwein, R. Clark, J.E. Scheffler, A. Wittinghofer, Mutational and kinetic analyses of the GTPase-activating protein (GAP)-p21 interaction: the C-terminal domain of GAP is not sufficient for full activity. *Mol.Cell Biol.* 12 (1992) 2050-2056.
- [115] C. Cales, J.F. Hancock, C.J. Marshall, A. Hall, The cytoplasmic protein GAP is implicated as the target for regulation by the ras gene product. *Nature* 332 (1988) 548-551.

- [116] H. Adari, D.R. Lowy, B.M. Willumsen, C.J. Der, F. McCormick, Guanosine triphosphatase activating protein (GAP) interacts with the p21 ras effector binding domain. *Science* 240 (1988) 518-521.
- [117] G.J. Clark, L.A. Quilliam, M.M. Hisaka, C.J. Der, Differential antagonism of Ras biological activity by catalytic and Src homology domains of Ras GTPase activation protein. *Proc.Natl.Acad.Sci.U.S.A* 90 (1993) 4887-4891.
- [118] G.A. Martin, A. Yatani, R. Clark, L. Conroy, P. Polakis, A.M. Brown, F. McCormick, GAP domains responsible for ras p21-dependent inhibition of muscarinic atrial K⁺ channel currents. *Science* 255 (1992) 192-194.
- [119] M. Henkemeyer, D.J. Rossi, D.P. Holmyard, M.C. Puri, G. Mbamalu, K. Harpal, T.S. Shih, T. Jacks, T. Pawson, Vascular system defects and neuronal apoptosis in mice lacking ras GTPase-activating protein. *Nature* 377 (1995) 695-701.
- [120] F. Parker, F. Maurier, I. Delumeau, M. Duchesne, D. Faucher, L. Debussche, A. Dugue, F. Schweighoffer, B. Tocque, A Ras-GTPase-activating protein SH3-domain-binding protein. *Mol.Cell.Biol.* 16 (1996) 2561-2569.
- [121] K. Irvine, R. Stirling, D. Hume, D. Kennedy, Rasputin, more promiscuous than ever: a review of G3BP. *The international journal of the developmental biology* 48 (2009) 1065-1077.
- [122] I.e. Gallouzi, F. Parker, K. Chebli, F. Maurier, E. Labourier, I. Barlat, J.P. Capony, B. Tocque, J. Tazi, A Novel Phosphorylation-Dependent RNase Activity of GAP-SH3 Binding Protein: a Potential Link between Signal Transduction and RNA Stability. *Mol.Cell.Biol.* 18 (1998) 3956-3965.
- [123] S.E. Salghetti, S.Y. Kim, W.P. Tansey, Destruction of myc by ubiquitin-mediated proteolysis: cancer-associated and transforming mutations stabilize myc. *The EMBO Journal* 18 (1999) 717-726.
- [124] L.P. Wen, K. Madani, G.A. Martin, G.D. Rosen, Proteolytic cleavage of ras GTPase-activating protein during apoptosis. *Cell Death.Differ.* 5 (1998) 729-734.
- [125] J.Y. Yang, C. Widmann, Antiapoptotic Signaling Generated by Caspase-Induced Cleavage of RasGAP. *Mol.Cell.Biol.* 21 (2001) 5346-5358.
- [126] J.Y. Yang, C. Widmann, The RasGAP N-terminal fragment generated by caspase cleavage protects cells in a Ras/PI3K/Akt-dependent manner that does not rely on NFkappa B activation. *J.Biol.Chem.* 277 (2002) 14641-14646.
- [127] J.Y. Yang, D. Michod, J. Walicki, B.M. Murphy, S. Kasibhatla, S.J. Martin, C. Widmann, Partial Cleavage of RasGAP by Caspases Is Required for Cell Survival in Mild Stress Conditions. *Mol.Cell.Biol.* 24 (2004) 10425-10436.

- [128] J.Y. Yang, J. Walicki, D. Michod, G. Dubuis, C. Widmann, Impaired Akt Activity Down-Modulation, Caspase-3 Activation, and Apoptosis in Cells Expressing a Caspase-resistant Mutant of RasGAP at Position 157. *Mol.Biol.Cell* 16 (2005) 3511-3520.
- [129] Early Breast Cancer Trialists' Collaborative Group (EBCTCG), Effects of chemotherapy and hormonal therapy for early breast cancer on recurrence and 15-year survival: an overview of the randomised trials. *Lancet* 365 (2005) 1687-1717.
- [130] G. Bonadonna, E. Brusamolino, P. Valagussa, A. Rossi, L. Brugnattelli, C. Brambilla, L.M. De, G. Tancini, E. Bajetta, R. Musumeci, U. Veronesi, Combination chemotherapy as an adjuvant treatment in operable breast cancer. *N.Engl.J.Med.* 294 (1976) 405-410.
- [131] A.M. Stessin, J.E. Meyer, D.L. Sherr, Neoadjuvant radiation is associated with improved survival in patients with resectable pancreatic cancer: an analysis of data from the surveillance, epidemiology, and end results (SEER) registry. *Int.J.Radiat.Oncol.Biol.Phys.* 72 (2008) 1128-1133.
- [132] B. Fisher, J. Bryant, N. Wolmark, E. Mamounas, A. Brown, E.R. Fisher, D.L. Wickerham, M. Begovic, A. DeCillis, A. Robidoux, R.G. Margolese, A.B. Cruz, Jr., J.L. Hoehn, A.W. Lees, N.V. Dimitrov, H.D. Bear, Effect of preoperative chemotherapy on the outcome of women with operable breast cancer. *J.Clin.Oncol.* 16 (1998) 2672-2685.
- [133] D. Mauri, N. Pavlidis, J.P. Ioannidis, Neoadjuvant versus adjuvant systemic treatment in breast cancer: a meta-analysis. *J.Natl.Cancer Inst.* 97 (2005) 188-194.
- [134] V.T. DeVita, Jr., E. Chu, A history of cancer chemotherapy. *Cancer Res.* 68 (2008) 8643-8653.
- [135] D. Michod, J.Y. Yang, J. Chen, C. Bonny, C. Widmann, A RasGAP-derived cell permeable peptide potently enhances genotoxin-induced cytotoxicity in tumor cells. *Oncogene* 23 (2004) 8971-8978.
- [136] D. Michod, C. Widmann, TAT-RasGAP317-326 requires p53 and PUMA to sensitize tumor cells to genotoxins. *Mol.Cancer Res.* 5 (2007) 497-507.

Glucose metabolism in cancer cells

Alessandro Annibaldi and Christian Widmann

Department of Physiology, Lausanne University, Lausanne, Switzerland

Correspondence to Christian Widmann, Department of Physiology, Rue du Bugnon 7, 1005 Lausanne, Switzerland
Tel: +41 21 692 5123; fax: +41 21 692 5505; e-mail: Christian.Widmann@unil.ch

Current Opinion in Clinical Nutrition and Metabolic Care 2010, 13:466–470

Purpose of review

Cancer cells alter their metabolism in order to support their rapid proliferation and expansion across the body. In particular, tumor cells, rather than fueling glucose in the oxidative phosphorylation pathway, generally use glucose for aerobic glycolysis. In this review, we discuss some of the mechanisms thought to be responsible for the acquisition of a glycolytic phenotype in cancer cells and how the switch towards glycolysis represents a selective growth advantage.

Recent findings

Glucose deprivation can activate oncogenes and these can upregulate proteins involved in aerobic glycolysis. In turn, proteins implicated in increased glycolysis can render tumor cells more resistant to apoptosis. Aerobic glycolysis induces acidification of the tumor environment, favoring the development of a more aggressive and invasive phenotype. Altering the pH around tumors might represent a way to hamper tumor development as suggested by a recent work demonstrating that bicarbonate, which increases the pH of tumors, prevented spontaneous metastatization.

Summary

The acquisition of a glycolytic phenotype by transformed cells confers a selective growth advantage to these cells. Interfering with aerobic glycolysis, therefore, represents a potentially effective strategy to selectively target cancer cells.

Keywords

apoptosis, cancer, glucose, glycolysis, oncogene

Curr Opin Clin Nutr Metab Care 13:466–470
© 2010 Wolters Kluwer Health | Lippincott Williams & Wilkins
1363-1950

Introduction

Carcinogenesis is a complex, multistep process that requires the elimination of several cell-imposed barriers such as antiproliferative responses, programmed cell death-inducing mechanisms, and senescence. This occurs mostly through mutations in oncogenes and tumor suppressor genes [1,2]. The tumor microenvironment plays a crucial role in the transition from precancerous lesions to carcinogenesis by exerting an adaptive pressure that selects cells for their clonal expansion [3–5]. Cellular energy metabolism is one of the main processes that is affected during the transition from normal to cancer cells. In particular, glucose metabolism is very often altered in tumor cells. Glycolysis is a catabolic process that converts one molecule of glucose to two pyruvates with the production of two ATP and two reduced nicotinamide adenine dinucleotide (NADH) molecules. Pyruvate in the presence of oxygen undergoes oxidation to CO₂ and H₂O in the oxidative phosphorylation pathway, resulting in the production of approximately 36 molecules of ATP. Alternatively, in the absence of oxygen, pyruvate is transformed into lactic acid in the anaerobic glycolysis pathway. However, conversion of glucose to lactic acid can occur in the presence of oxygen and this is known as the Warburg effect or aerobic glycolysis [6]. Most cancer

cells produce large amounts of lactate regardless of the availability of oxygen [7]. This increased aerobic glycolysis is considered by some to be the seventh hallmark of cancer [8] (the others, initially proposed by Hanahan and Weinberg [9], being limitless replicative potential, self-sufficiency in growth signals, resistance to apoptosis, insensitivity to antigrowth signals, sustained angiogenesis, and tissue invasion and metastasis).

In this review, we will discuss the different mechanisms responsible for the glycolysis switch in cancer and how they contribute to apoptosis resistance and survival of cancer cells. We will also present recent evidence indicating that interfering with glucose metabolism is a valuable anticancer approach.

Glucose utilization in tumors: the Warburg effect

Normal cell proliferation in tissues is controlled by the availability of growth regulating factors and by the interaction with surrounding cells. The availability of nutrients and oxygen, necessary for cell proliferation and metabolism, largely depends on blood supply. Initial tumor growth occurs in the absence of formation of new blood vessels. In this phase, tumor cells ignore

environmental growth-controlling constraints. They can do so by acquiring the ability to proliferate independently of growth signals, through, for example, mutations in receptor-associated signaling molecules, and by becoming insensitive to antigrowth stimuli, such as those mediated by cell-to-cell contacts [9,10].

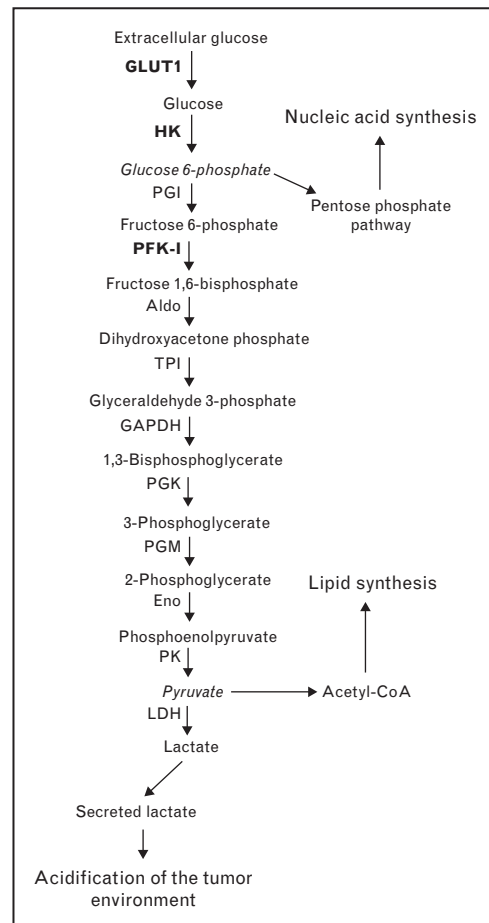
In the early carcinogenesis phase, uncontrolled cell proliferation moves tumor cells away from blood vessels and, therefore, from oxygen and nutrient supply. The only way oxygen and glucose can reach the inner cells of a non-vascularized tumor is by diffusion across the basement membrane and through the peripheral tumor-cell layers. However, partial oxygen pressure drops to very low values 100 μm away from blood vessels [11]. This implies that hypoxia and glucose shortage are rapidly generated in the inner mass of a growing tumor. Paradoxically, however, it is known since the 1920s [12] that tumor cells have a much higher rate of glucose consumption through a glycolysis pathway that does not send pyruvate to the Krebs cycle (i.e. the oxidative phosphorylation pathway) but that rather converts pyruvate to lactate: the so called Warburg effect [7] (Fig. 1). In fact, many tumors use this glucose to lactate pathway even in the presence of oxygen, explaining why the term aerobic glycolysis is often used as a substitute to the Warburg effect. It is important to note that the glycolytic switch occurring in cancer cells is not necessarily accompanied by a reduction in oxidative phosphorylation [13]. Nowadays, the augmented glycolytic activity of tumors is clinically exploited by positron emission tomography for the identification of metastatic lesions. This technique takes advantage of the increased ability of tumor cells to take up and metabolize glucose compared with normal tissues [5].

It would seem logical to assume that hypoxia is what drives tumor cells to fuel glucose in a nonoxidative 'glucose to lactate' pathway. However, it is currently believed that the glycolytic switch is acquired very early in carcinogenesis even before tumors experience hypoxia [7]. For example, lung cancers and leukemic cells, which are growing in the presence of oxygen, fuel glucose into the aerobic glycolysis pathway [14,15]. Consequently, the fact that, even in normoxic conditions, many tumors use aerobic glycolysis for their metabolic requirements indicates that the Warburg effect has functions that are not solely limited to hypoxia adaptation. We will come later to possible reasons why tumors turn on aerobic glycolysis but let us first discuss other responses induced by hypoxia in tumor cells.

Hypoxia adaptation and apoptosis resistance

A crucial molecule involved in the adaptation to hypoxia is the hypoxia-induced factor 1 (HIF-1). HIF-1 is a pleiotropic transcription factor that regulates genes

Figure 1 Glycolysis in cancer cells



The metabolic switch towards aerobic glycolysis commonly observed in cancer cells – the Warburg effect – is set after upregulation of some enzymes (indicated in bold) that play an important role in glucose metabolism. The increased glucose utilization through the glycolytic pathway generates metabolic intermediates (indicated in *italics*) that cancer cells need to sustain their rapid proliferation. One of these intermediates, glucose 6-phosphate is used for the synthesis of nucleic acid, through the pentose phosphate pathway, to allow rapid DNA replication. The abundant production of pyruvate stimulates lipid synthesis that is necessary for the formation of membranes in dividing tumor cells. Finally, secretion of lactate by the tumor cells induces acidification of the tumor microenvironment that creates a particular niche that favors further tumor progression, as well as inhibiting the action of some anticancer drugs. Aldo, aldolase; Eno, enolase; GAPDH, glyceraldehyde 3-phosphate dehydrogenase; GLUT1, glucose transporter 1; HK, hexokinase; LDH, lactate dehydrogenase; PFK-I, phosphofructokinase 1; PGI, phosphoglucose isomerase; PGK, phosphoglycerate kinase; PGM, phosphoglycerate mutase; PK, pyruvate kinase; TPI, triose phosphate isomerase.

involved in the hypoxia-induced metabolic switch, regulation of tumor pH, and angiogenesis [16]. The high glycolytic rate characteristic of hypoxic solid tumor is due in part to the greatly increased expression of hexokinase II (HK II) [17], a known transcriptional target of HIF-1. Hexokinase catalyses the first step in the glycolytic pathway where glucose is phosphorylated to

glucose-6-phosphate with conversion of one ATP to ADP (Fig. 1). There are four isoforms encoded by the mammalian genomes (I to IV) that are usually expressed at low levels in cells [18]. By increasing the expression level of HK II, hypoxia via HIF-1, can therefore modulate glucose metabolism.

HK II has additional features that are relevant in the context of cancer-cell apoptosis. HK II is normally associated with voltage-dependent anion channel (VDAC) [19], a 30 kDa pore protein inserted in the outer mitochondrial membrane that regulates the transport of metabolites in and out of the mitochondrial inter-membrane space [20]. Mitochondria are key components of the apoptotic cell-death process. Upon exposure to cell-death stimuli, mitochondria release cytochrome-*c* and other apoptogenic factors such as SMAC/DIABLO into the cytoplasm where they trigger caspase activation and apoptosis [21]. The release of cytochrome-*c* is orchestrated by members of the Bcl-2 family of proteins [22,23]. Among these proteins, only Bax and Bak are mandatory for the release of cytochrome-*c* [24] although the exact mechanism by which this happens is still debated. One model proposes that Bax, once activated by death stimuli, cooperates with VDAC to form a large cytochrome-*c* conducting channel through the mitochondrial membrane [25,26].

It can be envisioned that a protein interacting with VDAC, like HK II, has the potential to prevent the interaction of proapoptotic proteins with mitochondria and consequently interfere with apoptosis. Therefore in hypoxic tumors, the initial overexpression of HK II as a primary adaptation to hypoxia, may secondarily confer resistance to apoptosis. Supporting this notion is the observation that disruption of the binding of HK II to mitochondria, through activation of GSK3 β and phosphorylation of VDAC, potentiates chemotherapy-induced cytotoxicity in transformed cells [27]. Moreover, methyl jasmonate, an anticancer agent that interacts directly with mitochondria, is able to induce apoptosis selectively in cancer cells apparently by detaching hexokinases from mitochondria [28]. Recently, it has also been shown that the release of HK II from mitochondria potentiates cisplatin-induced cytotoxicity [29]. This was shown using a peptide that competed with HK II for VDAC binding and that enhanced cisplatin-induced apoptosis through Bak oligomerization and mitochondrial integrity loss.

The current evidence indicates, therefore, that hypoxia response in cancer cells, in addition to modulating the way they metabolize glucose, renders them more resistant to death stimuli. Hypoxic tumors are often more invasive and metastatic [30,31]. Whether this is linked to a higher resistance to apoptosis or to the altered glucose metabolism is currently not known.

Oncogenic stress and alteration of glucose metabolism

Hypoxia is not the only driving force that leads to abnormal glycolytic flux in cancer cells. It has been discovered in the last few years that oncogenes found in a wide variety of human cancers can directly activate HIF-1 and other components of glucose metabolism independently of hypoxia. One of such oncogenes is Akt. This serine/threonine kinase is involved in the modulation of several cellular processes such as proliferation, autophagy and cell metabolism [32,33]. Akt regulates factors involved in glucose metabolism, including HK II, whose association with mitochondria and its effect on apoptosis resistance was discussed in the previous section, phosphofruktokinase-1 (PFK-1) [34], one of the rate-controlling enzymes of glycolysis, and GLUT1, the most widely expressed glucose transporter [35]. Recently, Akt was coined the 'Warburg kinase' able to promote the metabolic changes that tumor cells experience en route to a more malignant state [36]. The fact that Akt promotes a glycolytic switch under normoxia conditions, without affecting the rate of oxidative phosphorylation, confirms that this occurs not only as an adaptation to low-oxygen flux but also when tumoral cells increase the production of metabolic intermediates required for rapid proliferation, such as pentose phosphates necessary for nucleic acid synthesis (Fig. 1).

These Akt-mediated metabolic changes render cancer cells dependent on aerobic glycolysis for their growth and survival. This can be seen for example in tumor cells bearing an activated form of Akt. These cells undergo rapid cell death when shifted to low-glucose conditions [37]. On the contrary, if tumor cells are given the chance to activate another metabolic pathway to sustain their high-energy demand, the addiction to aerobic glycolysis is overcome. This is indeed seen when cells are switched towards fatty acid metabolism by stimulating them with the AMPK activator 5-aminoimidazole-4-carboxamide ribonucleoside (AICAR) [38].

Another oncogene, K-Ras can alter glucose metabolism so as to provide tumor cells with a selective advantage. It has indeed recently been shown that expression of the GLUT1 glucose transporter is increased in cells with mutated K-Ras. Upregulation of this glucose receptor was associated with an increased glucose uptake, increased glycolysis and augmented lactate production, whereas mitochondrial functions and oxidative phosphorylation were not affected. When grown in low-glucose containing media, K-Ras mutated cells showed increased survival. Therefore, it was argued that agents able to inhibit glucose metabolism could selectively kill K-Ras mutant cells. Indeed the hexokinase inhibitor 3-bromopyruvate (3-BrPA) was found to be highly toxic to different cancer

cell lines bearing K-Ras mutation, but was much less toxic to cell lines lacking K-Ras mutation [39^{••}]. Interestingly, the K-Ras mutations that lead to low-glucose adaptations can be induced by glucose deprivation [39^{••}]. This suggests that a stress caused by nutrient shortage might be a favorable ground for the activation of oncogenes.

Aerobic glycolysis as a generator of a tumor friendly niche

There is evidence that an increased glycolysis rate contributes to the acquisition of resistance to chemical drugs by cancer cells, mainly through acidification of the tumor microenvironment. The large amounts of lactate secreted by tumor cells, as a direct consequence of the abnormal production of pyruvate, leads to acidification of the tumor surroundings [40]. Several anticancer drugs such as doxorubicin, mitoxantrone and vincristine are weak bases that are protonated in slightly acid tumor microenvironments. When protonated, these drugs cannot easily diffuse across the plasma membrane and consequently their cellular uptake is diminished. In this context it has recently been shown that addition of sodium bicarbonate in the drinking water raises the pH of the extracellular milieu in mice, which translated into a greater efficacy of doxorubicin to hamper the growth of xenotransplanted tumors [41]. The reverse situation was shown in another study where glucose administration to mice led to a decrease in the extracellular pH and a lower efficacy of doxorubicin on tumors [42]. In contrast to weak bases such as doxorubicin, weak acid anticancer drugs like chlorambucil are more efficacious when the pH of the extracellular milieu decreases [42]. These studies have important clinical implications because they suggest that appropriate modulation of the extracellular pH in patients with cancer based on the chemical properties of the used antitumor drugs could optimize the chemotherapy efficacy.

Additionally, pH lowering can influence more directly tumor progression and expansion. The extracellular conditions found within precancerous lesions (i.e. hypoxia, low-nutrient availability) typically results in necrosis or apoptosis of tumor cells through p53-dependent mechanisms and caspase-3-dependent mechanisms [43]. This initial beneficial response may, however, later favor the selection of cells that, in addition to upregulating glycolysis, acquire mutations allowing them to become immune to apoptotic-inducing pathways and potentially other antimalignant and anti-invasive checkpoints [5,9]. These cells are considered by some to be cancer stem-like cells [44]. The identification of these cancer stem-like cells and the mechanisms governing their anaerobic metabolic pathways may potentially open new perspectives in cancer treatment.

One peculiar feature of cancers is the ability to metastasize. Spontaneous metastasis consists in two main phases intravasation where transformed cells leave the primary tumor to the bloodstream and extravasation where tumor cells colonize new tissues. In-vitro studies have shown that tumor cell invasion can be stimulated by acidic conditions [45,46]. Moreover, acid pretreatment of tumor cells increases their ability to metastasize after injection in mice [47]. This effect could be attributed to an augmented release of cathepsin B that is involved in extracellular matrix remodeling. Recently, it has been shown that bicarbonate therapy significantly reduces the number and the size of metastases in a breast cancer mouse model by increasing tumor pH [48[•]]. Bicarbonate, by modulating the pH of the tumor environment, negatively affects the process of tumor cells extravasation without significantly influencing intravasation and circulation of tumor cells across the bloodstream [48[•]]. This finding is of high relevance if we consider that primary tumors rarely kill affected patients, but that it is rather formation of metastasis from primary tumors that is lethal. Therefore, strategies that aim at limiting spreading of primary tumors across the body could be highly beneficial for cancer patients.

Conclusion

Alteration of glucose metabolism can be the result of an adaptive response to the lack of oxygen or following activation of oncogenes. Aerobic glycolysis appears to represent a selective advantage for tumor cells as they become more resistant to apoptosis and acquire increased growth and invasive properties. At present it is still unclear if the molecular mechanisms controlling the switch towards aerobic glycolysis are directly involved in the acquisition of apoptosis resistance or whether this resistance is a secondary adaptation to hypoxia of a subpopulation of transformed cells in precancerous lesions. Regardless of the mechanisms, glycolysis upregulation represents a clear advantage for cancers cells and at the same time a target for new anticancer therapies.

Acknowledgements

We thank Dr Cécile Billotte for critical reading of the manuscript. C.W. is supported by grants from the Swiss National Science Foundation.

References and recommended reading

Papers of particular interest, published within the annual period of review, have been highlighted as:

- of special interest
- of outstanding interest

Additional references related to this topic can also be found in the Current World Literature section in this issue (pp. 504–505).

- 1 Bartkova J, Rezaei N, Liontos M, *et al.* Oncogene-induced senescence is part of the tumorigenesis barrier imposed by DNA damage checkpoints. *Nature* 2006; 444:633–637.
- 2 Luo J, Solimini NL, Elledge SJ. Principles of cancer therapy: oncogene and nononcogene addiction. *Cell* 2009; 136:823–837.

- 3 Gatenby RA, Smallbone K, Maini PK, *et al.* Cellular adaptations to hypoxia and acidosis during somatic evolution of breast cancer. *Br J Cancer* 2007; 97:646–653.
- 4 Liotta LA, Kohn EC. The microenvironment of the tumour-host interface. *Nature* 2001; 411:375–379.
- 5 Gatenby RA, Gillies RJ. Why do cancers have high aerobic glycolysis? *Nat Rev Cancer* 2004; 4:891–899.
- 6 Warburg O. On the origin of cancer cells. *Science* 1956; 123:309–314.
- 7 Vander Heiden MG, Cantley LC, Thompson CB. Understanding the Warburg effect: the metabolic requirements of cell proliferation. *Science* 2009; 324:1029–1033.
- 8 Yeung SJ, Pan J, Lee MH. Roles of p53, MYC and HIF-1 in regulating glycolysis: the seventh hallmark of cancer. *Cell Mol Life Sci* 2008; 65:3981–3999.
- 9 Hanahan D, Weinberg RA. The hallmarks of cancer. *Cell* 2000; 100:57–70.
- 10 Shaw RJ, Cantley LC. Ras, PI(3)K and mTOR signalling controls tumour cell growth. *Nature* 2006; 441:424–430.
- 11 Helmlinger G, Yuan F, Dellian M, *et al.* Interstitial pH and pO₂ gradients in solid tumors in vivo: high-resolution measurements reveal a lack of correlation. *Nat Med* 1997; 3:177–182.
- 12 Warburg O, Wind F, Negelein E. The metabolism of tumors in the body. *J Gen Physiol* 1927; 8:519–530.
- 13 Moreno-Sanchez R, Rodriguez-Enriquez S, Marin-Hernandez A, *et al.* Energy metabolism in tumor cells. *FEBS J* 2007; 274:1393–1418.
- 14 Nolop KB, Rhodes CG, Brudin LH, *et al.* Glucose utilization in vivo by human pulmonary neoplasms. *Cancer* 1987; 60:2682–2689.
- 15 Gottschalk S, Anderson N, Hainz C, *et al.* Imatinib (STI571)-mediated changes in glucose metabolism in human leukemia BCR-ABL-positive cells. *Clin Cancer Res* 2004; 10:6661–6668.
- 16 Pouyssegur J, Dayan F, Mazure NM. Hypoxia signalling in cancer and approaches to enforce tumour regression. *Nature* 2006; 441:437–443.
- 17 Rempel A, Mathupala SP, Griffin CA, *et al.* Glucose catabolism in cancer cells: amplification of the gene encoding type II hexokinase. *Cancer Res* 1996; 56:2468–2471.
- 18 Wilson JE. Isozymes of mammalian hexokinase: structure, subcellular localization and metabolic function. *J Exp Biol* 2003; 206:2049–2057.
- 19 Mathupala SP, Ko YH, Pedersen PL. Hexokinase II: cancer's double-edged sword acting as both facilitator and gatekeeper of malignancy when bound to mitochondria. *Oncogene* 2006; 25:4777–4786.
- 20 Colombini M. VDAC: the channel at the interface between mitochondria and the cytosol. *Mol Cell Biochem* 2004; 256–257:107–115.
- 21 Taylor RC, Cullen SP, Martin SJ. Apoptosis: controlled demolition at the cellular level. *Nat Rev Mol Cell Biol* 2008; 9:231–241.
- 22 Youle RJ, Strasser A. The BCL-2 protein family: opposing activities that mediate cell death. *Nat Rev Mol Cell Biol* 2008; 9:47–59.
- 23 Giam M, Huang DC, Bouillet P. BH3-only proteins and their roles in programmed cell death. *Oncogene* 2008; 27 (Suppl 1):S128–S136.
- 24 Wei MC, Zong WX, Cheng EH, *et al.* Proapoptotic BAX and BAK: a requisite gateway to mitochondrial dysfunction and death. *Science* 2001; 292:727–730.
- 25 Shimizu S, Narita M, Tsujimoto Y. Bcl-2 family proteins regulate the release of apoptogenic cytochrome c by the mitochondrial channel VDAC. *Nature* 1999; 399:483–487.
- 26 Shimizu S, Matsuoka Y, Shinohara Y, *et al.* Essential role of voltage-dependent anion channel in various forms of apoptosis in mammalian cells. *J Cell Biol* 2001; 152:237–250.
- 27 Pastorino JG, Hoek JB, Shulga N. Activation of glycogen synthase kinase 3 β disrupts the binding of hexokinase II to mitochondria by phosphorylating voltage-dependent anion channel and potentiates chemotherapy-induced cytotoxicity. *Cancer Res* 2005; 65:10545–10554.
- 28 Goldin N, Arzoino L, Heyfets A, *et al.* Methyl jasmonate binds to and detaches mitochondria-bound hexokinase. *Oncogene* 2008; 27:4636–4643.
- 29 Shulga N, Wilson-Smith R, Pastorino JG. Hexokinase II detachment from the mitochondria potentiates cisplatin induced cytotoxicity through a caspase-2 dependent mechanism. *Cell Cycle* 2009; 8:3355–3364.
- This article provides evidence that, HK II, a key enzyme upregulated in cancer cells to allow the installation of aerobic glycolysis, also inhibits the intrinsic apoptotic pathway.
- 30 Young SD, Marshall RS, Hill RP. Hypoxia induces DNA overreplication and enhances metastatic potential of murine tumor cells. *Proc Natl Acad Sci U S A* 1988; 85:9533–9537.
- 31 Cairns RA, Kalliomaki T, Hill RP. Acute (cyclic) hypoxia enhances spontaneous metastasis of KHT murine tumors. *Cancer Res* 2001; 61:8903–8908.
- 32 Manning BD, Cantley LC. AKT/PKB signaling: navigating downstream. *Cell* 2007; 129:1261–1274.
- 33 Jin S, DiPaola RS, Mathew R, *et al.* Metabolic catastrophe as a means to cancer cell death. *J Cell Sci* 2007; 120:379–383.
- 34 Deprez J, Vertommen D, Alessi DR, *et al.* Phosphorylation and activation of heart 6-phosphofructo-2-kinase by protein kinase B and other protein kinases of the insulin signaling cascades. *J Biol Chem* 1997; 272:17269–17275.
- 35 Barthel A, Okino ST, Liao J, *et al.* Regulation of GLUT1 gene transcription by the serine/threonine kinase Akt1. *J Biol Chem* 1999; 274:20281–20286.
- 36 Robey RB, Hay N. Is Akt the 'Warburg kinase'?-Akt-energy metabolism interactions and oncogenesis. *Semin Cancer Biol* 2009; 19:25–31.
- This review discusses the signaling events that participate in the installation of the Warburg effect in cancer cells and describes the evidence supporting a crucial role of the Akt kinases in this response.
- 37 Elstrom RL, Bauer DE, Buzzai M, *et al.* Akt stimulates aerobic glycolysis in cancer cells. *Cancer Res* 2004; 64:3892–3899.
- 38 Buzzai M, Bauer DE, Jones RG, *et al.* The glucose dependence of Akt-transformed cells can be reversed by pharmacologic activation of fatty acid β -oxidation. *Oncogene* 2005; 24:4165–4173.
- 39 Yun J, Rago C, Cheong I, *et al.* Glucose deprivation contributes to the development of KRAS pathway mutations in tumor cells. *Science* 2009; 325:1555–1559.
- This work is an important contribution for our understanding on the interplay between oncogenesis and nutrient deprivation in tumor cells.
- 40 Gerweck LE, Seetharaman K. Cellular pH gradient in tumor versus normal tissue: potential exploitation for the treatment of cancer. *Cancer Res* 1996; 56:1194–1198.
- 41 Raghunand N, He X, van SR, *et al.* Enhancement of chemotherapy by manipulation of tumour pH. *Br J Cancer* 1999; 80:1005–1011.
- 42 Gerweck LE, Vijayappa S, Kozin S. Tumor pH controls the in vivo efficacy of weak acid and base chemotherapeutics. *Mol Cancer Ther* 2006; 5:1275–1279.
- 43 Williams AC, Collard TJ, Paraskeva C. An acidic environment leads to p53 dependent induction of apoptosis in human adenoma and carcinoma cell lines: implications for clonal selection during colorectal carcinogenesis. *Oncogene* 1999; 18:3199–3204.
- 44 Bjerkvig R, Johansson M, Miletic H, *et al.* Cancer stem cells and angiogenesis. *Semin Cancer Biol* 2009; 19:279–284.
- 45 Glunde K, Guggino SE, Solaiyappan M, *et al.* Extracellular acidification alters lysosomal trafficking in human breast cancer cells. *Neoplasia* 2003; 5:533–545.
- 46 Rozhin J, Sameni M, Ziegler G, *et al.* Pericellular pH affects distribution and secretion of cathepsin B in malignant cells. *Cancer Res* 1994; 54:6517–6525.
- 47 Rofstad EK, Mathiesen B, Kindem K, *et al.* Acidic extracellular pH promotes experimental metastasis of human melanoma cells in athymic nude mice. *Cancer Res* 2006; 66:6699–6707.
- 48 Robey IF, Baggett BK, Kirkpatrick ND, *et al.* Bicarbonate increases tumor pH and inhibits spontaneous metastases. *Cancer Res* 2009; 69:2260–2268.
- This article has clear clinical relevance as it shows that raising the pH of breast tumors with bicarbonate efficiently blocks metastatization.

Objectives

OBJECTIVES

Our laboratory developed a tumor-specific sensitizer, TAT-RasGAP₃₁₇₋₃₂₆, able to potentiate the genotoxin-induced apoptosis in several cancer cell lines, but not in non tumoral cell lines. The active sequence of this peptide (amino acids 317-326 of RasGAP) was derived from the caspase-3-generated fragment N2 of RasGAP, previously shown to selectively sensitize malignant cells to genotoxin, and was fused to a cell permeable sequence (amino acids 48-57 of HIV TAT protein).

During my thesis I undertook the following research projects:

- I. Fragment N2, generated by the caspase-3 mediated proteolytic cleavage of RasGAP, specifically sensitizes tumor cells to genotoxin-induced apoptosis. This fragment exhibits a cytoplasmic localization in the cell and we wanted to ascertain whether changes in the sub-cellular location would impair fragment N2 ability to enhance genotoxin-induced apoptotic cell death.
- II. TAT-RasGAP₃₁₇₋₃₂₆ is an efficient tumor sensitizer *in vitro*. We tested the sensitizing properties of TAT-RasGAP₃₁₇₋₃₂₆ in *in vivo* settings using a tumor xenograft mouse model.
- III. G3BP1 (GAP SH3 Binding Protein 1) is a cytoplasmic protein described as binding to the SH3 of RasGAP on its sequence 317-326, which corresponds to the active sequence of our RasGAP-derived peptide. This observation, together with reports indicating G3BP1 as a protein involved in mRNA stability and adaptation to stress, made G3BP1 a potential effector of the TAT-RasGAP₃₁₇₋₃₂₆-mediated sensitization. We therefore checked if TAT-

RasGAP₃₁₇₋₃₂₆ modulated any of the G3BP1 functions or its cellular location and if the peptide needs G3BP1 to work.

- IV. The molecular mechanisms underlying the TAT-RasGAP₃₁₇₋₃₂₆-induced enhancement of apoptosis triggered by genotoxins is still poorly understood. Earlier reports showed that TAT-RasGAP₃₁₇₋₃₂₆ need a functional p53/Puma axis to exert its sensitizing properties, but this could be solely explained by the fact that in the absence of either p53 or Puma, cells cannot properly undergo apoptosis induced by genotoxins. Genotoxins kill tumor cells by triggering the intrinsic apoptotic pathway, a cell death pathway tightly controlled by the Bcl-2 family members. Hence we studied the importance of several members of this family, as well as the implication of p53, in the sensitization mechanism.
- V. Radiotherapy is one of the most commonly used anti-cancer treatments. We evaluated the ability of TAT-RasGAP₃₁₇₋₃₂₆ to sensitize several cancer cell lines and tumor xenografts, both p53 positive and negative, to γ -radiations.

Results

Part I

Introduction

RasGAP is a GAP (GTPase-activating protein) specific for Ras. The GAP activity resides within its C-terminus whereas the N-terminus is implicated in distinct signalling pathways.

Our group has previously shown that RasGAP is also a caspase 3 substrate. In presence of mild stress conditions, RasGAP is cleaved by caspase 3 at position 455 to generate a C-terminus fragment, named fragment C, and an N terminus fragment, called fragment N. Fragment N was reported to generate an anti-apoptotic response that depends on the activation of Ras/PI3K/Akt pathway. When stress conditions increase fragment N is further cleaved by caspase 3 at position 157 and this cleavage abrogates its anti-apoptotic function. The resulting fragments, called fragment N1 and fragment N2, do not play any role in the apoptotic response of normal cells. By contrast when over-expressed in cancer cells, fragment N2 sensitizes them to genotoxin-induced death.

We decided to look at fragment N2 localization in cancer cells to see if the sensitization event requires a specific sub-cellular location of this fragment.

Our data show that fragment N2 has an almost exclusive cytoplasmic localization, that is required for its sensitizing properties. Indeed, when we localize fragment N2 to other cellular compartments (i.e. mitochondria or endoplasmic reticulum), it loses its ability to favour the genotoxin-induced apoptosis of cancer cells. Taken together our results show that fragment N2-mediated sensitization of cancer cells to genotoxins strictly depends on its sub-cellular location.

Contribution

This work has been published in *Experimental Cell Research* in 2009 it is attached in the following section. I share the first authorship with Dr. David Michod. I performed part of the experiments done for the realization of the manuscript plus all the experiments of the revision.

available at www.sciencedirect.comwww.elsevier.com/locate/yexcr

Research Article

Role of the sub-cellular localization of RasGAP fragment N2 for its ability to sensitize cancer cells to genotoxin-induced apoptosis

Alessandro Annibaldi^{a,b,1}, David Michod^{a,b,1}, Linda Vanetta^{a,b}, Steeve Cruchet^{a,b}, Pascal Nicod^c, Gilles Dubuis^{a,b}, Christelle Bonvin^{a,b}, Christian Widmann^{a,b,*}

^aDepartment of Physiology, Lausanne University, Lausanne, Switzerland

^bDepartment of Cell Biology and Morphology, Lausanne University, Lausanne, Switzerland

^cUniversity Hospital Center, Lausanne, Switzerland

ARTICLE INFORMATION

Article Chronology:

Received 23 December 2008

Revised version received

12 March 2009

Accepted 14 March 2009

Available online 27 March 2009

Keywords:

RasGAP

Sensitization

Cancer

Apoptosis

Genotoxin

Fixation artefact

Immunocytochemistry

Sub-cellular localization

ABSTRACT

The specific sensitization of tumor cells to the apoptotic response induced by genotoxins is a promising way of increasing the efficacy of chemotherapies. The RasGAP-derived fragment N2, while not regulating apoptosis in normal cells, potentially sensitizes tumor cells to cisplatin- and other genotoxin-induced cell death. Here we show that fragment N2 in living cells is mainly located in the cytoplasm and only minimally associated with specific organelles. The cytoplasmic localization of fragment N2 was required for its cisplatin-sensitization property because targeting it to the mitochondria or the ER abrogated its ability to increase the death of tumor cells in response to cisplatin. These results indicate that fragment N2 requires a spatially constrained cellular location to exert its anti-cancer activity.

© 2009 Elsevier Inc. All rights reserved.

Introduction

One hallmark of cancer cells is their ability to evade apoptosis. Understanding the regulation of the apoptotic process can therefore lead to the development of new strategies to restore a normal apoptotic response in tumors to facilitate their elimination during anti-cancer therapies.

One of the mechanisms allowing cells to determine whether they should survive or commit suicide involves the sequential cleavage of RasGAP. This protein is a regulator of Ras- and Rho-

signaling [1,2]. It bears two caspase cleavage sites at position 455 and 157 [3]. In stressed cells having mildly activated caspase-3, RasGAP is only cleaved at position 455. This generates an N-terminal fragment called fragment N that induces a potent anti-apoptotic signal that depends on the activation of Ras, PI3K, and Akt [4] and that is crucially required for the survival of stressed cells [5]. In response to apoptotic stimuli, fragment N is further cleaved by caspase-3 and this abrogates its anti-apoptotic properties [6]. The resulting fragments (N1 and N2) do not appear to modulate apoptosis in normal cells [6]. In contrast, tumor cells are strongly

* Corresponding author. Department of Physiology, Rue du Bugnon 7/9, 1005 Lausanne, Switzerland. Fax: +41 21 692 5255.

E-mail address: Christian.Widmann@unil.ch (C. Widmann).

¹ These authors contributed equally to this work.

sensitized to genotoxin-induced death if they express fragment N2 [3,6,7]. The tumor sensitizing ability of fragment N2 lies within a 10 amino acid stretch located at position 317–326 [7]. A cell permeable synthetic peptide containing the 317–326 RasGAP sequence peptide, called TAT-RasGAP_{317–326}, is as potent as fragment N2 to sensitize cancer cells to genotoxins [7]. The molecular mechanism by which fragment N2 and TAT-RasGAP_{317–326} sensitize tumor cells is however not well understood although it has been recently demonstrated that a functional connection between p53 and PUMA is required [8].

Here we show that fragment N2 is almost exclusively located in the cytoplasm and that this location is required for its tumor sensitization properties.

Materials and methods

Cells and transfection

U2OS (LGC Promochem; ATCC no. HTB-96), HCT116 p53^{+/+}, and HCT116 p53^{-/-} cells [9] were maintained in DMEM containing 10% fetal calf serum (GIBCO/BRL) at 37 °C and 5% CO₂. They were transfected using the calcium/phosphate precipitation procedure [7] using 1 µg of the RasGAP-encoding plasmids and 0.5 µg of pEGFP-C1. HeLa cells were maintained in RPMI 1640 containing 10% newborn calf serum (NBCS) (catalog no. 26010-074; Invitrogen) at 37 °C and 5% CO₂. They were transfected using lipofectamine (GIBCO/BRL) [3]. The cells were submitted to the indicated experimental conditions 24 h following their transfection (unless indicated otherwise). Mouse embryonic fibroblasts (MEFs) were maintained in DMEM containing 10% NBCS at 37 °C and 5% CO₂.

Cell fractionation into nuclear and cytoplasmic fractions

U2OS cells were seeded at a density of 2×10^6 cells in 10 cm-plates and transfected the next day with the indicated constructs. Following an additional day in culture, the cells were solubilized in 400 µl lysis buffer (0.5% Triton X-100, 500 mM Tris-HCl pH 7.5, 137 mM NaCl, 10% glycerol, supplemented with one tablet of EDTA-free protease inhibitor [Roche] per 50 ml) and centrifuged at 16,000 g for 15 min at 4 °C. The supernatant, representing the cytoplasmic fraction, was collected and quantitated for protein content by Bradford assay. The pellet, containing nuclei, was rinsed once with 400 µl lysis buffer and then resuspended in 200 µl lysis buffer supplemented with 0.5% SDS. The nuclear lysate was sonicated and centrifuged at 16,000 g for 10 min at 4 °C. Protein content was then assessed by Bradford assay.

Sub-cellular fractionation into cytoplasmic, mitochondrial/ER, and nuclear fractions

U2OS cells were seeded and cultured as above. They were then washed with PBS and resuspended in 400 µl of hypotonic lysis buffer (10 mM Hepes pH 7.4, 10 mM MgCl₂, 42 mM KCl, supplemented with one tablet of EDTA-free protease inhibitor [Roche] per 50 ml) for 5 min on ice. Cells were scraped and then lysed using a Dounce homogenizer and centrifuged at 300 g for 5 min at 4 °C to collect crude nuclei that were further purified as described below. The supernatant was further centrifuged at 10,000 g for 10 min at 4 °C to collect mitochondria and ER. The

supernatant represents the soluble cytoplasmic fraction. Mitochondria/ER were resuspended in hypotonic lysis buffer supplemented with 1% Triton X-100, sonicated and centrifuged at 16,000 g for 10 min. The supernatant represents the mitochondria/ER protein fraction.

Nuclei were resuspended in hypotonic lysis buffer supplemented with 1% Triton X-100, sonicated and centrifuged 10 min at 16,000 g. Supernatant was discarded and nuclei were resuspended in lysis buffer (0.5% Triton X-100, 0.5% SDS, 500 mM Tris-HCl pH 7.5, 137 mM NaCl, 10% glycerol, supplemented with one tablet of EDTA-free protease inhibitor [Roche] per 50 ml), passed through a 26 gauge-needle several times to break the DNA, sonicated, and centrifuged 10 min at 16,000 g. The supernatant was used as the nuclear fraction.

Antibodies

The polyclonal rabbit anti-RasGAP antibody directed at the Src homology (SH) domains of RasGAP has been described before [10]. The polyclonal rabbit anti-RasGAP antibody directed at fragment N2 is from Alexis (catalog no. ALX-210-860). The monoclonal antibody specific for the hemagglutinin (HA) tag was purchased as ascites from BabCo (catalog no. MMS-101R). This antibody was adsorbed on HeLa cell lysates to decrease non-specific binding as described previously [3]. Secondary antibodies were donkey anti-mouse indocarbocyanine (Cy3)-conjugated antibody and donkey anti-rabbit Cy3-conjugated antibody (Jackson ImmunoResearch, catalog no. 715-165-151 and 711-165-152, respectively). The histone H3 antibody is from MBL (catalog no. JM 3623). The tubulin antibody is from Serotec (catalog no. MCA77G). The calreticulin antibody is from Cell Signaling (catalog no. 2891). The mouse monoclonal antibody specific for the cytochrome c oxidase subunit 5A is from Mitosciences (catalog no. MS409).

Plasmids

pEGFP-C1 and *pEGFP-C3* encode the green fluorescent protein and are from Clontech. The extension .dn3 indicates that the backbone plasmid is pcDNA3 (Invitrogen). *HA-GAP.dn3* encodes the full-length human RasGAP protein bearing an HA tag (MGYPYDVP-DYAS) at the amino terminal end [3]. *HA-GAP-N.dn3*, *HA-N1.dn3*, and *HA-N2.dn3* encode the HA-tagged (at the N-terminus) versions of fragments N, N1, and N2, respectively [3]. *GFP-GAPC* is a fusion protein between GFP and RasGAP fragment C, bearing an HA tag at the carboxy-terminal end (fragment C cannot be expressed in cells unless fused to GFP [3]).

GFP-HA-GAP encodes a fusion protein between GFP and the HA-tagged form of full-length RasGAP. It was constructed by subcloning the 3911 bp BamHI/EcoRI fragment from *HA-GAP.dn3* into *pEGFP-C1* opened with BglII and EcoRI. *GFP-HA-N* encodes a fusion protein between GFP and the HA-tagged form of fragment N. It was constructed by subcloning the 1429 bp XhoI fragment from *HA-GAPN'.dn3* into *pEGFP-C3* opened with the same enzyme. *HA-GAPN'.dn3* is almost identical to *HA-GAP-N* but for the BamHI site replaced with a XhoI site. It was constructed by annealing oligonucleotides #187 (GATCTCTCGAGAAA) and #188 (GATCTTCTCGAGA) and subcloning them into *HA-GAP-N* opened with BamHI. *GFP-HA-N2* encodes a fusion protein between GFP and the HA-tagged form of fragment N2. It was constructed by subcloning the 967 bp ApaI fragment from *HA-N2.dn3* into *pEGFP-C1* opened with the same enzyme. Plasmid *HA-N2-RKQERFNR-Bcl-X_L TMB.dn3* encodes the

HA-tagged fragment N2 fused to the mitochondrial targeting sequence of Bcl-X_L. It was constructed as follows: *GFP-C3* (corresponding to plasmid EGFP-X-TMB[Bcl-x] in [11]) was PCR-amplified with the N2-Bcl-X_L-sense oligo [AATAT GCGGCCGC (NotI) AGCCGAGAGCCGAAAGGGCCAGGAAC (nucleotides 777–802 of the human Bcl-X_L mRNA; NM_001191)] and with the C3 anti-sense oligo [GTTTCAGGTTTCAGGGGAGGTG; sequence 1583–1562 of GFP-C3]. The 155 bp PCR fragment was cut with NotI and XbaI and subcloned in plasmid *HA-N2-no stop.dn3* opened with the same enzymes. The latter plasmid is similar to plasmid *HA-N2.dn3* but does not bear a stop codon at the end of the coding sequence of fragment N2. It was generated as follows: *HA-N2.dn3* was PCR-amplified using the sense oligo 644 [GCGTGGATAGCGGTTTGACTC (nucleotides 644–664 of pcDNA3)] and the anti-sense oligo ND157x [AAAAAAAA (trailer) GCGGCCGC (NotI) GTC GAC TGT GTC ATT GAG TAC (human RasGAP D455–V449; the 6 nucleotides preceding the NotI site creating a new Sall site)]. The 1206 bp fragment was cut with Bsu36 and NotI. The resulting 784 bp fragment was subcloned in *HA-N2.dn3* opened with the same enzymes. Plasmid *HA-N2-Bcl-2.dn3* encodes the HA-tagged fragment N2 fused to the intracellular membrane targeting domain of Bcl-2. It was constructed as follows: *GFP-C2* (corresponding to plasmid EGFP-BH2X-TMB[Bcl-2] in [11]) was PCR-amplified with the sense oligo N2-Bcl-2-sense [AATAT GCGGCCGC (NotI) G ATCCAGGATAACGGAGGCTGGGATG (human Bcl-2 amino acids 189–239)] and the anti-sense oligo N2-Bcl-2-AS [N2-Bcl-2-AS; #342; sequence 1780–1751 of GFP-C2): TGATCAGTTAT TCTAGA (XbaI) T G (mutation to remove the Dam methylation site) CGGTGGATCATC]. The resulting 374 bp fragment was digested with NotI and XbaI and subcloned in *HA-N2-no stop.dn3* opened with the same enzymes. Plasmid *HA-N2-AAGQEAFA-Bcl-X_L TMB.dn3* is similar to *HA-N2-RKGQERFNR-Bcl-X_L TMB.dn3* but bears mutations in the sequences upstream of the trans-membrane domain that disrupt the mitochondrial targeting (see Fig. 4). It was generated as follows: *HA-N2-RKGQERFNR-Bcl-X_L TMB.dn3* was PCR-amplified with the sense primer Mutated Bcl-X_L TMB (CAGTCGAC [feeder] GCGGCCGC [NotI] AGCCGAGAGC gc A gc TGGCCAGGAA gc CTCAAC gc CTGGTTCCTGACGGGCATGAC [nucleotides 777–833 of human Bcl-X_L mRNA (NM_001191) with mutations indicated by lower case letters; these mutations also introduce an additional PvuII site) and the anti-sense primer Sp6 (CTAGCATTAGGTGACACTATAG [pcDNA3 nucleotides 1021–999]). The 204 bp PCR fragment was then cut with NotI and ApaI and the resulting 141 bp fragment subcloned into the template plasmid opened with the same enzymes.

N(D157A).pgx encodes a fusion protein between GST and fragment N. It was constructed by PCR amplification of plasmid N (D157A).dn3 with the sense oligo [TTGGTT (feeder) GGATCC (BamHI) ATG ATG GCG GCC GAG (amino acids 1–5 of RasGAP)] and with the anti-sense oligo [TACCTAGCATGAACAGATTG (a sequence that is not found in pcDNA3 and that has no use in the present context) AGGGGCAACAACAGATG (a pcDNA3 sequence downstream of the multiple cloning sites)]. The resulting 1517 bp fragment was cut with BamHI and XhoI and subcloned in plasmid pGEX-KG opened with the same enzymes. *N(D157A).dn3* was constructed by subcloning the SacII/BglII 1.2 kb fragment of h-RasGAP (no 3'-UTR).dn3 into *HA-N(D157A).dn3* opened with the same enzyme. *HA-N(D157A).dn3* encodes the HA-tagged caspase-resistant version of fragment N [3].

h-RasGAP (no 3'-UTR).dn3 was constructed by PCR amplification of h-RasGAP.dn3 (using the Pfu polymerase) using the sense oligonucleotide (CTCATGCAAGGGAAGGGCAA: human RasGAP

mRNA nucleotides 2001–2020; accession no. M23379) and the anti-sense oligonucleotide (CG [feeder]; GCGGCCGC [NotI]; CTACCTGACATCATTGGTTTTTGT [RasGAP cDNA sequence 3331–3308 accession no. 34190380]). The PCR fragment (1.1 kb) was then digested with NotI/EcoRV and subcloned in h-RasGAP.dn3 opened with the same enzyme. h-RasGAP.dn3 encodes the human RasGAP mRNA (clone 101) [nucleotides 1–3987] [12].

The names of the plasmids used for the production of lentiviruses end with .lti. Plasmids *HA-N(D157A).lti* (previously called N-D157A.lti) was described earlier [5]; as were plasmids *HA-N2.lti* and *HA-RasGAP (no 3'-UTR).lti* [6].

All the PCR-generated plasmids were sequenced to check that no PCR-mediated errors were generated.

Immuno-cytochemistry

Cells were grown on glass coverslips and transfected. Two days post-transfection, the cells were fixed as follows (all the steps were performed at room temperature). The cells on coverslips were washed with 4 ml of PBS [116 mM NaCl, 10.4 mM Na₂HPO₄, 3.2 mM KH₂PO₄ (pH 7.4)], fixed with 3 ml PBS, 3% formaldehyde, 3% sucrose for 10 min, washed thrice with PBS, permeabilized with 2 ml of PBS, 0.2% Triton X-100 for 10 min, washed thrice with PBS,

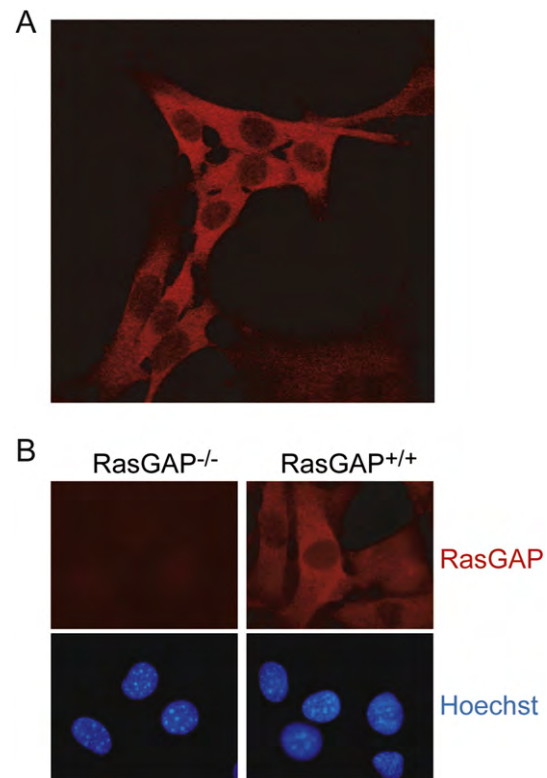


Fig. 1 – The endogenous full-length RasGAP protein is predominantly cytoplasmic. (A) MEFs derived from wild-type mice were stained with a 1/300 dilution of a polyclonal anti-RasGAP antibody recognizing the SH domains of the protein and photographed using a confocal microscope. (B) MEFs derived from RasGAP knock-out (*RasGAP*^{-/-}) or wild-type (*RasGAP*^{+/+}) mice were stained as above together with the Hoechst dye to label the nuclei. They were photographed using a microscope equipped with normal transmission optics.

and incubated 30 min with 3 ml of filtered serum-containing culture medium. After three additional PBS washes, the coverslips were incubated for 1 h with the primary antibody diluted in DMEM, 10% newborn calf serum. The coverslips were washed 3 times over 30 min in PBS and then incubated 1 h with a 1/100 dilution of labelled secondary antibodies in DMEM, 10% newborn calf serum. The coverslips were washed 3 more times in PBS and labelled when indicated with 10 µg/ml Hoechst 33342 (Molecular Probe) before being mounted (Vectashield mounting medium, Vector laboratories Inc). Confocal images were captured with a Leica SP5 AOBs confocal microscope. Other images were taken with a Zeiss Axioplan 2 imaging microscope.

Apoptosis measurements

Apoptosis was determined by scoring the number of cells displaying pycnotic nuclei. Nuclei of live cells were labelled with Hoechst 33342 (10 µg/ml final concentration) for about 5 min and the cells were then analyzed (at least 200 cells per condition) using an inverted Zeiss Axiovert 25 microscope equipped with fluorescence and transmitted light optics. Assessment of apoptosis was performed one day after treatment of the cells. The pEGFP-C1 plasmid was included in the transfection solution to label the transfected cells with GFP. The extent of apoptosis was assessed in transfected cells only.

Lentivirus

Recombinant lentiviruses were produced as previously described [13].

Statistical analysis

Statistical analyses were performed with Microsoft Excel (XP edition) using the two-tailed unpaired student *t*-test. Significance is indicated by an asterisk when $p < 0.05/n$, where p is the probability derived from the *t*-test analysis and n is the number of comparisons performed (Bonferroni correction). In Fig. 4C, statistical significance was assessed by ANOVA using the R program (<http://www.r-project.org/>).

Results

Sub-cellular location of RasGAP and its caspase-generated fragments

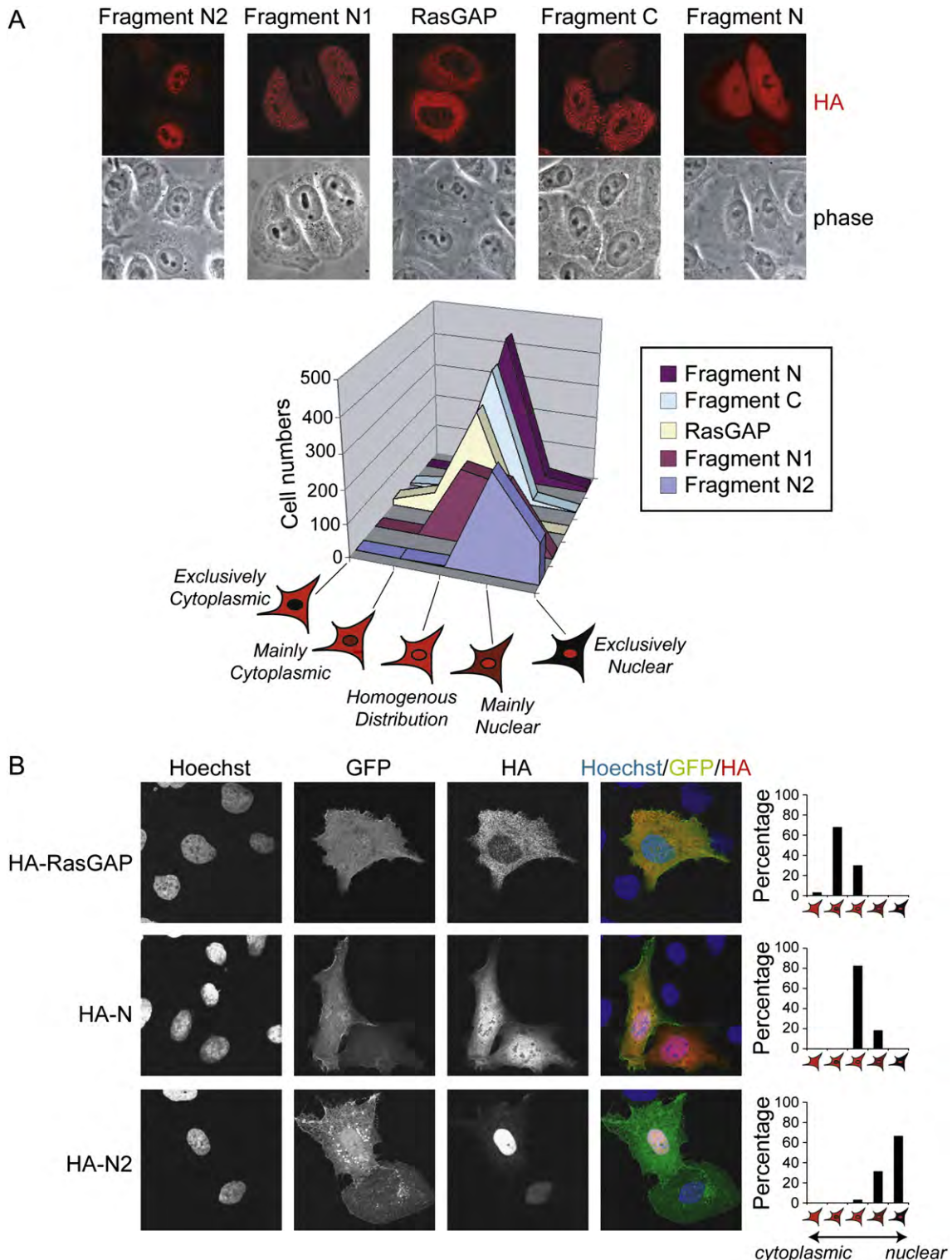
The sub-cellular location of endogenous RasGAP was first assessed in MEFs. Fig. 1A shows that the endogenous RasGAP protein is mainly localized in the cytoplasm, as anticipated from earlier studies demonstrating GAP activity in cytoplasmic extracts [14,15]. The specificity of the anti-RasGAP antibody was demonstrated by the absence of staining in RasGAP^{-/-} MEFs (Fig. 1B). There are no currently available antibodies that can discriminate RasGAP from its cleavage products by immuno-cytochemistry. To assess the sub-cellular distribution of caspase-generated RasGAP fragments, HeLa cells were therefore transfected with plasmids encoding HA-tagged versions of RasGAP or its fragments. The location of the various constructs was assessed by immuno-cytochemistry (Fig. 2A, upper part) and the proportions of cells displaying a given cytoplasmic versus nuclear distribution ratio scored as shown in the lower part of Fig. 2A. In comparison with the endogenous protein, over-expressed full-length RasGAP had an increased nuclear distribution but the nuclear staining was never more intense than the cytoplasmic one. Fragments N and C had a similar cellular location as the full-length protein. Fragment N1, in contrast, had a nuclear staining that was as strong as or stronger than the cytoplasmic staining. This was even more pronounced when fragment N2 was over-expressed. About one third of fragment N2-transfected cells expressed the protein exclusively in the nucleus and for the remaining ones, the cytoplasmic staining remained very low. None of the other constructs used here displayed an exclusively nuclear location. The predominant nuclear location of fragment N2 was confirmed in the U2OS osteosarcoma cell line (Fig. 2B).

Two approaches were employed to evaluate the degree of over-expression of full-length RasGAP that is achieved in U2OS cells. First, U2OS cells were transfected or not with a plasmid encoding the HA-tagged form of full-length RasGAP. The expression of RasGAP was then evaluated by measuring the intensity of the

Fig. 2 – Fragment N2 has a predominant nuclear location in fixed cells. (A) HeLa cells were transfected with plasmids encoding the indicated HA-tagged proteins and fragments. The location of the constructs was assessed by immuno-cytochemistry using an anti-HA antibody. The lower part of the panel graphically depicts the number of cells having a given cytoplasmic versus nuclear distribution ratio (from exclusively cytoplasmic to exclusively nuclear as schematized under the horizontal axis). **(B)** U2OS cells were transfected with plasmids encoding the indicated HA-tagged constructs together with a plasmid encoding the GFP protein. The cells were then visualized by fluorescence microscopy and the cellular location of the transfected RasGAP-derived constructs scored as described in panel A. **(C)** U2OS cells were either left untreated or transfected with a construct encoding HA-RasGAP. The cells were fixed 24 h later and subjected to immuno-cytochemistry using an anti-RasGAP fragment N2 antibody. Images were taken with a confocal microscope and the intensity of the RasGAP signal was quantitated using the ImageJ software (1.34n version). In the transfected cells, only the cells with a clear increase in RasGAP levels were recorded. Results correspond to the mean ± SD ($n = 25$ cells). **(D and E)** U2OS cells were infected or not with a lentivirus encoding the HA-tagged form of RasGAP. Two days later, the cells were either fixed and subjected to immuno-cytochemistry analysis using an anti-HA antibody (panel D), counted after trypsinization, or lysed. Different quantities of the lysates were loaded on a SDS-PAGE gel along with known quantities of purified GST-fragment N recombinant protein. A Western blot was then performed using an antibody recognizing the N2 portion of RasGAP (panel E, upper part). The quantity of RasGAP in the lysates was calculated using the standard curve obtained by plotting the Western blot signals of the GST-fragment N recombinant proteins against their molar quantities (panel E, lower part). Recording the number of cells in the culture wells prior to lysis allowed for the conversion of “number of RasGAP molecules in a given quantity of lysate” to “number of RasGAP molecules per cell”.

immuno-fluorescence signal on confocal microscopy images (Fig. 2C). There was about a 7-fold increase in RasGAP expression levels in the U2OS cells transfected with the RasGAP-encoding plasmid. The second experiment was performed on U2OS cells infected or not with a lentivirus encoding the HA-tagged form of RasGAP. The amount of virus used led to virtually all of the cells to over-express RasGAP (Fig. 2D). The quantity of RasGAP expressed in the cells was determined by Western blot analysis using an anti-RasGAP antibody by comparing the signal obtained with known

amounts of purified GST-fragment N recombinant protein (that bears the epitope recognized by the antibody used in the Western blot) with the signals derived from cell lysates (Fig. 2E). This analysis revealed that an U2OS cell expresses about 400,000 RasGAP molecules while an U2OS cell infected with a lentivirus encoding RasGAP expresses on average about 2 million RasGAP molecules. These two approaches indicate therefore that the level of over-expression of RasGAP in U2OS cells, whether achieved by transfection or following lentiviral infection, is ~5–7 fold.



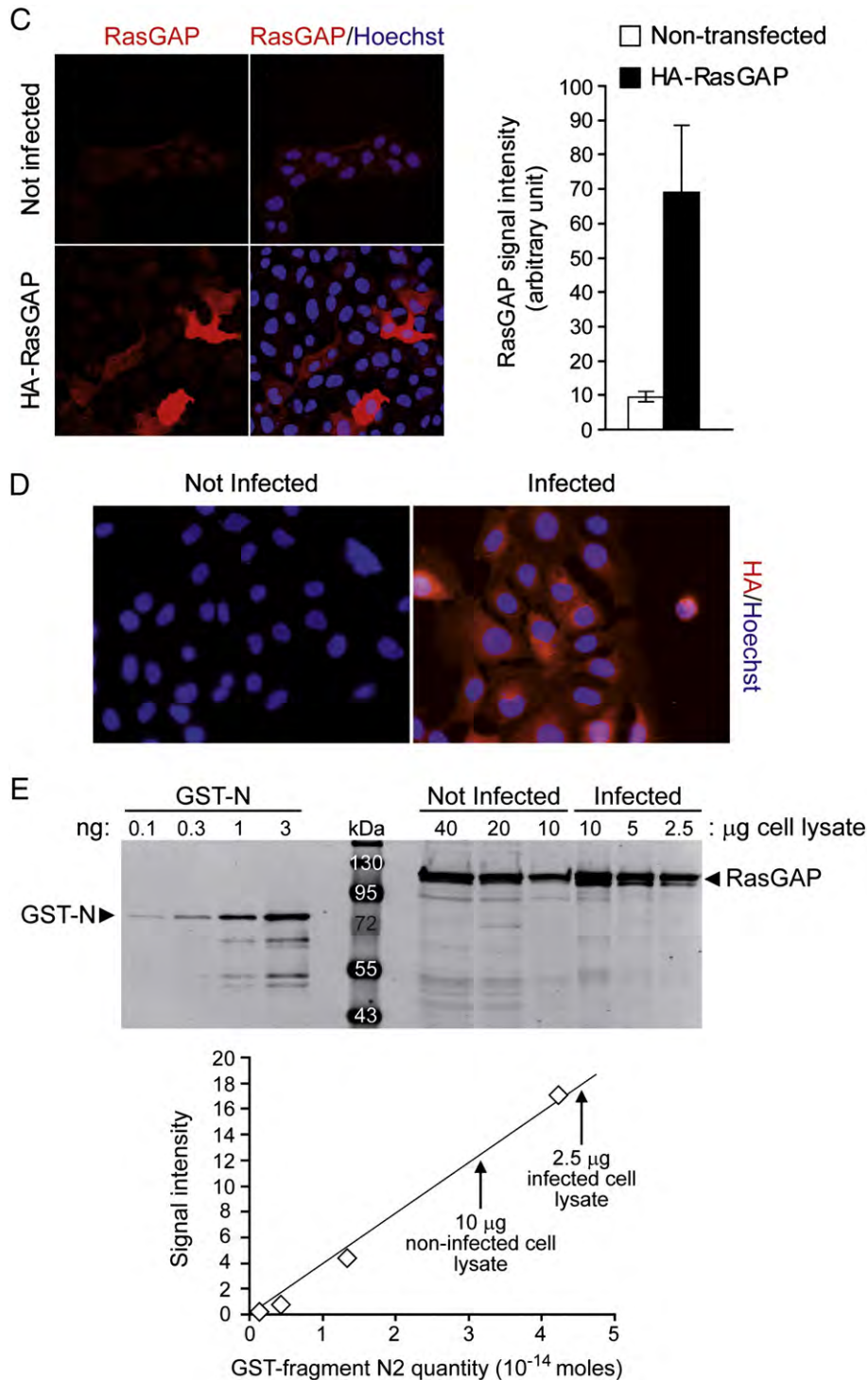


Fig. 2 (continued).

Additional experiments showed however that the location in fixed cells of fragment N2, but not of fragment N or RasGAP, is artefactual. Live imaging of U2OS cells transfected with a plasmid encoding a fusion protein between GFP and fragment N2 revealed cells with a strong green cytoplasmic labelling (Fig. 3A; compare with Fig. 2). Fragment N2 fused to GFP was still functional as a genotoxin-sensitizer (Fig. 3B) indicating that the GFP moiety did not interfere with its anti-cancerous function.

Sub-cellular fractionation of HA-fragment N2-transfected U2OS cells into a nuclear histone H3-containing fraction, and a cytoplasmic tubulin-containing fraction (Fig. 3C) confirmed the predominant cytoplasmic location of fragment N2. In contrast to what was observed with fragment N2, the locations of the parental RasGAP protein and fragment N were similar in live and fixed cells and more or less matched the distribution pattern observed in sub-cellular fractions (Figs. 2 and 3): fragment N

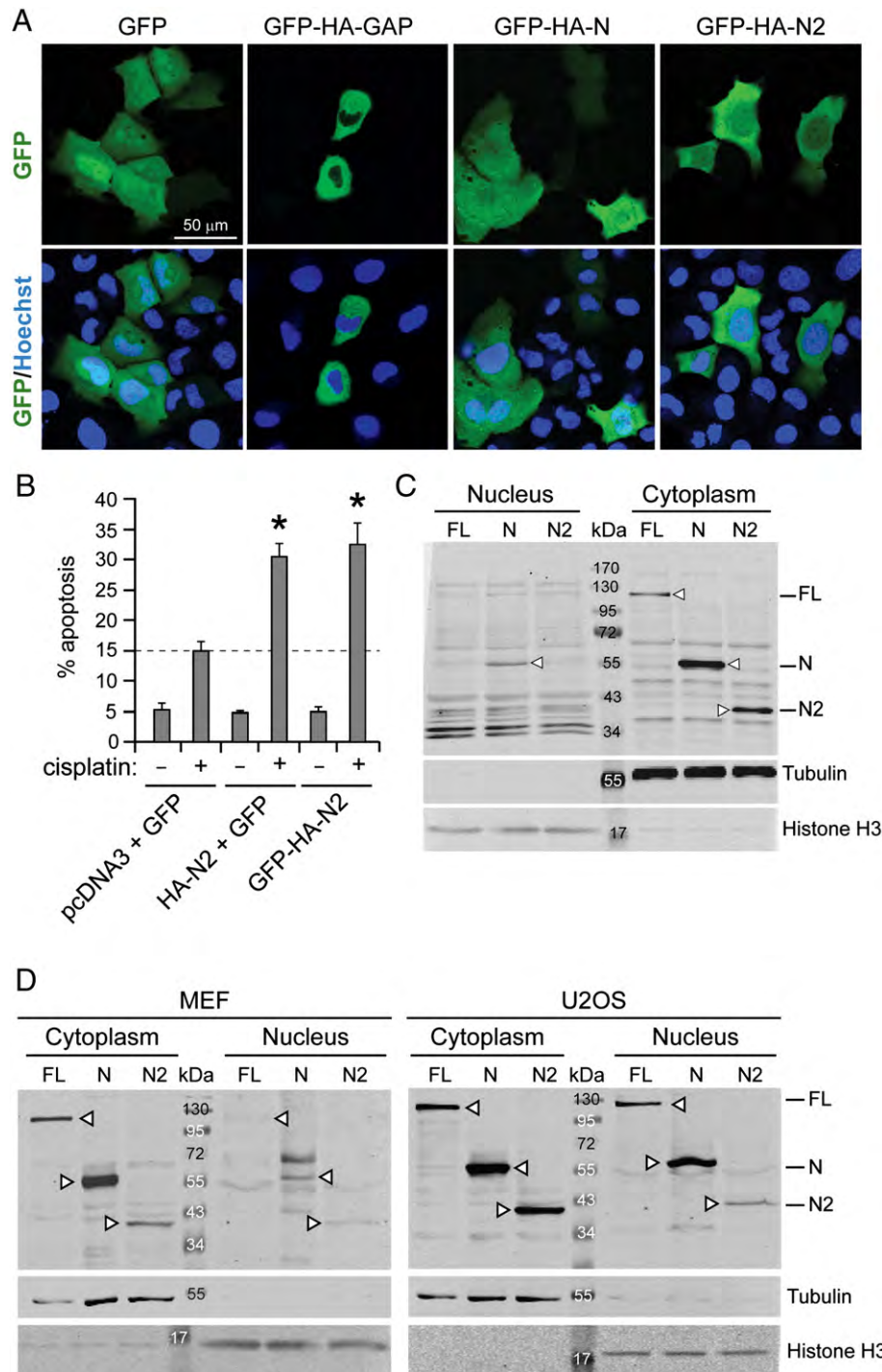


Fig. 3 – Fragment N2 is mainly located in the cytoplasm of living cells. (A) U2OS cells were transfected with plasmids encoding the indicated GFP-tagged constructs. Immediately following Hoechst staining, the cells were visualized while still alive, by fluorescence confocal microscopy. (B) U2OS cells were transfected with the indicated constructs. They were then incubated with increasing concentrations of cisplatin and one day later apoptosis was determined in the transfected cell population. The results correspond to the mean \pm SD of three independent experiments. Statistical analysis was performed to assess the significance of the sensitization induced by the N2-containing constructs (i.e. comparisons of control cells treated with cisplatin with the other cisplatin-treated cells; 2 comparisons). (C) U2OS cells were transfected with plasmids encoding the HA-tagged forms of full-length RasGAP, fragment N or fragment N2. Nuclear and cytoplasmic fractions (see [Materials and methods](#)) were then analyzed by Western blotting using an anti-HA antibody to detect RasGAP and its fragments. Tubulin and histone H3 were used as markers for the cytoplasm and nucleus, respectively. (D) U2OS and MEFs were infected with the same amount of HA-RasGAP, HA-N and HA-N2-expressing lentiviruses and 48 h later they were lysed and the lysates were fractionated as described in (C).

was localized in the cytoplasm and in the nucleus and full-length RasGAP was predominantly detected in the cytoplasm (see also Fig. 1).

As fragment N2 does not sensitize non-cancer cells (e.g. mouse embryonic fibroblasts [MEFs]) to genotoxin-induced apoptosis [6], it was of interest to determine whether the cytoplasmic location of

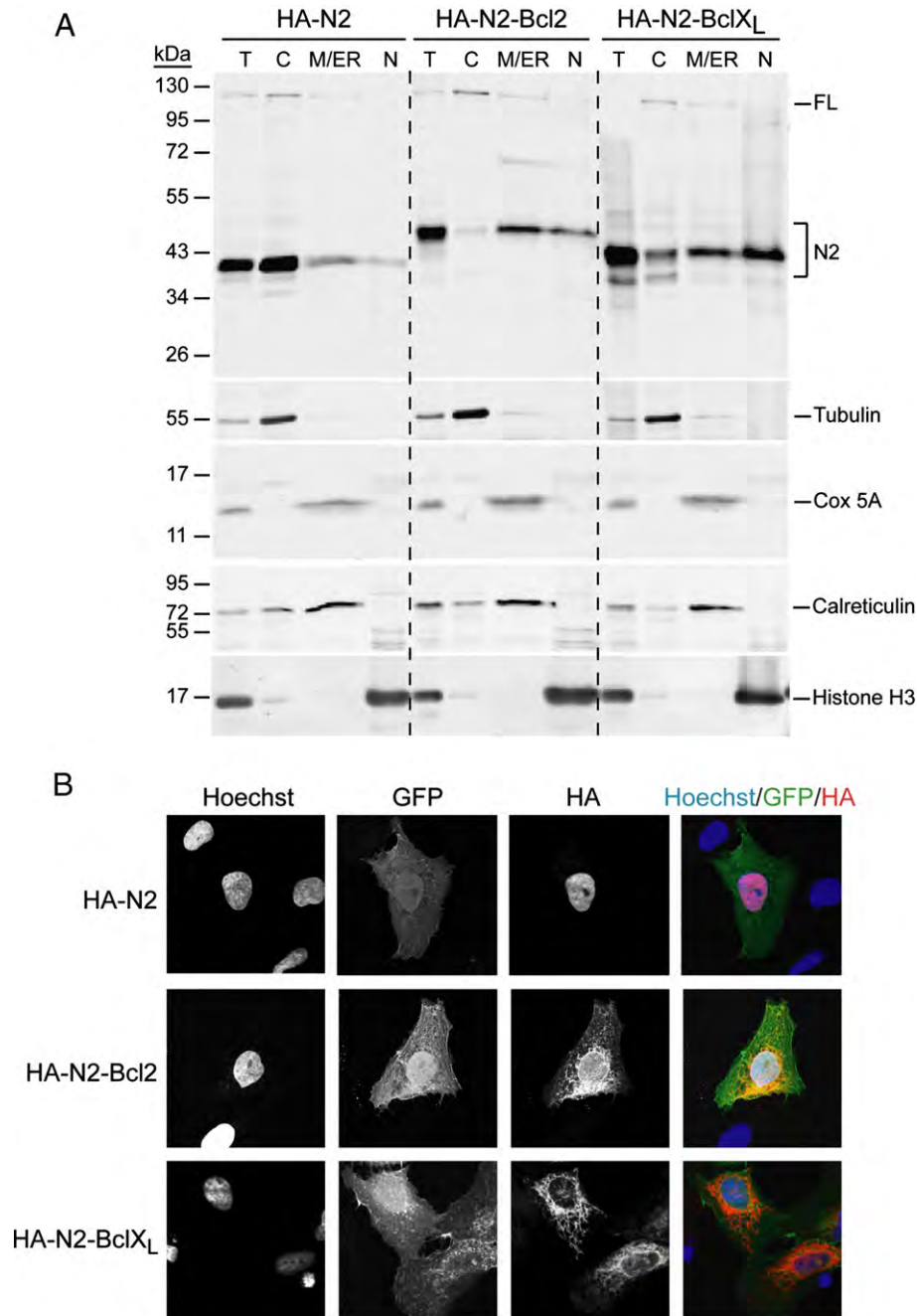


Fig. 4 – Mitochondria and ER-targeted fragment N2 does not sensitize tumor cells to genotoxins. (A) U2OS cells were transfected with plasmids encoding the indicated HA-tagged constructs. The cells were then lysed to generate a total cell extract (T) or separated into soluble cytoplasmic (C), mitochondria/ER-containing (M/ER), and nuclear (N) fractions as described in **Materials and methods**. The presence of the indicated proteins was assessed by Western blot. The RasGAP-specific antibody used here recognizes the N2 region of RasGAP. FL, full-length RasGAP; N2, the various forms of fragment N2. **(B)** U2OS cells were transfected with plasmids encoding the indicated HA-tagged constructs together with a plasmid encoding the GFP protein. Following Hoechst staining, fixed cells were visualized by fluorescence confocal microscopy. **(C)** U2OS cells transfected with the indicated constructs together with a plasmid encoding the GFP protein were incubated with increasing concentrations of cisplatin. Apoptosis in the GFP-positive cells was determined 24 h later. The results correspond to the mean \pm SD of three independent experiments. The asterisk denotes a statistical difference between cells expressing wild-type N2 and the other conditions (for all the possible comparisons). No statistical differences were detected within the conditions found in the bracket.

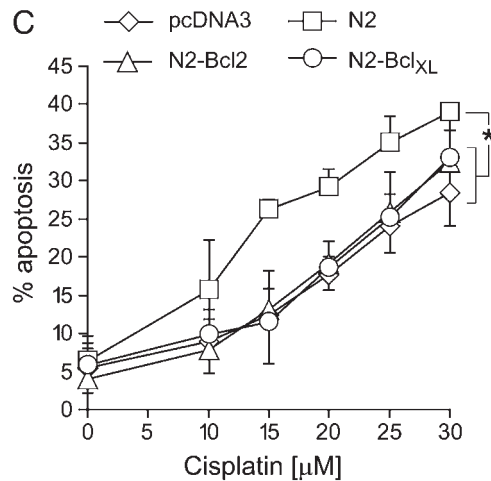


Fig. 4 (continued).

fragment N2 was a specific characteristic of cancer cells (such as U2OS or HeLa cells) or whether fragment N2 was also mainly found in the cytoplasm of normal cells. We therefore assessed the sub-cellular location of fragment N2 in MEFs. Full-length RasGAP and fragment N were also analyzed for comparison. As MEFs are poorly transfectable, we used lentiviral infection to ectopically express the proteins (the amount of viruses used led to 100% of the cells being infected; not shown and Fig. 2D). As controls, U2OS cells were similarly infected. Fig. 3D shows that fragment N2 was mostly detected in the cytoplasmic fraction of both MEF and U2OS infected cells. The cytoplasmic location of fragment N2 is therefore not a specific feature of cancer cells.

In infected cells, low but clearly detectable amounts of fragment N2 were found in the nuclear fraction. As fragment N2 was not observed in the nuclear fraction of transfected U2OS cells (see Fig. 3C), this suggests that lentiviruses somehow affect the sub-cellular distribution of fragment N2 in cells. Lentiviruses perturbed to seemingly a greater extent the sub-cellular distribution of full-length RasGAP and fragment N since there were obviously more of these proteins in the nuclear fraction of infected U2OS cells in comparison to what was observed in transfected U2OS cells. The main message of Fig. 3D however is that the sub-cellular distribution pattern of fragment N2 does not seem to be grossly different between cancer and non-cancer cells.

The results described above indicate that fragment N2 is found in the cytoplasm but they do not tell whether fragment N2 is associated or not with a cytoplasmic organelle (e.g. mitochondria). To assess this point, U2OS cells expressing the HA-tagged form of the fragment were separated into nuclear, organelle-free cytoplasmic, and mitochondria/ER-containing fractions. The purity of these fractions were assessed using the tubulin cytoplasmic marker, the cytochrome *c* oxidase subunit 5A (Cox) mitochondrial marker, the calreticulin ER marker, and the histone H3 nuclear marker. Fig. 4A (left part) shows that the majority of fragment N2 is found in the soluble fraction. A minor portion of fragment N2 was distributed in the mitochondria/ER-containing fraction. An even smaller portion was detected in the nuclear fraction.

The cytoplasmic location of fragment N2 is required for its tumor sensitization properties

The data presented above indicate that fragment N2 is mainly a soluble protein present in the cytoplasm but they also show that a small fraction of fragment N2 can be associated with organelles (mitochondria and/or the ER). We reasoned that if the presence of fragment N2 in the cytoplasm is important for its ability to sensitize tumor cells to genotoxin-induced death, experimentally relocating fragment N2 away from the cytoplasm onto given organelles should negatively affect its sensitization properties. Conversely, if the location of fragment N2 on a given organelle favors or is required for its sensitization properties, such relocation should positively affect its ability to sensitize tumor cells to genotoxins. Specific sequences in Bcl-2 family members have been shown to target proteins to various organelles. For example, amino acids 136–170 of human Bcl-X_L targets the protein to mitochondria while amino acids 189–239 of human Bcl-2 targets it to intracellular membranes including the endoplasmic reticulum and perinuclear membranes [11]. We therefore generated plasmids encoding HA-tagged fragment N2 bearing these targeting sequences at the carboxy-terminal end. The targeting capacity of the Bcl-2 and Bcl-X_L sequences was assessed by sub-cellular fractionation and immuno-cytochemistry. Fig. 4A shows that both the Bcl-2 and Bcl-X_L sequences induce a relocation of fragment N2 from a soluble cytoplasmic fraction to mitochondrial/ER and nuclear fractions. The presence of some N2-Bcl-2 fusion protein in the nuclear fraction could be expected from the earlier demonstration that the Bcl-2 sequence used here (amino acids 189–239 of human Bcl-2) targets protein to intracellular membranes including perinuclear membranes [11]. In contrast, it is currently unclear why the Bcl-X_L mitochondrial targeting sequence (amino acids 136–170 of human Bcl-X_L) [11] led some of the N2-Bcl-X_L fusion proteins ending up in the nuclear fraction. Despite the fact that fragment N2 artefactually associates with the nucleus of fixed cells, the Bcl-2 and Bcl-X_L sequences were able to relocate fragment N2 to the mitochondria and ER/nuclear membranes in fixed cells (Fig. 4B). Importantly, this change in sub-cellular location abrogated the ability of fragment N2 to sensitize tumor cells to cisplatin-induced apoptosis (Fig. 4C).

It could be argued that it is the mere addition of sequences at the carboxy-terminal end of fragment N2 that inhibits its sensitization properties. To assess this issue, four point mutations were introduced in the X domain preceding the trans-membrane domain (TM) and the basic amino acids (B) in the mitochondrial targeting sequence of Bcl-X_L (Fig. 5A). These mutations have been shown to abrogate mitochondria targeting [11]. Fig. 5B shows that fragment N2 bearing such a mutated sequence at its COOH-terminus was no longer retained in the cytoplasm but predominantly redistributed to the nucleus of fixed cells. This was accompanied by a recovered ability to sensitize tumor cells to cisplatin-induced apoptosis (Fig. 5C). This suggests that it is the modification of the sub-cellular location of fragment N2 that causes its inability to sensitize tumors to genotoxins rather than the addition of sequences at its C-terminal end.

Fragment N2 and shorter peptides derived from it have been shown to sensitize tumor cells, but not normal cells, to genotoxin-induced death [6,7] and to photodynamic therapy [16]. It is however not known whether this sensitization property could also be seen in association with apoptotic stimuli that are not supposed

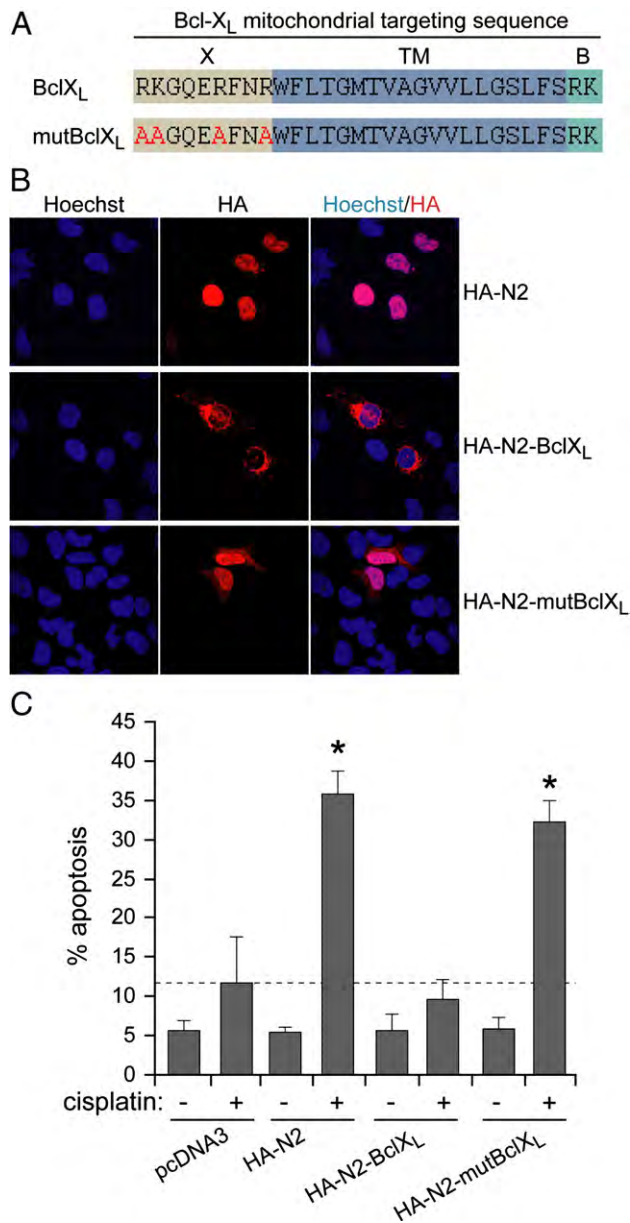


Fig. 5 – The presence of additional sequences at the carboxy-terminal end of fragment N2 does not hamper its ability to sensitize tumor cells to cisplatin. (A) The Bcl-X_L mitochondrial targeting sequence is shown. The mutations known to abrogate mitochondrial targeting are indicated in red. (B and C) U2OS cells were transfected with plasmids encoding the indicated HA-tagged constructs together with a plasmid encoding GFP. In panel B, the cells were treated as in Fig. 2B. In panel C, the cells were processed as described in Fig. 3B (only the cells expressing GFP were analyzed). In panel C, statistical analysis was performed to assess the significance of the sensitization induced by the N2-containing constructs (i.e. comparisons of control cells treated with cisplatin with the other cisplatin-treated cells; 3 comparisons).

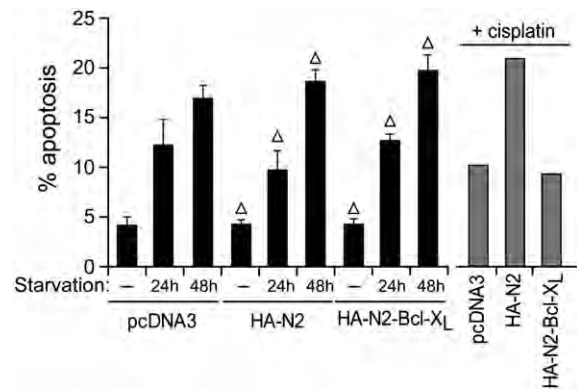


Fig. 6 – Fragment N2 does not sensitize cells to starvation-induced apoptosis. U2OS cells were transfected with the indicated plasmids together with a plasmid encoding the GFP protein. Eight hours later, the cells were starved for 24 or 48 h (black bars). Apoptosis was then determined in the GFP-expressing cells. Results correspond to the mean \pm SD ($n = 3$ determinations). Statistical analysis was performed to assess the difference between cells transfected with pcDNA3 and the other transfected cells for a given condition (i.e. no starvation or starvation for 24 h and 48 h). The triangles indicate that the p value for the indicated comparison was > 0.05 (not significant). As a control to assess the functionality of the plasmids, the cells were incubated with 15 μ M cisplatin for 22 h after which apoptosis was determined in the GFP-expressing cells (grey bars). Results are expressed as the mean of two determinations. As expected, HA-N2 sensitized U2OS cells to cisplatin-induced apoptosis, while the HA-N2-Bcl-X_L construct did not.

to specifically target tumor cells (e.g. starvation). Moreover, targeting fragment N2 on organelles that abrogates the capacity of fragment N2 to sensitize tumor cells to genotoxin-induced death might not affect the capacity of fragment N2 to promote apoptosis of tumor cells to non-genotoxin-induced apoptosis. We assessed these points by determining whether fragment N2, or fragment N2 coupled to the mitochondrial targeting Bcl-X_L sequence, can sensitize U2OS cells to starvation-induced apoptosis. As shown in Fig. 6, U2OS cells expressing or not the two forms of fragment N2 underwent similar apoptosis in response to starvation. This indicates that fragment N2 specifically sensitizes tumor cells to certain (e.g. genotoxins), but not all, death stimuli and that fragment N2 targeted to the mitochondria does not acquire sensitization properties that would be absent in the cytoplasmic form of fragment N2.

Discussion

Fragment N2 generated upon the full processing of RasGAP by caspases is able to sensitize tumor cells, but not normal cells, to genotoxin-induced apoptosis [7]. Here we show that fragment N2 is almost strictly located in the cytoplasm of cells and is only minimally associated with the nucleus or organelles such as the mitochondria or the endoplasmic reticulum. Earlier work has demonstrated that fragment N2 requires PUMA to exert its anti-cancerous function [8]. PUMA, a transcriptional target of p53,

belongs to the BH3-only pro-apoptotic members of the Bcl-2 family of proteins [17,18]. It favors cell death by antagonizing pro-survival Bcl-2 family members (e.g. Mcl-1, Bcl-2, Bcl-X_L). The ability of PUMA to promote cell death appears to be strictly dependent on Bax, a BH1-2-3 Bcl-2 family member that is able, upon activation, to induce the release of cytochrome *c* from mitochondria, which in turn results in caspase activation [19]. Yet, fragment N2 does neither alter PUMA levels nor the activity or expression of p53 that controls PUMA expression [8]. It has therefore been hypothesized that fragment N2 modulates the concerted action of p53 and PUMA at the mitochondria level to increase the sensitivity of tumor cells to the action of genotoxins [8]. The data presented here however show that fragment N2 loses its anti-tumor property if located on mitochondria. Fragment N2 might therefore modulate PUMA action before mitochondria are targeted. One possibility would be that fragment N2 alters the expression of other Bcl-2 family members so that the balance between anti- and pro-apoptotic Bcl-2 proteins is tilted in favor of the latter. In this context, it has to be mentioned that fragment N2 does not induce a decrease in the expression of the anti-apoptotic Mcl-1 protein [8]. Additional work will be required to determine the cytoplasmic mode of action of fragment N2 that sensitizes tumor cells to genotoxin-induced death.

The present work also provides a striking example of a sub-cellular location artefact induced by cell fixation. Fragment N2 is virtually absent from the nucleus in living cells but has a predominant nuclear location in fixed cells. Permeabilization and fixation of cells for immuno-fluorescence studies are known to potentially induce improper nuclear targeting of proteins [20]. The example of fragment N2 and others [21–23] clearly emphasize the need of additional approaches (i.e. microscopy of live cells) to be used when the sub-cellular location of proteins of interest is analyzed.

Acknowledgments

We thank Dr. Christoph Borner for the gifts of the EGFP-BH2X-TMB [Bcl-2] and EGFP-X-TMB[Bcl-x], Dr. Bert Vogelstein for the HCT116 cell lines and Dr. Didier Trono for the TRIP-PGK-ATGm-MCS-WHV lentiviral vector. This work was supported by grants from the Swiss National Science Foundation and from Oncosuisse.

REFERENCES

- [1] A. Bernards, J. Settleman, GAP control: regulating the regulators of small GTPases, *Trends Cell Biol.* 14 (2004) 377–385.
- [2] S.V. Kulkarni, G. Gish, P. Van der Geer, M. Henkemeyer, T. Pawson, Role of p120 ras-GAP in directed cell movement, *J. Cell Biol.* 149 (2000) 457–470.
- [3] J.-Y. Yang, C. Widmann, Antiapoptotic signaling generated by caspase-induced cleavage of RasGAP, *Mol. Cell Biol.* 21 (2001) 5346–5358.
- [4] J.-Y. Yang, C. Widmann, The RasGAP N-terminal fragment generated by caspase cleavage protects cells in a Ras/PI3K/Akt-dependent manner that does not rely on NF κ B activation, *J. Biol. Chem.* 277 (2002) 14641–14646.
- [5] J.-Y. Yang, D. Michod, J. Walicki, B.M. Murphy, S. Kasibhatla, S. Martin, C. Widmann, Partial cleavage of RasGAP by caspases is required for cell survival in mild stress conditions, *Mol. Cell Biol.* 24 (2004) 10425–10436.
- [6] J.-Y. Yang, J. Walicki, D. Michod, G. Dubuis, C. Widmann, Impaired Akt activity down-modulation, caspase-3 activation, and apoptosis in cells expressing a caspase-resistant mutant of RasGAP at position 157, *Mol. Biol. Cell* 16 (2005) 3511–3520.
- [7] D. Michod, J.Y. Yang, J. Chen, C. Bonny, C. Widmann, A RasGAP-derived cell permeable peptide potentially enhances genotoxin-induced cytotoxicity in tumor cells, *Oncogene* 23 (2004) 8971–8978.
- [8] D. Michod, C. Widmann, TAT-RasGAP317-326 requires p53 and PUMA to sensitize tumor cells to genotoxins, *Mol. Cancer Res.* 5 (2007) 497–507.
- [9] F. Bunz, A. Dutriaux, C. Lengauer, T. Waldman, S. Zhou, J.P. Brown, J.M. Sedivy, K.W. Kinzler, B. Vogelstein, Requirement for p53 and p21 to sustain G2 arrest after DNA damage, *Science* 282 (1998) 1497–1501.
- [10] M. Valius, J. Secrist, A. Kazlauskas, The GTPase-activating protein of ras suppresses platelet-derived growth factor β receptor signaling by silencing phospholipase c- γ 1, *Mol. Cell Biol.* 15 (1995) 3058–3071.
- [11] T. Kaufmann, S. Schlipf, J. Sanz, K. Neubert, R. Stein, C. Borner, Characterization of the signal that directs Bcl-x_L, but not Bcl-2, to the mitochondrial outer membrane, *J. Cell Biol.* 160 (2003) 53–64.
- [12] C. Widmann, S. Gibson, G.L. Johnson, Caspase-dependent cleavage of signaling proteins during apoptosis. A turn-off mechanism for anti-apoptotic signals, *J. Biol. Chem.* 273 (1998) 7141–7147.
- [13] J.-Y. Yang, J. Walicki, A. Abderrahmani, M. Cornu, G. Waeber, B. Thorens, C. Widmann, Expression of an uncleavable N-terminal RasGAP fragment in insulin-secreting cells increases their resistance toward apoptotic stimuli without affecting their glucose-induced insulin secretion, *J. Biol. Chem.* 280 (2005) 32835–32842.
- [14] M. Trahey, F. McCormick, A cytoplasmic protein stimulates normal N-ras p21 GTPase, but does not affect oncogenic mutants, *Science* 238 (1987) 542–545.
- [15] J.B. Gibbs, M.D. Schaber, W.J. Allard, I.S. Sigal, E.M. Scolnick, Purification of ras GTPase activating protein from bovine brain, *Proc. Natl. Acad. Sci. U. S. A.* 85 (1988) 5026–5030.
- [16] O. Pittet, D. Petermann, D. Michod, T. Krueger, C. Cheng, H.B. Ris, C. Widmann, Effect of the TAT-RasGAP317-326 peptide on apoptosis of human malignant mesothelioma cells and fibroblasts exposed to meso-tetra-hydroxyphenyl-chlorin and light, *J. Photochem. Photobiol. B* 88 (2007) 29–35.
- [17] V. Labi, M. Erlacher, S. Kiessling, A. Villunger, BH3-only proteins in cell death initiation, malignant disease and anticancer therapy, *Cell Death. Differ.* 13 (2006) 1325–1338.
- [18] R.J. Youle, A. Strasser, The BCL-2 protein family: opposing activities that mediate cell death, *Nat. Rev. Mol. Cell Biol.* 9 (2008) 47–59.
- [19] J. Yu, Z. Wang, K.W. Kinzler, B. Vogelstein, L. Zhang, PUMA mediates the apoptotic response to p53 in colorectal cancer cells, *Proc. Natl. Acad. Sci. U. S. A.* 100 (2003) 1931–1936.
- [20] M.A. Melan, G. Sluder, Redistribution and differential extraction of soluble proteins in permeabilized cultured cells. Implications for immunofluorescence microscopy, *J. Cell Sci.* 101 (1992) 731–743.
- [21] M. Lundberg, M. Johansson, Is VP22 nuclear homing an artifact? *Nat. Biotechnol.* 19 (2001) 713–714.
- [22] I. Behrmann, T. Smyczek, P.C. Heinrich, L.H. Schmitz-Van de, W. Komyod, B. Giese, G. Muller-Newen, S. Haan, C. Haan, Janus kinase (Jak) subcellular localization revisited: the exclusive membrane localization of endogenous Janus kinase 1 by cytokine receptor interaction uncovers the Jak-receptor complex to be equivalent to a receptor tyrosine kinase, *J. Biol. Chem.* 279 (2004) 35486–35493.
- [23] M. Lundberg, M. Johansson, Positively charged DNA-binding proteins cause apparent cell membrane translocation, *Biochem. Biophys. Res. Commun.* 291 (2002) 367–371.

Results

Part II

Introduction

Cancer is a class of diseases that exhibit significant heterogeneity in term of genetic aberrations, cell proliferation rate and cell surface markers. Nevertheless one common feature of cancer cells is represented by apoptosis evasion. The design of strategies targeting the sensitivity of malignant cells to apoptosis could therefore help the improvement of the currently used anti-cancer regimens. In this sense one promising approach is represented by therapies relying on the utilization of genotoxins combined to compounds interfering with the apoptotic resistance of cancer cells. This might therefore enhance the genotoxin-induced death response, selectively in cancer cells.

It was previously discovered that the RasGAP cleavage fragment N2 selectively sensitizes cancer cells to genotoxins *in vitro* while having no effect on non-cancer cell. The shortest sequence of fragment N2 still bearing this property, that corresponds to amino acids 317-326, was also determined. This sequence was fused to the TAT cell permeation sequence and the resulting peptide, called TAT-RasGAP₃₁₇₋₃₂₆, was able to enter tumoral cells and sensitize them to genotoxins.

In the present study we wanted to assess if the TAT-RasGAP₃₁₇₋₃₂₆ sensitizes tumors in *in vivo* conditions. To answer this question we first synthesized the Retro-Inverso form of the peptide, called RI- TAT-RasGAP₃₁₇₋₃₂₆, by converting its amino acids from the natural L-form to the protease-resistant D-form. We found that the RI-TAT-RasGAP₃₁₇₋₃₂₆ is more stable in culture medium and biological fluids compared to the L-form; this property is most likely due to its resistance to protease-mediated degradation.

Subsequently we evaluated the toxicity of the RI- TAT-RasGAP₃₁₇₋₃₂₆. We determined the lethal dose and the causes of the RI- TAT-RasGAP₃₁₇₋₃₂₆-induced mice death.

Next we sub-cutaneously implanted nude mice with HCT1116 tumor cells and we look at the tumor development in presence of two different genotoxins (cisplatin and doxorubicin) alone or in combination with the RI- TAT-RasGAP₃₁₇₋₃₂₆.

Our data show that the RI- TAT-RasGAP₃₁₇₋₃₂₆ significantly reduces tumor growth when administrated together with doses of genotoxins that by themselves only poorly reduce tumor growth. Importantly, the RI- TAT-RasGAP₃₁₇₋₃₂₆ by itself has no effect on tumor growth.

Contribution

This work has been published in the Journal of the National Cancer Institute in 2009 and it is attached in the following section. I share the first authorship of this paper with Dr. David Michod. I performed all the experiments done for the revision of this paper.

Effect of RasGAP N2 Fragment-Derived Peptide on Tumor Growth in Mice

David Michod, Alessandro Annibaldi, Stephan Schaefer, Christine Dapples, Bertrand Rochat, Christian Widmann

Peptides that interfere with the natural resistance of cancer cells to genotoxin-induced apoptosis may improve the efficacy of anticancer regimens. We have previously reported that a cell-permeable RasGAP-derived peptide (TAT-RasGAP₃₁₇₋₃₂₆) specifically sensitizes tumor cells to genotoxin-induced apoptosis in vitro. Here, we examined the in vivo stability of a protease-resistant D-form of the peptide, RI-TAT-RasGAP₃₁₇₋₃₂₆^D and its effect on tumor growth in nude mice bearing subcutaneous human colon cancer HCT116 xenograft tumors. After intraperitoneal injection, RI-TAT-RasGAP₃₁₇₋₃₂₆^D persisted in the blood of nude mice for more than 1 hour and was detectable in various tissues and subcutaneous tumors. Tumor-bearing mice treated daily for 7 days with RI-TAT-RasGAP₃₁₇₋₃₂₆^D (1.65 mg/kg body weight) and cisplatin (0.5 mg/kg body weight) or doxorubicin (0.25 mg/kg body weight) displayed reduced tumor growth compared with those treated with either genotoxin alone (n=5–7 mice per group; *P*=.004 and *P*=.005, respectively; repeated measures analysis of variance [ANOVA, two-sided]). This ability of the RI-TAT-RasGAP₃₁₇₋₃₂₆^D peptide to enhance the tumor growth inhibitory effect of cisplatin was still observed at peptide doses that were at least 150-fold lower than the dose lethal to 50% of mice. These findings provide the proof of principle that RI-TAT-RasGAP₃₁₇₋₃₂₆^D may be useful for improving the efficacy of chemotherapy in patients.

J Natl Cancer Inst 2009;101:828–832

Chemotherapeutic drugs kill tumor cells by activating apoptosis. If this activation is compromised (eg, through additional gene mutations), a tumor may develop resistance to the anticancer drugs (1,2). Consequently, strategies to restore tumor sensitivity to apoptosis are promising approaches for treating cancer. Much is now known about the mode of action of proteins that regulate cell death in cancer cells. This knowledge has led to the design of peptides that, in vitro, can perturb the resistance of cancer cells to anticancer agents (3,4). However, few studies have examined the efficacy of those peptides as anticancer compounds in vivo (3).

We have previously reported that fragment N2, a caspase-generated polypeptide from RasGAP, a regulator of Ras- and Rho-dependent pathways, strongly sensitizes tumor cells, but not normal cells, to genotoxin-induced apoptosis (5,6). The tumor sensitization property of the N2 fragment is contained within a 10-amino acid sequence (amino acids 317–326) (7). A synthetic peptide (called TAT-RasGAP₃₁₇₋₃₂₆) corresponding to this sequence fused to a

cell-permeable peptide derived from the human immunodeficiency virus TAT protein was found to efficiently increase the extent of apoptosis induced by a variety of genotoxins (7) and other anticancer treatments (8) in several tumor cell lines. Although it is now known that tumor cells must be able to activate the p53 and p53-upregulated modulator of apoptosis (PUMA) pathway for them to undergo TAT-RasGAP₃₁₇₋₃₂₆ peptide-mediated sensitization to genotoxin-induced apoptosis (9), the molecular mechanisms underlying the apoptosis sensitization property of TAT-RasGAP₃₁₇₋₃₂₆ remain to be characterized in detail. Here, we assessed the ability of TAT-RasGAP₃₁₇₋₃₂₆ to increase the efficacy of genotoxins in an in vivo context.

We first examined the functional stability of the peptide in biological fluids because it has been shown that peptides that are susceptible to proteolytic degradation can rapidly lose their function (10,11). Indeed, the ability of the natural L-form of TAT-RasGAP₃₁₇₋₃₂₆ (L-TAT-RasGAP₃₁₇₋₃₂₆) to sensitize cisplatin-treated human p53-positive

osteosarcoma U2OS cells (12) to undergo apoptosis [assessed by scoring the percentage of cells displaying pycnotic nuclei (9)] decreased as a function of increasing peptide preincubation time in serum-containing medium, suggesting that this peptide is sensitive to degradation by serum proteases (Figure 1, A). This sensitivity to degradation is likely to adversely affect the antitumor activity of the peptide in vivo. One way to render a peptide more resistant to proteolytic degradation is to convert its amino acids from the natural L-form to the protease-resistant D-form. To best mimic the structure of the natural peptide, the sequence of the D-peptide is generally inverted, generating the so-called retro-inverso form (13,14). After preincubation in serum-containing medium for up to 2 days, the retro-inverso form of TAT-RasGAP₃₁₇₋₃₂₆ (RI-TAT-RasGAP₃₁₇₋₃₂₆^D) showed almost no decrease in its ability to sensitize U2OS cells to cisplatin-induced apoptosis (Figure 1, A). This finding suggests that RI-TAT-RasGAP₃₁₇₋₃₂₆^D is a more stable compound than L-TAT-RasGAP₃₁₇₋₃₂₆. Dose-response analyses indicated that RI-TAT-RasGAP₃₁₇₋₃₂₆^D was more effective than L-TAT-RasGAP₃₁₇₋₃₂₆ in sensitizing U2OS cells to the apoptosis-inducing action of cisplatin (Figure 1, B and C), a likely reflection of its higher stability compared with L-TAT-RasGAP₃₁₇₋₃₂₆.

Another parameter that can affect the efficacy of an anticancer compound in vivo is its rate of clearance from the circulation. We used liquid chromatography coupled with mass spectrometry to examine the persistence of RI-TAT-RasGAP₃₁₇₋₃₂₆^D in blood samples taken at various times from

Affiliations of authors: Department of Physiology (DM, AA, CW), Department of Pathology (SS, CD), and Quantitative Mass Spectrometry Facility, University Hospital Center (BR), University of Lausanne, Lausanne, Switzerland.

Correspondence to: Christian Widmann, PhD, Department of Physiology, University of Lausanne, Rue du Bugnon 7/9, 1005 Lausanne, Switzerland (e-mail: christian.widmann@unil.ch).

See "Funding" and "Notes" following "References."

DOI: 10.1093/jnci/djp100

© The Author 2009. Published by Oxford University Press. All rights reserved. For Permissions, please e-mail: journals.permissions@oxfordjournals.org.

CONTEXT AND CAVEATS

Prior knowledge

Peptides that interfere with the natural resistance of cancer cells to genotoxin-induced apoptosis in vitro, such as TAT-RasGAP^{317-326'}, a cell-permeable RasGAP-derived peptide, may improve the efficacy of anticancer regimens in vivo.

Study design

Examination of the in vitro and in vivo stability of a protease-resistant D-form of the peptide, RI-TAT-RasGAP^{317-326'}, and its effect on tumor growth in nude mice bearing subcutaneous human colon cancer HCT116 xenograft tumors.

Contribution

RI-TAT-RasGAP³¹⁷⁻³²⁶ was stable in biological fluids, and after injection into mice, it persisted in the bloodstream for more than 1 hour, reached distant tissues and subcutaneous tumors, was effective at doses at least 150-fold below the dose lethal to 50% of mice, and improved the efficacy of genotoxins.

Implications

RI-TAT-RasGAP³¹⁷⁻³²⁶ may be useful for improving the efficacy of chemotherapy in patients.

Limitations

Tumors in nude (ie, immunocompromised) mice may not behave the same as syngeneic tumors in immunocompetent mice.

From the Editors

that cisplatin in combination with the peptide hampers tumor growth better than cisplatin alone.

In the second type of experiment, HCT116 cells were injected subcutaneously into the left and right upper flanks of 7-week-old female nude mice (2.5×10^5 cells injected per flank). One week later, when visible tumors had developed, the mice were injected intraperitoneally once per day for 1 week with PBS, RI-TAT-RasGAP³¹⁷⁻³²⁶ (1.65 mg/kg body weight), or cisplatin (0.5 mg/kg body weight) or doxorubicin (0.25 mg/kg body weight; catalog no. D1515, Sigma-Aldrich), alone or in combination with RI-TAT-RasGAP³¹⁷⁻³²⁶ ($n=4-7$ mice per group). We tested doxorubicin because it is structurally different from cisplatin and has a different mode of action (15). The orthogonal dimensions of

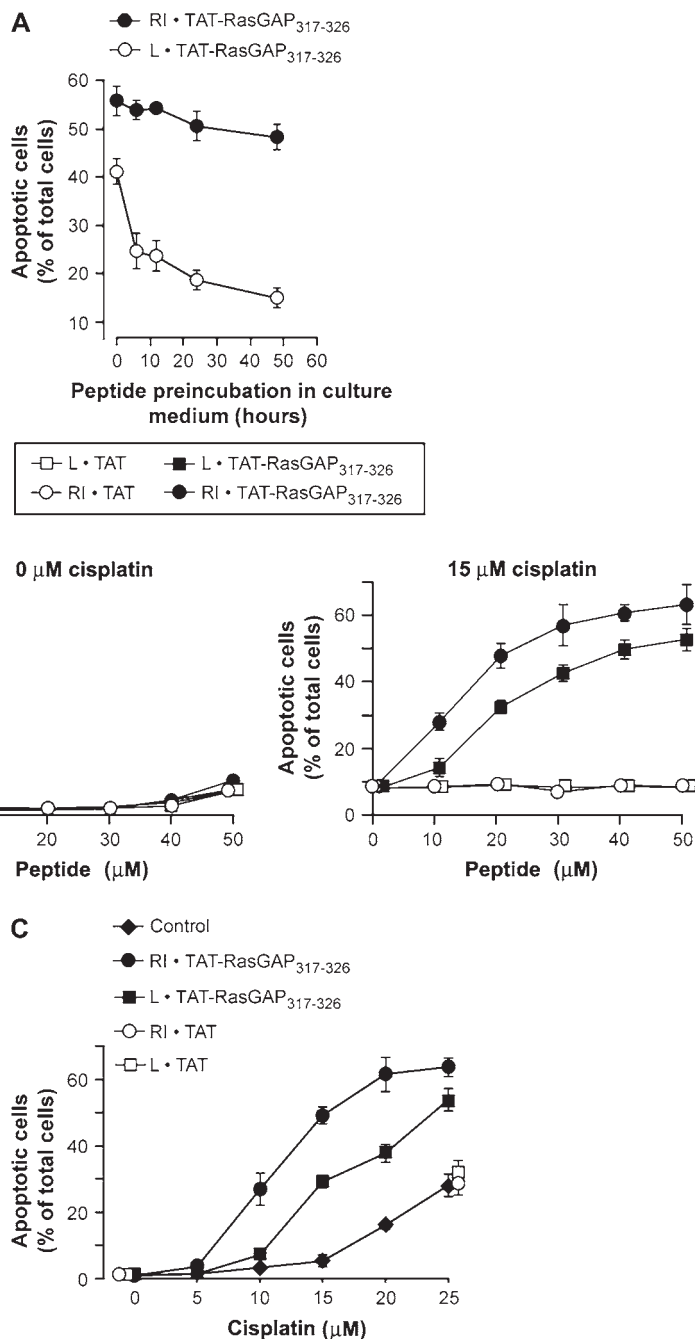
a 7-week-old female NMRI Nu/Nu (nude) mouse (Janvier, Le Genest-St-Isle, France) that received a single intraperitoneal injection with the peptide at 3.3 mg/kg body weight. All experiments involving mice were approved by the State of Vaud Veterinary Office (Lausanne, Switzerland). RI-TAT-RasGAP³¹⁷⁻³²⁶ was detectable in the circulation as early as 15 minutes after injection and for at least 90 minutes after injection; peak concentrations were observed 1 hour after the injection of the peptide (Supplementary Figure 1, A and B, available online). By contrast, we could not detect the peptide in blood samples obtained from two mice that were similarly injected with L-TAT-RasGAP³¹⁷⁻³²⁶ (data not shown), consistent with the notion that the L-peptide is less stable, or more rapidly cleared, than the retro-inverso form. The observation that RI-TAT-RasGAP³¹⁷⁻³²⁶ could be detected in the circulation for relatively long periods of time suggested that it might be able to reach distant tissues, including tumors, after it is injected into mice. To test this possibility, a nude mouse bearing a visible tumor derived from subcutaneous injection of human colon cancer HCT116 cells was injected intraperitoneally with RI-TAT-RasGAP³¹⁷⁻³²⁶ (4.8 mg/kg body weight). The mouse was killed approximately 1 hour after peptide injection, and its liver, lungs, brain, and the tumor were removed and processed for peptide detection by mass spectrometry. RI-TAT-RasGAP³¹⁷⁻³²⁶ was detectable in the liver and lungs of this mouse but was not found in the brain (Supplemental Figure 1, C, available online), suggesting that it may not cross the blood-brain barrier. Importantly, RI-TAT-RasGAP³¹⁷⁻³²⁶ was also detected in the subcutaneous tumor.

We next evaluated the toxicity of RI-TAT-RasGAP³¹⁷⁻³²⁶ in nude mice that were injected intraperitoneally twice per week for 4 weeks with RI-TAT-RasGAP³¹⁷⁻³²⁶ or RI-TAT (a control peptide consisting of the retro-inverso form of the TAT peptide) (dose range=0.8–7.2 mg peptide/kg body weight; $n=3-4$ mice per group). Intraperitoneal injection of RI-TAT-RasGAP³¹⁷⁻³²⁶ at a dose of 4.8 mg/kg of mouse body weight was lethal (three of the three injected mice died, all within 45–60 minutes after the first injection), whereas a dose of 2.4 mg/kg body weight was not,

even after repeated injections (three of the three injected mice were alive after the eighth injection) (Supplementary Table 1, available online). These results indicate that the dose of RI-TAT-RasGAP³¹⁷⁻³²⁶ that is lethal to 50% of mice (ie, the LD₅₀) is between 2.4 and 4.8 mg/kg body weight. The lethality induced by high doses of RI-TAT-RasGAP³¹⁷⁻³²⁶ did not seem to be due to the presence of the cell-permeable TAT peptide because none of the three mice injected intraperitoneally with RI-TAT at a dose of 4.8 mg/kg body weight died. Necropsy revealed that the cause of death in mice injected with lethal doses of RI-TAT-RasGAP³¹⁷⁻³²⁶ appeared to be massive hemorrhages in the lungs and kidneys (Supplementary Figure 1, D, available online). No damage to the liver, pancreas, or spleen was observed (data not shown).

We next conducted two types of in vivo experiments to examine the effect of RI-TAT-RasGAP³¹⁷⁻³²⁶ on the efficacy of cisplatin against tumors, in particular under conditions in which the doses of cisplatin had poor or marginal effects. In the first experiment, 7-week-old female nude mice were injected intraperitoneally with 1.5×10^6 HCT116 cells. Beginning the next day, the mice were injected intraperitoneally twice per week for 4 weeks with phosphate-buffered saline (PBS), cisplatin (1 mg/kg body weight; catalog no. P4394, Sigma-Aldrich, St Louis, MO), RI-TAT-RasGAP³¹⁷⁻³²⁶ (2.4 mg/kg body weight), or cisplatin plus RI-TAT-RasGAP³¹⁷⁻³²⁶ ($n=15-24$ mice per group). At the end of the treatment period, the mice were killed by cervical dislocation, and their tumors were removed, weighed (when possible), and scored empirically as follows: tumors weighing more than 1 mg (score 5), tumors weighing more than 0.5 mg up to 1 mg (score 4), tumors weighing more than 0.1 mg up to 0.5 mg (score 3), vascularized tumors grouped in clumps but too small to be weighed (score 2), or nonvascularized dispersed tumors too small to be weighed (score 1). Mice treated with RI-TAT-RasGAP³¹⁷⁻³²⁶ plus cisplatin developed statistically significantly fewer tumors with higher scores than mice treated with cisplatin alone ($P=.032$, two-sample location exact two-sided Wilcoxon test; all statistical analyses were performed using SAS/STAT software v9.1.3, SAS Institute, Inc. (Cary, NC) (Figure 2, A). This finding indicates

Figure 1. Effects of the L and the RI forms of TAT-RasGAP₃₁₇₋₃₂₆ on cisplatin-induced apoptosis in U2OS cells. Sequences of the peptide used in the figure: RI-TAT-RasGAP₃₁₇₋₃₂₆' DTRLNTVWM-WGRRRQRKKRG (D-amino acid); L-TAT-RasGAP₃₁₇₋₃₂₆' GRKKRRQRRRGGWMMVVTNLRTD (L-amino acid); RI-TAT, RRRQRKKRG (D-amino acid); and L-TAT, GRKKRRQRRR (L-amino acid). Apoptosis was assessed by counting the cells that displayed a pycnotic nucleus. The results presented in each panel correspond to the mean percentage of apoptotic cells for three independent experiments; **error bars** correspond to 95% confidence intervals. **A)** Peptide functional stability assay. U2OS cells were incubated for 20 hours with 15 μ M cisplatin plus the indicated peptides, which were previously preincubated for the indicated times in Dulbecco's modified Eagle medium containing 10% newborn calf serum. Apoptosis was then assessed. **B)** Tumor cell sensitization in response to increasing peptide concentrations. U2OS cells were treated for 20 hours with increasing concentrations of the indicated peptides in the absence (**left panel**) or presence (**right panel**) of 15 μ M cisplatin. Apoptosis was then assessed. **C)** Tumor cell sensitization induced by the peptides in response to increasing cisplatin concentrations. U2OS cells were treated for 20 hours without (Control) or with (20 μ M final concentration) the indicated peptides in the presence of increasing concentrations of cisplatin. Apoptosis was then assessed. The values for L-TAT and RI-TAT are slightly offset for better visualization. L=natural; RI=retro-inverso.



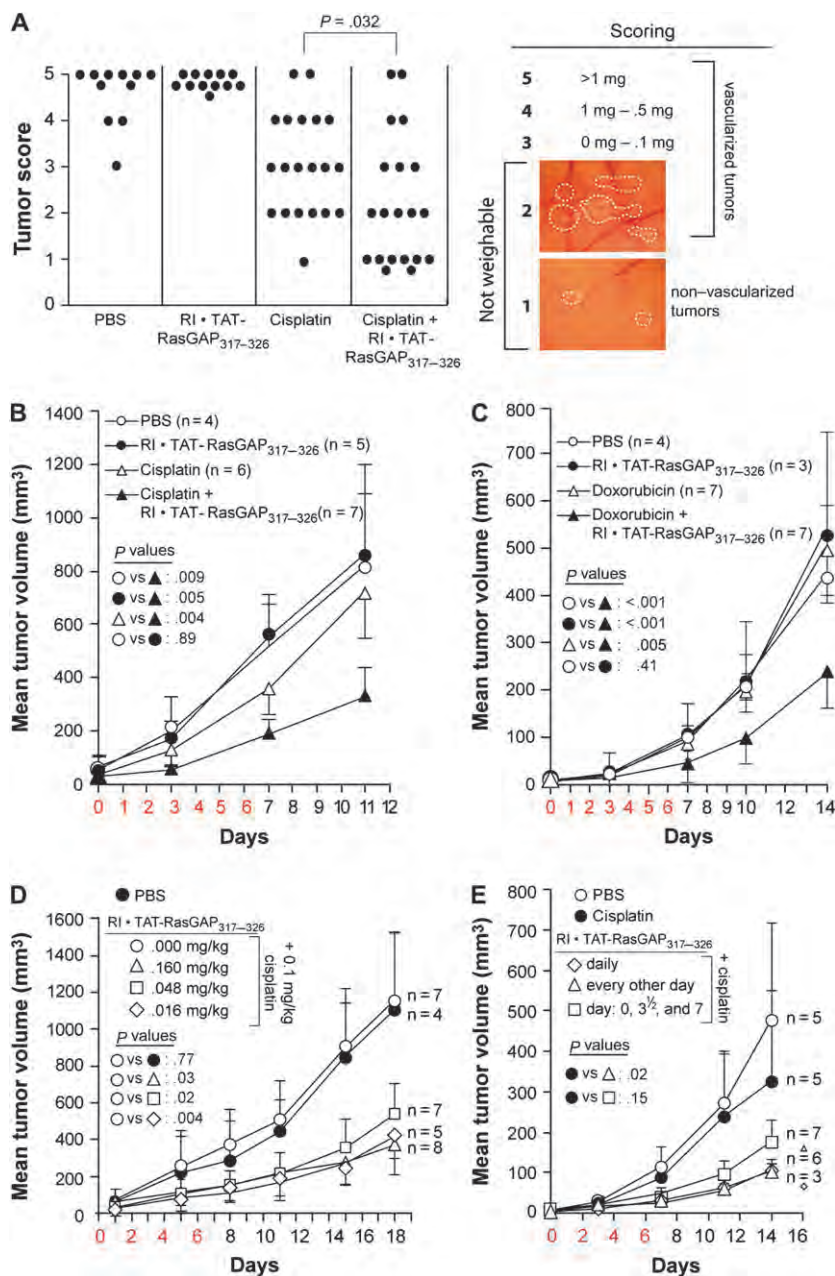
the tumors were measured daily with the use of a caliper on isoflurane-anesthetized mice, beginning on the first day of treatment injection (day 0, ie, when tumors were just visible), for up to 13 days. Tumor volume was calculated as [(largest orthogonal dimension)² × (smallest orthogonal dimension) × ($\pi/6$)]. When a mouse developed tumors on both flanks, the volumes of the two tumors were averaged to get a single value for that mouse to allow statistical comparisons with mice that developed only one tumor. All mice in a given experiment

were killed by cervical dislocation while still anesthetized when the largest tumors exceeded a specific threshold volume (500–1000 mm³, depending on the experiment). Mice treated with RI-TAT-RasGAP₃₁₇₋₃₂₆ plus either cisplatin or doxorubicin developed statistically significantly smaller tumors than mice treated with RI-TAT-RasGAP₃₁₇₋₃₂₆ ($P=.005$ and $P<.001$, respectively) or with the respective genotoxin alone ($P=.004$ and $P=.005$, respectively; repeated measures analysis of variance [ANOVA, two-sided]) (Figure 2, B and C).

Compared with PBS, RI-TAT-RasGAP₃₁₇₋₃₂₆ by itself had no effect on tumor growth ($P=.89$ and $P=.41$ for the cisplatin and doxorubicin experiments, respectively; repeated measures ANOVA [two-sided]). These data demonstrate that RI-TAT-RasGAP₃₁₇₋₃₂₆ can inhibit the growth of already formed and detectable tumors when used in combination with a genotoxin (cisplatin or doxorubicin).

Given our finding that one injection of a lethal dose of TAT-RasGAP₃₁₇₋₃₂₆ led to hemorrhages in lungs and kidneys

Figure 2. In vivo chemosensitizing efficacy of RI-TAT-RasGAP₃₁₇₋₃₂₆. **A** Effect of RI-TAT-RasGAP₃₁₇₋₃₂₆ on intraperitoneal tumors. Nude mice (7-week-old females) were injected with 1.5 million HCT116 cells intraperitoneally. The following day and thereafter twice a week, the mice were injected intraperitoneally with PBS, 2.4 mg/kg of RI-TAT-RasGAP₃₁₇₋₃₂₆, 1 mg/kg cisplatin, or a combination of cisplatin and RI-TAT-RasGAP₃₁₇₋₃₂₆. After 28 days, the mice were killed and the development of the tumors scored (score 5, tumors weighing more than 1 mg; score 4, tumors weighing between 0.5 and 1 mg; score 3, tumors weighing between 0.1 and 0.5 mg; score 2, vascularized tumors grouped in clumps but too small to be weighed; and score 1, nonvascularized dispersed tumors too small to be weighed); examples of tumors with scores 1 and 2 are shown on the right in **(A)**. Mice that did not show any presence of tumors (ie, mice in which the tumors did not “take”) were excluded from the analysis (PBS: four mice excluded of 15 injected; RI-TAT-RasGAP₃₁₇₋₃₂₆: three mice excluded of 15 injected; cisplatin: one mouse excluded of 21 injected; cisplatin + RI-TAT-RasGAP₃₁₇₋₃₂₆: four mice excluded of 24 injected); the proportion of excluded mice did not differ statistically significantly among the groups (Fisher exact test, $P = .225$). The **dots** represent individual mice. Statistical analysis for the difference between the cisplatin and the cisplatin + RI-TAT-RasGAP₃₁₇₋₃₂₆ groups was performed with a two-sample location exact two-sided Wilcoxon test. **B and C**) Cisplatin- and doxorubicin-sensitizing effect of RI-TAT-RasGAP₃₁₇₋₃₂₆ on subcutaneous tumors. Nude mice (7-week-old females) were injected subcutaneously with 250000 HCT116 cells on the left and right upper flanks. Seven days later, the mice that developed visible tumors were injected each day for 7 consecutive days (in **red** in the figure) with PBS (300 μ L), RI-TAT-RasGAP₃₁₇₋₃₂₆ (1.65 mg/kg in 300 μ L PBS), cisplatin (0.5 mg/kg in 300 μ L PBS), or RI-TAT-RasGAP₃₁₇₋₃₂₆ plus cisplatin **(B)**. In the experiment described in **(C)**, cisplatin was replaced with 0.25 mg/kg doxorubicin. Tumor volume was plotted as a function of time (for mice that developed tumors on both flanks, the two tumor volumes were averaged). The number of mice analyzed is indicated in the figure. Mean values are plotted, and **error bars** correspond to 95% confidence intervals. **D**) Dose–response analysis of the in vivo sensitizing effect of the peptide. Nude mice were treated and analyzed as in **(B)** but with the conditions indicated in the figure. **E**) Peptide injection frequency. Nude mice were injected subcutaneously with 500000 HCT116 cells and treated as described in **(D)**, except that 0.16 mg/kg body weight RI-TAT-RasGAP₃₁₇₋₃₂₆ was injected on the indicated days [open diamonds, triangles, and squares; cisplatin was injected every day as in **(D)**]. The P values in **(B–E)** are from repeated measures ANOVA (two-sided). ANOVA=analysis of variance; PBS=phosphate-buffered saline; RI=retro-inverso.



(Supplementary Figure 1, D, available online), we assessed whether the nonlethal dose of RI-TAT-RasGAP₃₁₇₋₃₂₆ that enhanced the sensitivity of tumors to cisplatin and doxorubicin in the previous experiment had any effect on these organs. Non-tumor-bearing mice were injected with PBS, RI-TAT-RasGAP₃₁₇₋₃₂₆, cisplatin, or RI-TAT-RasGAP₃₁₇₋₃₂₆ plus cisplatin as described above (n=2 mice per group); the mice were killed by cervical dislocation after the last injection (ie, 8 days after the first injection), and histological sections of

their lungs and kidneys were prepared. We observed no damage to these organs in any of the mice (Supplementary Figure 1, E, available online). Thus, a nonlethal dose of RI-TAT-RasGAP₃₁₇₋₃₂₆ (1.65 mg/kg body weight), which was only approximately two- to three fold lower than the lethal dose (~5 mg/kg body weight), did not appear to cause visible alterations in the lungs or kidneys, even when it was administered in the presence of cisplatin.

To examine if RI-TAT-RasGAP₃₁₇₋₃₂₆ doses lower than 1.65 mg/kg body weight

could exert a genotoxin-sensitizing effect on tumor growth in mice, we used the experimental design described above but with decreasing doses of injected RI-TAT-RasGAP₃₁₇₋₃₂₆ and with a dose of cisplatin that is at the threshold of inducing an inhibitory effect on tumor growth by itself. This dose of cisplatin was determined by injecting mice with various doses of cisplatin only (range=0.005–1 mg/kg body weight) using the injection protocol shown in Figure 2, B. The highest dose of cisplatin tested that did not reduce tumor growth was found to be

0.1 mg/kg body weight (data not shown). HCT116 tumor-bearing mice were treated with PBS or RI-TAT-RasGAP³¹⁷⁻³²⁶ (at doses of 0, 0.16, 0.048, or 0.160 mg/kg body weight) combined with cisplatin at 0.1 mg/kg body weight (n=4–8 mice per group). Cisplatin alone (0.1 mg/kg body weight) had no effect on the growth of HCT116 tumors compared with PBS ($P=.77$; repeated measures ANOVA [two-sided]) (Figure 2, D). However, cisplatin plus RI-TAT-RasGAP³¹⁷⁻³²⁶ at 0.16 mg/kg body weight efficiently inhibited tumor growth compared with cisplatin alone ($P=.03$; repeated measures ANOVA [two-sided]). Importantly, RI-TAT-RasGAP³¹⁷⁻³²⁶ at 0.016 mg/kg body weight, a dose more than 150-fold lower than the estimated LD₅₀ (ie, between 2.4 and 4.8 mg/kg body weight), also improved the efficacy of cisplatin to inhibit the growth of HCT116 tumors compared with cisplatin alone ($P=.004$; repeated measures ANOVA [two-sided]).

We also examined the effect of varying the frequency of RI-TAT-RasGAP³¹⁷⁻³²⁶ peptide injection on tumor growth. HCT116 tumor-bearing mice were injected for 1 week with RI-TAT-RasGAP³¹⁷⁻³²⁶ (0.16 mg/kg body weight), daily, every other day, or every 3.5 days, in combination with a daily injection of cisplatin (0.1 mg/kg body weight) (n=3–7 mice per group). Control mice were injected daily with PBS or cisplatin alone. Tumor volumes were measured every 3–4 days. Injection of the peptide every other day sensitized tumor cells to cisplatin (every-other-day peptide injection + cisplatin vs cisplatin only: $P=.02$; repeated measures ANOVA [two-sided]) as efficiently as daily injection of the peptide (every-other-day peptide injection + cisplatin vs daily peptide injection + cisplatin: $P=.94$; repeated measures ANOVA [two-sided]). Injection of the peptide every 3.5 days also sensitized the tumors somewhat to cisplatin (every 3.5 days peptide injection + cisplatin vs cisplatin only: $P=.15$; repeated measures ANOVA [two-sided]) but with reduced efficiency compared with daily or every-other-day injections of the peptide. These results indicate that RI-TAT-RasGAP³¹⁷⁻³²⁶ does not need to be injected every day along with cisplatin to exert its sensitization property, probably because of its increased resistance to degradation in biological fluids.

A limitation of this study is that tumors in immunocompromised mouse models

(eg, nude mice) may not behave as syngeneic tumors in immunocompetent mice. Indeed, there is now clear evidence that the immune system positively modulates some anticancer therapies (16). For example, doxorubicin-induced death of colon carcinoma cells implanted in syngeneic mice elicits an immune response that favors the elimination of the tumor cells (17). The efficacy of RI-TAT-RasGAP³¹⁷⁻³²⁶ against human tumors implanted in nude mice might therefore be attenuated by the lack of an intact immune system in nude mice.

The properties of RI-TAT-RasGAP³¹⁷⁻³²⁶ described here in mouse tumor models indicate that this peptide has the potential to be used in humans to sensitize tumor cells to genotoxin treatments (ie, to enhance the antitumor effect of genotoxins): it is stable in biological fluids, it persists in the bloodstream for more than 1 hour after intraperitoneal injection, it reaches distant tissues and organs (including subcutaneous tumors), its efficacious doses are at least 100-fold below the LD₅₀, and it greatly improves the efficacy of genotoxins. To our knowledge, this peptide is the only compound that has been shown to improve the efficacy of genotoxins and that behaves strictly as a chemosensitizer, that is, it has no effect on tumors by itself (4). This compound would therefore have the potential to improve the efficacy of chemotherapeutic agents that are currently used in the clinic, particularly in situations in which doses of genotoxin have to be lowered to reduce side effects.

References

1. Debatin K-M. Apoptosis pathways in cancer and cancer therapy. *Cancer Immunol Immunother*. 2004;53(3):153–159.
2. Schmitt CA, Lowe SW. Apoptosis and therapy. *J Pathol*. 1999;187(1):127–137.
3. Mendoza FJ, Espino PS, Cann KL, Bristow N, McCrea K, Los M. Anti-tumor chemotherapy utilizing peptide-based approaches—apoptotic pathways, kinases, and proteasome as targets. *Arch Immunol Ther Exp (Warsz)*. 2005;53(1):47–60.
4. Michod D, Widmann C. DNA-damage sensitizers: potential new therapeutical tools to improve chemotherapy. *Crit Rev Oncol Hematol*. 2007;63(2):160–171.
5. Yang J-Y, Widmann C. Antiapoptotic signaling generated by caspase-induced cleavage of RasGAP. *Mol Cell Biol*. 2001;21(23):5346–5358.
6. Yang J-Y, Walicki J, Michod D, Dubuis G, Widmann C. Impaired Akt activity downmodulation, caspase-3 activation, and apoptosis in cells expressing a caspase-resistant mutant

of RasGAP at position 157. *Mol Biol Cell*. 2005;16(8):3511–3520.

7. Michod D, Yang JY, Chen J, Bonny C, Widmann C. A RasGAP-derived cell permeable peptide potently enhances genotoxin-induced cytotoxicity in tumor cells. *Oncogene*. 2004;23(55):8971–8978.
8. Rehm M, Huber HJ, Dussmann H, Prehn JH. Systems analysis of effector caspase activation and its control by X-linked inhibitor of apoptosis protein. *EMBO J*. 2006;25(18):4338–4349.
9. Michod D, Widmann C. TAT-RasGAP³¹⁷⁻³²⁶ requires p53 and PUMA to sensitize tumor cells to genotoxins. *Mol Cancer Res*. 2007;5(5):497–507.
10. Widmann C, Maryanski JL, Romero P, Corradin G. Differential stability of antigenic MHC class I-restricted synthetic peptides. *J Immunol*. 1991;147(11):3745–3751.
11. Blanchet JS, Valmori D, Dufau I, et al. A new generation of Melan-A/MART-1 peptides that fulfill both increased immunogenicity and high resistance to biodegradation: implication for molecular anti-melanoma immunotherapy. *J Immunol*. 2001;167(10):5852–5861.
12. Ponten J, Saksela E. Two established in vitro cell lines from human mesenchymal tumours. *Int J Cancer*. 1967;2(5):434–447.
13. Chorev M, Goodman M. Recent developments in retro peptides and proteins—an ongoing topochemical exploration. *Trends Biotechnol*. 1995;13(10):438–445.
14. Fischer PM. The design, synthesis and application of stereochemical and directional peptide isomers: a critical review. *Curr Protein Pept Sci*. 2003;4(5):339–356.
15. Momparler RL, Karon M, Siegel SE, Avila F. Effect of adriamycin on DNA, RNA, and protein synthesis in cell-free systems and intact cells. *Cancer Res*. 1976;36(8):2891–2895.
16. de la Cruz-Merino L, Grande-Pulido E, Alberto-Tamarit A, Codes-Manuel de Villena ME. Cancer and immune response: old and new evidence for future challenges. *Oncologist*. 2008;13(12):1246–1254.
17. Casares N, Pequignot MO, Tesniere A, et al. Caspase-dependent immunogenicity of doxorubicin-induced tumor cell death. *J Exp Med*. 2005;202(12):1691–1701.

Funding

Swiss National Science Foundation (31003A_119876 to C.W.). D. Michod and C. Widmann are coinventors of the TAT-RasGAP³¹⁷⁻³²⁶ compound as a genotoxin sensitizer (patent owned by the University of Lausanne) and may receive royalties from patent licensing if the compound is commercialized. The authors did not receive any specific support from private or institutional bodies that might have commercial interests in the patented product.

Notes

D. Michod and A. Annibaldi contributed equally to this work.

We thank Dr Rudolf Kraftsik for the statistical analyses of the data.

Manuscript received April 30, 2008; revised February 19, 2009; accepted March 27, 2009.

Results

Part III

Introduction

Peptides enhancing the genotoxin-induced cell death in cancer cells could improve the efficacy of anti-cancer regimens and the survival of cancer patients. Our group discovered that fragment N2, generated by the caspase 3-mediated cleavage of RasGAP, favours the genotoxin-induced apoptosis of cancer cells. These sensitizing properties reside within a 10 amino acids stretch (317-326) that was fused to the TAT cell permeation sequence. The resulting peptide, called TAT-RasGAP₃₁₇₋₃₂₆, still bears sensitizing properties *in vitro* and *in vivo*. The molecular mechanisms by which TAT-RasGAP₃₁₇₋₃₂₆ fulfills its anti-cancer properties is not well understood.

One potential candidate to explain how TAT-RasGAP₃₁₇₋₃₂₆ delivers its pro-apoptotic effect in the presence of genotoxins was the RasGAP SH3 binding protein 1 (G3BP1). G3BP1 is an endoribonuclease known to associate to RasGAP in proliferating cells. Interestingly G3BP1 binds the SH3 domain of RasGAP in correspondence to the ten amino acids stretch (amino acids 317-326) that composes the TAT-RasGAP₃₁₇₋₃₂₆ peptide. This evidence, together with others showing that G3BP1 is involved in the regulation of mRNA stability, in the cell adaptation to several kinds of stresses and that it is over-expressed in various human tumors (e.g. breast cancer), prompted us to ascertain if G3BP1 was the TAT-RasGAP₃₁₇₋₃₂₆ effector.

In this report we show not only that G3BP1 is not involved at all in the TAT-RasGAP₃₁₇₋₃₂₆-mediated sensitization of malignant cells to apoptosis, but also that neither RasGAP nor fragment N2 (the caspase-3-generated RasGAP fragment from which the sensitizing sequence 317-326 was derived) are G3BP1 binding partners.

Contribution

This work has been published in Plos ONE in 2011 and it is attached in the following section. All the experiments were performed by me. *In silico* protein docking assays were performed by Aline Dousse.

Revisiting G3BP1 as a RasGAP Binding Protein: Sensitization of Tumor Cells to Chemotherapy by the RasGAP 317–326 Sequence Does Not Involve G3BP1

Alessandro Annibaldi¹, Aline Dousse¹, Sophie Martin², Jamal Tazi², Christian Widmann^{1*}

¹ Department of Physiology, University of Lausanne, Lausanne, Switzerland, ² Institut de Génétique Moléculaire de Montpellier UMR 5535, IFR 122, Centre National de Recherche Scientifique, Montpellier, France

Abstract

RasGAP is a multifunctional protein that controls Ras activity and that is found in chromosomal passenger complexes. It also negatively or positively regulates apoptosis depending on the extent of its cleavage by caspase-3. RasGAP has been reported to bind to G3BP1 (RasGAP SH3-domain-binding protein 1), a protein regulating mRNA stability and stress granule formation. The region of RasGAP (amino acids 317–326) thought to bind to G3BP1 corresponds exactly to the sequence within fragment N2, a caspase-3-generated fragment of RasGAP, that mediates sensitization of tumor cells to genotoxins. While assessing the contribution of G3BP1 in the anti-cancer function of a cell-permeable peptide containing the 317–326 sequence of RasGAP (TAT-RasGAP_{317–326}), we found that, in conditions where G3BP1 and RasGAP bind to known partners, no interaction between G3BP1 and RasGAP could be detected. TAT-RasGAP_{317–326} did not modulate binding of G3BP1 to USP10, stress granule formation or *c-myc* mRNA levels. Finally, TAT-RasGAP_{317–326} was able to sensitize G3BP1 knock-out cells to cisplatin-induced apoptosis. Collectively these results indicate that G3BP1 and its putative RasGAP binding region have no functional influence on each other. Importantly, our data provide arguments against G3BP1 being a genuine RasGAP-binding partner. Hence, G3BP1-mediated signaling may not involve RasGAP.

Citation: Annibaldi A, Dousse A, Martin S, Tazi J, Widmann C (2011) Revisiting G3BP1 as a RasGAP Binding Protein: Sensitization of Tumor Cells to Chemotherapy by the RasGAP 317–326 Sequence Does Not Involve G3BP1. PLoS ONE 6(12): e29024. doi:10.1371/journal.pone.0029024

Editor: Laszlo Buday, Hungarian Academy of Sciences, Hungary

Received: August 11, 2011; **Accepted:** November 18, 2011; **Published:** December 19, 2011

Copyright: © 2011 Annibaldi et al. This is an open-access article distributed under the terms of the Creative Commons Attribution License, which permits unrestricted use, distribution, and reproduction in any medium, provided the original author and source are credited.

Funding: This work was supported by Swiss National Science Foundation grant 31003A_119876 (to CW). The funder had no role in study design, data collection and analysis, decision to publish, or preparation of the manuscript.

Competing Interests: CW is a coinventor of the TAT-RasGAP_{317–326} compound as a genotoxin sensitizer (patent owned by the University of Lausanne) and may receive royalties from patent licensing if the compound is commercialized. Patent numbers and dates are WO 2005000887 (30.6.2003) and WO 2010097720 (30.1.2009). This does not alter the authors' adherence to all the PLoS ONE policies on sharing data and materials. The authors did not receive any specific support from private or institutional bodies that might have commercial interests in the patented product.

* E-mail: Christian.Widmann@unil.ch

Introduction

There is an ongoing need to improve current anti-tumor regimens to reduce the rate of death due to cancer. In this context, we discovered earlier that the caspase-3-generated RasGAP N-terminal fragment (RasGAP_{158–455}), called N2, was able to selectively sensitize cancer cells, but not healthy cells, to genotoxin-induced apoptosis [1]. RasGAP amino acids 317 to 326 within fragment N2 were found to carry this sensitizing activity [2]. A cell-permeable peptide containing this sequence (the so-called TAT-RasGAP_{317–326} peptide) was then generated [2]. This peptide potently enhances the efficacy of genotoxins to selectively kill cancer cells, both in *in vivo* [3] and *in vitro* [2] settings. TAT-RasGAP_{317–326} does not induce apoptosis by itself making it a pure sensitizer compound [2–4]. The understanding of its mode of action is of particular relevance in the context of the mechanisms allowing cancer cells to resist apoptosis. It is known that TAT-RasGAP_{317–326} favors genotoxin-induced mitochondrial outer membrane depolarization (MOMP) and caspase-3 activation [5]. The RasGAP-derived peptide requires a functional p53/PUMA axis to induce its genotoxin-sensitization effect [5]. However, this might only reflect the fact that genotoxins require the p53/PUMA axis to optimally kill

cancer cells [6,7]. At present, the direct molecular target(s) of TAT-RasGAP_{317–326} are unknown and the cellular events underlying its sensitizing properties are only minimally understood.

GAP SH3 Binding Protein 1 (G3BP1) is one of the molecules described to interact with RasGAP. This was first reported by Parker *et al.* in 1996 [8] who identified and cloned a molecule able to bind to the SH3 domain of RasGAP. Incidentally, this interaction only took place in serum-stimulated cells. The binding between RasGAP and G3BP1 could be prevented by a peptide corresponding to sequence 317–326 found within the RasGAP SH3 domain. These data were corroborated by two other reports showing that G3BP1 binds to RasGAP in proliferating cells [9] and that the G3BP1 domain responsible for these binding was the nuclear transfer factor 2 (NTF2)-like domain, located at its N-terminus [10]. This domain was also described to mediate the binding of the yeast orthologue of G3BP1 (Bre5) to the Ubp3 deubiquitinating enzyme [11]. G3BP1 seems not to be a substrate of USP10, the Ubp3 mammalian orthologue, but it appears to inhibit the capacity of USP10 to cleave ubiquitin chains [12]. The C-terminal portion of G3BP1 contains two canonical RNA recognition motifs (RRMs) indicating that G3BP1 has RNA-binding capacities. Indeed G3BP1 was reported to co-immuno-

precipitate with mRNAs and to bind to and cleave the 3' untranslated region (3'UTR) of the *c-myc* mRNA *in vitro* [9]. Interestingly, the endoribonuclease activity of G3BP1 is governed by its phosphorylation status. In proliferating cells, when G3BP1 is hypo-phosphorylated, it loses its ability to cleave mRNA whereas in quiescent cells, when it is hyper-phosphorylated, it does cleave mRNAs [9]. This observation suggested a possible role of G3BP1 in coupling extra-cellular stimuli to mRNA stability. This hypothesis is supported by the finding that G3BP1 is implicated in stress granule (SG) assembly [13]. SGs correspond to cytoplasmic loci where mRNAs are stored during stress conditions and where the decision to degrade or convert them into translationally active mRNA protein complexes (mRNPs) is taken once the stress has subsided [14–16]. Formation of stress granules in cells may inhibit apoptosis [17].

The observation that G3BP1 binds to RasGAP on the very same sequence that mediates the tumor sensitizing activity of fragment N2 and the fact that G3BP1 is over-expressed in some cancer cells made G3BP1 a good candidate for the TAT-RasGAP_{317–326} peptide ability to lower the resistance specifically in cancer cells. We therefore investigated whether the known functions attributed to G3BP1 could be modulated by TAT-RasGAP_{317–326} and whether G3BP1 was required for the peptide to sensitize tumor cells to genotoxin-induced apoptosis.

Materials and Methods

Cell lines and transfection

U2OS (LGC Promochem; ATCC n° HTB-96), HCT116 [18], HEK293T [19], HeLa cells (LGC Promochem; ATCC n° CCL-2), and CCL39 cells (LGC Promochem; ATCC n° CCL-39), as well as wild-type and G3BP1 knock-out mouse embryonic fibroblasts (MEFs) [20] were maintained in DMEM (Invitrogen reference n°61965) containing 10% fetal calf serum (GIBCO/BRL reference n°10270-106, lot n°41Q6001K) at 37°C and 5% CO₂. HEK293T and U2OS cells were transfected using the calcium/phosphate precipitation procedure [2,21].

Buffers

The composition of phosphate buffered saline (PBS) is 116 mM NaCl, 10.4 mM Na₂HPO₄, 3.2 mM KH₂PO₄ (pH 7.4). The Stag lysis buffer is made of 50 mM Hepes pH 7.4, 150 mM NaCl, 1.5 mM MgCl₂, 1 mM EGTA pH 8.0, 10% glycerol, 1% Triton X-100, and is supplemented with one tablet of EDTA-free inhibitor (Roche) per 50 ml. The composition of sample buffer 2X is 25 mM 2-amino-2-(hydroxymethyl)-1,3-propanediol (Tris) HCl pH 6.5, 10% glycerol, 6% SDS, 0.02% of bromophenol blue and 100 mM freshly added dithiothreitol (DTT). The 1% Triton X-100 lysis buffer is made of 20 mM Hepes pH 7.4, 150 mM NaCl, 1% Triton X-100, 1 mM MgCl₂, 1 mM EGTA and 1 mM NaVO₄ supplemented with one tablet of EDTA-free inhibitor [Roche] per 50 ml. The RIPA-like lysis buffer is made of 50 mM Tris-HCl pH 7.4, 150 mM NaCl, 1% NP-40, 0.25% deoxycholic acid, 1 mM EGTA and 1 mM NaVO₄ supplemented with one tablet of EDTA-free inhibitor (Roche) per 50 ml. The composition of sample buffer 5X is 250 mM Tris-HCl pH 7, 10% SDS, 30% glycerol, 5% β-mercaptoethanol. Tris buffer saline (TBS) is made of 20 mM Tris base, 130 mM NaCl, pH 7.6.

Antibodies

The monoclonal antibody specific for the hemagglutinin (HA) tag was purchased as ascites from BabCo (reference n°MMS-101R). This antibody was adsorbed on HeLa cell lysates to

decrease non-specific binding as described previously [22]. Mouse anti-human G3BP1 was from BD Transduction Laboratories (reference n°611127). The rabbit polyclonal anti human TIA-1 antibody was from Santa Cruz (reference n°sc-28237). The anti S-Protein HRP-conjugated antibody was from Novagen (reference n°69047). The anti-GST antibody was from Upstate (reference n°06-332). The polyclonal rabbit anti-c-Myc antibody was from Cell Signaling (reference n°9402). The polyclonal rabbit anti-RasGAP antibody directed at the Src homology (SH) domains of RasGAP was from Enzo Life Sciences (reference n°ALX-210-860-R100). The monoclonal mouse anti-SV40 large T antigen was from BD Pharmingen (reference n°554149). The rabbit anti-USP10 antibody was provided by Dr. Olivier Staub (University of Lausanne, Switzerland). The monoclonal mouse anti-V5 antibody was from Invitrogen (reference n°46-0705). Secondary antibodies were donkey anti-mouse fluorescein-conjugated antibody and donkey anti-rabbit Cy3-conjugated antibody (Jackson ImmunoResearch, reference n°715-095-1507 and 711-165-152, respectively).

Plasmids

The extension *.dn3* indicates that the backbone plasmid is pcDNA3 (#1) (Invitrogen). *S-tag* corresponds to the first 15 amino acids of the S-peptide of RNase A (amino acids 1–15 of RNase A). The S-tag is able to bind with high affinity to the S protein (amino acid 21–124 of RNase A) [23,24]. **TRIP-PGK-IRESNEO-WHV** (#350) is a lentiviral vector bearing the neomycine resistance. The **pEGFP-C1** plasmid (#6) encodes the green fluorescent protein and is from Clontech. The **hG3BP1.dn3** plasmid (#322) encodes human G3BP1 [8]. **HA-rRhoGAP.prc** (#196) encodes the HA-tagged form of rat p190RhoGAP. The **6xHis-Stag-mUSP10.dn3** plasmid (#646) encoding the poly-histidine- and S-tagged form of mouse USP10 was described earlier [25]. **HA-hRasGAP.dn3** (#118), previously called HA-GAP.dn3 [22], encodes the HA-tagged form of human RasGAP. **HA-hRasGAP[158–455].dn3** (#145), previously called HA-N2.dn3 [22], encodes the HA-tagged form of fragment N2. **HA-hRasGAP[1–455](D157A).dn3** (#352), previously called N-D157A.dn3 [22], encodes the HA-tagged caspase-3-resistant form of fragment N. **V5-hRasGAP[3–455](D157A).dn3** (#585) encodes a V5-tagged version of the caspase-3-resistant form of fragment N that lacks its first two methionine residues (to prevent potential internal translation events). It was constructed by PCR amplifying HA-hRasGAP[1–455](D157A).dn3 with oligonucleotide #559 [AA (feeder sequences) GGTACC (KpnI site) GCCACC (Kozak sequence) ATG GGA AAA CCA ATA CCA AAT CCA CTA GGC CTA GAC AGT ACA (V5 tag) GCG GCC GAG GCC GGC AGTG (sequences complementary to RasGAP from third amino acid on; nucleotides 124–133 of the human RasGAP mRNA; entry M23379)] and oligonucleotide #560 [GCA ACG AAG TGG GCA GTT TG (sequences lying within the human RasGAP mRNA downstream of the SacII site; nucleotides 489–469 of human RasGAP mRNA; entry M23379)]. The resulting 427 bp PCR fragment was cut with KpnI and SacII and subcloned in HA-hRasGAP[1–455](D157A).dn3 opened with the same enzymes. **V5-hRasGAP[3–1931].dn3** (#686) encodes a V5-tagged version of human RasGAP that lacks its first two methionine residues (to prevent potential internal translation events). It was made by subcloning the SpeI/SacII fragment of V5-hRasGAP[3–455](D157A).dn3 into HA-hRasGAP.dn3 opened with the same enzymes. **HA-hG3BP1.dn3** (#541) encodes an HA-tagged version of human G3BP1. It was produced by PCR amplifying the hG3BP1.dn3 plasmid with oligonucleotide #501 [AAAA (feeder sequences), GGATCC (BamHI site),

GGATCC (Kozak sequence), ATG GGC TAC CCG TAC GAC GTG CCG GAC TAC GCT TCT (HA tag), ATG GTG ATG GAG AAG CCT AG (nucleotides 172–191 of the human G3BP1 mRNA; NCBI entry NM_005754) and oligonucleotide #502 [TTTTT (feeder sequences), GTCGAC (SalI site) TTC ACT GCC GTG GCG CAA GCC CCC TTC (nucleotides 1573–1547 of the human G3BP1 mRNA; NCBI entry NM_005754). The resulting 1465 bp fragment was blunted with T4 DNA polymerase (Promega reference n°M421A), digested with BamHI and subcloned into pcDNA3 opened with BamHI and EcoRV. **Stag-GFP.dn3** (#647) encodes an S-tagged form of the green fluorescent protein (GFP). It was generated by PCR amplifying plasmid pEGFP-C1 with oligonucleotide #686 [AAAAAA (feeder), GGATCC (BamHI site), GCCACC (Kozak sequence), ATG AAA GAA ACC GCT GCT GCT AAA TTC GAA CGC CAG CAC ATG GAC AGC (S-tag), ATG GTG AGC AAG GGC GAG GA (first 20 coding nucleotides of GFP)] and with oligonucleotide #687 [AAA (feeder), CCG TCG ACT GCA GAA TTC GAA GC (nucleotides of pEGFP-C1 surrounding the EcoRI site; underlined)]. The amplified PCR fragment was then digested with BamHI and EcoRI and subcloned into pcDNA3 opened with the same enzymes. **Stag-hRasGAP[158–455].dn3** (#754) encodes the S-tagged form of fragment N2 and was constructed by PCR amplifying plasmid HA-hRasGAP[158–455].dn3 with oligonucleotide #796 [TAAGCAG (feeder sequence), AAGCTT (HindIII), CTCGAG (XhoI), CCACC (Kozak sequence; the last nucleotide of the XhoI recognition site provides the G at the –6 Kozak position), ATG GCG (start codon and alanine codon), AAA GAA ACC GCT GCT GCT AAA TTC GAA CGC CAG CAC ATG GAC AGC (S-tag) TCT CTG GAT GGA CCA GAA TA (first 21 base pairs of fragment N2) and oligonucleotide #679 [GCA TTT AGG TGA CAC TAT AG (nucleotides 1018–999 of pcDNA3)]. The resulting 1027-base pairs PCR fragment was then digested with HindIII and subcloned in HA-hRasGAP[158–455].dn3 opened with the same enzyme. **SV40LargeTantigen.pBABE-puro** (#731) encodes the SV40 large T antigen (Addgene; plasmid 13970). **SV40LargeTantigen.lti-neo** (#738) similarly encodes the large T antigen but in a lentiviral expression vector. It was constructed by subcloning the BamHI 2187 base pairs fragment of SV40LargeTantigen.pBABE-puro into TRIP-PGK-IRESNEO-WHV opened with the same enzyme. **Non-target.pLKO-puro** (#584) corresponds to a pLKO.1-puro lentiviral expression vector containing a shRNA insert that does not target human and mouse genes (Sigma Aldrich, reference n°SHC002). **shRNA-hG3BP1.pLKO-puro** (#641) encodes a shRNA targeting a sequence within the 3'UTR of the human G3BP1 mRNA (nucleotides 1976–1997 of entry NM_005754). It was purchased from Sigma Aldrich. **6xHis-hRasGAP[279–343].pET28** (#544) encodes a histidine-tagged form of the SH3 domain of RasGAP. It was constructed as follows. HA-hRasGAP(no 3'UTR).dn3 (#424) [1] was amplified by PCR using oligonucleotide #505 [AT (feeder) CATATG (NdeI site) AGA AGG CGT GTA CGA GCT AT (human RasGAP; nucleotides 959–978 of NCBI entry M23379)] and oligonucleotide #506 [AT (feeder) GCGGCCG (NotI site) CTA (stop codon) CCG GCC CAC CTC CTC TAC TA (human RasGAP; nucleotides 1143–1122 of NCBI entry M23379)]. The amplified fragment was cut with the NdeI and NotI restriction enzymes and the resulting 192 base pair fragment was subcloned into vector pET-28a(+) (#543) opened with the same enzymes. A PCR-generated A to G silent mutation was found at position 1129 (numbering based on NCBI entry M23379) in 6xHis-hRasGAP[279–343].dn3. **His-TAT-GFP** (#130) encodes a fusion protein made of a stretch of 6 histidine residues, the TAT sequence, and GFP.

S-TAG pull down

Two millions U2OS cells were seeded in a six-well plate and the next day transfected using the calcium/phosphate precipitation procedure. After an additional 24-hour period, cells were lysed in Stag lysis buffer and 1 mg of the lysates were incubated with 1 μ l of biotinylated S-protein (Novagen; reference n°69218) for 3 hours at 4°C. Thirty μ l of streptavidin beads (GE Healthcare BioSciences; reference n°17-5113-01) were then added to the samples and the incubation resumed for an additional 1-hour period. Pull down complexes were then washed 3 times with PBS, 1% NP40 and solubilized in 30 μ l of sample buffer 2X.

Immunoprecipitation

One million cells (either CCL39 or U2OS) were seeded in 10-cm plates and 24 hours later the cells were lysed in 1% Triton X-100 lysis buffer. Alternatively, one million HEK 293T cells were seeded in 10-cm plates and 24 hours later they were transfected using the calcium/phosphate precipitation procedure. After an additional 24-hour period they were lysed in RIPA-like lysis buffer. Protein content was measured by Bradford. Seven hundreds μ g of total protein were immunoprecipitated with 1 μ g of the anti-RasGAP antibody overnight at 4°C with rotation at 9 rpm. Twenty μ l of G protein sepharose beads (GE Healthcare; reference n°17-0618-01) were then added for an additional 2 hour period. Immunocomplexes were then washed three times with washing buffer (50 mM Tris-HCl pH 7.4, 150 mM NaCl, 1% NP-40) and solubilized in 30 μ l of sample buffer 2X. Samples were heated 10 minutes at 95°C before loading.

Quantitative PCR

RNA was isolated with the “High Pure RNA isolation kit” (Roche; reference n° 11828665001) according to the manufacturer’s instruction. The RNA was then reverse-transcribed with the “Transcriptor high fidelity cDNA kit” (Roche; reference n°05 091 284 001) as per the manufacturer’s instruction. Quantitative PCR assays were carried out on a real-time PCR detection system (iQ5; Bio-Rad) using iQ SYBR Green Supermix (Bio-Rad; reference n° 170–8862) using primers at a 500 nM concentration. The sequences of the *c-myc* specific primers were GGA CGA CGA GAC CTT CAT CAA (oligonucleotide #728, nucleotide 926–946 of *c-myc* mRNA, NCBI entry: NM_002467.3) and CCA GCT TCT CTG AGA CGA GCT T (oligonucleotide #729, nucleotide 996–1017 of *c-myc* mRNA, NCBI entry: NM_002467.3). The 18S ribosomal RNA was used for normalization. The primers used to amplify this RNA were GCA ATT ATT CCC CAT GAA CG (oligonucleotide #774, nucleotide 1617–1636, NCBI entry: NR_003278.1) and GGC CTC ACT AAA CCA TCC AA (oligonucleotide #775, nucleotide 1720–1739, NCBI entry: NR_003278.1).

Western blotting

Two hundred thousand cells were seeded in six-well plates and 24 hours later they were subjected to the treatments indicated in the figures after which they were lysed in sample buffer 5X. Proteins were quantitated using the Bradford method. Equal amounts of proteins were subjected to SDS-PAGE and then transferred onto a nitrocellulose membrane (Biorad; reference n°162 0115). The membranes were blocked with TBS containing 0.1% Tween-20 and 5% non-fat milk and incubated overnight at 4°C with the indicated primary antibodies used at 1:1000 dilution. Blots were then washed with TBS-Tween 0.1%, incubated with the appropriate secondary antibody (1:5000 dilution) 1 hour at room temperature and subsequently visualized with the Odyssey

infrared imaging system (LICOR Biosciences, Bad Homburg, Germany).

Lentivirus

Recombinant lentiviruses were produced as described [26]. Briefly, HEK293T cells were co-transfected using the calcium phosphate DNA precipitation method [21] with 50 µg of the lentiviral vector (TRIP-PGKATGm-MCS-WHV) containing the cDNA of interest (i.e. G3BP1 shRNA), 2.5 µg of the envelope protein-coding plasmid (pMD.G), and 7.5 µg of the packaging construct (pCMVDR8.91). Two days after transfection, the virus-containing medium was harvested. Infection of the cells was performed as follows. Hexadimethrine bromide (Polybrene; Sigma; reference n°52495) was added to cells cultured in six-well plates at a final concentration of 5 µg/ml followed by the addition of the lentivirus. The plates were then centrifuged 45 minutes at 800 *g* and placed 24 hours at 37°C in a 5% CO₂ humidified atmosphere. The medium was then replaced with fresh medium, and the cells were further cultured for an additional 48 hour period before being used in specific experiments.

Immunocytochemistry

Two hundred thousand cells were seeded in six-well plates containing glass coverslips and 24 hours later they were transfected with the calcium/phosphate precipitation procedure. One day post-transfection, the cells were fixed as follows (all steps were performed at room temperature). The cells on coverslips were washed with 4 ml of PBS, fixed with 3 ml PBS, 3% formaldehyde, 3% sucrose for 10 minutes, washed thrice with PBS, permeabilized with 2 ml of PBS, 0.2% Triton X-100 for 10 min, washed thrice with PBS, and incubated 30 minutes with 3 ml of filtered serum-containing culture medium. After three additional PBS washes, the coverslips were incubated for 1 hour with the primary antibody diluted in DMEM, 10% newborn calf serum. The coverslips were washed 3 times over 30 minutes in PBS and then incubated 1 hour with a 1/100 dilution of labeled secondary antibodies in DMEM, 10% newborn calf serum. The coverslips were washed 3 more times in PBS and labeled when indicated with 10 µg/ml Hoechst 33342 (Molecular Probe) before being mounted (Vectashield mounting medium, Vector laboratories Inc). Confocal images were captured with a Leica SP5 AOBs confocal microscope.

Determination of G3BP1 nuclear content

Confocal images were converted to tif format and opened with the Adobe Photoshop Elements 5.0 software. Pictures of Hoechst-stained cells were used to create masks of the nuclei that were then overlaid on the pictures of G3BP1-stained cells in order to delimitate the nuclear area. The nuclear G3BP1 signal image was then opened using the ImageJ software (1.34n version) and the nuclear signal was quantitated. Similarly, the total G3BP1 staining was quantitated for each picture with the ImageJ software (in this case the cell contours were manually drawn). The nuclear G3BP1 signal was calculated as the percentage of the total G3BP1 cell staining.

Peptides

TAT and TAT-RasGAP_{317–326} are retro-inverso peptides (i.e. synthesized with D-amino acids in the opposite direction compared to the natural sequence). The TAT moiety corresponds to amino acids 48–57 of the HIV TAT protein (RRRQRRKKRG) and the RasGAP_{317–326} moiety corresponds to amino acids 317–326 of the human RasGAP protein (DTRLNTVWMW). These two moieties are separated by two

glycine linker residues in the TAT-RasGAP_{317–326} peptide. The peptides were synthesized at the Department of Biochemistry, University of Lausanne, Switzerland, using Fmoc technology, purified by HPLC and tested by mass spectrometry.

Protein production and purification

Plasmids coding for recombinant proteins were expressed in BL21 *E. coli*. Bacteria were grown overnight in lysogeny broth (LB) medium (casein enzymic hydrolysate 10 g/l, yeast extract 5 g/l, NaCl 170 mM, pH 7.5). The induction of the recombinant proteins was performed by the addition of 0.1 mM isopropyl-beta-thiogalactoside (IPTG) to the culture medium when it reached an optical density at 600 nm of 0.6. After 4 hours of induction, the cells were harvested and resuspended in 5 ml Buffer A [HEPES 50 mM, magnesium acetate 200 mM, NaCl 500 mM, Triton X-100 0.1%, lysozyme 2 mg/ml, 0.5% β-mercaptoethanol and 10 µg/ml DNaseI, supplemented with one tablet of EDTA-free inhibitor (Roche) per 50 ml]. In order to fully lyse the cells, the suspension was sonicated (Heischer DmBH sonicator, 0.9 cycles per second, 80% amplitude) 4 times 30 seconds on ice and then centrifuged 20 minutes at 9'000 *g* at 4°C. A sample of the lysate was kept to verify the induction of the protein. GST-tagged proteins were then purified. The glutathione-sepharose beads (Amersham Pharmacia Biotech; reference n°17-0756-01) were washed 3 times with PBS and then incubated with the lysate at 4°C with rotation (Labinco rotary mixer, 12 rpm). The beads were washed thrice with PBS. To elute the recombinant protein, the beads were incubated with 500 µl of glutathione elution buffer (50 mM Tris pH 8, 10 mM reduced glutathione [Sigma reference n°G-4251]) for 15 minutes at 4°C with rotation. The beads were then pulled down at 4'000 *g* and the supernatant was collected. Histidine-N2 recombinant proteins were produced as described above, except that nickel beads were used (Ni-NTA agarose, Qiagen; reference n°1000632) instead of glutathione-Sepharose beads. The elution step was then performed with buffer A (see above) supplemented with 25 mM imidazole (Sigma reference n°I2399).

Statistics

All the statistical analyses were done with Microsoft Excel (XP edition) using the unpaired Student's *t* test. Significance is indicated by an asterisk when $P < 0.05/n$, where *P* is the probability derived from the *t* test analysis and *n* is the number of comparisons done (Bonferroni correction).

In silico protein docking assays

The G3BP1 NTF2 domain structure (PDB entry #2Q90) was first refined using Maestro v90211 in order to complete and refine the loops. Molecular dynamics simulations were conducted using the AMBER 11.0 force field from the NAMD 2.7 package. Using AmberTools 11.0, the resulting system was solvated in a rectangular box extending 12 Å around the molecule using TIP3P water molecules. Sodium and chloride ions were added to neutralize the system. Five thousand steps of energy minimization were applied on the entire system. Following minimization, the system was equilibrated with 5'000 steps of water-only molecular dynamics at 150°K, the system was heated from 0 to 300°K for 100 picoseconds. After heating, a 5 nanosecond production simulation was conducted with a 1 picosecond time step at a pressure of 1 bar and a temperature of 300°K. The RasGAP SH3 domain (PDB entry #2JO5) was optimized using the same method. The docking was performed using Hex 5.1 standard parameters. The 150 best poses out of 10'000 were collected and analyzed. The resulting complexes were ranked according to their free interactions energy. The same docking method was applied to

the SH3 domain of RasGAP and sequence 190–233 of UBP3, the USP10 yeast orthologue (PDB entry #2QJY).

Results

No evidence for a RasGAP-G3BP1 interaction

Previous data indicated that G3BP1 binds to a discrete sequence of RasGAP within its SH3 domain that corresponds to amino acids 317–326 of the protein [8]. As fragment N2 bears this SH3 domain, we postulated that it should allow fragment N2 to bind to G3BP1. However, Figure 1 shows that in HEK 293T cells fragment N2 failed to pull down G3BP1 in conditions where USP10, a deubiquitinating enzyme known to interact with G3BP1 [12], did. It could be argued that the 317–326 sequence is not accessible on fragment N2 while it would be exposed on the parental full-length protein. We therefore assessed if an interaction between RasGAP and G3BP1 could be demonstrated. Figure 2 indicates that RasGAP could not co-immunoprecipitate with G3BP1, while it did with p190 RhoGAP, a known RasGAP binding partner [27,28]. G3BP1 binding to RasGAP has been reported in the CCL39 (Chinese hamsters lung fibroblast) cell line [9]. Conceivably, this interaction could be cell-type specific. Therefore, we immunoprecipitated RasGAP from both CCL39 cells and U2OS cells. Figure 3 shows that endogenous RasGAP

protein interacted with p190 RhoGAP in both cell lines. In these conditions, no interaction could be detected between RasGAP and G3BP1.

TAT-RasGAP_{317–326} does not affect the binding of G3BP1 to USP10

It might be argued that the G3BP1-RasGAP interaction is transient and difficult to detect by the techniques we have used here. This interaction might nevertheless occur and one could hypothesize that TAT-RasGAP_{317–326} sensitizes tumor cells by modulating G3BP1 functions by either inhibiting the binding of RasGAP to G3BP1 or by mimicking the binding of RasGAP to G3BP1. One of the reported functions of G3BP1 is to bind to and inhibit USP10 [12]. We therefore assessed if TAT-RasGAP_{317–326} could prevent the binding of G3BP1 to this protein. Figure 4 shows that the interaction of G3BP1 to USP10 was unaffected by TAT-RasGAP_{317–326}, indicating that the peptide does not affect the inhibitory function of G3BP1 on USP10.

TAT-RasGAP_{317–326} does not impair stress granule formation

In response to environmental stress (i.e. heat and oxidative conditions) eukaryotic cells stop the translation of constitutive

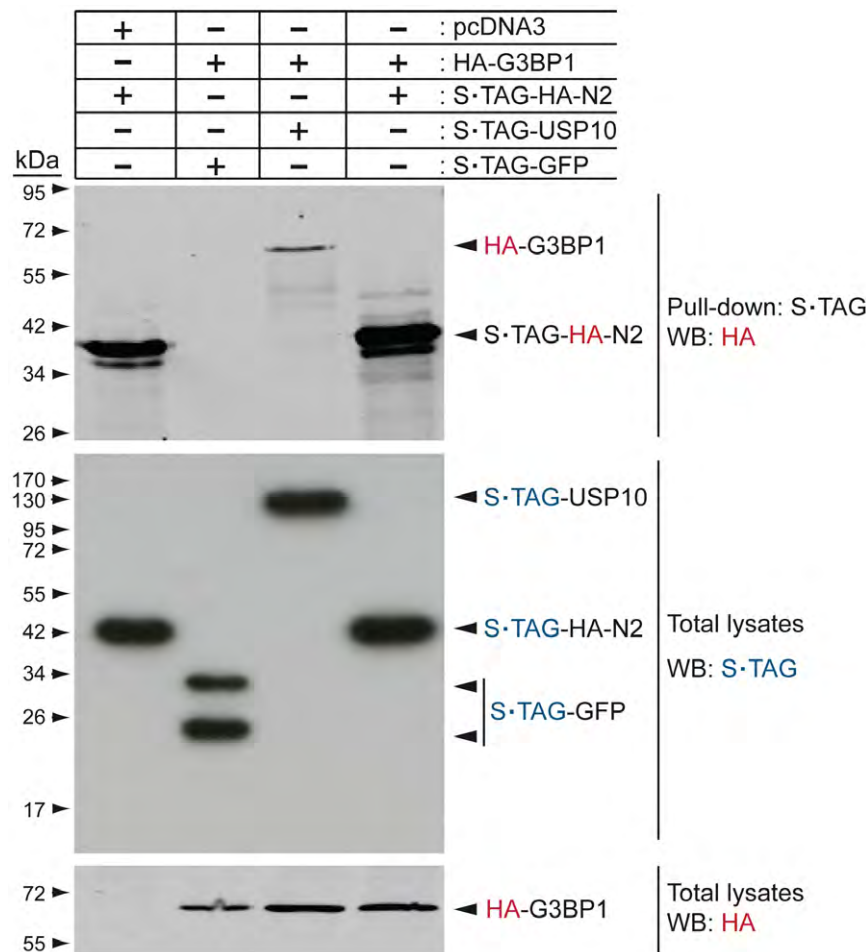


Figure 1. G3BP1 does not bind to RasGAP-derived fragment N2. Lysates (1 mg) from HEK293T cells that had been transfected with the indicated plasmids were subjected to S-TAG pull-down. Pulled-down complexes were then analyzed by Western blotting using an HA-specific antibody. In parallel, 50 μ g of total cell lysates were subjected to Western blot analysis using antibodies recognizing HA or the S-TAG. doi:10.1371/journal.pone.0029024.g001

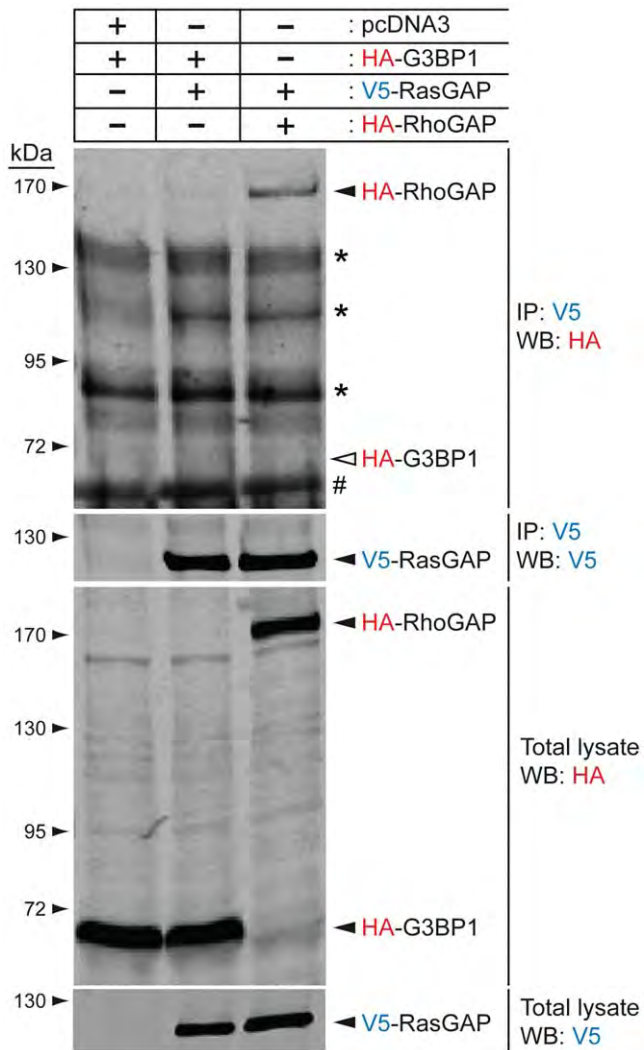


Figure 2. Ectopically-expressed RasGAP and G3BP1 fail to interact in conditions where RasGAP binds to RhoGAP. Lysates (1 mg) from HEK293T cells that had been transfected with the indicated plasmids were immunoprecipitated with an anti-V5 antibody. Immunoprecipitated complexes and cell lysates (50 μ g) were analyzed by Western blotting using HA- and V5-specific antibodies. Asterisks: non-specific bands; #: immunoglobulin heavy chains; white arrowhead: expected migration of HA-G3BP1.
doi:10.1371/journal.pone.0029024.g002

expressed mRNAs that are then routed to phase-dense cytoplasmic granules called stress granules (SGs). Many RNA-binding proteins participate in SG assembly including G3BP1, which together with TIA-1, is a SG marker [16]. An attractive hypothesis was that TAT-RasGAP_{317–326} mediates its sensitization effect by inhibiting the capacity of G3BP1 to participate in SG formation when cells are subjected to cytotoxic stresses. Therefore we tested if cisplatin was able to induce SG formation in U2OS cells and if TAT-RasGAP_{317–326} could impair this stress-induced response. As shown in Figure 5A, formation of SGs after treatment with arsenite was observed, but cisplatin did not induce SG assembly. Consequently, it is unlikely that the ability of TAT-RasGAP_{317–326} to sensitize U2OS cells to genotoxin-induced apoptosis relies on an effect on SGs. Nevertheless, to assess whether TAT-RasGAP_{317–326}, in conditions where SGs are efficiently induced, modulates their

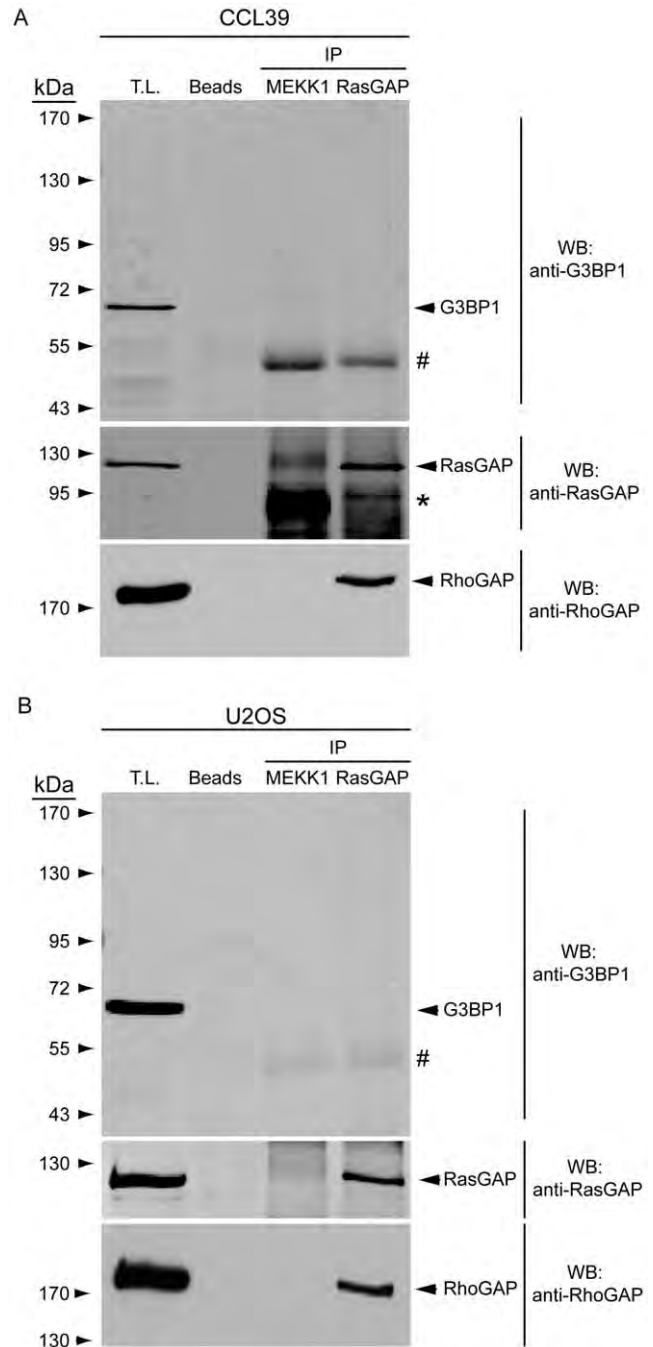


Figure 3. Endogenous RasGAP binds to RhoGAP but does not associate with G3BP1. Non-confluent, exponentially growing CCL39 cells (panel A) or U2OS cells (panel B) were lysed in 1% Triton X-100 lysis buffer and 1 mg of total protein extracts were immunoprecipitated with an anti-RasGAP antibody. Immunoprecipitated complexes and cell lysates (50 μ g) were analyzed by Western blotting using G3BP1- and p190 RhoGAP-specific antibodies. T.L.: total lysate; asterisks: non-specific bands; #: immunoglobulin heavy chains.
doi:10.1371/journal.pone.0029024.g003

assembly, U2OS cells were pre-incubated with TAT-RasGAP_{317–326} and then incubated with arsenite. Figure 5B–C shows that the peptide did not affect the number of SG per cell or the number of cells exhibiting SGs. To directly evaluate whether TAT-RasGAP_{317–326} affects SG formation induced by G3BP1, U2OS cells

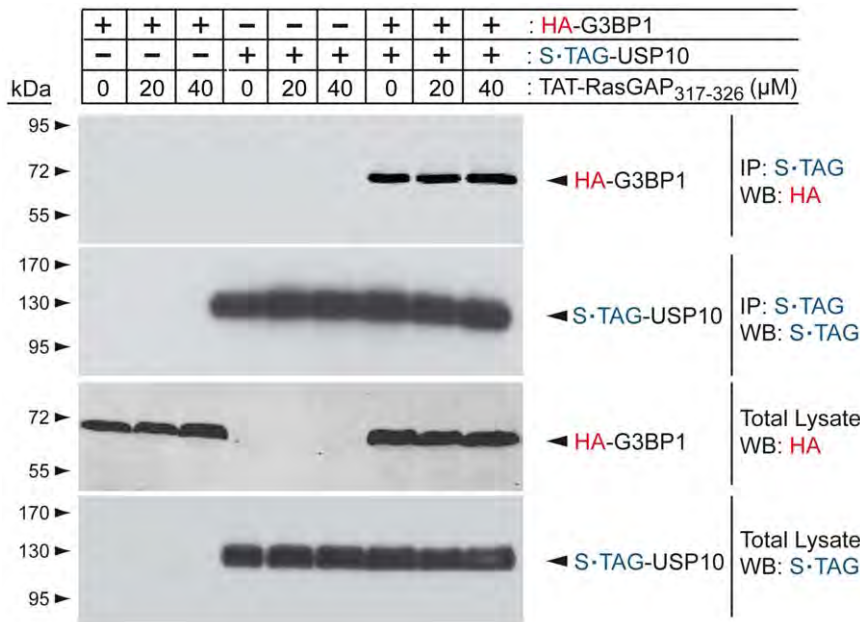


Figure 4. TAT-RasGAP_{317–326} does not affect the binding of G3BP1 to USP10. HEK293T cells were transfected with the indicated plasmids. Eight hours later, they were treated with the indicated concentrations of TAT-RasGAP_{317–326} for an additional 20 hour period at which time they were lysed. Lysates (1 mg) were subjected to S-TAG pull-down. Pulled-down complexes were analyzed by Western blotting using HA- and S-TAG specific antibodies. In parallel 50 µg of total cell lysates were subjected to Western blotting analysis using the same antibodies.
doi:10.1371/journal.pone.0029024.g004

were transfected with a GFP-tagged form of G3BP1 and incubated or not with the RasGAP-derived peptide. In this case again, the presence of TAT-RasGAP_{317–326} did not alter the formation of SGs (Figure 5D–E). Altogether, these results show, not only that genotoxins do not induce SG formation, but also that TAT-RasGAP_{317–326} does not affect the ability of G3BP1 to mediate the formation of SGs.

TAT-RasGAP_{317–326} does not sensitize cancer cells through the modulation of *c-myc* mRNA levels

The endoribonuclease activity of G3BP1 was first reported by its ability to cleave the 3' untranslated region (UTR) of the *c-myc* transcript [9,29]. This transcription factor regulates the expression of hundreds of gene controlling many cellular functions including cell survival and cell death [30]. It is an oncogene (one of the first to have been characterized actually) that is deregulated in many cancer types [31]. It plays a role in apoptosis by modulating proteins belonging to the Bcl-2 family, such as the pro-apoptotic BH3 only protein Bim [32,33]. The 3' UTR of the *c-myc* mRNA regulates its stability but how it does so is unclear. There are reports indicating that the 3' UTR favors *c-myc* mRNA decay [34,35], while another one provides indirect evidence that the 3' UTR contributes to *c-myc* mRNA stabilization [29]. If TAT-RasGAP_{317–326} modulates the ability of G3BP1 to cleave the *c-myc* mRNA it could affect the sensitivity of cells to apoptosis, in particular if c-Myc protein levels are increased because this can lead to cancer cell apoptosis, potentially via induction of Bim expression [36,37]. We therefore checked if TAT-RasGAP_{317–326} modulated *c-myc* mRNA levels and whether it affected c-Myc and Bim protein expression. Figure 6 shows that TAT-RasGAP_{317–326} did not modulate *c-myc* mRNA or c-Myc protein levels. Similarly, Bim expression was not affected by the peptide (Figure 6B). The levels of c-Myc and Bim were efficiently decreased by Actinomycin D, a transcription inhibitor, indicating that the

experimental conditions used in the figure allow detecting down-modulation of c-Myc and Bim. Finally, G3BP1 protein levels did not appear to be affected by TAT-RasGAP_{317–326} but an effect of the peptide on the transcription or translation of G3BP1 cannot be ruled out as the half-life of G3BP1 is considerably longer than c-Myc or Bim (Figure 6B). Collectively these results do not support the possibility that TAT-RasGAP_{317–326} modulates the endoribonuclease activity of G3BP1 to mediate its tumor sensitization property.

TAT-RasGAP_{317–326} does not affect G3BP1 subcellular location

Another possibility we wanted to explore concerned G3BP1 localization. It was reported that in quiescent MEFs, G3BP1 relocalizes to the nucleus and that this relocalization modulates its phosphorylation status and endoribonuclease activity [29]. Specifically, when G3BP1 translocates to the nucleus, it becomes phosphorylated on serine 149 and it functions as an active endoribonuclease whereas in proliferating cells, possibly in association with RasGAP, it is dephosphorylated and loses its ability to cleave RNAs [29]. Therefore we assessed whether TAT-RasGAP_{317–326} could alter the sub-cellular location of G3BP1. In HeLa cells, three-dimensional reconstructions of confocal sections indicated that G3BP1 was mainly located on a flat section of the cytoplasm and was absent in areas directly above or below the nucleus (egg-on-a-plate configuration) (Figure 7A). This permitted quantitation of the nuclear G3BP1-specific signal to be performed on conventional epifluorescence images (Figure 7B), which revealed that 15–20% of G3BP1 was localized in the nucleus (Figure 7C). This nuclear location was not affected by the RasGAP-derived peptide however, indicating that the mechanism by which TAT-RasGAP_{317–326} sensitizes tumor cells to genotoxin-induced apoptosis does not rely on modulation of the nuclear G3BP1 content.

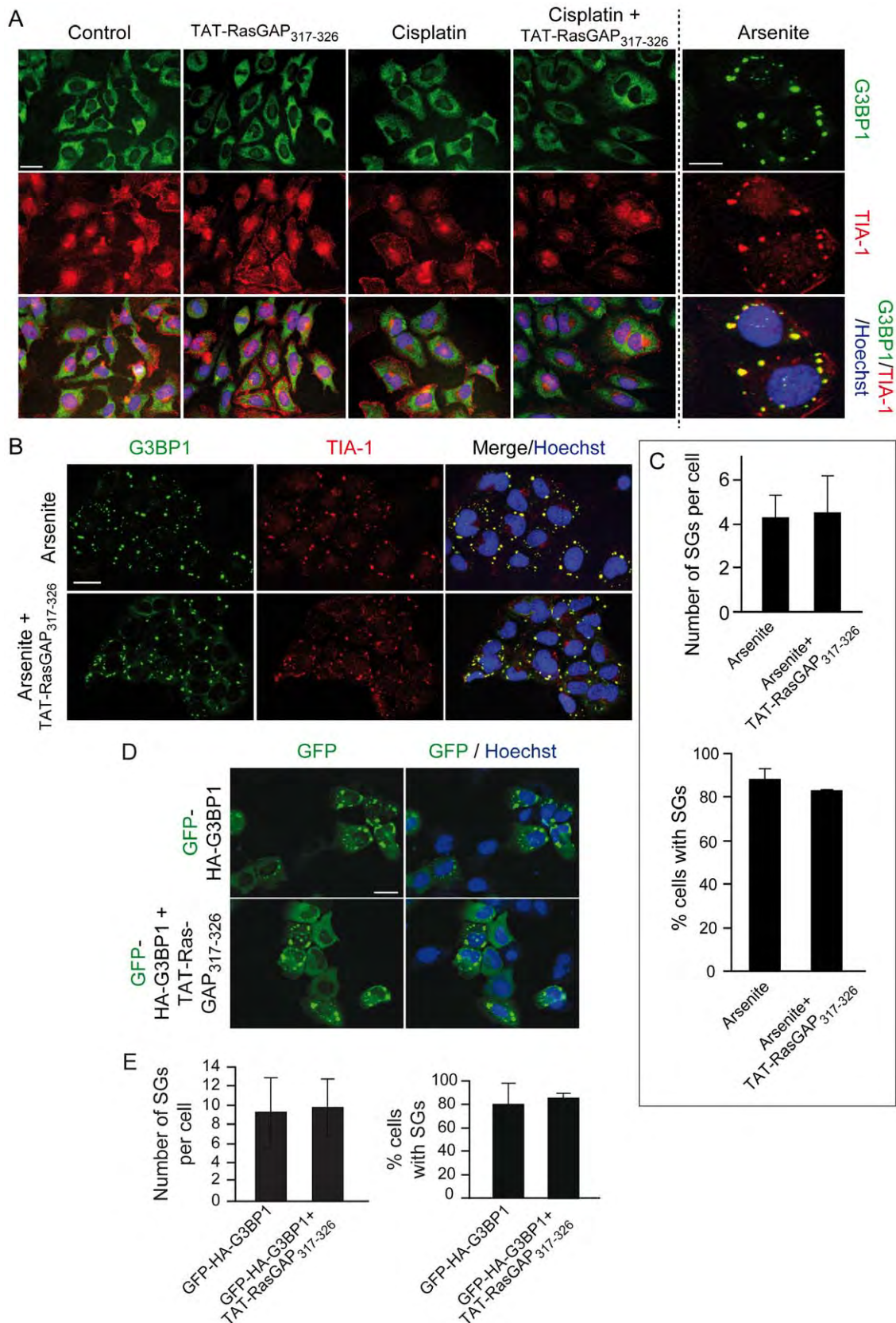


Figure 5. TAT-RasGAP₃₁₇₋₃₂₆ does not affect G3BP1-induced SG formation. **A.** U2OS cells were left untreated or incubated with 15 μ M cisplatin, 20 μ M TAT-RasGAP₃₁₇₋₃₂₆, or a combination of the two compounds for 22 hours. Alternatively, the cells were treated with 200 μ M arsenite for 2 hours. The cells were then processed for immunofluorescence analysis using TIA-1- and G3BP1-specific antibodies. Nuclei were stained with Hoechst 33342. Images were taken with a fluorescent microscope (Nikon Eclipse 90i). Scale bar: 20 μ m for the first 4 columns, 5 μ m for the last

column. **B–C.** U2OS cells were pre-incubated or not with 20 μM TAT-RasGAP_{317–326} for 18 hours and then treated with arsenite (200 μM , 2 hours). The cells were then processed as in panel A. Scale bar: 20 μm . Quantitation of the number of SGs per cells and the percentage of cells with SGs is shown in panel C. **D–E.** U2OS cells were transfected with a plasmid encoding GFP-HA-G3BP1 and 6 hours later were incubated or not with 20 μM TAT-RasGAP_{317–326} for an additional 22 hour period. Cells were then fixed and their nuclei stained with Hoechst 33342. Scale bar: 20 μm . Panel E shows the quantitation of the number of SGs per cells as well as the percentage of cells with SGs.
doi:10.1371/journal.pone.0029024.g005

G3BP1 ablation does not abolish TAT-RasGAP_{317–326}-mediated sensitization of cancer cells to cisplatin

The evidence provided so far indicates that G3BP1 is not a (strong) RasGAP or fragment N2 binding partner and that TAT-RasGAP_{317–326} does not modulate any of the known G3BP1 functions. To unequivocally determine whether G3BP1 is needed for TAT-RasGAP_{317–326}-mediated tumor sensitization, we used tumor cells in which G3BP1 was silenced and transformed MEFs from G3BP1 knock-out mice. Silencing G3BP1 using shRNA directed at the 3' UTR of its mRNA resulted in 90% reduction in G3BP1 levels in U2OS cells (Figure 8A–B). This however did not prevent TAT-RasGAP_{317–326} from sensitizing the cells to cisplatin-induced death (Figure 8C). Earlier work has demonstrated that TAT-RasGAP_{317–326} does not sensitize non-cancer cells to cisplatin-induced apoptosis [2]. MEFs, which are non-cancer cells, were indeed not experiencing more cisplatin-induced death in presence of the peptide (Figure 8F). It is however possible to transform MEFs with the SV40 large T antigen [38]. We therefore expressed the large T antigen in MEFs via lentiviral infection (Figure 8D) and, as expected, this rendered them sensitive to the genotoxin-sensitizing effect of TAT-RasGAP_{317–326} (Figure 8F). However, the peptide displayed identical sensitizing efficacy in large T-transformed MEFs lacking or not G3BP1 (Figure 8G). G3BP1 is therefore dispensable for TAT-RasGAP_{317–326} to mediate its genotoxin-sensitizing effect on cancer cells.

Discussion

The tumor-sensitizing activity of fragment N2 towards genotoxin-induced apoptosis resides in a 10 amino acid stretch corresponding to amino acids 317–326 of RasGAP [2]. This

peptidic sequence fused to a cell-permeable peptide (the so-called TAT-RasGAP_{317–326} peptide) is indeed capable of favoring the death of several tumor cell lines to various genotoxins [2]. Amino acids 317–326 of RasGAP correspond exactly to the sequence reported to mediate the binding of RasGAP to G3BP1 [8]. G3BP1 is a protein regulating mRNA stability, stress granule formation, and other cellular functions (reviewed in [39]). Formation of stress granules in cells has been reported to inhibit apoptosis [17]. Additionally, G3BP1 is over-expressed in certain tumors such as breast cancers [40]. As G3BP1 binds to amino acid 317–326 of RasGAP, an attractive hypothesis to explain how TAT-RasGAP_{317–326} sensitizes specifically tumor cells to genotoxin-induced death was that the peptide inhibits the ability of G3BP1 to form stress granule and consequently, as stress granules may exert anti-apoptotic properties [16], decreases the resistance of cancer cells towards apoptosis. This hypothesis would predict that cells lacking G3BP1 would not be sensitized by TAT-RasGAP_{317–326}. The evidence reported in the present study demonstrates that this hypothesis is incorrect. First, genotoxins did not induce the formation of stress granules in cancer cells. Formation of stress granules cannot therefore represent a protective mechanism against genotoxins in these cells. Secondly, TAT-RasGAP_{317–326} did not modulate stress granules in conditions known to induce their formation (e.g. in the presence of arsenite). Third, the peptide efficiently sensitizes tumor cells lacking G3BP1 to genotoxin-induced death. It can therefore be unequivocally concluded that G3BP1 plays no role in the anti-tumor activity of TAT-RasGAP_{317–326}.

The non-implication of G3BP1 in the function of TAT-RasGAP_{317–326} led us to reassess the reported interactions of G3BP1 with RasGAP. The RasGAP-G3BP1 interaction was first

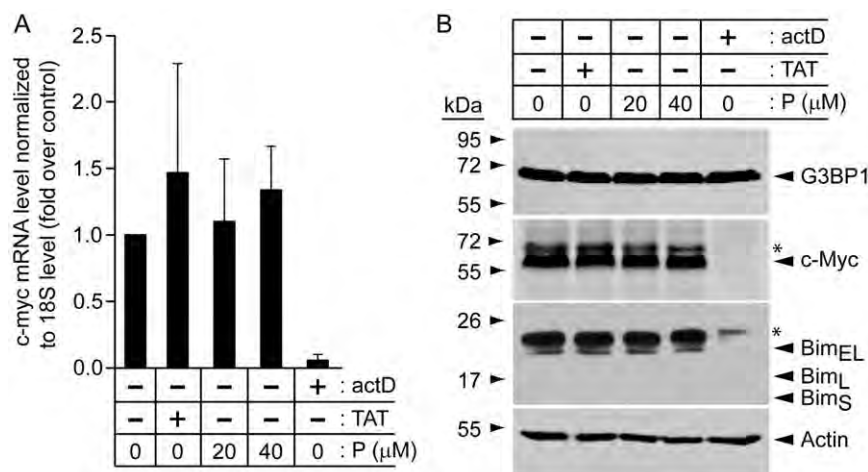


Figure 6. TAT-RasGAP_{317–326} does not affect *c-myc* mRNA and protein levels or expression of the *c-Myc* target Bim. **A.** HeLa cells were treated or not for 24 hours with 20 μM TAT, 20 or 40 μM TAT-RasGAP_{317–326} (P), or 1 $\mu\text{g/ml}$ actinomycin D (actD). Quantitative RT-PCR was then used to measure *c-myc* mRNA levels. **B.** Alternatively, the cells were lysed and 50 μg of protein extracts were analyzed by Western blotting using the indicated antibodies. Note that the Bim gene encodes three different forms of the protein, the expected migrations of which are indicated. Asterisks indicate non-specific bands.
doi:10.1371/journal.pone.0029024.g006

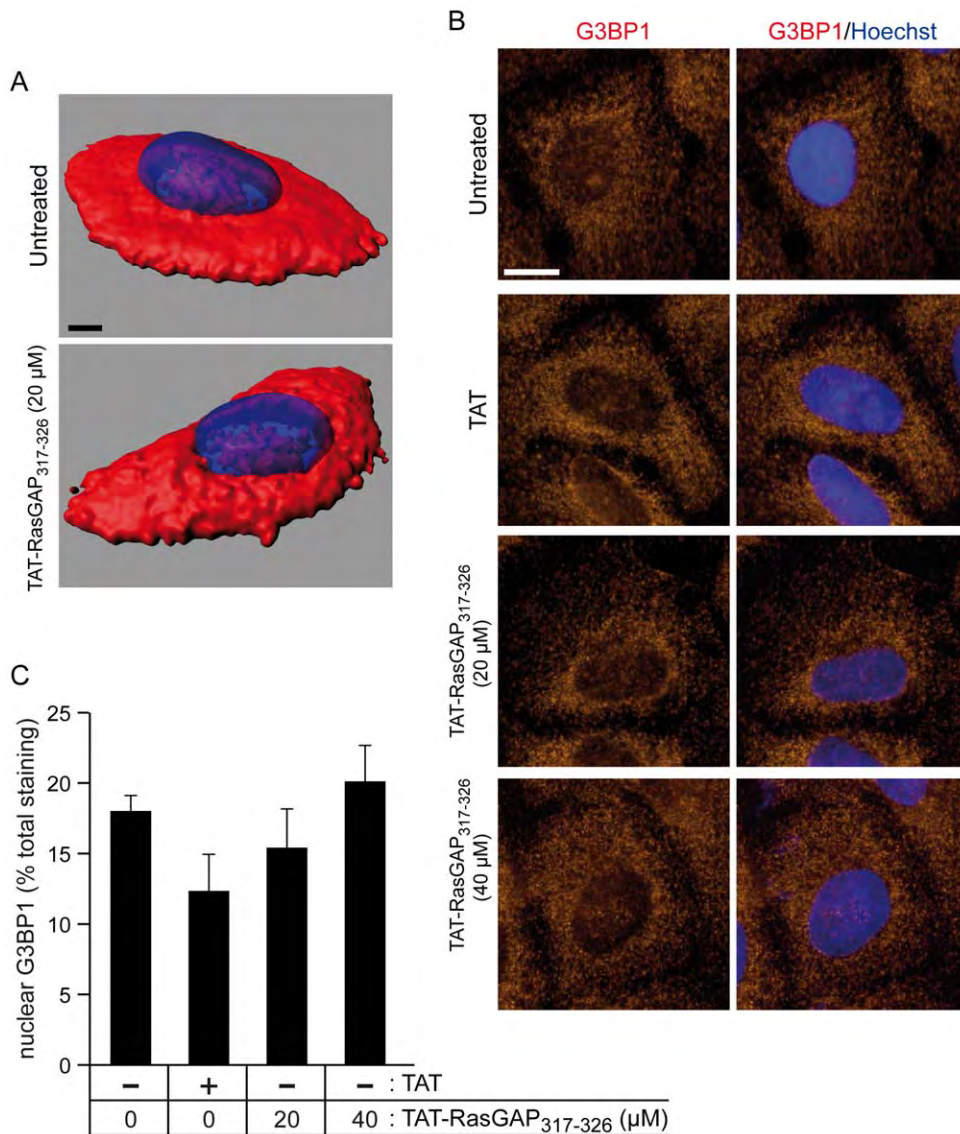


Figure 7. TAT-RasGAP₃₁₇₋₃₂₆ does not affect G3BP1 nuclear localization. A. HeLa cells were left untreated or treated for 18 hours with TAT (20 μM), TAT-RasGAP₃₁₇₋₃₂₆ (20 or 40 μM). Immunocytochemistry against G3BP1 was then performed (the nuclei were stained in blue with the Hoechst 33342 dye) and confocal z-stacks were acquired. Three-dimensional images were then built with the Imaris software. Representative examples of untreated and TAT-RasGAP₃₁₇₋₃₂₆-treated cells are shown (scale bar: 5 μm). Alternatively, images were taken using conventional epifluorescence microscopy (scale bar: 10 μm). Panel B depicts representative examples and panel C shows the corresponding quantifications performed on 80 cells as described in the methods. doi:10.1371/journal.pone.0029024.g007

reported in 1996 [8]. In this report, it was shown by Far Western blotting that a fusion protein between GST and the SH3 domain of RasGAP bound to G3BP1 from ER22 cell lysates and that this binding could be prevented by the addition of a peptide corresponding to the 317–326 RasGAP amino acid sequence. We were not able to reproduce these data using U2OS cell lysates and a recombinant histidine-tagged SH3 domain of RasGAP as a probe in the Far Western blotting procedure (data not shown). Moreover, in conditions where RasGAP and G3BP1 bound to known partners (i.e. p190 RhoGAP and USP10, respectively), no interaction between G3BP1 and RasGAP was detected (Figures 1, 2, 3). We used exponentially growing cells for these experiments as it was reported that G3BP1 does not interact with RasGAP in quiescent cells [9]. The results

presented in Figures 1, 2, and 3 contrast with reports showing binding of RasGAP to G3BP1 by co-immunoprecipitation methods [8,9] and by using GST pull-down assays [10]. It has to be noted however that these studies did not provide controls excluding a non-specific binding to beads for example. The interaction between RasGAP and G3BP1 might be occurring in very specific situations. It has been reported that G3BP1 only binds to serum-stimulated cells [8,9] and only after specific cyclical periods of time following the stimulation: association detected 1 hour, 8 hours and 16 hours after serum addition but no association seen 10 minutes, 20 minutes, 2 hours, 4 hours following serum addition [9]. Whether such pattern of G3BP1-RasGAP association correlates with a known physiological cell cycle has not been defined.

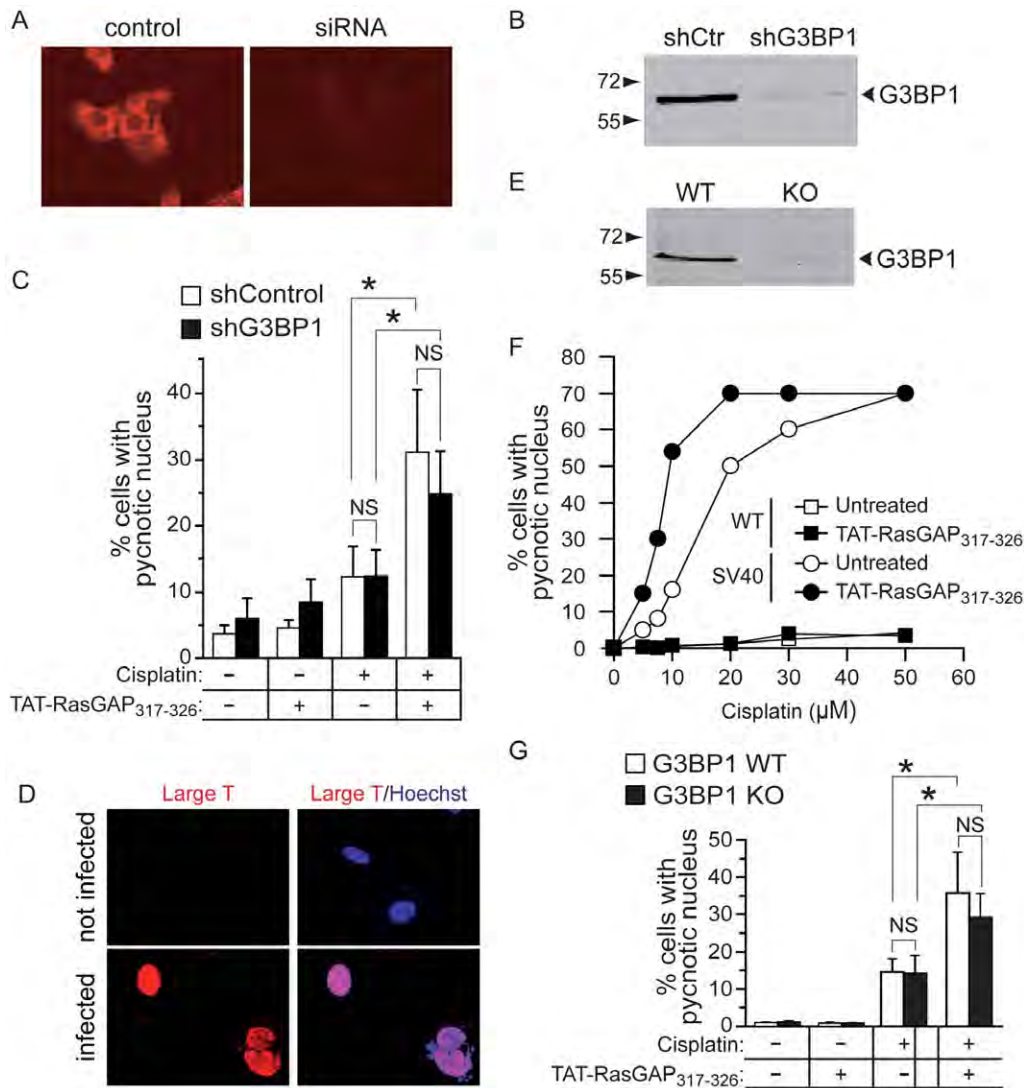


Figure 8. G3BP1 silencing does not affect TAT-RasGAP₃₁₇₋₃₂₆-mediated sensitization of cancer cells to cisplatin-induced apoptosis.

A, B. U2OS were infected with a non-target shRNA control vector or a G3BP1 shRNA-expressing lentivirus. After 72 hours, cells were analyzed by immunocytochemistry (panel A) and Western blotting (panel B) for the presence of G3BP1. **C.** Infected cells were incubated with 20 μM cisplatin and 20 μM TAT-RasGAP₃₁₇₋₃₂₆ for 22 hours as indicated on the figure. Apoptosis was then scored. **D.** MEFs were infected or not with a large T antigen-expressing lentivirus and 3 days later the expression of the large T antigen was assessed by immunocytochemistry. **E.** G3BP1 expression in wild-type (WT) and G3BP1 knock-out (KO) SV40 large T antigen-transformed MEFs was assessed by Western blotting. **F.** Alternatively, these cells were incubated with increasing concentrations of cisplatin in the presence or in the absence of TAT-RasGAP₃₁₇₋₃₂₆ for 22 hours. Apoptosis was then measured by scoring the number of cells with pycnotic nuclei. **G.** Wild-type (WT) and G3BP1 knock-out (KO) SV40 large T-transformed MEFs were treated as in panel C. Asterisks indicate statistically significant differences; NS: not significant.

doi:10.1371/journal.pone.0029024.g008

We also tried to crosslink RasGAP to G3BP1 in U2OS cell lysates to visualize a 180 kDa RasGAP-G3BP1 complex, as previously shown [9], but our analysis failed to reveal such a complex (data not shown). We were therefore unable to reveal a binding between G3BP1 and either RasGAP or the SH3 domain-containing fragment N2 of RasGAP, even when we used techniques, conditions (e.g. cells incubated with serum) and cell lines (e.g. CCL39) used by others to report this interaction. A similar lack of interaction between RasGAP and G3BP1 has been reported earlier by another laboratory [12]. It is pertinent to mention here that RasGAP was not found in the proteins identified by mass spectrometry in the cellular material pulled down with an anti-G3BP1 antibody (Sophie Martin and Jamal Tazi, unpublished results). The reverse was also true, i.e. G3BP1 was not identified by mass spectrometry in the

cellular material pulled down with an anti-RasGAP antibody (Hadi Khalil and Christian Widmann, unpublished results). Last, we took advantage of the recently crystallized structure of the NTF2 domain of human G3BP1 (PDB; <http://www.pdb.org>; #3QN) and the previously published structure of the RasGAP SH3 domain [41] to conduct molecular dynamics and docking simulations. This analysis failed to reveal a preferred binding site between the NTF2 domain of G3BP1 and the SH3 domain of RasGAP (Figure 9A). As a control, the ability of USP10 to dock to G3BP1 was also tested. Figure 9B shows that there was a preferred interaction conformation between these two proteins at sites demonstrated to interact in the crystal structure made of these two proteins [42]. In light of all our results, the possibility that RasGAP is not a genuine G3BP1 partner has to be considered.

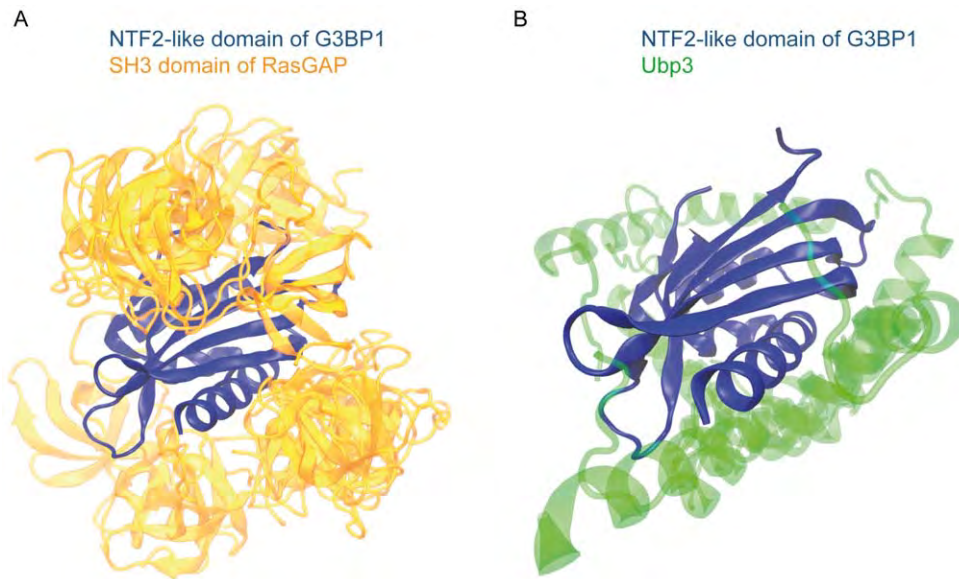


Figure 9. *In silico* assessment of G3BP1 binding to RasGAP. *In silico* docking assays were performed as described in the methods with the SH3 domain of RasGAP on either the G3BP1 NTF2-like domain (panel A) or sequence 190–233 of Ubp5, the yeast orthologue of USP10 (panel B). The 15 best interactions are presented in the figure. While the interactions of G3BP1 and USP10 were of similar nature (note the superposition of the USP10 structures in green), there was no preferred docking interaction between the SH3 domain of RasGAP and G3BP1.
doi:10.1371/journal.pone.0029024.g009

Acknowledgments

We thank Yannick Kremp from the Cellular Imaging Facility of the University of Lausanne for 3D confocal image reconstruction, Dr. Véronique Leblanc and Dr. Bruno Tocqué for the gift of the hG3BP1.dn3 plasmid, Dr. Olivier Staub for the gift of the 6xHis-Stag-mUSP10.dn3 plasmid and the anti-USP10 antibody, Dr. Didier Trono for the gift of plasmid TRIP-PGK-IRESNEO-WHV, Dr. Ole Kristensen for the gift of

the pET28(+) plasmid, and Dr. Jeff Settleman for the gift of HA-rRhoGAP.prc.

Author Contributions

Conceived and designed the experiments: AA CW. Performed the experiments: AA AD. Analyzed the data: AA CW. Contributed reagents/materials/analysis tools: SM JT. Wrote the paper: AA CW. Discussed the results and edited the paper: AA AD SM JT CW.

References

- Yang J-Y, Walicki J, Michod D, Dubuis G, Widmann C (2005) Impaired Akt activity down-modulation, caspase-3 activation, and apoptosis in cells expressing a caspase-resistant mutant of RasGAP at position 157. *Mol Biol Cell* 16: 3511–3520.
- Michod D, Yang JY, Chen J, Bonny C, Widmann C (2004) A RasGAP-derived cell permeable peptide potently enhances genotoxin-induced cytotoxicity in tumor cells. *Oncogene* 23: 8971–8978.
- Michod D, Annibaldi A, Schaefer S, Dapples C, Rochat B, et al. (2009) Effect of RasGAP N2 fragment-derived peptide on tumor growth in mice. *J Natl Cancer Inst* 101: 828–832.
- Pittet O, Petermann D, Michod D, Krueger T, Cheng C, et al. (2007) Effect of the TAT-RasGAP_{317–326} peptide on apoptosis of human malignant mesothelioma cells and fibroblasts exposed to *meso*-tetra-hydroxyphenyl-chlorin and light. *J Photochem Photobiol B* 88: 29–35.
- Michod D, Widmann C (2007) TAT-RasGAP_{317–326} requires p53 and PUMA to sensitize tumor cells to genotoxins. *Mol Cancer Res* 5: 497–507.
- Yu J, Wang Z, Kinzler KW, Vogelstein B, Zhang L (2003) PUMA mediates the apoptotic response to p53 in colorectal cancer cells. *Proc Natl Acad Sci USA* 100: 1931–1936.
- Villunger A, Michalak EM, Coultas L, Mullauer F, Bock G, et al. (2003) p53- and drug-induced apoptotic responses mediated by BH3-only proteins puma and noxa. *Science* 302: 1036–1038.
- Parker F, Maurier F, Delumeau I, Duchesne M, Faucher D, et al. (1996) A Ras-GTPase-activating protein SH3-domain-binding protein. *Mol Cell Biol* 16: 2561–2569.
- Gallouzi I-E, Parker F, Chebli K, Maurier F, Labourier E, et al. (1998) A novel phosphorylation-dependent RNase activity of GAP-SH3 binding protein: a potential link between signal transduction and RNA stability. *Mol Cell Biol* 18: 3956–3965.
- Kennedy D, French J, Guitard E, Ru K, Tocque B, et al. (2001) Characterization of G3BPs: tissue specific expression, chromosomal localisation and rasGAP(120) binding studies. *J Cell Biochem* 84: 173–187.
- Stark LA, Dunlop MG (2005) Nucleolar sequestration of RelA (p65) regulates NF- κ B-driven transcription and apoptosis. *Mol Cell Biol* 25: 5985–6004.
- Soncini C, Berdo I, Draetta G (2001) Ras-GAP SH3 domain binding protein (G3BP) is a modulator of USP10, a novel human ubiquitin specific protease. *Oncogene* 20: 3869–3879.
- Tourriere H, Chebli K, Zekri L, Courselaud B, Blanchard JM, et al. (2003) The RasGAP-associated endoribonuclease G3BP assembles stress granules. *J Cell Biol* 160: 823–831.
- Anderson P, Kedersha N (2006) RNA granules. *J Cell Biol* 172: 803–808.
- Ivanov PA, Nadezhkina ES (2006) Stress granules: RNP-containing cytoplasmic bodies arising in stress: structure and mechanism of organization. *Molecular Biology* 40: 937–944.
- Buchan JR, Parker R (2009) Eukaryotic stress granules: the ins and outs of translation. *Mol Cell* 36: 932–941.
- Arimoto K, Fukuda H, Imajoh-Ohmi S, Saito H, Takekawa M (2008) Formation of stress granules inhibits apoptosis by suppressing stress-responsive MAPK pathways. *Nat Cell Biol* 10: 1324–1332.
- Waldman T, Kinzler KW, Vogelstein B (1995) p21 is necessary for the p53-mediated G1 arrest in human cancer cells. *Cancer Res* 55: 5187–5190.
- DuBridge RB, Tang P, Hsia HC, Leong PM, Miller JH, et al. (1987) Analysis of mutation in human cells by using an Epstein-Barr virus shuttle system. *Mol Cell Biol* 7: 379–387.
- Zekri L, Chebli K, Tourriere H, Nielsen FC, Hansen TV, et al. (2005) Control of fetal growth and neonatal survival by the RasGAP-associated endoribonuclease G3BP. *Mol Cell Biol* 25: 8703–8716.
- Jordan M, Schallhorn A, Wurm FM (1996) Transfecting mammalian cells: optimization of critical parameters affecting calcium-phosphate precipitate formation. *Nucleic Acids Res* 24: 596–601.
- Yang J-Y, Widmann C (2001) Antiapoptotic signaling generated by caspase-induced cleavage of RasGAP. *Mol Cell Biol* 21: 5346–5358.
- Gilmanshin R, VanBeek J, Callender R (1996) Study of the ribonuclease S-peptide/S-protein complex by means of Raman difference spectroscopy. *Journal of Physical Chemistry* 100: 16754–16760.
- Backer MV, Gaynutdinov TI, Gorshkova II, Crouch RJ, Hu T, et al. (2003) Humanized docking system for assembly of targeting drug delivery complexes. *J Control Release* 89: 499–511.

25. Boulkroun S, Ruffieux-Daidie D, Vitagliano JJ, Poirot O, Charles RP, et al. (2008) Vasopressin-inducible ubiquitin-specific protease 10 increases ENaC cell surface expression by deubiquitylating and stabilizing sorting nexin 3. *Am J Physiol Renal Physiol* 295: F889–F900.
26. Dull T, Zufferey R, Kelly M, Mandel RJ, Nguyen M, et al. (1998) A third-generation lentivirus vector with a conditional packaging system. *J Virol* 72: 8463–8471.
27. Moran MF, Polakis P, McCormick F, Pawson T, Ellis C (1991) Protein-tyrosine kinases regulate the phosphorylation, protein interactions, subcellular distribution, and activity of p21ras GTPase-activating protein. *Mol Cell Biol* 11: 1804–1812.
28. Settleman J, Albright CF, Foster LC, Weinberg RA (1992) Association between GTPase activators for Rho and Ras families. *Nature* 359: 153–154.
29. Tourriere H, Gallouzi I-E, Chebli K, Capony J-P, Mouaikel J, et al. (2001) RasGAP-associated endoribonuclease G3BP: selective RNA degradation and phosphorylation-dependent localization. *Mol Cell Biol* 21: 7747–7760.
30. Fernandez PC, Frank SR, Wang L, Schroeder M, Liu S, et al. (2003) Genomic targets of the human c-Myc protein. *Genes Dev* 17: 1115–1129.
31. Meyer N, Penn LZ (2008) Reflecting on 25 years with MYC. *Nat Rev Cancer* 8: 976–990.
32. Egle A, Harris AW, Bouillet P, Cory S (2004) Bim is a suppressor of Myc-induced mouse B cell leukemia. *Proc Natl Acad Sci U S A* 101: 6164–6169.
33. Hemann MT, Bric A, Teruya-Feldstein J, Herbst A, Nilsson JA, et al. (2005) Evasion of the p53 tumour surveillance network by tumour-derived MYC mutants. *Nature* 436: 807–811.
34. Herrick DJ, Ross J (1994) The half-life of c-myc mRNA in growing and serum-stimulated cells: influence of the coding and 3' untranslated regions and role of ribosome translocation. *Mol Cell Biol* 14: 2119–2128.
35. Yeilding NM, Rehman MT, Lee WM (1996) Identification of sequences in c-myc mRNA that regulate its steady-state levels. *Mol Cell Biol* 16: 3511–3522.
36. Strasser A, Puthalakath H, Bouillet P, Huang DC, O'Connor L, et al. (2000) The role of bim, a proapoptotic BH3-only member of the Bcl-2 family in cell-death control. *Ann N Y Acad Sci* 917: 541–548.
37. O'Connor L, Strasser A, O'Reilly LA, Hausmann G, Adams JM, et al. (1998) Bim: a novel member of the Bcl-2 family that promotes apoptosis. *EMBO J* 17: 384–395.
38. Ahuja D, Saenz-Robles MT, Pipas JM (2005) SV40 large T antigen targets multiple cellular pathways to elicit cellular transformation. *Oncogene* 24: 7729–7745.
39. Irvine K, Stirling R, Hume D, Kennedy D (2004) Rasputin, more promiscuous than ever: a review of G3BP. *Int J Dev Biol* 48: 1065–1077.
40. French J, Stirling R, Walsh M, Kennedy HD (2002) The expression of Ras-GTPase activating protein SH3 domain-binding proteins, G3BPs, in human breast cancers. *Histochem J* 34: 223–231.
41. Ross B, Kristensen O, Favre D, Walicki J, Kastrop JS, et al. (2007) High resolution crystal structures of the p120 RasGAP SH3 domain. *Biochem Biophys Res Commun* 353: 463–468.
42. Li K, Zhao K, Ossareh-Nazari B, Da G, Dargemont C, et al. (2005) Structural basis for interaction between the Ubp3 deubiquitinating enzyme and its Bre5 cofactor. *J Biol Chem* 280: 29176–29185.

Results

Part IV

Introduction

This section contains unpublished data obtained in the context of understanding the molecular mechanisms that underlie the TAT-RasGAP₃₁₇₋₃₂₆-mediated sensitization of cancer cells to genotoxin-induced apoptosis. Deciphering the mode of action of TAT-RasGAP₃₁₇₋₃₂₆ might be critically important to unravel how cancer cells resist genotoxic stress and to design new more targeted and efficient anti-cancer strategies.

The manuscript presented in this part shows that TAT-RasGAP₃₁₇₋₃₂₆ potentiates the genotoxin-mediated activation of Bax, a member of the Bcl-2 family that acts as effector of the mitochondrial apoptotic pathway.

Contribution

This work has been entirely carried out by me; it is presented below as manuscript.

Introduction

The modulation of tumor cell sensitivity to genotoxic agents is one major issue in anticancer research. The development of small molecules able to selectively increase the susceptibility of cancer cells to genotoxin-induced cell death would ameliorate the efficacy of chemotherapy and offer incalculable benefits to cancer suffering patients. Our laboratory earlier developed a cell permeable peptide whose active sequence was derived from the SH3 domain of the RasGAP protein [1]. This peptide, TAT-RasGAP₃₁₇₋₃₂₆, was shown to selectively sensitize several cancer cell lines, but non non-cancer cell lines, to genotoxin-induced apoptosis, while having no effect by itself [1]. TAT-RasGAP₃₁₇₋₃₂₆ was also demonstrated to be a chemosensitizer *in vivo* in a tumor xenograft mouse model [2]. Understanding how TAT-RasGAP₃₁₇₋₃₂₆ delivers its pro-apoptotic effect would potentially give new insights into the mechanism allowing cancer cells to resist apoptosis. This would therefore allow the development of more target-specific anti-cancer strategies.

Genotoxins are DNA-damaging substances that prevalently exert their anti-tumor activity by causing apoptosis in cancer cells through the mitochondrial pathway [3-5]. The genotoxin-induced DNA-damage response is orchestrated by a series of kinases (e.g. the ataxia-telangiectasia mutated, ATM) [6;7] that sense the extent of the damage and activate downstream effectors. One of the key DNA damage response effector is p53, a transcription factor that regulates the expression of genes mainly involved in cell cycle arrest (e.g. p21) and apoptosis (e.g. Puma and Bax) [8]. Puma and Bax are two Bcl-2 family members, a family of proteins that tightly controls the mitochondrial membrane integrity [9]. When the balance between pro and anti-apoptotic members of this family tips in favor of the anti-apoptotic players, mitochondrial membrane integrity is lost with consequent release of cytochrome *c* that leads to caspase activation and apoptosis [10].

We earlier showed that TAT-RasGAP₃₁₇₋₃₂₆ does not modulate the MAPK signaling pathways (p38, ERK and JNK), the NF- κ B transcriptional activity and it does not influence the AKT protein levels and phosphorylation status [1;11]. We also provided evidence suggesting that a functional p53/Puma apoptotic axis is needed by the peptide to potentiate the genotoxin-induced cell death, even though their protein levels are not altered by TAT-RasGAP₃₁₇₋₃₂₆ [11].

The aim of this study is to gain a deeper insight into the molecular events allowing TAT-RasGAP₃₁₇₋₃₂₆ to potentiate the genotoxin-activated mitochondrial cell death pathway.

Materials and methods

Chemicals

Cisplatin (Sigma, ref. n°P4394) was diluted in water at a final concentration of 1 mg/ml and stored at -80°C. TNF α (Pierce, ref. n°RTNFA10) was diluted in water at a concentration of 10 μ g/ml. Cycloheximide (Sigma, ref. n°C7698) was diluted in methanol and stored at -20 °C. Paraformaldehyde (PFA) and HCl were from Acros (ref. n°30525-89-4 and 7647-01-0, respectively). Hoechst 33342 (Molecular Probe, Invitrogen, ref. n°H21492) was diluted in water at a concentration of 10 mg/ml and used at a final concentration of 10 μ g/ml. The pan-caspase inhibitor MX1013 was a kind gift from Maxim Pharmaceuticals (San Diego, CA). Tris, sodium dodecyl sulfate (SDS), mannitol and sucrose were from Sigma (ref. n°T1503, L4390, M4125 and S0389 respectively). HEPES (4-(2-hydroxyethyl)-1-piperazineethanesulfonic acid) was from Applichem (ref. n°A3724). NaCl, EGTA (ethylenedis[oxymethylenenitrilo]tetraacetic acid) and bromophenol blue were from Acros (ref. n°7647-14-5, 67-42-5, and 115-39-9, respectively). CHAPS (3-[(3-Cholamidopropyl)dimethylammonio]-1-propanesulfonate), EDTA (ethylenediaminetetraacetic acid), dithiothreitol (DTT), KCl and glycerol were from Fluka

(ref. n°26680, 03620, 43817, 60130 and 49780, respectively). G-Sepharose beads were from GE Healthcare (ref. n°17-0618-01). Nitrocellulose membranes were from Biorad (ref. n°162 0115). MgCl₂ was from Eurobio (ref. n°018023). EDTA-free Protease Inhibitor Cocktail Tablets were from Roche Applied Science (ref. n°1873580). Polyoxyethylene (20) sorbitan monolaurate (Tween 20) was from AppliChem (ref. n° 90005-64-5).

Buffers

The composition of phosphate buffered saline (PBS) is 116 mM NaCl, 10.4 mM Na₂HPO₄, 3.2 mM KH₂PO₄ (pH 7.4). The composition of the isotonic mitochondrial buffer (MB) is 10 mM HEPES (pH 7.4), 210 mM mannitol, 70 mM sucrose, 1 mM EDTA supplemented with one tablet of EDTA-free inhibitor (Roche) per 50 ml. The KCl buffer is made of 10 mM HEPES (pH 7.4), 125 mM KCl, 0.5 mM EGTA, 4 mM MgCl₂ and 5mM KHPO₄. 1% CHAPS lysis buffer is made of 5 mM MgCl₂, 137 mM NaCl, 1 mM EDTA, 1 mM EGTA, 1% Chaps, 20 mM Tris-HCl, supplemented with one tablet of EDTA-free Protease Inhibitor Cocktail (Roche) per 50 ml. MonoQ-c buffer is made of 70 mM β-glycerophosphate, 0.5% Triton X-100, 2 mM MgCl₂, 1 mM EGTA, 100 μM Na₃VO₄, 1 mM dithiothreitol, 20 μg/ml aprotinin supplemented with one tablet of complete EDTA-free Protease Inhibitor Cocktail per 50 ml.

Peptides

TAT and TAT-RasGAP317-326 are retro-inverso peptides (i.e. synthesized with D-amino acids in the opposite direction compared to the natural sequence). The TAT moiety corresponds to amino acids 48-57 of the HIV TAT protein (RRRQRRKKRG) and the RasGAP317-326 moiety corresponds to amino acids 317-326 of the human RasGAP protein (DTRLNTVWMW). These two moieties are separated by two glycine linker residues in the

TAT-RasGAP317-326 peptide. The peptides were synthesized at the Institute of Biochemistry, University of Lausanne, Switzerland, using Fmoc technology, purified by HPLC and tested by mass spectrometry.

Cell lines

U2OS, HCT116 were cultured in DMEM (Invitrogen, ref. n°61965) supplemented with 10% heat-inactivated fetal bovine serum (FBS; Invitrogen, ref. n°10270-106) in 5% CO₂ at 37°C. HeLa cells were cultured in RPMI (Invitrogen, ref. n°61870) supplemented with 10% heat-inactivated FBS in 5% CO₂ at 37°C. Culturing of the cells prior to performing the experiments described in this article was performed in six-well plates by seeding 100'000 cells (Figure 1; Figure 2, right graph), 150'000 (Figure 5, U2OS and HeLa cells), 200'000 (Figure 5, HCT116 cells), or 250'000 cells (Figure 2, left graph; Figure 3) in the wells 24 hours before being treated as indicated in the figures. B Mouse embryonic fibroblast (MEFs) knock-out (KO) for Bcl-XL, Bcl-2, Mcl-1, Bim, Bmf and Bid were generously provided by Dr David Huang. MEFs KO for Bax, Bak, Bax/Bak and Bad were generously provided by Dr Stansley Korsmeyer. Culturing of the KO MEFs prior to performing the experiments described in this article was performed in six-well plates by seeding 150'000 cells (Figure 8).

Starvation

Cells were washed three times with PBS and incubated for 24 hours with medium lacking FBS.

UV illumination

Cells in culture dishes with the lid removed were illuminated with UV-C using the UV lamp of a cell culture hood (Fortuna from Scanlaf 1200) delivering an intensity of 0.25 J/m² per

second. The cells were then incubated in their culture medium for the indicated periods of time in 5% CO₂ at 37°C.

Apoptosis quantitation

Cells were fixed in 2% PFA and nuclei labeled with Hoechst 33342. Apoptotic cells (i.e. cells displaying a pycnotic nucleus) were counted under a Nikon Eclipse TS100 microscope. When apoptosis was assessed on a population of transfected cells, only green cells (i.e. cells having incorporated the transfected plasmids) were counted.

Statistics

Statistical analyses were performed with the SAS/STAT software (version 9.1.3; SAS Institute, Cary, NC) using one-way ANOVA procedures followed by post-hoc Bonferroni (Dunn) t tests.

Mitochondria purification and cytochrome c release assay

HeLa cells were harvested in PBS and centrifuged 10 minutes at 1000 x g. Cells were then resuspended in isotonic mitochondrial buffer (MB), broken by twenty passages through a 25G1 0.5- by 25-mm needle fitted on a 2 ml syringe and centrifuged at 1500 x g 5 minutes. This procedure was repeated twice and supernatants from each step were pooled and centrifuged 5 minutes at 1500 x g. Supernatant was collected, centrifuged 5 minutes at 2000 x g and further centrifuged 10 minutes at 90000 x g. Pellet was then resuspended in MB and centrifuged 10 minutes at 7000 x g and the pellet, representing the mitochondrial fraction, was finally resuspended in MB. Mitochondrial content was quantitated by Bradford. 30 µg of mitochondria were incubated in KCl buffer with or without the recombinant protein tBid in a total volume of 100 µl for 30 minutes at room temperature. Samples were then centrifuged at

12000 x g 5 minutes, supernatants and pellets were then used to determine the cytochrome c release.

Transfection

Cells were transfected using Lipofectamine 2000 (GibcoBRL, ref. n°18324-012) according to the manufacturer's instructions. Briefly, the indicated plasmids, together with 0.5 mg of GFP-encoding plasmid, were diluted in 250 ml DMEM without FBS. The amount of DNA used in the transfection was kept constant to 4 mg by adding the appropriate quantities of pcDNA3 plasmid. In parallel, 8 ml of lipofectamine were added to 250 ml of DMEM without FBS and kept at room temperature for 5 minutes. Finally, the DNA-containing medium was added drop by drop to the lipofectamin-containing medium and the resulting 500 ml mix was added to cells. Five hours later, cells were washed once with fresh medium (DMEM supplemented with FBS) and cultured for an additional 20 hour period in the presence of the treatments indicated in the figures.

Coimmunoprecipitation and immunoblotting

7.5x10⁵ U2OS and HeLa cells and 10⁶ HCT116 cells were seeded in 10 cm plates and the next day treated as shown in the figures. Sixteen hours later, the cells were lysed in 300 µl of 1% CHAPS lysis buffer and 700 µg of the lysate proteins were immunoprecipitated overnight with 1.5 µg of the 6A7 anti-Bax antibody (Figure 4) or 1.5 µg of the anti-Bcl-XL antibody (Figure 6). Immunoprecipitates were captured on 30 µl of protein G-Sepharose at 4 °C for 2 hours. Immunocomplexes were then washed three times in CHAPS lysis buffer and eluted in 30 µl of 2X sample buffer [25 mM Tris-HCl pH 7.5, 10% glycerol, 6% SDS, 0.02% of bromophenol blue and 100 mM freshly added DTT]. The immunoprecipitates and 50 µg of total cell lysates were separated by SDS-PAGE and then transferred onto nitrocellulose

membrane. The membranes were blocked with TBS (20 mM Tris, 130 mM NaCl, pH 7.6) containing 0.1% Tween 20 and 5% non-fat milk (TBS-TM) and incubated overnight at 4°C with a 1/1000 dilution of the N-20 anti-Bax antibody (Figure 4) or 1/1000 dilutions of the antibodies directed at the proteins indicated in the other figures. Blots were then washed with TBS containing 0.1% Tween 20 (TBS-T), incubated 1 hour at room temperature with the appropriate fluorophore-conjugated secondary antibody (1:5'000 dilution) and subsequently visualized with the Odyssey infrared imaging system (LICOR Biosciences, Bad Homburg, Germany).

Western blotting

Cells were lysed in 100 µl of monoQ-c buffer. Visualization and quantitations of the bands were performed using the Odyssey infrared imaging device and software (Licor, Homburg, Germany).

Antibodies

The anti-PUMA rabbit polyclonal IgG, the anti-Bid rabbit polyclonal antibody and the anti-Bcl-XL rabbit polyclonal IgG and the anti-Caspase-3 rabbit polyclonyl IgG were from Cell Signaling (ref. n°4976, 2002, 2764 and 9665, respectively). The 6A7 anti-Bax mouse monoclonal IgG1 and the N-20 anti-Bax rabbit polyclonal IgG were from SantaCruz (ref. n°sc-23959 and n°sc-493, respectively). The anti-Bcl-2 mouse monoclonal IgG1 was from Upstate (ref. n°05-341), the Y37 anti-Mcl-1 rabbit monoclonal IgG was from Abcam (ref. n°ab32087), the 3C5 anti-Bim rat monoclonal IgG2a and the 1E1-1-10 anti-cIAP1 rat monoclonal IgG2a were from Enzo Life Sciences (ref. n°ALX-804-527-C100 and n°ALX-803-335-C100, respectively), the 48/hILP/XIAP anti-XIAP mouse monoclonal IgG1 was from BD Biosciences (ref. n°610762). The anti-cytochrome c rabbit polyclonal antibody was

a gift from Dr, Jean-Claude Martinou. Secondary antibodies were goat anti-mouse IRDye800-conjugated antibody (Rockland, ref. n°610-132-121), goat anti-rabbit Alexa Fluor 680-conjugated antibody (Molecular Probes, ref. n°A21109) and donkey anti-rabbit HRP-conjugated antibody (Jackson immunoresearch ref n ° 711-035-152).

Plasmids

The pcDNA3 expression vector is from Invitrogen. pEGFP-C1 (Clontech) encodes the green fluorescent protein. Puma.cmv (Origene) encodes human Puma. hTPP53.dn3 encodes the human p53. It was generated by subcloning the 1900 bp EcoRI/BamHI fragment from hTP53.lti (gift from Richard Iggo) into pcDNA3 opened with the same two enzymes. **TRIP-PGK-IRESNEO-WHV (#350)** is a lentiviral vector bearing the neomycine resistance **SV40LargeTantigen.pBABE-puro (#731)** encodes the SV40 large T antigen (Addgene; plasmid 13970). **SV40LargeTantigen.lti-neo (#738)** similarly encodes the large T antigen but in a lentiviral expression vector. It was constructed by subcloning the BamHI 2187 base pairs fragment of SV40LargeTantigen.pBABE-puro into TRIP-PGK-IRESNEO-WHV opened with the same enzyme. The extension .lti indicates that the backbone is a lentiviral vector. The extension .cmv indicates that the backbone is the pCMV-AC vector. The extension .dn3 indicates that the backbone plasmid is pcDNA3.

Results

TAT-RasGAP₃₁₇₋₃₂₆ sensitizes diverse cancer cells to genotoxin-induced apoptosis but not to TNF α -induced apoptosis and variably to starvation- and UV-induced apoptosis

We demonstrated earlier that TAT-RasGAP₃₁₇₋₃₂₆ sensitizes various cancer cell lines to apoptosis induced by genotoxins such as cisplatin [1]. These compounds induce apoptosis via the intrinsic apoptosis pathway [3;4]. To gain further insight about the manner by which TAT-RasGAP₃₁₇₋₃₂₆ exerts its tumor sensitization effect, HeLa, U2OS, and HCT116 cancer cells were treated with additional pro-apoptotic compounds, including TNF α that induces cell death via the extrinsic apoptotic pathway. Figure 1 shows that TAT-RasGAP₃₁₇₋₃₂₆ favors apoptosis induced by cisplatin in the three different cancer cell lines, confirming earlier results [1;11]. However, TAT-RasGAP₃₁₇₋₃₂₆ does not sensitize all tumor cell lines to UV- or growth factor deprivation-induced apoptosis, despite that these treatments activate the intrinsic apoptotic pathway [12;13]. None of the tumors is sensitized by the peptide to the extrinsic pathway stimulator TNF α [14;15] in presence of cycloheximide, a protein synthesis inhibitor that prevents the expression of anti-apoptotic proteins that would otherwise counteract the pro-apoptotic abilities of TNF α [16;17]. These results indicate that TAT-RasGAP₃₁₇₋₃₂₆ exerts a pro-apoptotic role only in conditions where the intrinsic cell death pathway is engaged. However since the cancer cell lines used here are type II cells [18;19], i.e. they need the mitochondrial pathway to fully activate caspase-3 in response to extrinsic death stimuli [20], it is unclear why TAT-RasGAP₃₁₇₋₃₂₆ does not have any sensitizing effect on these cell lines when incubated with TNF α . One possibility could be that the peptide requires protein translation (blocked by cycloheximide) to mediate its effect. Possibly therefore, the activation of the mitochondrial pathway upon TNF α treatment is not pronounced enough for TAT-RasGAP₃₁₇₋₃₂₆ to operate.

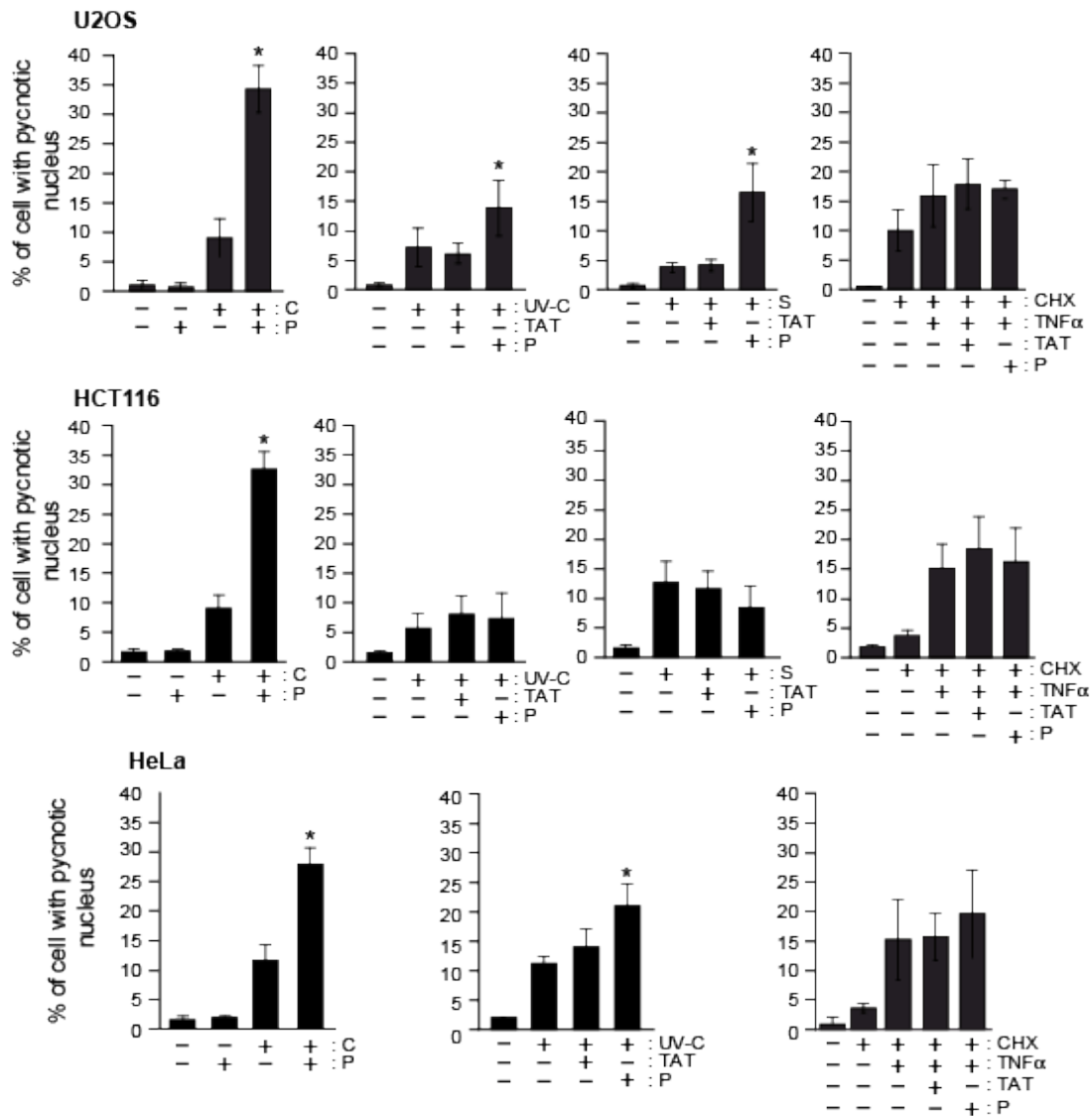


Figure 1. Ability of TAT-RasGAP₃₁₇₋₃₂₆ to sensitize tumor cell to various cell death stimuli. U2OS, HeLa and HCT116 were subjected to UV-C illumination or treated during 24 hours with various apoptotic stimuli as indicated in the figure. Cells were then fixed and apoptosis was counted by scoring pycnotic nuclei. C: cisplatin 30 μ M, P: TAT-RasGAP₃₁₇₋₃₂₆ 20 μ M, TAT: 20 μ M, UV-C: 20 J/m² (U2OS), 25 J/m² (HeLa and HCT116), S: starvation, CHX: cycloheximide 10 μ g/ml, TNF α : 1 ng/ml (U2OS and HeLa), 0,5 ng/ml (HCT116). The results correspond to the mean \pm 95% CI of at least three independent experiments. The asterisks indicate a statistically significant difference (as assessed by impaired t-test between cells treated or not with TAT-RasGAP₃₁₇₋₃₂₆ in the presence of the apoptogenic stimulus).

TAT-RasGAP₃₁₇₋₃₂₆ does not sensitize cells to PUMA over-expression

We previously reported that TAT-RasGAP₃₁₇₋₃₂₆ requires an intact p53/Puma axis to deliver its genotoxin-sensitizing effect in cancer cells [11]. To determine if the peptide potentiates the pro-apoptotic activity of PUMA, Puma was ectopically expressed in U2OS cells to levels comparable to those induced by cisplatin (Figure 2A). This does not lead to apoptosis whether

the cells were incubated with TAT-RasGAP₃₁₇₋₃₂₆ or not (Figure 2B, squares). In contrast, the peptide efficiently sensitizes tumor cells to cisplatin-induced apoptosis (Figure 2B, circles). PUMA is a p53 transcription target that may, once synthesized, need p53 to exert its full pro-apoptotic actions [21]. Figure 3 shows that ectopic expression of p53 in U2OS cells induces apoptosis. However this is neither modulated by PUMA nor by TAT-RasGAP₃₁₇₋₃₂₆. Taken together these data suggest that TAT-RasGAP₃₁₇₋₃₂₆ does not directly amplify the DNA-damage-induced p53/PUMA arm. Hence, even though cisplatin requires p53 and PUMA to induce apoptosis [11], this genotoxin may modulate other pro-apoptotic signals that are targeted by TAT-RasGAP₃₁₇₋₃₂₆ to induce cell death in cancer cells. Additionally, the results presented in Figure 3 do not support the model proposed by Chipuk and collaborators where PUMA and p53 collaborate to induce apoptosis [21].

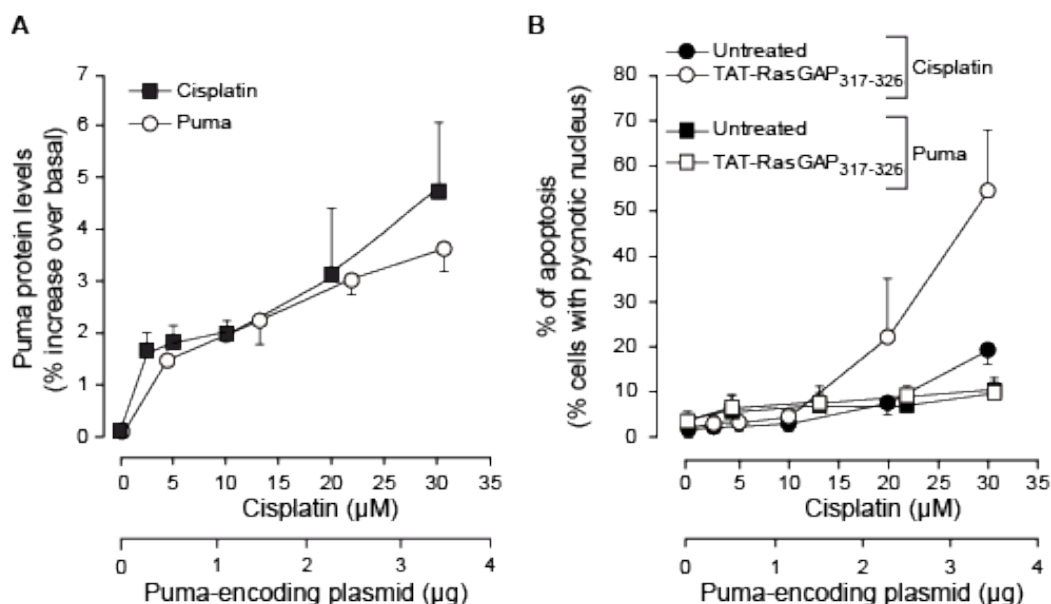


Figure 2. Increase in Puma expression levels does not make tumor cells sensitive to TAT-RasGAP₃₁₇₋₃₂₆. U2OS were treated with increasing concentrations of cisplatin or transfected with the indicated amount of a Puma-encoding plasmid in the presence or not of TAT-RasGAP₃₁₇₋₃₂₆ (20 µM) for 22 hours. Apoptotic cell percentage (B) and Puma protein levels (A) were then quantitated. Results correspond to the mean \pm 95% CI of three independent experiments.

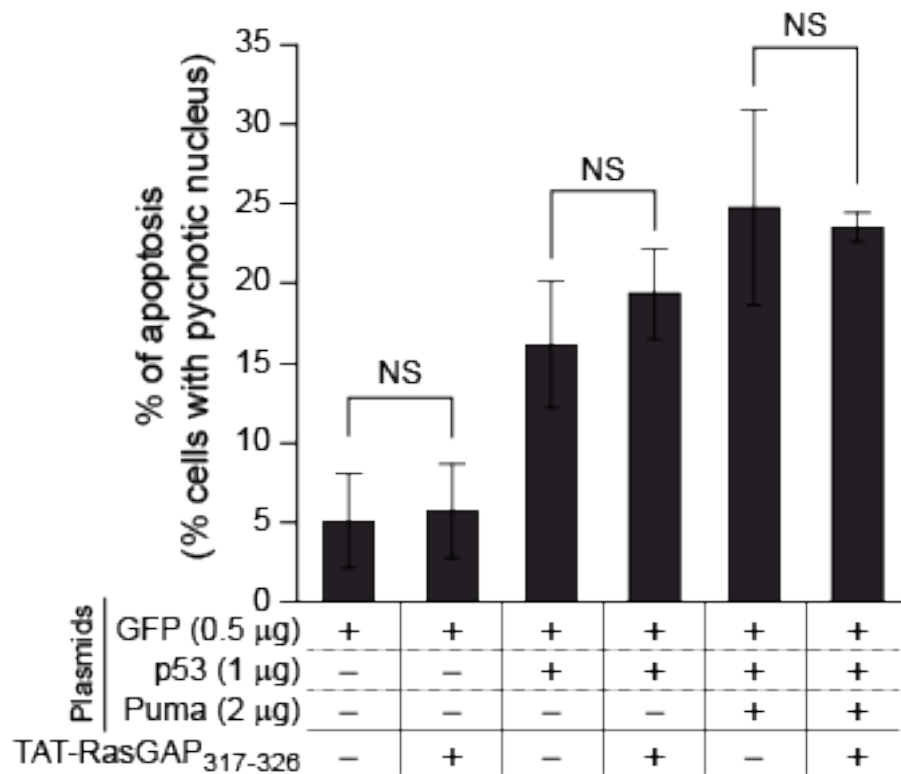


Figure 3. p53, in combination or not with Puma, does not sensitize cancer cells to TAT-RasGAP₃₁₇₋₃₂₆. U2OS were transfected with the indicated plasmids and treated or not with 20 μ M of TAT-RasGAP₃₁₇₋₃₂₆ for 22 hours. Apoptosis was then determined. Results correspond to the mean \pm 95% CI of four independent experiments. NS, no statistically significant difference

TAT-RasGAP₃₁₇₋₃₂₆ affects long term survival of cancer cells independently of p53

The observation that the RasGAP-derived peptide does not amplify the p53/Puma axis led us to reconsider the implication of p53 in the TAT-RasGAP₃₁₇₋₃₂₆-mediated sensitization of cancer cells. Cells lacking an intact p53/Puma axis show a drastically reduced apoptotic rate when exposed to genotoxin treatment [1], but their overall resistance to genotoxins might not be affected. Figure 4B shows that the overall survival of HCT116 p53^{-/-} tumor cells, tested by colony formation assay, is reduced by cisplatin treatment and, more importantly, TAT-RasGAP₃₁₇₋₃₂₆ significantly augments the cisplatin-mediated impairment in cell survival (Figure 4). The same TAT-RasGAP₃₁₇₋₃₂₆-mediated effect is observed, as expected, in HCT116 p53 WT cells treated with cisplatin (Figure 4A). Moreover TAT-RasGAP₃₁₇₋₃₂₆ by itself has no effect on the clonogenic survival as well as the cell permeable sequence TAT, alone or in combination with cisplatin. These data led us to the conclusion that, contrary to

what previously hypothesized, p53 is dispensable for the TAT-RasGAP₃₁₇₋₃₂₆-mediated sensitization of malignant cells.

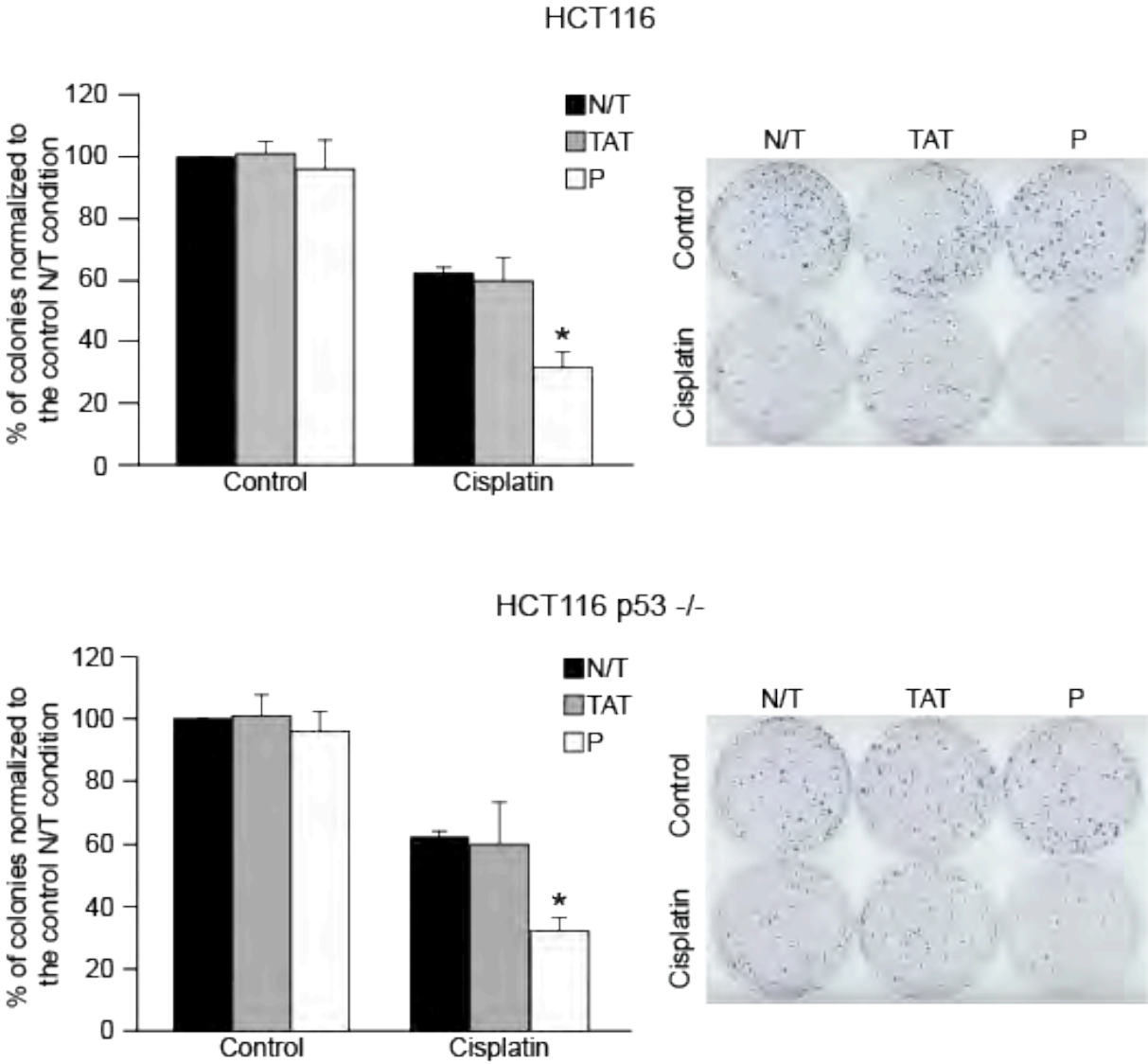


Figure 4. TAT-RasGAP₃₁₇₋₃₂₆ sensitizes cancer cells to cisplatin-induced cell death irrespective of the p53 status. HCT116 and HCT116 p53^{-/-} were treated with 1 μM cisplatin in the presence or not of 20 μM TAT-RasGAP₃₁₇₋₃₂₆ (P) or 20 μM TAT for 3 days. Culture medium was then replaced with fresh medium and after an additional 10-day period the number of colonies was recorded. N/T:untreated. The results correspond to the mean +/- 95%CI of at least three independent experiments. The asterisks indicate a statistically significant difference (as assessed by ANOVA between cells treated or not with TAT-RasGAP₃₁₇₋₃₂₆ in the presence of cisplatin).

TAT-RasGAP₃₁₇₋₃₂₆ increases cisplatin-induced Bax activation.

Tumor cells sensitized by TAT-RasGAP₃₁₇₋₃₂₆ to genotoxin-induced apoptosis show increased caspase-3 activation and more pronounced mitochondrial membrane depolarization [11]. This suggests that the RasGAP-derived peptide acts upstream of cytochrome c release from mitochondria. Consequently, Bax, which is required for outer mitochondrial membrane permeabilization, cytochrome c release, and caspase activation [10], should be more activated by genotoxins in the presence of TAT-RasGAP₃₁₇₋₃₂₆. Figure 5A shows indeed that, while the peptide alone does not affect Bax activity, it increases cisplatin-induced Bax stimulation. There is evidence that caspase activation induces a positive feedback loop to increase Bax activation and cytochrome c release from the mitochondria [22]. To determine if TAT-RasGAP₃₁₇₋₃₂₆ modulates this feedback loop, the experiment shown in Figure 5A was performed in the presence of the pan-caspase inhibitor MX1013 [23;24] that efficiently blocks executioner caspase activity (Figure 5B). This experiment shows that caspase inhibition does not prevent TAT-RasGAP₃₁₇₋₃₂₆ from enhancing cisplatin-mediated Bax activation (Figure 5C). Altogether, these experiments indicate that the mechanisms underlying TAT-RasGAP₃₁₇₋₃₂₆-mediated apoptosis sensitization occur upstream or at the level of mitochondria.

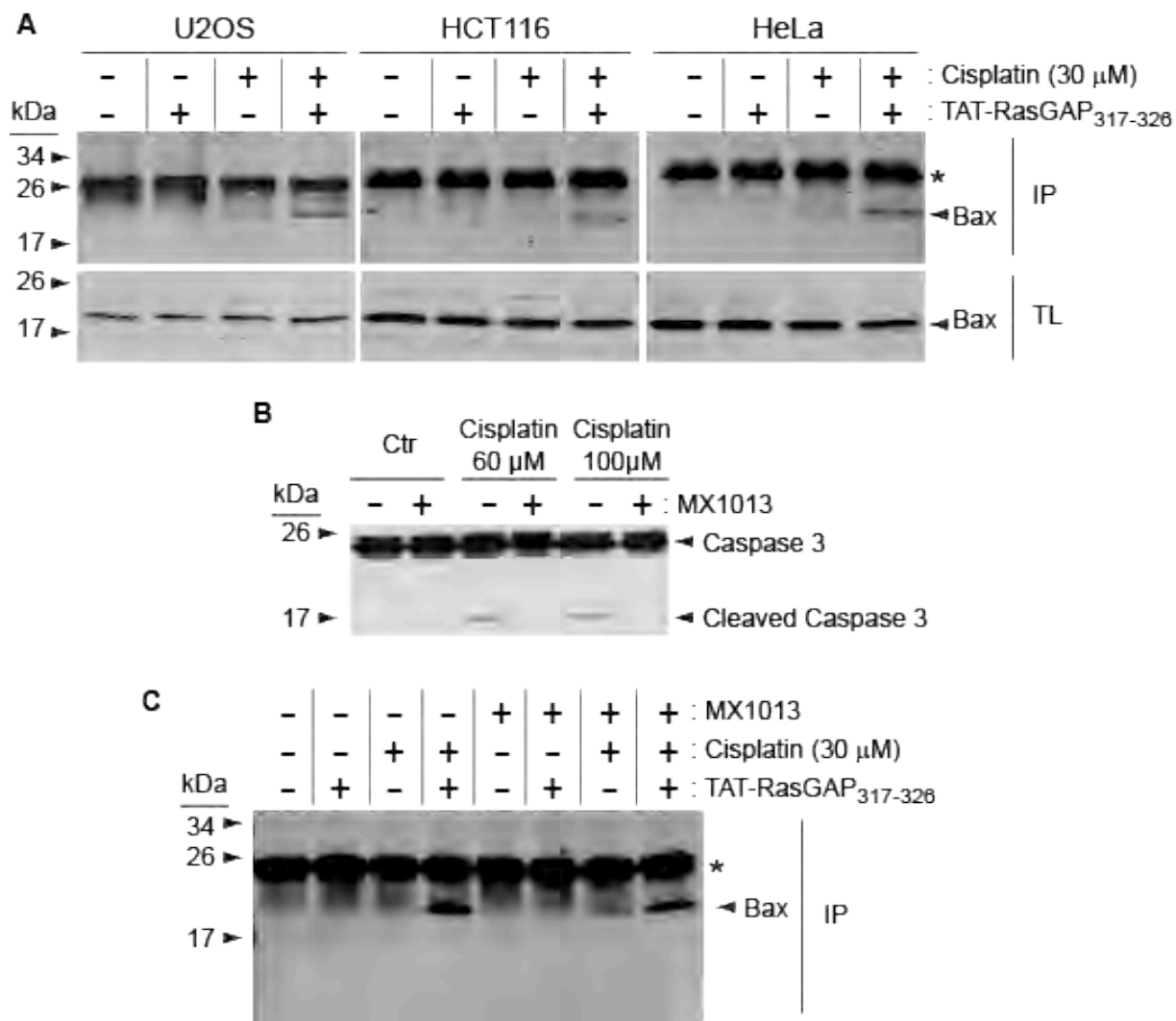


Figure 5. TAT-RasGAP₃₁₇₋₃₂₆ favors, in a caspase-independent manner, the ability of cisplatin to activate Bax.

A. U2OS, HeLa and HCT116 were treated for 16 hours with 20 μ M TAT-RasGAP₃₁₇₋₃₂₆ and/or with 30 μ M of cisplatin as indicated in the figure. The cells were then lysed and the activated form of Bax detected after immunoprecipitation (see methods). IP, immunoprecipitate; TL, total lysate; *, non-specific band.

B. HCT116 were either left untreated or treated with the indicated concentration of cisplatin for 20 hours, in the presence or not of the pan-caspase inhibitor MX1013. The cells were then lysed and the cleavage of Caspase-3 was assessed by Western blot.

C. U2OS cells were processed as in panel A in the presence or not of 10 μ M of the pan-caspase inhibitor MX1013.

TAT-RasGAP₃₁₇₋₃₂₆ does not modulate any of the Bcl-2 and IAP family members

Bax activation is controlled by pro- and anti-apoptotic members of the Bcl-2 family of proteins [9;10]. Conceivably, TAT-RasGAP₃₁₇₋₃₂₆ could favor genotoxin-induced apoptosis by increasing the levels of pro-apoptotic Bcl-2 family members and/or decreasing the levels of the anti-apoptotic members. However, the peptide does neither modulate the pro-apoptotic

Bim, Puma and Bid proteins nor the anti-apoptotic Bcl-X_L, Bcl-2 and Mcl-1 proteins (Figure 6). Another possibility that could explain how TAT-RasGAP₃₁₇₋₃₂₆ favors apoptosis is inhibition of inhibitor of apoptosis (IAP) family proteins. However, the peptide does not alter cellular levels of cIAP1, cIAP2 and XIAP (Figure 6). Therefore, modulation of the expression of IAPs and Bcl-2 family members is not the mechanism used by TAT-RasGAP₃₁₇₋₃₂₆ to favor Bax activation and apoptosis. However, this does not exclude the possibility that the peptide affects the activity of these proteins.

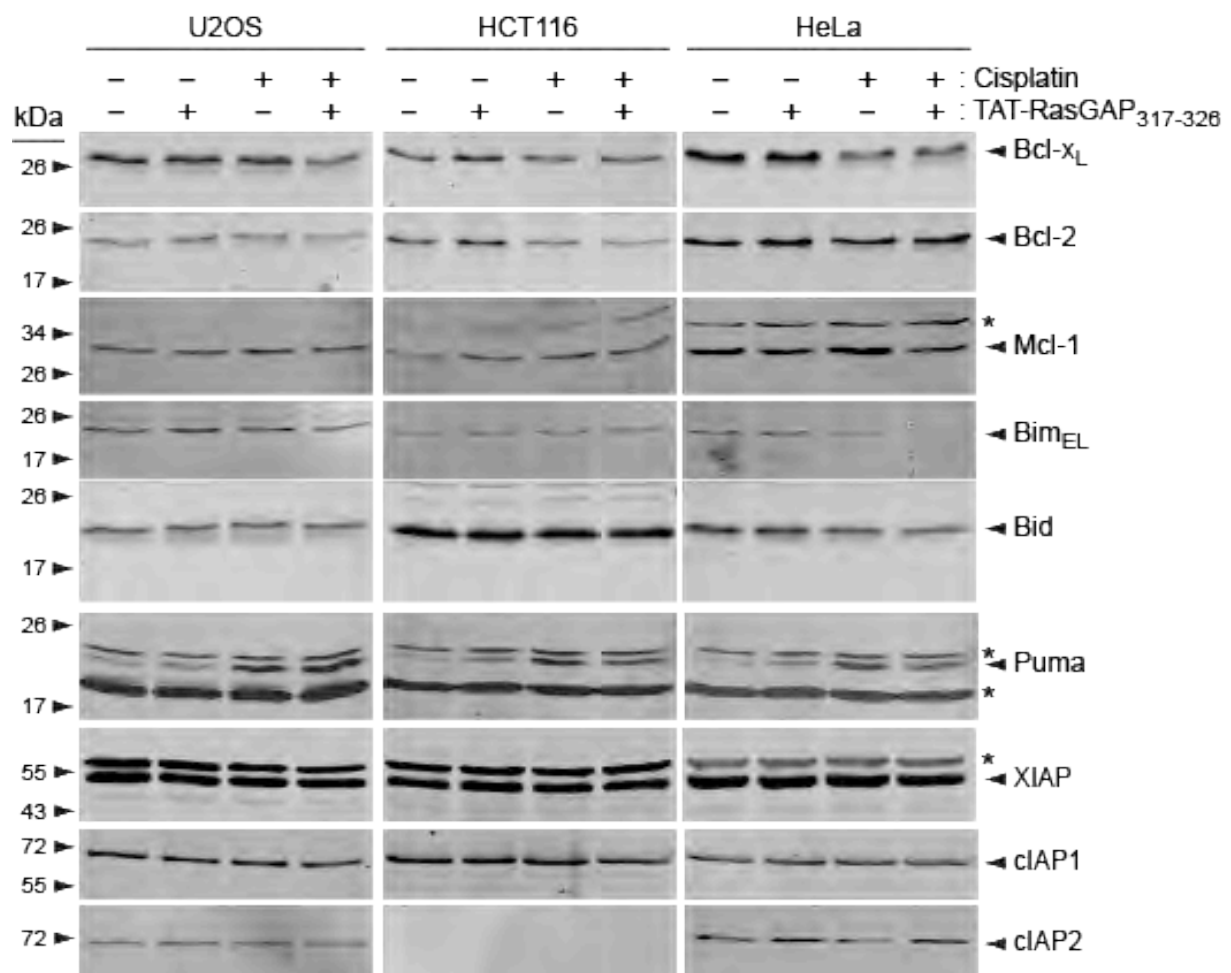


Figure 6. TAT-RasGAP₃₁₇₋₃₂₆ does not modulate Bcl-2 family protein levels. U2OS, HCT116 and HeLa were treated as shown in the figure for 22 hours (TAT-RasGAP₃₁₇₋₃₂₆, 20 μ M; cisplatin, 30 μ M). Cells were then lysed and total protein extracts were immunoblotted with antibodies specific for the indicated proteins (*: non-specific band). cIAP2 is not detected in HCT116.

The ability of Bcl-X_L to bind p53 and Puma is not impaired by TAT-RasGAP₃₁₇₋₃₂₆

Bcl-X_L is one of the main anti-apoptotic proteins that bind to and neutralize pro-apoptotic proteins such as PUMA [25]. Additionally, the p53 tumor suppressor binds to Bcl-X_L, antagonizing the latter's anti-apoptotic activity [26]. TAT-RasGAP₃₁₇₋₃₂₆ may promote apoptosis by displacing Bcl-X_L from its pro-apoptotic binding partners. However, cisplatin-induced increased binding of Bcl-X_L to p53 or to PUMA is unaffected by the peptide (Figure 7). Therefore, TAT-RasGAP₃₁₇₋₃₂₆ does not appear to modulate Bcl-X_L functionality.

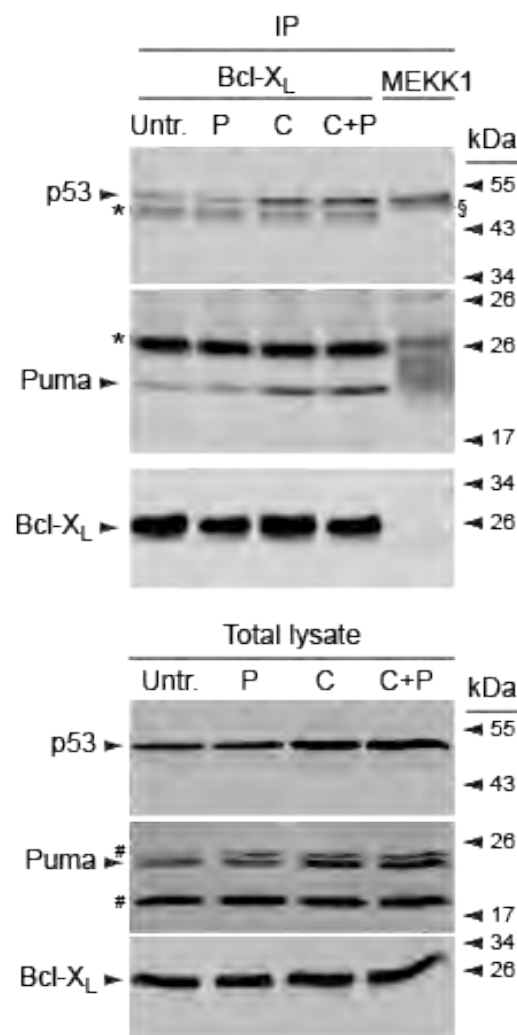


Figure 7. TAT-RasGAP₃₁₇₋₃₂₆ does not affect the ability of Bcl-XL to bind to p53 or Puma. Cells were treated as shown in the figure (C: 30 μM cisplatin; P: 20 μM TAT-RasGAP₃₁₇₋₃₂₆). Bcl-XL was immunoprecipitated from cell lysates and its association with p53 and Puma was analysed by Western blot. In parallel, proteins expression was assessed on total protein extracts. *, immunoglobulin light chains; #, non-specific bands. The immunoglobulin heavy chains of the MEKK1 antibody (§) are shifted up compared to the corresponding chains of the Bcl-XL-specific antibody.

Targeted disruption of individual Bcl-2 family members does not prevent TAT-RasGAP₃₁₇₋₃₂₆-mediated tumor cell sensitizing

Large T antigen-transformed MEFs lacking specific Bcl-2 family member were used to investigate the role of this protein family in the capacity of TAT-RasGAP₃₁₇₋₃₂₆ to sensitize tumor cells to genotoxin-induced apoptosis. MEFs are not cancer cells and hence are not susceptible to TAT-RasGAP₃₁₇₋₃₂₆-mediated genotoxin sensitization. However, transforming MEFs with the SV40 large T antigen renders them sensitive to the peptide (*Annibaldi, A., Plos One, 2011*). Figure 8 shows that transformed MEFs lacking the pro-apoptotic Bim, Bmf, Bad, Bax, or Bak proteins, or the anti-apoptotic Bcl-X_L, Bcl-2, or Mcl-1 proteins are efficiently sensitized by TAT-RasGAP₃₁₇₋₃₂₆ to cisplatin-induced apoptosis. As expected, transformed MEFs lacking both Bax and Bak are totally resistant to cisplatin-induced death [27]. Similarly, transformed MEFs lacking Bid are totally resistant to cisplatin-induced apoptosis, consistent with the notion that Bid is a main cell death effector in DNA-damage response [28;29]. These results indicate that taken individually Bim, Bmf, Bad, Bax, Bak, Bcl-X_L, Bcl-2, or Mcl-1 and dispensable for TAT-RasGAP₃₁₇₋₃₂₆ to mediate its tumor sensitization activity.

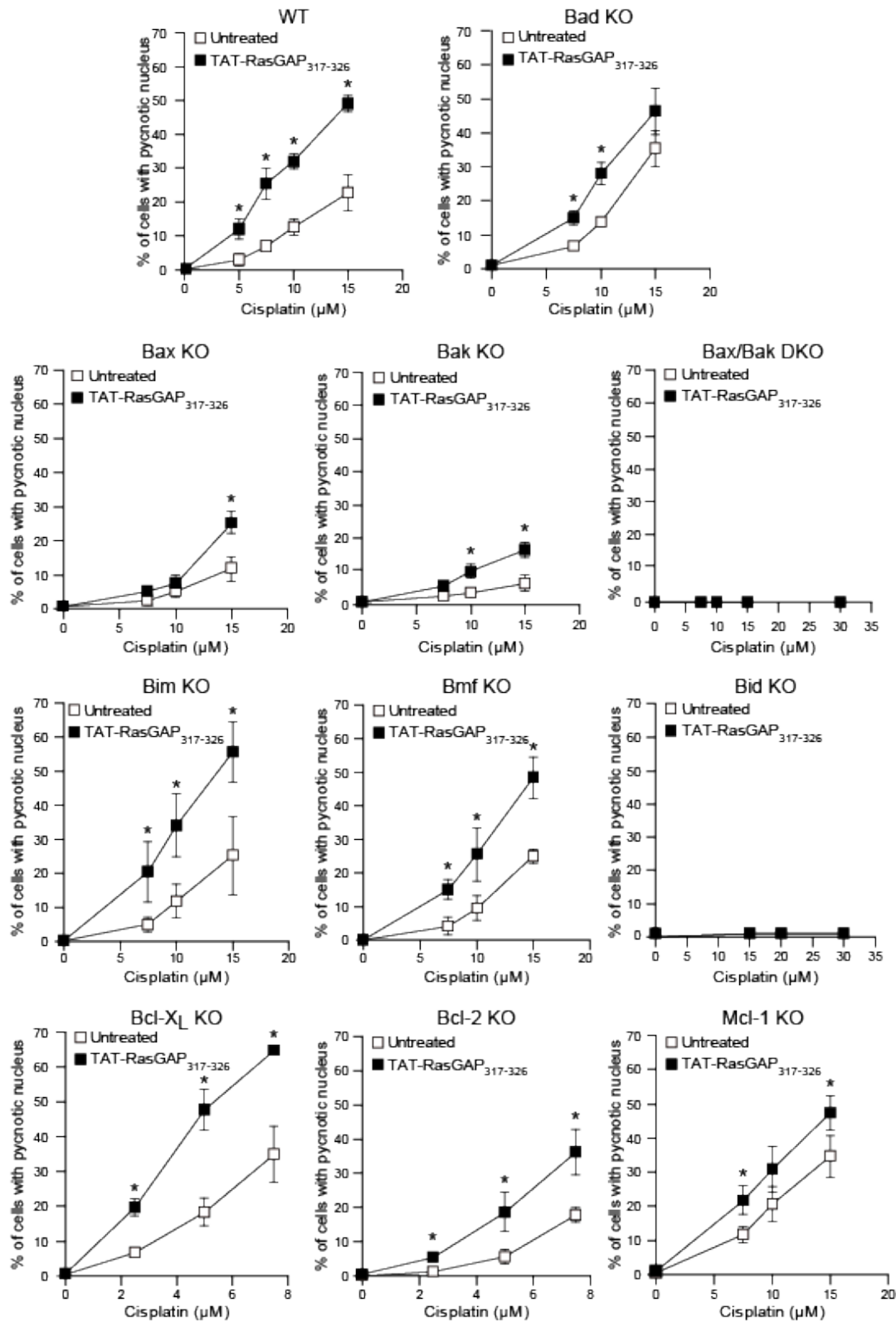


Figure 8. Role of single Bcl-2 family proteins in the TAT-RasGAP₃₁₇₋₃₂₆-mediated sensitization to cisplatin-induced apoptosis.

SV40-transformed MEFs KO for the indicated Bcl-2 family proteins were treated as indicated in the figure for 22 hours. Cells were then fixed and apoptosis was counted by scoring pycnotic nuclei. TAT-RasGAP₃₁₇₋₃₂₆: 20 μM . The results correspond to the mean \pm 95%CI of at least three independent experiments. The asterisks indicate a statistically significant difference (as assessed by unpaired t-test between cells treated or not with TAT-RasGAP₃₁₇₋₃₂₆ in the presence cisplatin).

TAT-RasGAP₃₁₇₋₃₂₆ enhances cisplatin-induced Bax activation via tBid

The absence of apoptosis observed in Bid KO MEFs does not allow us to conclude if TAT-RasGAP requires Bid to sensitize tumors. To address this point we used HeLa-purified mitochondria, taking advantage of the fact that Bax is weakly associated with the mitochondrial membrane in an inactive configuration [30;31]. The addition of recombinant tBid to the isolated mitochondria was shown to trigger Bax oligomerization, insertion into the outer mitochondrial membrane and cytochrome *c* release [30;32]. If TAT-RasGAP₃₁₇₋₃₂₆ needs tBid to fulfill its sensitizing functions, we predict that the peptide should favor the tBid-induced cytochrome *c* release. Consistently with our prediction, figure 9 shows that tBid induces cytochrome *c* release in a dose dependent manner and that TAT-RasGAP₃₁₇₋₃₂₆ enhances the tBid-mediated cytochrome *c* release, while having no effect by itself. These data support a role for tBid in the above-mentioned TAT-RasGAP₃₁₇₋₃₂₆-induced activation of Bax that results then in mitochondrial membrane depolarization and cytochrome *c* release.

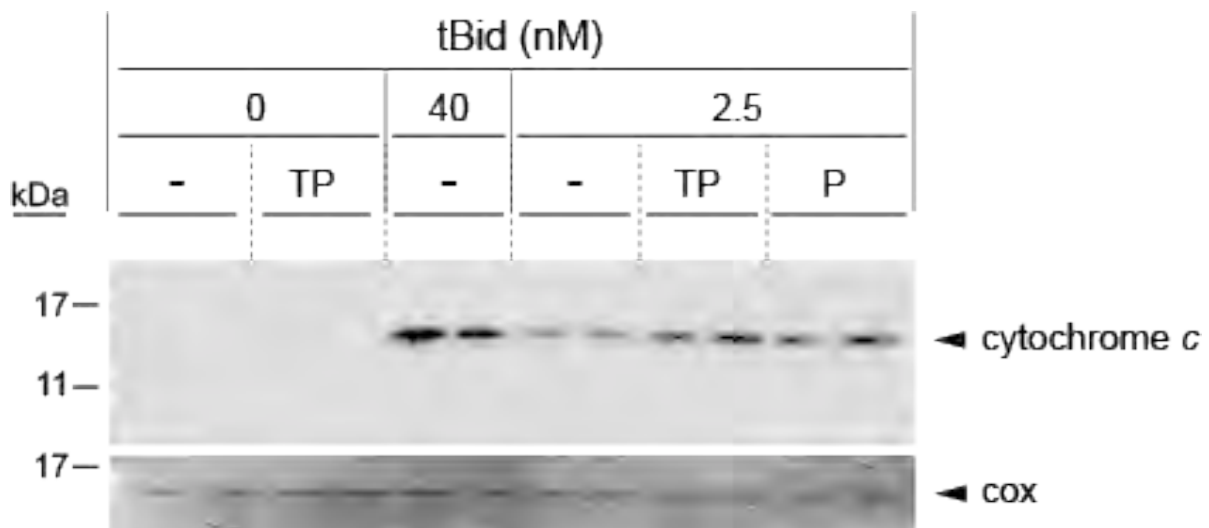


Figure 9. TAT-RasGAP₃₁₇₋₃₂₆ enhances the tBid-induced cytochrome *c* release.

30 μ g of HeLa-isolated mitochondria were left untreated or incubated with the indicated concentrations of recombinant tBid in the presence or not of 1 μ M TAT-RasGAP₃₁₇₋₃₂₆ (TP) or 1 μ M RasGAP₃₁₇₋₃₂₆ (P) as indicated in the figure for 30 minutes at room temperature. Supernatants were analysed for cytochrome *c* release and mitochondrial pellets for Cox as gel-loading control. These blots are representative of 4 different experiments.

Discussion

This study provides advances in the understanding on the mode of action of TAT-RasGAP₃₁₇₋₃₂₆. Firstly, it clarifies the role played by p53 (and Puma) in TAT-RasGAP₃₁₇₋₃₂₆-mediated sensitization of tumor cells to genotoxin-induced apoptosis. Secondly, it shows that this peptide enhances Bax activation, providing a mechanistic basis for its sensitizing capacity.

Earlier work has indicated that TAT-RasGAP₃₁₇₋₃₂₆ required a functional p53-PUMA axis to favor apoptosis of cisplatin-stimulated tumor cells [11]. We therefore hypothesized that increased expression of p53 and Puma in cancer cells, which occurs when cells are treated with cisplatin, would render them sensitive to TAT-RasGAP₃₁₇₋₃₂₆. However, this proved not to be the case. Moreover, tumor cells lacking p53, even though highly resistant to cisplatin-induced apoptosis in short-term experiments [11], were nevertheless less able to survive long-term cisplatin treatment when co-treated with TAT-RasGAP₃₁₇₋₃₂₆. This indicates that the RasGAP-derived peptide does not require p53 to exert its tumor sensitization activity. Hence, p53 and Puma are not targets of TAT-RasGAP₃₁₇₋₃₂₆. The apparent requirement of p53 and Puma for the genotoxin-sensitizing function of the peptide in short-term apoptosis assays most likely results from the fact that genotoxins inefficiently induce apoptosis of tumor cells lacking a functional p53-Puma axis [33]. In other words, the absence of TAT-RasGAP₃₁₇₋₃₂₆-mediated sensitization observed in p53- or Puma-negative cells merely reflects the fact these cells cannot properly undergo genotoxin-induced apoptosis. Measuring cell death in short-term assays (e.g. within the first 24 hours of treatment) might lead to an underestimation of the killing potential of genotoxins, as long-term cell survival is not taken into account. This may particularly be the case in cells bearing mutations in apoptosis-controlling proteins. Tumor cells lacking p53 can bypass the primary apoptotic decision, which takes place shortly after the administration of an apoptotic stimulus, and undergo several cell divisions before dying. This can occur either by p53-independent apoptosis or as a result of mitotic catastrophe

or necrotic cell death [34]. The observation that TAT-RasGAP₃₁₇₋₃₂₆, in combination with cisplatin, reduces the viability of p53-negative tumor cells demonstrates that this peptide can also positively reinforce p53-independent cell death mechanism(s) that occur in a more delayed manner compared to short-term apoptosis.

Bid is a BH3-only Bcl-2 family member bearing a caspase-8 recognition site. Caspase 8-mediated cleavage of Bid at asp59 generates a C-terminal fragment, called truncated Bid (tBid), which translocates to mitochondria to induce the release of cytochrome *c* through the oligomerization of Bax [30]. Consistently with previous reports, we found that Bid-deficient cells are fully resistant to cisplatin [28] (Figure 8). Thus, similarly to p53 and Puma, Bid is also required for genotoxin-induced apoptosis of at least some cancer cells. Consequently, the use of Bid knockout cells did not allow us to assess the involvement of Bid in TAT-RasGAP₃₁₇₋₃₂₆-mediated tumor cell sensitization to genotoxins. To circumvent this limitation, we used a cell free assay in which the release of cytochrome *c* is induced by recombinant tBid. This approach showed that TAT-RasGAP₃₁₇₋₃₂₆ is able to increase the capacity of tBid to activate Bax as assessed by augmented cytochrome-*c* release. This is consistent with our observation that the peptide increases cisplatin-induced Bax activation in cells (Figure 5). Two possibilities can be proposed to explain this observation: i) the peptide pre-sensitizes Bax (and/or Bak) so that they can be better activated by direct stimulators such as tBid, Puma, or Bim; ii) the peptide makes truncated forms of Bid more potent in activating Bax. At present, we cannot discriminate between these two possibilities but the following arguments need to be taken into consideration. First, Bax activation does not result from a peptide-induced balance shift between the expression levels of pro- and anti-apoptotic Bcl-2 family members. Indeed, the protein levels of Bcl-2, Bcl-X_L, Mcl-1, Bim, Puma, and Bid were not modulated by TAT-RasGAP₃₁₇₋₃₂₆ (Figure 6). Moreover, many Bcl-2 family proteins (Bcl-2, Bcl-XL, Mcl-1, Bim, Bmf and Bad) were shown to be dispensable individually for the

sensitizing activity of the peptide. Second, the ability of TAT-RasGAP₃₁₇₋₃₂₆ to increase genotoxin-induced Bax activation did not require caspase activation (Figure 5C). Therefore, the peptide does not amplify a positive feedback loop on Bax activation induced by the activation of caspases following cytochrome c release [22]. The fact that caspase inhibition does not prevent TAT-RasGAP₃₁₇₋₃₂₆ from increasing genotoxin-induced Bax activation would rule out the implication of tBid generation in this process. Additionally, stimuli activating the extrinsic apoptotic pathway, hence caspase-8 and potentially the formation of tBid were not killing tumor cells better in the presence of the peptide (Figure 1). However, Bid can be cleaved by other cellular protease such as calpains and cathepsins [35] and there are indications that calpain-induced Bid cleavage plays an important role in cisplatin-induced apoptosis [36]. Taken together our data led us to the elaboration of the model proposed in Figure 10. Future studies will determine whether TAT-RasGAP₃₁₇₋₃₂₆ targets Bax directly or indirectly.

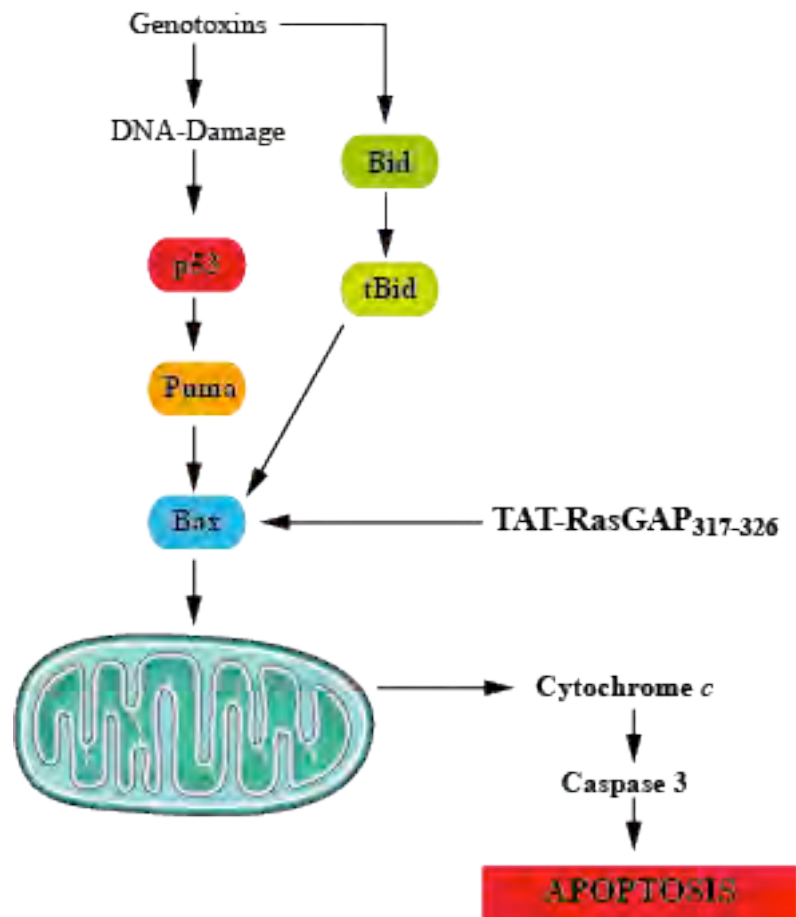


Figure 10. Proposed model for the TAT-RasGAP₃₁₇₋₃₂₆ mode of action.

Genotoxin-induced DNA damage triggers an apoptotic cell death response that requires the p53/Puma axis as well as the generation of tBid for the full activation of Bax. Activation of Bax mediates mitochondrial membrane permeabilization and cytochrome c release with the consequent activation of caspase 3 and induction of apoptosis. TAT-RasGAP₃₁₇₋₃₂₆ enhances the genotoxin-mediated activation of Bax in a tBid-dependent manner.

Reference list

- [1] D. Michod, J.Y. Yang, J. Chen, C. Bonny, C. Widmann, A RasGAP-derived cell permeable peptide potently enhances genotoxin-induced cytotoxicity in tumor cells. *Oncogene* 23 (2004) 8971-8978.
- [2] D. Michod, A. Annibaldi, S. Schaefer, C. Dapples, B. Rochat, C. Widmann, Effect of RasGAP N2 Fragment-Derived Peptide on Tumor Growth in Mice. *J.Natl.Cancer Inst.*2009) djp100.
- [3] K.M.P.D.K.G. Debatin, Chemotherapy: targeting the mitochondrial cell death pathway. *Oncogene*2009).
- [4] S.H. Kaufmann, W.C. Earnshaw, Induction of apoptosis by cancer chemotherapy. *Exp.Cell Res.* 256 (2000) 42-49.
- [5] S. Fulda, K.M. Debatin, Extrinsic versus intrinsic apoptosis pathways in anticancer chemotherapy. *Oncogene* 25 (2006) 4798-4811.
- [6] B.B. Zhou, J. Bartek, Targeting the checkpoint kinases: chemosensitization versus chemoprotection. *Nat.Rev.Cancer* 4 (2004) 216-225.
- [7] Y. Shiloh, ATM and related protein kinases: safeguarding genome integrity. *Nat.Rev.Cancer* 3 (2003) 155-168.
- [8] E. Michalak, A. Villunger, M. Erlacher, A. Strasser, Death squads enlisted by the tumour suppressor p53. *Biochem.Biophys.Res.Comm.* 331 (2005) 786-798.
- [9] R.J. Youle, A. Strasser, The BCL-2 protein family: opposing activities that mediate cell death. *Nat Rev Mol Cell Biol* 9 (2008) 47-59.
- [10] J.E. Chipuk, D.R. Green, How do BCL-2 proteins induce mitochondrial outer membrane permeabilization? *Trends in Cell Biology* 18 (2008) 157-164.
- [11] D. Michod, C. Widmann, TAT-RasGAP317-326 requires p53 and PUMA to sensitize tumor cells to genotoxins. *Mol.Cancer Res.* 5 (2007) 497-507.
- [12] S. Bialik, V.L. Cryns, A. Drincic, S. Miyata, A.L. Wollowick, A. Srinivasan, R.N. Kitsis, The mitochondrial apoptotic pathway is activated by serum and glucose deprivation in cardiac myocytes. *Circ.Res.* 85 (1999) 403-414.
- [13] T.R. Dunkern, G. Fritz, B. Kaina, Ultraviolet light-induced DNA damage triggers apoptosis in nucleotide excision repair-deficient cells via Bcl-2 decline and caspase-3/-8 activation. *Oncogene* 20 (2001) 6026-6038.
- [14] M.O. Hengartner, The biochemistry of apoptosis. *Nature* 407 (2000) 770-776.
- [15] H. Walczak, P.H. Krammer, The CD95 (APO-1/Fas) and the TRAIL (APO-2L) apoptosis systems. *Exp.Cell Res.* 256 (2000) 58-66.

- [16] J.R. Muppidi, J. Tschopp, R.M. Siegel. Life And Death Decisions: Secondary Complexes and Lipid Rafts in TNF Receptor Family Signal Transduction. *Immunity* 21[4], 461-465. 1-10-2004.
- [17] I. Lavrik, A. Golks, P.H. Krammer, Death receptor signaling. *J Cell Sci* 118 (2005) 265-267.
- [18] N. Ozoren, W.S. El-Deiry, Defining characteristics of Types I and II apoptotic cells in response to TRAIL. *Neoplasia*. 4 (2002) 551-557.
- [19] M. Mandal, S.B. Maggirwar, N. Sharma, S.H. Kaufmann, S.C. Sun, R. Kumar, Bcl-2 prevents CD95 (Fas/APO-1)-induced degradation of lamin B and poly(ADP-ribose) polymerase and restores the NF-kappaB signaling pathway. *J.Biol.Chem.* 271 (1996) 30354-30359.
- [20] C. Scaffidi, S. Fulda, A. Srinivasan, C. Friesen, F. Li, K.J. Tomaselli, K.M. Debatin, P.H. Krammer, M.E. Peter, Two CD95 (APO-1/Fas) signaling pathways. *EMBO J.* 17 (1998) 1675-1687.
- [21] J.E. Chipuk, L. Bouchier-Hayes, T. Kuwana, D.D. Newmeyer, D.R. Green, PUMA Couples the Nuclear and Cytoplasmic Proapoptotic Function of p53. *Science* 309 (2005) 1732-1735.
- [22] S.A. Lakhani, A. Masud, K. Kuida, G.A. Porter, Jr., C.J. Booth, W.Z. Mehal, I. Inayat, R.A. Flavell, Caspases 3 and 7: key mediators of mitochondrial events of apoptosis. *Science* 311 (2006) 847-851.
- [23] W. Yang, J. Guastella, J.C. Huang, Y. Wang, L. Zhang, D. Xue, M. Tran, R. Woodward, S. Kasibhatla, B. Tseng, J. Drewe, S.X. Cai, MX1013, a dipeptide caspase inhibitor with potent in vivo antiapoptotic activity. *Br.J.Pharmacol.* 140 (2003) 402-412.
- [24] H. Jaeschke, A. Farhood, S.X. Cai, B.Y. Tseng, M.L. Bajt, Protection against TNF-induced liver parenchymal cell apoptosis during endotoxemia by a novel caspase inhibitor in mice. *Toxicol.Appl.Pharmacol.* 169 (2000) 77-83.
- [25] A. Strasser, S. Cory, J.M. Adams, Deciphering the rules of programmed cell death to improve therapy of cancer and other diseases. *EMBO J.* 30 (2011) 3667-3683.
- [26] M. Mihara, S. Erster, A. Zaika, O. Petrenko, T. Chittenden, P. Pancoska, U.M. Moll, p53 has a direct apoptogenic role at the mitochondria. *Mol.Cell* 11 (2003) 577-590.
- [27] M.C. Wei, W.X. Zong, E.H. Cheng, T. Lindsten, V. Panoutsakopoulou, A.J. Ross, K.A. Roth, G.R. MacGregor, C.B. Thompson, S.J. Korsmeyer, Proapoptotic BAX and BAK: a requisite gateway to mitochondrial dysfunction and death. *Science* 292 (2001) 727-730.
- [28] I. Kaminer, R. Sarig, Y. Zaltsman, H. Niv, G. Oberkovitz, L. Regev, G. Haimovich, Y. Lerenthal, R.C. Marcellus, A. Gross, Proapoptotic BID is an ATM effector in the DNA-damage response. *Cell* 122 (2005) 593-603.

- [29] S.N. Shelton, M.E. Shawgo, J.D. Robertson, Cleavage of Bid by executioner caspases mediates feed forward amplification of mitochondrial outer membrane permeabilization during genotoxic stress-induced apoptosis in Jurkat cells. *J.Biol.Chem.* 284 (2009) 11247-11255.
- [30] R. Eskes, S. Desagher, B. Antonsson, J.C. Martinou, Bid Induces the Oligomerization and Insertion of Bax into the Outer Mitochondrial Membrane. *Mol.Cell.Biol.* 20 (2000) 929-935.
- [31] K.G. Wolter, Y.T. Hsu, C.L. Smith, A. Nechushtan, X.G. Xi, R.J. Youle, Movement of Bax from the cytosol to mitochondria during apoptosis. *J.Cell Biol.* 139 (1997) 1281-1292.
- [32] S. Desagher, A. Osen-Sand, A. Nichols, R. Eskes, S. Montessuit, S. Lauper, K. Maundrell, B. Antonsson, J.C. Martinou, Bid-induced Conformational Change of Bax Is Responsible for Mitochondrial Cytochrome c Release during Apoptosis. *J.Cell Biol.* 144 (1999) 891-901.
- [33] A. Villunger, E.M. Michalak, L. Coultas, F. Mullauer, G. Bock, M.J. Ausserlechner, J.M. Adams, A. Strasser, p53- and Drug-Induced Apoptotic Responses Mediated by BH3-Only Proteins Puma and Noxa. *Science* 302 (2003) 1036-1038.
- [34] Y. Ma, R. Conforti, L. Aymeric, C. Locher, O. Kepp, G. Kroemer, L. Zitvogel, How to improve the immunogenicity of chemotherapy and radiotherapy. *Cancer Metastasis Rev.* 30 (2011) 71-82.
- [35] X.M. Yin, Bid, a BH3-only multi-functional molecule, is at the cross road of life and death. *Gene* 369 (2006) 7-19.
- [36] A. Mandic, K. Viktorsson, L. Strandberg, T. Heiden, J. Hansson, S. Linder, M.C. Shoshan, Calpain-mediated Bid cleavage and calpain-independent Bak modulation: two separate pathways in cisplatin-induced apoptosis. *Mol.Cell Biol.* 22 (2002) 3003-3013.

Results

Part V

Introduction

Radiotherapy is one of the most commonly used anti-cancer therapies. Its toxicity towards tissues surrounding the tumoral mass still remains a major concern in radio-oncology. In this work we wanted to ascertain if TAT-RasGAP₃₁₇₋₃₂₆ sensitizes cancer cells to radiation-induced cell death, augmenting the killing efficacy of γ -irradiations. We provided evidence showing that TAT-RasGAP₃₁₇₋₃₂₆ efficiently potentiates the cytotoxicity of γ -irradiations in several cancer cell lines, but not in non-cancer cell lines, and, in combination with radiotherapy, it delays the tumoral growth in a xenograft mouse model. This suggests that TAT-RasGAP₃₁₇₋₃₂₆ might be a good therapeutical tool to augment the efficiency of radiotherapy, allowing a reduction of the curative doses with consequent reduction or elimination of side effects in cancer suffering patients.

Contribution

I carried out this study in collaboration with Dr. David Viertl, we equally contributed to the data presented below in form of manuscript.

Introduction

Radiotherapy is the treatment of choice in numerous tumor treatments and has offered incalculable benefits for cancer patients [1]. Radio-therapy induces DNA strand breaks that are lethal for the cell when extensive enough [4]. Despite technical improvements, radiation toxicity remains the major obstacle to effective therapy. Indeed, the toxic effects of radiotherapy on healthy tissues often limit the dose of γ -radiation that can be administered to tumors [2].

Therapeutic gain is defined by an increase in tumor control probability without a parallel increase in the severity of side effects. In an ideal setting, the probability of normal tissue damage should be minimal at a dose level that induces maximal probability of tumor control. Several strategies of combined modality treatments have been developed in order to improve the therapeutic index. The concept of using a radio-sensitizer was established in Heidelberger's studies in 1958 by giving a drug in conjunction with radiotherapy to strengthen the effect of radiation [6]. Most of the clinical research published has reported successful use of traditional cytotoxic agents, nucleoside analogues or platinum compounds to improve radiotherapy. More recently non-DNA targeting compound such as growth factor inhibitors or inhibitors of tumor vasculature are being studied. However, most of these compounds show limitations in clinical use because of their intrinsic toxicity or limited radio-sensitizing effect [7]. Ideally, an optimal radio-sensitizer should exert no side effects by itself while being able to improve the potency of ionizing radiation.

Our laboratory developed a chemosensitizer, TAT-RasGAP₃₁₇₋₃₂₆, able to sensitize tumor cell lines and human tumor xenografts to chemotherapy [9]. In this study we explore the radiosensitizing properties of the TAT-RasGAP₃₁₇₋₃₂₆. In particular, we show that TAT-RasGAP₃₁₇₋₃₂₆ sensitizes tumor cell lines and human tumor xenografts to radiotherapy irrespective of the p53 status.

Materials and methods

Cell lines

HCT116, HCT116 p53 ^{-/-} and HaCaT were cultured in DMEM (Invitrogen, ref. n°61965) supplemented with 10% heat-inactivated fetal bovine serum (FBS; Invitrogen, ref. n°10270-106) in 5% CO₂ at 37°C. HeLa cells were cultured in RPMI (Invitrogen, ref. n°61870) supplemented with 10% heat-inactivated FBS in 5% CO₂ at 37°C

Peptide synthesis

The HIV-TAT₄₈₋₅₇ (GRKKRRQRRR) and TAT-RasGAP₃₁₇₋₃₂₆ (GRKKRRQRRRGGWMWVTNLRTD) peptides were synthesized at the Institute of Biochemistry, University of Lausanne, Switzerland using Fmoc technology, purified by HPLC and tested by mass spectrometry. Peptides were diluted at a concentration of 1 mM in H₂O and stored at -20°C

Colony Formation Assay (CFA)

Five hundred cells were seeded on 100 x 20 mm tissue culture dishes in 8 ml fresh culture medium. The following day they were irradiated (0, 1, 2, 4 Gy) using a Philips RT 250 gamma-irradiator and treated. In experiments combining TAT-RasGAP₃₁₇₋₃₂₆ and irradiation, cells were irradiated immediately after the addition of TAT or TAT-RasGAP₃₁₇₋₃₂₆. After two weeks from the irradiation cells were fixed and stained with 0.5 % crystal violet in methanol/acetic acid (3:1, v/v). Colonies containing ≥ 50 cells were counted. Each experiment was repeated at least three times and the average of experiments was plotted with interval of confidence (95%).

Xenograft mouse model

All experiments were performed according to the principles of laboratory animal care and Swiss legislation. The protocol was specifically approved by the cantonal veterinary service (VD 2243). Female homozygous athymic *Foxn1^{nu/nu}* nude mice (Harlan) of 6 to 8 weeks of age were subcutaneously injected on the left and right lower flanks with 0.7×10^6 cells. After 5 days mice displaying tumor volume of 10 mm^3 were randomly assigned to the different groups of treatment. Treated mice received every day, for 10 consecutive days, 3 Gy of γ -radiations on the lower back, with or without intraperitoneal injection of either TAT-RasGAP₃₁₇₋₃₂₆ (1.65 mg/kg in 200 μ l of PBS) or PBS (200 μ l). Mice not exposed to irradiation were intraperitoneally injected either with PBS (200 μ l) or with TAT-RasGAP₃₁₇₋₃₂₆ (1.65 mg/kg in 200 μ l of PBS). Tumors were measured 3 times a week and tumor volume was calculated as $\text{length} \times \text{width} \times \text{height} \times \pi/6$. When tumors reached 800 mm^3 mice were sacrificed.

Statistical analysis

The R statistic software was used (<http://www.r-project.org/>). For CFAs, statistical differences between groups were determined by ANOVA followed by the post-hoc Tukey HSD test for multiple comparisons. For the *in vivo* experiments statistical differences between groups were determined by repeated measures ANOVA. Significant difference ($p < 0.05$) is indicated by *.

Results

TAT-RasGAP₃₁₇₋₃₂₆ sensitizes cancer cells, but not normal cells, to γ -radiations

The radiosensitizing capacities of TAT-RasGAP₃₁₇₋₃₂₆ were assessed by colony formation assay. Two different cancer cell lines WT for p53 (HCT116 and HeLa) and one lacking p53 (HCT116 p53 ^{-/-}) showed reduced clonogenicity when exposed to increasing doses of γ -radiations. Interestingly, TAT-RasGAP₃₁₇₋₃₂₆, while having no effect alone, in combination with γ -radiations significantly reduces the clonogenic potential of the analyzed tumoral cell lines, irrespective of the p53 status (Figure 1). It has also to be noticed that the cell permeable sequence TAT, alone or in combination with γ -radiations, has no influence on the number of colonies. On the contrary, the clonogenicity of a non tumoral cell line, HaCaT, exposed to irradiations, is not affected by the RasGAP-derived peptide (figure 1). These results are consistent with the previously reported specificity of TAT-RasGAP₃₁₇₋₃₂₆ for cancer cells [8] and prove that the RasGAP-derived peptide sensitizes cancer cells to γ -radiations, independently of the p53 status.

Tumor sensitizing activity of TAT-RasGAP₃₁₇₋₃₂₆

In order to evaluate the ability of TAT-RasGAP₃₁₇₋₃₂₆ to sensitize tumors in *in vivo* settings nude mice were subcutaneously injected with HCT116 tumoral cells and the tumoral growth was recorded over time in the presence of the indicated treatment (Figure 2A). Mice treated with radiotherapy plus TAT-RasGAP₃₁₇₋₃₂₆ developed statistically significant smaller tumor than mice treated with radiotherapy or with TAT-RasGAP₃₁₇₋₃₂₆ alone.

P53 is deleted or mutated in about 50% of human tumor [10] and this has been correlated with tumor resistance to radiotherapy [3;5]. Therefore we wondered whether our RasGAP-derived

peptides would keep its tumor sensitizing properties in p53-deficient tumors. Figure 2B shows that radiotherapy delays the tumoral growth of the p53 KO HCT116 xenografts, but it is evident that p53 deficient tumors are much more resistant to γ -radiations than p53 proficient tumors (compare 2A with 2B, open squares). Interestingly, when TAT-RasGAP₃₁₇₋₃₂₆ was co-administrated with radiotherapy, the p53 negative tumor growth was dramatically reduced, to more or less the same extent as the p53 positive tumors (compare 2A with 2B, filled triangles). Taken together these results show that, consistently with what was observed in vitro, TAT-RasGAP₃₁₇₋₃₂₆ sensitizes tumors to radiotherapy irrespective of the p53 status.

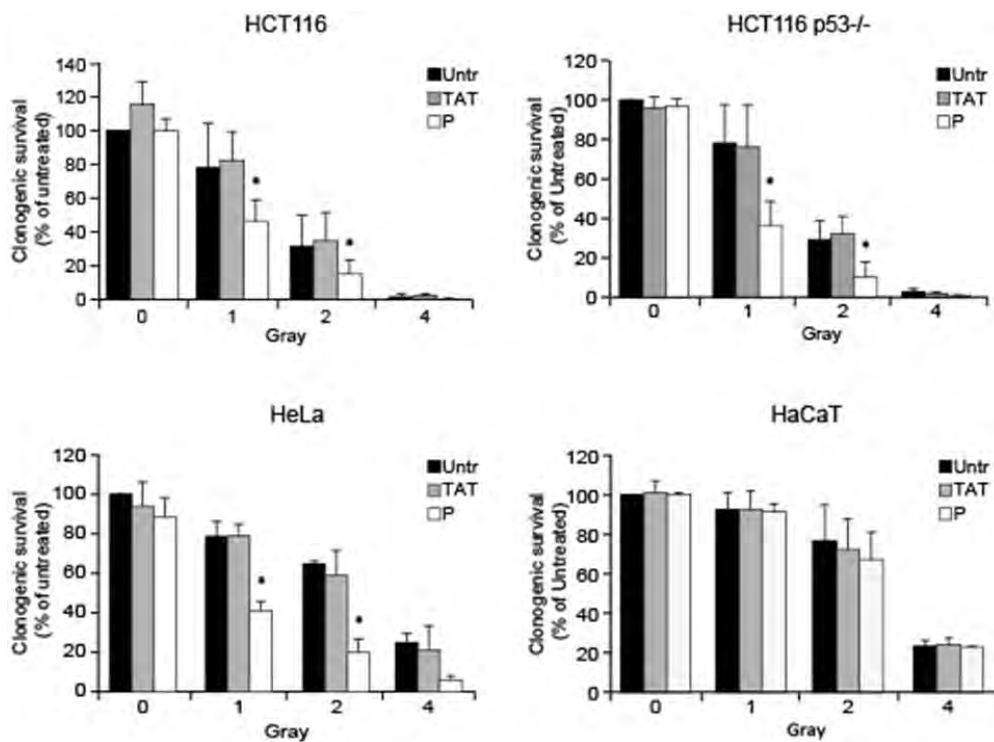


Figure 1. TAT-RasGAP₃₁₇₋₃₂₆ selectively sensitizes cancer cells to irradiation. HCT116, HCT116 p53^{-/-}, HeLa and non-tumoral HaCaT cells were subjected to the indicated doses of γ -radiation in the presence or not of 20 μ M TAT-RasGAP₃₁₇₋₃₂₆ (P) and 20 μ M TAT. Two weeks later, the number of colonies was recorded. The results correspond to the mean \pm 95%CI of at least independent experiments. The asterisks indicate a statistically significant difference (as assessed by ANOVA between cells treated or not with TAT-RasGAP₃₁₇₋₃₂₆ in the presence of the indicated doses of γ -radiations).

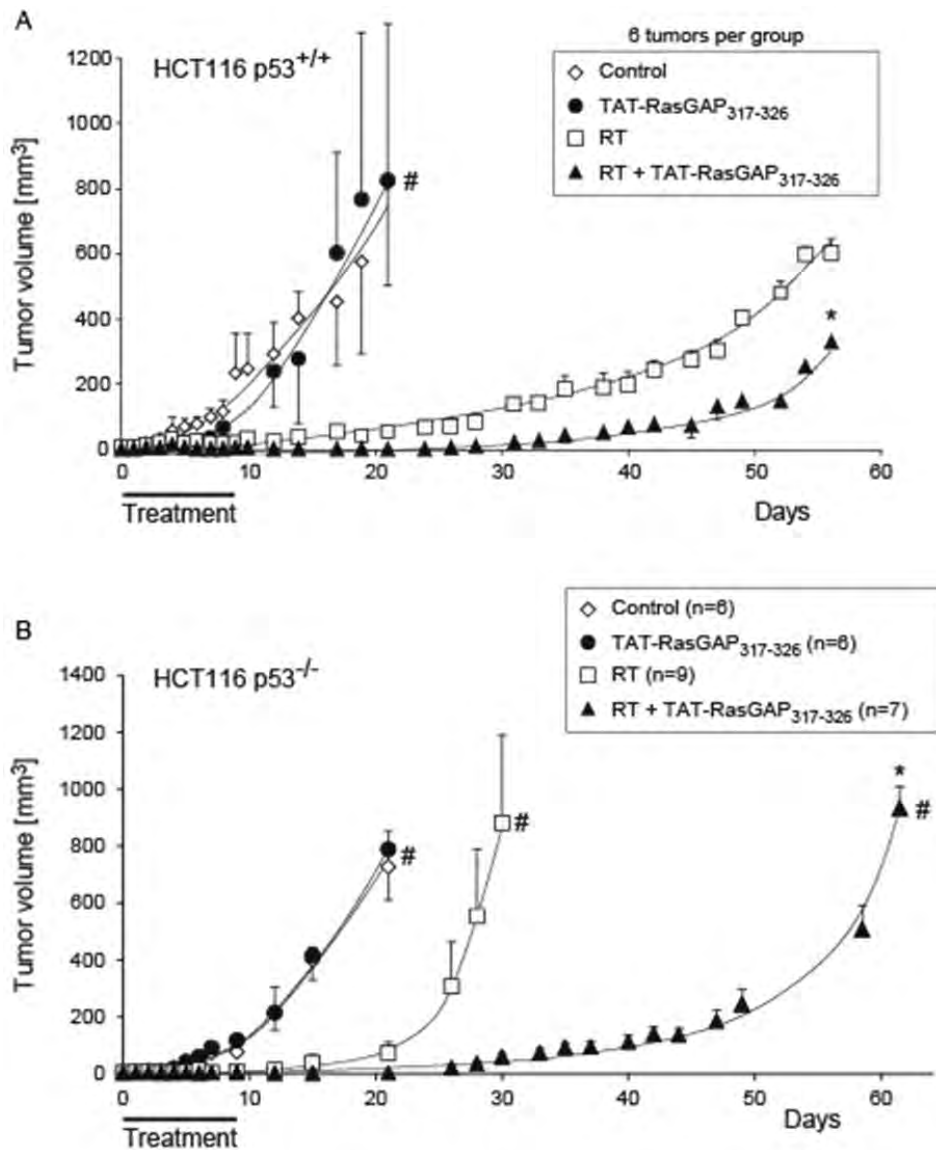


Figure 2. TAT-RasGAP317-326 greatly impairs radiotherapy-treated tumor development.

Mice bearing wild-type (A) and p53 knock-out (B) HCT116 xenografts were subjected to one of the following treatments:

- 1) Intraperitoneal PBS injections and no irradiation.
- 2) Intraperitoneal TAT-RasGAP317-326 injections (every day, 1.65 mg peptide per kg of mouse in 300 microliter of PBS) and no irradiation.
- 3) Intraperitoneal PBS injection and gamma-irradiation (3 Gy; gamma-irradiation was performed 1 hour after the peptide injection).
- 4) Intraperitoneal TAT-RasGAP317-326 injections and gamma-irradiation.

The treatments (i.e. peptide injections followed by irradiation) were performed every day for 10 days without interruption. The size of the tumors was monitored 3 times a week. #: mice were sacrificed when the tumors reached a volume of about 800 mm³. Asterisks indicate a statically significant difference (as assessed by ANOVA repeted measures between groups subjected to irradiation and irradiation plus TAT-RasGAP317-326)

Discussion

This study started the characterization of a new TAT-RasGAP₃₁₇₋₃₂₆ facet. In fact, we demonstrate that the RasGAP-derived peptide is able to synergize with γ -radiations for the elimination of malignant cells. In particular, consistently with the results obtained combining TAT-RasGAP₃₁₇₋₃₂₆ to genotoxins, the RasGAP-derived peptide sensitizes different cancer cell lines and human tumor xenografts to irradiation. Moreover, as previously reported, TAT-RasGAP₃₁₇₋₃₂₆ does not have any pro-apoptotic function in non-cancer cells and no side effects on mice.

Importantly, the TAT-RasGAP₃₁₇₋₃₂₆-mediated sensitization to γ -radiations occurs independently of p53. P53 deletion or mutation are found in around half of human malignancies and are associated with tumor insensitivity to irradiation. In this work we showed that p53 deficient HCT116-generated tumors are effectively more radio-resistant than their p53 positive counterparts. Nevertheless, TAT-RasGAP₃₁₇₋₃₂₆ is somehow able to convert p53 negative tumors into p53 proficient-like tumors, restoring their normal sensitivity to γ -radiations. The provided data are of high clinical and therapeutical importance because they show not only that TAT-RasGAP₃₁₇₋₃₂₆ is able to enhance the tumor killing potential of γ -radiations but also that it might be used to overcome the tumor resistance to radiotherapy due to p53 deletion/mutations.

Reference list

- [1] J. Bernier, E.J. Hall, A. Giaccia, Radiation oncology: a century of achievements. *Nat.Rev.Cancer* 4 (2004) 737-747.
- [2] S.A. Bhide, C.M. Nutting, Recent advances in radiotherapy. *BMC.Med.* 8 (2010) 25.
- [3] J.M. Brown, B.G. Wouters, Apoptosis, p53, and tumor cell sensitivity to anticancer agents. *Cancer Res.* 59 (1999) 1391-1399.
- [4] C.F. Dunne-Daly, Principles of radiotherapy and radiobiology. *Semin.Oncol.Nurs.* 15 (1999) 250-259.
- [5] D.A. Haas-Kogan, S.S. Kogan, G. Yount, J. Hsu, M. Haas, D.F. Deen, M.A. Israel, p53 function influences the effect of fractionated radiotherapy on glioblastoma tumors. *Int.J.Radiat.Oncol.Biol.Phys.* 43 (1999) 399-403.
- [6] C. HEIDELBERGER, L. GRIESBACH, O. CRUZ, R.J. SCHNITZER, E. GRUNBERG, Fluorinated pyrimidines. VI. Effects of 5-fluorouridine and 5-fluoro-2'-deoxyuridine on transplanted tumors. *Proc.Soc.Exp.Biol.Med.* 97 (1958) 470-475.
- [7] M.R. Horsman, L. Bohm, G.P. Margison, L. Milas, J.F. Rosier, G. Safrany, E. Selzer, M. Verheij, J.H. Hendry, Tumor radiosensitizers--current status of development of various approaches: report of an International Atomic Energy Agency meeting. *Int.J.Radiat.Oncol.Biol.Phys.* 64 (2006) 551-561.
- [8] D. Michod, J.Y. Yang, J. Chen, C. Bonny, C. Widmann, A RasGAP-derived cell permeable peptide potently enhances genotoxin-induced cytotoxicity in tumor cells. *Oncogene* 23 (2004) 8971-8978.
- [9] D. Michod, A. Annibaldi, S. Schaefer, C. Dapples, B. Rochat, C. Widmann, Effect of RasGAP N2 Fragment-Derived Peptide on Tumor Growth in Mice. *J.Natl.Cancer Inst.* 2009) djp100.
- [10] B. Vogelstein, D. Lane, A.J. Levine, Surfing the p53 network. *Nature* 408 (2000) 307-310.

Discussion and Perspectives

DISCUSSION AND PERSPECTIVES

The most used anti-cancer regimens rely on the utilization of DNA-damaging agents: genotoxins for the chemotherapy and ionizing radiations for radiotherapy. Unfortunately, these two kinds of therapies, besides targeting cancer cells, also damage healthy cells leading to the generation of side effects. Signaling circuits regulating apoptosis are often altered in cancer [1]. Strategies aimed to fix or to amplify the apoptotic circuitry in cancer cells would improve the killing potential of anti-cancer treatments. This approach would allow a reduction of the therapeutical doses, without affecting the toxicity of the treatments towards malignant cells, with consequent prevention of harmful effect on healthy tissues. In this sense cancer research devotes a lot of efforts to the design and development of therapeutic peptides targeting the apoptotic signaling pathway [2]

Our laboratory early demonstrated that a cell permeable RasGAP-derived peptide, TAT-RasGAP₃₁₇₋₃₂₆, is able to selectively sensitize several cancer cell lines, but not non-cancer cell lines, to genotoxin-induced apoptosis [3]. This finding represented a very attractive starting point for a translational study where the potential of TAT-RasGAP₃₁₇₋₃₂₆ as sensitizer could be tested in pre-clinical and clinical models.

In the present work I first wanted to check if the ability of TAT-RasGAP₃₁₇₋₃₂₆ to sensitize human cancer-derived cell lines to genotoxins could be extended to human tumors implanted in mice. In part I we showed that human tumors xenografted in nude mice treated with TAT-RasGAP₃₁₇₋₃₂₆ plus cisplatin or doxorubicin grow significantly slower than tumors implanted in mice treated with the peptide or the genotoxin alone [4]. Importantly, the doses of cisplatin and doxorubicin we used have almost no effect on the tumoral growth by themselves and do not induce any

detectable toxic effects in treated mice. Similarly, TAT-RasGAP₃₁₇₋₃₂₆ alone has no effect on the tumoral growth, demonstrating that the RasGAP-derived peptide strongly potentiates the genotoxin capacity to shrink tumors. These findings are of particular interest from a clinical and therapeutical point of view because they represent the proof of principle that TAT-RasGAP₃₁₇₋₃₂₆ may be used to augment the efficacy of chemotherapy in cancer suffering patients, especially when the therapeutical doses have to be lowered to avoid harmful side effects.

As mentioned above, radiotherapy is a widely used anti-tumor therapy and, in spite of the excellent advances made in term of delivery to the tumoral mass, its toxicity towards tumor surrounding tissues still remains a limitation. In part V we showed that TAT-RasGAP₃₁₇₋₃₂₆ sensitizes both human tumor cell lines and human tumor xenografts to radiotherapy. Importantly, this tumor sensitization occurs irrespective of the p53 status. Indeed, p53-deficient human colon cancer HCT116 cells, as well as HCT1116 p53-positive cells, were sensitized to radiotherapy and the expected resistance of p53-negative tumor xenografts to γ -radiations was overridden by TAT-RasGAP₃₁₇₋₃₂₆. These findings are relevant for two reasons: i) they show that TAT-RasGAP₃₁₇₋₃₂₆ is a good radio-sensitizer *in vivo* and its application may be envisaged in cancer suffering patients to increase the efficacy of radiotherapy and limit side effects; ii) p53-deleted/mutated cancers represent around half of the human malignancies [5] and the fact that TAT-RasGAP₃₁₇₋₃₂₆ overcomes their resistance to irradiation greatly extends the potential field of use of our peptide.

Although the presented data highlight the *in vivo* therapeutical potential of TAT-RasGAP₃₁₇₋₃₂₆, further pre-clinical study will have to be performed in order to be able to start a phase I of clinical trials. In particular two points will be object of future studies: bio-distribution and anti-tumoral effect on immune-competent mice. Bio-distribution studies will be performed using a ¹²⁵I-radiolabeled peptide in mice; they will give us a clear view of the incorporation, accumulation

and elimination of TAT-RasGAP₃₁₇₋₃₂₆ in various organs as well as in tumors. The immune system was described to significantly contribute to the elimination of tumors subjected to specific chemotherapeutic agents (e.g. oxaliplatin) or radiotherapy. Hence we will evaluate the ability of TAT-RasGAP₃₁₇₋₃₂₆ to potentiate the effect of γ -radiations in a syngeneic mouse model using B16F10 melanoma cell line that can grow subcutaneously in immune-competent C57BL/6 mice.

Understanding the mode of action allowing TAT-RasGAP₃₁₇₋₃₂₆ to sensitize cancer cells to genotoxin-induced apoptosis would be of great relevance for anti-cancer therapy. Indeed it might help to identify a (new) mechanism of cancer resistance to apoptosis induced by genotoxins and to design more targeted and efficient anti-tumor strategies. Our first candidate that could potentially act as TAT-RasGAP₃₁₇₋₃₂₆ effector was G3BP1 (RasGAP SH3 Binding Protein 1). Indeed G3BP1 was reported to bind to RasGAP on the very same sequence that forms the active peptide sequence (amino acids 317-326) [6]. Evidence we provided in part III shows that G3BP1 is not involved at all in the TAT-RasGAP₃₁₇₋₃₂₆-mediated sensitization to genotoxin-induced apoptosis, as shown by G3BP1 KO MEFs that are still sensitive to the peptide [7]. Moreover the lack of interaction reported between G3BP1 and RasGAP or the RasGAP-derived fragment N2 (the fragment from which the peptide active sequence 317-326 was identified) pushed us to reconsider G3BP1 as a RasGAP binding protein.

Earlier study conducted in our laboratory showed that TAT-RasGAP₃₁₇₋₃₂₆ potentiates the genotoxin-induced mitochondrial apoptotic pathway by an enhancement of the mitochondrial membrane depolarization and an increased processing of caspase 3 [8]. It was also shown that p53 and Puma are required by the sensitization event to occur but their protein levels are not modulated by TAT-RasGAP₃₁₇₋₃₂₆ [8]. We now know that the p53/Puma axis is only required for the TAT-RasGAP₃₁₇₋₃₂₆-mediated sensitization to short term apoptosis, whose induction needs the

presence of p53, but it is dispensable for the peptide-mediated impairment of cell survival observed long term after the administration of genotoxins. This last observation suggests that TAT-RasGAP₃₁₇₋₃₂₆ might also potentiate p53-independent mechanisms of cell death occurring with a slower kinetic than short-term apoptosis (e.g mitotic catastrophe).

In order to explain the increased mitochondrial membrane depolarization observed when TAT-RasGAP₃₁₇₋₃₂₆ is combined to genotoxins, we assessed the activation status of Bax. Bax is a member of the Bcl-2 family, a group of protein that tightly regulates mitochondrial integrity [9;10]. Particularly, Bax is directly able to trigger the mitochondrial membrane permeabilization and the release of cytochrome *c* [11;12]. Our data demonstrate that TAT-RasGAP₃₁₇₋₃₂₆ potentiates the genotoxin-mediated activation of Bax. We also show that this peptide-mediated enhancement of Bax activation is most likely Bid-dependent. Bid is a member of the Bcl-2 family belonging to the BH3-only sub-group. In cell-free system truncated Bid (from now on referred to as tBid) was shown to directly activate Bax, leading to mitochondrial cytochrome *c* release [11;12]. In this study, using HeLa-isolated mitochondria, known to contain inactive Bax, we show that the addition of tBid triggers cytochrome *c* release. Interestingly, the t-Bid-mediated cytochrome *c* release was potentiated by TAT-RasGAP₃₁₇₋₃₂₆. This suggests that the peptide most probably needs tBid to enhance the activation of Bax, which is then translated into an increase of cytochrome *c* release and, in a cellular system, into more apoptosis.

However it remains to be determined if TAT-RasGAP₃₁₇₋₃₂₆ directly favors the tBid-mediated activation of Bax or if it needs a mitochondrial or cytoplasmic protein (HeLa-isolated mitochondria still contain cytoplasmic material). To answer this question a much purer system will be employed: rat liver-isolated mitochondria that do not contain at all cytoplasmic material, including Bax [13], which has to be provided as recombinant protein. Using this system it would

be possible to ascertain if TAT-RasGAP₃₁₇₋₃₂₆ needs the presence of a cytoplasmic protein. However if TAT-RasGAP₃₁₇₋₃₂₆ would still favor cytochrome *c* release in rat liver mitochondria, the possibility that this effect is mediated by a mitochondrial protein cannot be ruled out. This issue will be addressed by using liposomes (synthetic vesicles made of lipid bilayer, containing a fluorescent compound) [14] incubated with Bax and tBid in the presence or not of TAT-RasGAP₃₁₇₋₃₂₆ and the release of the fluorescent compound will be used as read-out for membrane permeabilization.

The understanding of how TAT-RasGAP₃₁₇₋₃₂₆ favors the activation of Bax could allow the design and development of more specific strategies to potentiate the genotoxin-mediated cell death process in cancer cells and therefore to improve chemo and radiotherapy with high beneficial effects for cancer patients.

Reference list

- [1] D. Hanahan, R.A. Weinberg, Hallmarks of cancer: the next generation. *Cell* 144 (2011) 646-674.
 - [2] D. Barras, C. Widmann, Promises of apoptosis-inducing peptides in cancer therapeutics. *Curr.Pharm.Biotechnol.* 12 (2011) 1153-1165.
 - [3] D. Michod, J.Y. Yang, J. Chen, C. Bonny, C. Widmann, A RasGAP-derived cell permeable peptide potently enhances genotoxin-induced cytotoxicity in tumor cells. *Oncogene* 23 (2004) 8971-8978.
 - [4] D. Michod, A. Annibaldi, S. Schaefer, C. Dapples, B. Rochat, C. Widmann, Effect of RasGAP N2 Fragment-Derived Peptide on Tumor Growth in Mice. *J.Natl.Cancer Inst.*2009) djp100.
 - [5] A.M. Goh, C.R. Coffill, D.P. Lane, The role of mutant p53 in human cancer. *J.Pathol.* 223 (2011) 116-126.
 - [6] F. Parker, F. Maurier, I. Delumeau, M. Duchesne, D. Faucher, L. Debussche, A. Dugue, F. Schweighoffer, B. Tocque, A Ras-GTPase-activating protein SH3-domain-binding protein. *Mol.Cell.Biol.* 16 (1996) 2561-2569.
 - [7] A. Annibaldi, A. Dousse, S. Martin, J. Tazi, C. Widmann. Revisiting G3BP1 as a RasGAP Binding Protein: Sensitization of Tumor Cells to Chemotherapy by the RasGAP 317–326 Sequence Does Not Involve G3BP1. 20-12-2011.
- Ref Type: Generic
- [8] D. Michod, C. Widmann, TAT-RasGAP317-326 requires p53 and PUMA to sensitize tumor cells to genotoxins. *Mol.Cancer Res.* 5 (2007) 497-507.
 - [9] R.J. Youle, A. Strasser, The BCL-2 protein family: opposing activities that mediate cell death. *Nat Rev Mol Cell Biol* 9 (2008) 47-59.
 - [10] A. Strasser, S. Cory, J.M. Adams, Deciphering the rules of programmed cell death to improve therapy of cancer and other diseases. *EMBO J.* 30 (2011) 3667-3683.
 - [11] S. Desagher, A. Osen-Sand, A. Nichols, R. Eskes, S. Montessuit, S. Lauper, K. Maundrell, B. Antonsson, J.C. Martinou, Bid-induced Conformational Change of Bax Is Responsible for Mitochondrial Cytochrome c Release during Apoptosis. *J.Cell Biol.* 144 (1999) 891-901.

- [12] R. Eskes, S. Desagher, B. Antonsson, J.C. Martinou, Bid Induces the Oligomerization and Insertion of Bax into the Outer Mitochondrial Membrane. *Mol.Cell.Biol.* 20 (2000) 929-935.
- [13] D. Arnoult, P. Parone, J.C. Martinou, B. Antonsson, J. Estaquier, J.C. Ameisen, Mitochondrial release of apoptosis-inducing factor occurs downstream of cytochrome c release in response to several proapoptotic stimuli. *J.Cell Biol.* 159 (2002) 923-929.
- [14] S. Lucken-Ardjomande, S. Montessuit, J.C. Martinou, Contributions to Bax insertion and oligomerization of lipids of the mitochondrial outer membrane. *Cell Death.Differ.* 15 (2008) 929-937.

Standard protocols from the Widmann's laboratory used during this thesis work

Reagents

1. HEPES buffer (2X) pH 7.05 (23°C):

1.1. Important note: always calibrate the pH meter before starting preparing the HEPES buffer.

1.2. Composition.

Chemicals	Final concentration	Source/Company	Code/quantities
NaCl	280 mM	Fluka	71380 (1 kg)
KCl	10 mM	Fluka	60130 (1 kg)
Na ₂ HPO ₄	1.5 mM	Merck	1.06586.0500 (500 g)
D-glucose•H ₂ O	12 mM	Merck	1.08342.1000 (1 kg)
HEPES	50 mM	Fluka	54461 (250 g)

1.3. Recipe.

Chemicals	For 500 ml
NaCl	8 g
KCl	0.38 g
Na ₂ HPO ₄	0.1 g
D-glucose•H ₂ O	1.1 g
HEPES	5 g
Adjust pH with NaOH (1 N, then 0.1 N) to 7.05 (23°C)	See 1.4

1.4. Add ddH₂O to about 450 ml, then adjust to pH 6.8-6.9 with 1 N NaOH, and finally to pH 7.05 with 0.1 N NaOH. Complete to 500 ml with ddH₂O. Control that the pH is still at 7.05.

1.5. Sterilize through a 0.22 µm 500 ml Stericups (Millipore #SCGPU05RE). Under a sterile hood, aliquot in 50 ml tubes (40 ml per tube). Write the lot number and the date on the tubes (**the lot number should be indicated in your laboratory book**). Store at -20°C.

2. Others

Chemicals	Source/Company	Code/quantities	Solvent	[stock]	Storage	Sterile
NaOH	Fluka	#71690 (500 g)	ddH ₂ O	10 N	Room temp.	no
Chloroquine	Sigma	C6628 (25g)	PBS	25 mM	-20°C	yes
CaCl ₂ •2H ₂ O (MW 147.02)	Acros	207780010 (1 kg)	ddH ₂ O	2.5 M	4°C	yes
Gelatin	Fluka	48722 (500 g)	PBS	0.1%	4°C	yes
DMEM, glutamax I, 4.5 g/l glucose, sans sodium pyruvate	Gibco	61965026 (500 ml)				
Newborn calf serum (NBCS), heat inactivated	Gibco	26010041 (500 ml)				

2.1. Preparation of NaOH solutions.

NaOH can cause irreversible damage to the eyes. It is thus mandatory to wear glasses when preparing or using NaOH solutions. The preparation of 10 N NaOH involves a highly exothermic reaction, which can cause breakage of glass container. Prepare this solution with extreme care in plastic beakers. To 80 ml of H₂O, slowly add 40 g of NaOH pellets, stirring continuously. As an added precaution, place the beaker on ice. When the pellets have dissolved completely, adjust the volume to 100 ml with H₂O. Store the solution in a plastic

container at room temperature (plastic containers are to be used because NaOH slowly dissolves glassware). Sterilization is not necessary.

2.2. Preparation of a 25 mM chloroquine solution.

In a 50 ml Falcon tube, add 0,645 gr of chloroquine and complete to 50 ml with ddH₂O. Transfer to a 50 ml syringe and sterilize through a 0.22 µm filter (Millex – GV filters [Millipore #SLGV025LS]). Under a sterile hood, aliquote in 15 ml tubes (10 per tube). Write the lot number and the date on the tubes (**the lot number should be indicated in your laboratory book**).

2.3. Preparation of a 2.5 M CaCl₂ solution.

In a 50 ml Falcon tube, add 18.4 g of CaCl₂•2H₂O and complete to 50 ml with ddH₂O. Transfer to a 50 ml syringe and sterilize through a 0.22 µm filter (Millex – GV filters [Millipore #SLGV025LS]). Under a sterile hood, aliquote in 15 ml tubes (10 per tube). Write the lot number and the date on the tubes (**the lot number should be indicated in your laboratory book**).

2.4. Preparation of a PBS/0.1% gelatin solution (500 ml).

Add 0.5 g gelatin and 50 ml PBS 10X to 450 ml ddH₂O in a glass bottle. Autoclave and store at 4°C.

Procedure

Day 0.

1. Plate cells in appropriate medium (use gelatinized dishes if required).

Cells	Number per 10 cm dish	Number per well (6 well-plates)	medium	Gelatinized dish
HEK 293 and derived cell lines	2·10 ⁶	350'000	DMEM; 10% NBCS	yes
COS cells			DMEM; 10% NBCS	no

1.1. Gelatinization of the dishes.

Place the indicated volume of PBS/0.1% gelatin in the dish (tilt the plate to cover the entire surface with the solution). Wait at least 10 min. Just before adding the cells to the plates, aspirate the PBS/0.1% gelatin (do not allow the plates to dry).

Dish size	Volume of PBS/01% gelatin
10 cm	2-5 ml
6 well plates	0.5 ml

Day 1.

2. Prewarm the HEPES 2X buffer in a 37°C water bath (at least 20 min). In case the buffer is thawed, mix very well before using.
3. Add the DNA in the indicated volume of H₂O. Add the corresponding volume of 2.5 M calcium solution. Mix **10 times** by pipetting the solution up and down. Allow 20-30 min the solution to equilibrate.

Cells	Dish size	Volume of medium in the dish	DNA amount	Volume of water in which the DNA is added	Volume of 2.5 M calcium to be added
HEK293	10 cm	10 ml	5-20 µg	450 µl	50 µl
	6 well plate	2 ml	2 µg	90 µl	10 µl

4. Add 25 µM chloroquine to the cell culture medium (not necessary to change the medium).
Note: if the cells are grown in RPMI medium (e.g. HeLa cells), you have to replace it with DMEM because RPMI medium is not compatible with the present transfection technique.

Dish size	Volume of medium	Volume of stock
10 cm	10 ml	10 µl
6 well plates	2 ml	2 µl

5. Place the plates back in the incubator for at least 10 min.
6. Add the indicated volume of prewarmed (37°C) 2X HEPES buffer to the DNA/calcium solution, mix 5 times by pipetting the solution up and down. Incubate for 1 minute exactly (starting from the moment the HEPES has been added to the DNA; not from the time when the mixing is finished). Put the DNA-HEPES mix in the culture medium (rock the plate left to right and up and down 2 times).

Dish size	Volume of HEPES 2X to be added
10 cm	500 µl
6 well plate	100 µl

7. Incubate the cells at 37°C for 8-16 hours (**always mention this time of incubation in your laboratory book**). Replace the transfection medium with normal culture medium containing penicillin and streptomycin [use a 1:100 dilution of a Penicillin-Streptomycin Glutamine 100X solution (10'000 units/ml penicillin G; 10 mg/ml streptomycin sulfate; 29,2 mg/ml L-glutamine; 10 mM sodium citrate; 0.14% NaCl {GibcoBRL #10378-016})] to avoid contamination (the DNA used for the transfection is generally not sterile!).
8. Expected transfection efficiencies (count at least 500 cells).

Cells	Transfection efficiency
HEK293	30-80%
COS	30-40%

9. **In your laboratory book, always mention how long after step 7 were the cells analyzed.**

References

1. Jordan et al. - Nucl. Acid Res. (1996) **24**:596 (#3461)

Reagents

Chemicals	Source/Company	Code/quantities
Lipofectamine 2000 (1 mg/ml)	Gibco/Invitrogen	11668-019 (1.5 ml)
RPMI1640 Medium	SIGMA	R8758 (500 ml)
DMEM	SIGMA	D5796 (500 ml)
Newborn calf serum, heat inactivated	SIGMA	N4637 (500 ml)
15 ml polystyrene round-bottom tube	Becton Dickinson	352057

Procedure

Day 0.

1. Plate cells in appropriate medium according to Table I.

Table I

Cells	Number per 10 cm dish	Number per well of 6 well-plates	medium
HeLa cells	$0.5-2 \cdot 10^6$ (use $0.5 \cdot 10^6$ cells for P-Akt assay)	$4 \cdot 10^5$	RPMI, 10% NBCS

Day 1.

- a. Add the required DNA amounts at the bottom of sterile Eppendorf tubes (see column 3 of Table II). Using a 2 ml plastic pipette, add the serum-free medium (for the volume of medium to be used, please refer to column 3 of Table II). Using the same plastic pipette, transfer the required volume of serum-free medium to the 15 ml polystyrene round-bottom tubes (for the volume of medium to be used, please refer to column 4 of Table II).
- b. Mix the Lipofectamine 2000 stock solution gently before use, centrifuge quickly to pellet the drops to the bottom of the tube, and then add the Lipofectamine 2000 to the serum-free medium that has been placed in the 15 ml tubes (for the volume of Lipofectamine 2000 to be used, please refer to the column 4 of table II). Mix gently and incubate 5 minutes at room temperature.
- c. Using 1 ml tips, add the diluted DNA drop by drop to the diluted lipofectamine2000. Mix gently and incubate 20 min at room temperature.
- d. Just before the next step, wash the plates twice with serum-free culture medium (see column 5 of Table II for the volumes to be used).

- e. Add serum-free culture medium to the DNA + lipofectamine mix with a 5 ml plastic pipette and, using the same plastic pipette, add this mixture to the cells (refer to column 6 of Table II for the volumes to be used).
- f. Incubate 5 hours at 37°C in a CO₂ incubator
- g. After 5 hours replace the medium with serum-containing medium (use twice as much as the volumes indicated in column 5 of Table II). The cells can then be processed according to the experimental design.

Table II

1	2	3	4	5	6
Cells	Dish size	Total DNA amount (µg) and Dilution Volume (µl)	Lipofectamine 2000 (µl) and Dilution Volume (µl)	Washing steps (volume to be used)	Volumes of serum-free medium to be added to the Lipofectamine-DNA mix
HeLa	10 cm dish	7 µg in 600 µl	8-10 µl in 600µl	5 ml	3.8 ml
HeLa	6 well-plate	4 µg in 250 µl	4 µl in 250 µl	2 ml	1.5 ml

Apparatus

Transfer tank located in the drawers next to Christian's office door. It is the transparent tank containing red-black electrode module inside. Gel cassettes and sponges are either in the drawer above the one containing the tanks or above the sink in the middle of the lab.

Materials and reagents

1. Plastic sheets, commercial Enhanced chemiluminescence (ECL) solution and other reagents.

1.1. Materials and reagents.

Materials and reagents	Source/Company	Code/quantities
Plastic sheets Kapak Tubular Roll Stock [9.5''x250' #5 Scotchpak (2 Mil)].	Kapak Parkdale Drivewe, Minneapolis, Minnesota 55416 • 1681	
Tris	Sigma	T1503 5Kg
Tween	Acros	p7949 100ml
Milk		
ECL reagent Supersignal West Femto Substrate	Pierce	#34095
Ponceau S	Acros	161470250 (25 g)

1.2. Ponceau S Staining Solution [0.1%(w/v) Ponceau S in 5% (v/v) acetic acid]

- 1g Ponceau S
 - 50ml acetic acid
 - Make up to 1 liter with ddH₂O
- Store at 4°C. Do not freeze.

Alternative recipe: 0.2% (w/v) Ponceau S in 3% (v/v) acetic acid.

1.3. Tris-buffer saline (TBS; 18 mM HCl, 130 mM NaCl, 20 mM Tris pH 7.2)

- 30ml HCl
- 152g NaCl
- 48g Tris base
- Up to 1L dH₂O

1.4. TBS/tween

- 19L dH₂O
- 1L 20X TBS
- 0.1% Tween (final concentration)

1.5. TBS/milk

- 5% powdered milk (25g for 500ml of TBS/tween)
- TBS/tween
- Alternatively some primary antibodies work better if they are diluted in 5% BSA (5%BSA in TBS/tween)

2. Home-made ECL solution.

2.1. Composition of the stocks.

Chemicals	Stock concentration	Final concentration	Source/Company	Code/quantities
Luminol (3-aminophthalhydrazide)	250 mM (1 g in 22.7 ml DMSO). Make 1.5 ml aliquotes	1.25 mM	Sigma	A-8511 (1 g)
P-coumaric acid	90 mM (0.5 g in 33.3 ml DMSO). Make 660 µl aliquotes.	0.2 mM	Acros	12109-0250 (25 g)
Tris	1 M pH 8.5	100 mM	Boehringer Mannheim	708976 (1 kg); IBCM stock
H ₂ O ₂ 30%	30%	0.01%	Merck	1.07210.0250 (250 ml)

Solution 1: 2.5 mM luminol and 0.4 mM coumaric acid in 100 mM Tris pH 8.5.

Solution 2: 0.02% H₂O₂ in 100 mM Tris pH 8.5.

3. Home-made enhanced ECL solution *Note: for the moment this is not working (use the above recipe instead).*

3.1. Composition of the stocks.

Chemicals	Stock concentration	Final concentration	Source/Company	Code/quantities
Luminol (3-aminophthalhydrazide)	250 mM	1.25 mM	Sigma	A-8511 (1 g)
p-iodophenol	(in DMSO)	50 µM		
Tris	1 M pH 8.5	100 mM	Boehringer Mannheim	708976 (1 kg); IBCM stock
H ₂ O ₂ 30% (8.82 M)	30%	2 mM	Merck	1.07210.0250 (250 ml)

Procedure

1. General remarks.

- 1.1. The conditions of incubation of the blots have to be adapted for each antigen and each antibody used. Therefore, the procedures presented in the following sections have to be considered as general guidelines and should not be assumed to work in all cases. Indications of possible improvements when the conditions are not found optimal will be mentioned.
- 1.2. Always centrifuge the tubes containing the antibodies before usage.
- 1.3. In principle, do not incubate two blots in the same bag.
- 1.4. Never touch the blot with bare hands. Use gloves and move the blots with tweezers.
- 1.5. The following procedure should be considered only for the small gels (see SOP12.1).

2. Migration on gels.

Percentage of acrylamide	Separation
8%	40-200 kDa
10%	30-200 kDa
12%	20-200 kDa
4-20%	7-250 kDa
8-16%	15-250 kDa

3. Transfer to membranes.

3.1. After migration, proteins are transferred to nitrocellulose filters (Schleicher and Schuell, BA83 0.2, μm , no. 401380) or PVDF membranes. Instruction on how to do this can be found in the same drawer as the material used for the transfer and for the SDS-PAGE (see SOP 12.1).

3.2. Transfer buffers.

David has recently tested the two following buffers. According to him, transfer buffer II works better.

Composition of transfer buffer I.

Chemicals	Stock solution	Final concentration	Source/Company	Code/quantities
CAPS	1M pH11	10 mM	Acros	172621000 (100 g)
Methanol		10%	Fluka	65543 (5 l)

CAPS 1M stock solution (500 ml): 110 g CAPS (MW 221.3) and 20 g NaOH in water. The pH should be 11. Store in the dark at 4°C.

Prepare the transfer buffer (5 liters) directly in the transfer tank (50 ml CAPS 1M, 500 ml methanol, and water up to 5 liters).

Methanol evaporation ensures that the buffer does not heat too much. Therefore the transfer buffers cannot be used too many times. Without methanol, the buffer would boil during the transfer!

Transfer o/n at 600 mA.

Composition of the transfer buffer II.

Chemicals	10X stock (1 liter)	Final concentration (1X transfer buffer)	Source/Company	Code [quantities]
Tris	30.2 g	1 mM	Biosolve ltd	20092388 [4 kg]
Glycine	144 g	8 mM	ACROS	120070050 [5 kg]
SDS	10 ml of a 10% solution in water	0.001%	Biosolve ltd	19822359 [0.5 kg]

Prepare the transfer buffer 1X (5 liters) directly in the transfer tank.

Add 500 ml of the 10X buffer, 1 liter of methanol and water up to 5 liters.

Transfer 5 hours at 660 mA.

Currently the situation with the transfer buffers is like this: they are located above the sink were other materials for the transfer can also be found (sponges, etc.), There are several bottles of 10x transfer buffer. In order to make 1x transfer buffer, mix 100 ml of the 10X preparation with 700ml of water and 200ml of some alcohol (methanol or ethanol).

3.3 After preparing the transfer tank, place the top on and plug it into a power supply machine (make sure that the plus and minus plugs are connected right: you do not want your proteins to be released on the wrong side directly into the transfer buffer). Transfer is usually preformed at 250 mA (constant amperage) for one hour or one hour and twenty minutes.

- 3.4 Check if the protein markers have been transferred (one should see the markers on the membrane and not on the gel).

4. This protocol should be used when there are no particular problems to get a strong signal
 - 4.1. Ponceau S Stain for Western blots.

Background. *This is a rapid and reversible staining method for locating protein bands on Western blots. Sensitivity is somewhat less than Coomassie blue and produces reddish pink stained bands; minor components may be difficult to resolve. The stain is useful because it does not appear to have a deleterious effect on the sequencing of blotted polypeptides and is therefore one method of choice for locating polypeptides on Western blots for blot-sequencing. The stain binds strongly to nylon-based filter media but is fine for nitrocellulose and PVDF membranes. Incubate the membrane for up to an hour in staining solution with gentle agitation. Rinse the membrane in distilled water until the background is clean. The stain can be completely removed from the protein bands by continued washing. Stain solution can be re-used up to 10 times.*

How we use it in the laboratory. Incubate the blot in Ponceau for 2-3 min to visualize the proteins and to determine whether the transfer was homogeneous. With a pen, mark the position of the molecular weight markers. The blots are then subjected to the following incubations.
 - 4.2. wash 3x 20 min at room temperature with TBS/0.1% Tween 20 (TBS/Tween; found in the big tank next to the sink near the entrance of the laboratory).
 - 4.3. 45-60 min at room temperature with TBS/5% powdered milk (TBS/milk).
 - 4.4. overnight with the primary antibody (in TBS/milk) at 4°(in a cold room).
 - 4.5. 3x 20 min at room temperature with TBS/Tween.
 - 4.6. 45 min at room temperature with TBS/milk.
 - 4.7. 45 min with the secondary antibody (in TBS/milk) at room temperature (if the secondary antibody bears a fluorochrome sensitive to light [e.g. antibodies required for the odyssey detection; see SOP 17], make sure that incubation is performed in a black box).
 - 4.8. 3x 20 min at room temperature with TBS/tween (in the dark).

5. Detection of the secondary antibodies on films.
 - 5.1. This method should be used only for antibodies and antigens that do not generate strong signals. If this is not the case, detect the secondary antibodies with the BioRad Fluor-S imager (refer to SOP 2.0) or even better with the Odyssey apparatus (see SOP 17).
 - 5.2. Check that the developer has been turned on and is ready to be used.
 - 5.3. Prepare a cassette that should contain a fluorescent ladder (to position your film on the blot later on).
 - 5.4. Wash a glass plate thoroughly (first with soap, rinse with water and finally with ethanol).
 - 5.5. Prepare the ECL reagent by mixing equal volumes of solutions I and II. You need about 1 ml for each 10 cm² of your blot.
 - 5.6. Cut some Kappak plastic sheet that will be used to contain your blot during the exposure to films. Seal it but leave one side open.
 - 5.7. Take the blot with tweezers and touch some absorbing paper with one of its corner to remove the liquid in excess. Place the blot on the glass plate with the transferred proteins up. Pour the ECL reagent on the blot. Check that the whole surface is covered and wait one minute.
 - 5.8. With tweezers, transfer the blot in the Kappak bag. Remove the bubbles and seal the bag. Using absorbing paper, remove the liquid on the exterior of the bag. Place the bag in the cassette as close as possible to the fluorescent ladder. Tape the bag on one side.
 - 5.9. Immediately, go to the dark room with the sealed blot, the films and a cassette. Place a film on the blot. Close the cassette. Wait one minute. Remove the first film that you insert in the developer. While the first film develops, place a second one on the blot and close the cassette. When the first film comes out, check the intensity of the signal. If it is weak, expose the second film for 5-15 min. If it is too strong, develop the second film immediately (it will of course be too dark too) and expose a third film to 5-15 seconds. If the film has to be exposed for 1-2 seconds, tape it on the other side of the cassette. This will ensure that when you close the lids, the film will not move. Note again that if the signal is strong, you should not use this technique (see point 3.1).
 - 5.10. Keep all the films (the overexposed ones are often used to position the molecular weight markers). All the films should be labeled (**do it immediately**) with the date, the experiment number, the exposure time, the type of ECL used, and the experimental conditions for each lane. Also try (when possible) to identify the bands on your blots.

6. Detection of the secondary antibodies with the BioRad Fluor-S imager.

- 6.1. Refer to SOP 2.0.
 - 6.2. In this case also, the images obtained should be labeled: date, the experiment number, the exposure time, the type of ECL used, and the experimental conditions for each lane. Also try (when possible) to identify the bands on your blots.
 7. Quantitation of the ECL signal.
 - 7.1. In principle, quantitation should not be performed using films because the signal on films is not linear (you need more than one photon to activate the silver grains) and saturates rapidly.
 - 7.2. If possible, quantitation should be performed using the BioRad Fluor-S imager. Please refer to SOP 2.0.
 8. Detection of the secondary antibodies using the Odyssey system (Licor).
 - 8.1. Refer to SOP 17.
 9. No signal
 - 9.1. Increase the incubation with the antibodies: o/n incubation with the first antibody and 2-4 hours with the secondary antibody. Perform the incubations at 4°C.
 - 9.2. Reduce the “stringency” of the incubation buffer. Milk containing buffer can possibly quench a fraction of the antibody. The following buffers are ranked from highest to lowest stringency: milk-containing buffer, BSA containing-buffer, tween-containing buffer, PBS or Tris buffer.
 10. How to store antibodies.
 - 10.1. It is possible to reuse antibodies many times and this should be done whenever the antibody is rare and not available commercially. The solution containing the antibody needs to contain 0.05% azide (NaN_3) and 10 mM EDTA.
 11. Very important: after completion of the Western blot procedure, always store the nitrocellulose membranes in Kappak bags at -20°C for further potential use.
-

References

1. Widmann et al. *Biochem. J.* (1995) **310**:203 (#3461)
2. Yang et al. *Mol. Cell Biol.* (2001) **21**:5346 (#3666)

Reagents

Chemicals/medium	Source/Company	Code/quantities
JETstar maxi	Genomed	20 prep (#220020)
Isopropanol		
Glycerol		
Tris		
EDTA		

TE: Tris 10 mM pH 7.4, EDTA 1 mM.

Bacteria culture

1. For most plasmids, inoculate 250 ml of LB with the appropriate antibiotic (see SOP 8.0) with:
 - a tip that has touched a colony on an Agar plate
 - a few ml of a mini-prep culture
 - a chunk of a glycerol stock taken with a yellow tip
2. Incubate o/n at 37°C in a shaker.
3. If required, take 1 ml of the culture to prepare a glycerol stock (put this one ml in an Eppendorf tube, centrifuge in an Eppendorf centrifuge at 4'000 rpm for 5 min, discard the supernatant and resuspend the pellet in 300-500 µl of a sterile 10% glycerol solution; store at -70°C).

Maxi prep

1. Principle.

The procedure employs a modified alkaline/SDS method to prepare the cleared lysate. After neutralization, the lysate is applied onto a JETstar column and the plasmid DNA is bound to the anion exchange resin. Washing the resin removes RNA and all other impurities. Afterwards, the purified plasmid is eluted from the column and finally concentrated by alcohol precipitation. The supplier says that the JETstar purified plasmid DNA is of a higher quality than 2 x CsCl purified plasmid DNA. The expected yield for a maxi column is between 300-500 µg of DNA.
2. Centrifuge the cultures in 250 ml bottles at 5'000 rpm for 5-10 min at 4°C using the GSA rotor in the Sorvall RC-5B centrifuge. Check that the rotor is clean before and after use. Clean if necessary and always remove any liquid present.
3. Place the column on the "blue cow". Add 30 ml of solution E4 in the column and let flow by gravity.
4. Note: RNase must be added to solution E1 prior to its first use. Just pour the lyophilized RNase powder into bottle E1 and mix. Add the sticker indicating that the RNase has been added, the date and your name.

Discard the supernatant. Resuspend the pellet in 10 ml of solution E1.
5. Add 10ml of solution E2 and mix gently. Incubate 5min at room temp on a rocker (Rocker Inotech; shake 9, timer 5, frequency 17).
6. Add 10 ml of solution E3 and mix immediately by inverting the bottle 5 times. Transfer to a 50 ml blue Falcon tube (do not use yellow Falcon tube since they are more fragile and may break during the centrifugation). Centrifuge at 9'000 rpm for 10 min at 20°C using the SLA 600TC rotor in the Sorvall RC-5B centrifuge.
7. Pour the supernatant on the column and let flow by gravity. Wash the resin with 60 ml of solution E5.
8. Place the column on a 50 ml blue Falcon tube and secure the column on the tube with tape. Add 15 of solution E6 and let flow by gravity.

9. Add 10.5 of isopropanol. Mix and incubate on ice for at least 1 hour (alternatively, the tube can be stored o/n at -20°C).
 10. Centrifuge at 10'000 rpm for 30 min at 4°C using the SLA 600TC rotor in the Sorvall RC-5B centrifuge. Discard the supernatant being very careful not to loose the pellet that is not always firmly adherent (sometimes not at all).
 11. Add about 20 ml of 70% ethanol. Centrifuge at 10'000 rpm for 10 min at 4°C using the SLA 600TC rotor in the Sorvall RC-5B centrifuge. Discard the supernatant as above. Aspirate all the residual drops with a long white tip.
 12. Resuspend the pellet in 500 μl of TE.
 13. Measure the concentration with the spectrophotometer using a 1/100 dilution in a quartz cuvette. One OD at 260 nm corresponds to 50 $\mu\text{g}/\text{ml}$ of DNA. The ratio between the OD at 260 nm and the OD at 280 nm should be between 1.8 and 2.0.
 14. Write down the concentration of the maxi prep in the plasmid files as well as on the tube.
-

Materials and reagents

1. coverslips keep in ethanol 100%

Materials and reagents	Source/Company	Code/quantities
PBS 10 X	?	?
0.2% TX-100 in PBS		
PBS 1X, 3% paraformaldehyde, 3% sucrose		
Gelatin	Fluka	48722 (500 g)
Mounting medium		
Antibody		

1.1. Preparation of a PBS/0.1% gelatin solution (500 ml).

Add 0.5 g gelatin and 50 ml PBS 10X to 450 ml ddH₂O in a glass bottle. Autoclave and store at 4°C.

2. List of antibodies

Name of Ab	Name of epitope or antigen	Origin of Ab	Source	Company or source	Dilution

Procedure

Preparation of coverslips

Growing cells on coverslips

1. In a sterile hood, take a coverslip from the ethanol bottle with tweezers. Set fire to the ethanol by passing quickly the coverslip over the flame. When all the ethanol has burnt and evaporated, place it in the appropriate culture plastic-ware. If required, coat the wells and the coverslips with PBS/0.1% gelatin for at least 10 minutes. Remove the PBS/gelatin if present and add the cells to the wells. Transfect or infect the cells if required.

Immunocytochemistry

1. Fill the required number of wells of 6-well plates with ~3ml PBS 1X (these 6-well plates can be used over and over). With tweezers, transfer the coverslips to the 6-well plates (face up). This can be performed under a sterile hood with sterile devices if the rest of the cells (i.e. cells not on the coverslips) have to be kept in culture.
2. After this step, the procedure can be continued on the bench. Use ~20°C solutions (solutions that have been kept at room temperature).
3. Aspirate the PBS 1X and put gently 3ml of PBS 1X, 2% paraformaldehyde, 3% sucrose. Incubate 15 min in the dark (*fixation step*).
4. Wash very carefully with 3 ml PBS 1X.
5. Add very carefully 3ml 0.2% TX-100 in PBS 1X. Incubate the coverslips 10 min in the dark. (*permeabilization of the membrane*)
6. Wash very carefully with 3 ml PBS 1X.
7. Put 3 ml of sterile filtered serum-containing medium for 15 min in the dark (old sera can be used; filtrate the medium through 0.2 µm Millipore filter). These media are kept in the cold room. Take what is needed for

the experiment (do not forget to include volumes used to dilute the antibodies) under a sterile hood and work according to cell culture standards.

8. Place some parafilm on a **clean** portion of the bench. Stretch the parafilm and fix it on the table with tape.
9. Dilute the first antibody in filtered medium and place 50 μ l drops on the parafilm (1 drop per coverslip).
10. Take the coverslips with tweezers, remove the excess medium by touching a Kleenex tissue with the edge of the coverslip, and place the coverslip on the drop, face down.
11. Cover the coverslips with a lid (typically the top part of a foam box used for the shipping of frozen biological goods) with paper taped on the interior side that must be moistened with water to reduce the extent of evaporation of the medium containing the antibodies. Incubate one hour.
12. Prepare a small becher containing PBS 1X.
13. Place 50 μ l drops containing the second antibody (or any kind of labeling reagent) on a stretched parafilm (see #8-9).
14. Take the coverslips with tweezers, remove the excess medium by touching a Kleenex tissue with the edge of the coverslip, hold the coverslip ~5 seconds in the PBS-containing becher, remove the excess liquid and place the coverslip on the drop, face down. Cover with a lid as described in #11 and incubate for a further hour.
15. Take the coverslips with tweezers, remove the excess medium by touching a Kleenex tissue with the edge of the coverslip and place the coverslips face-up into the 6-well plate still filled with the filtered serum-containing medium.
16. Perform 6 incubations with PBS 1X in the dark. The incubations should last at least 20 min (preferably 30 min). If the coverslips float up (which happens especially during the last washes), push them to the bottom of the wells with the tweezers.
17. Clean the required number of slides to mount the coverslips.
18. For each coverslip, place 2 μ l of mounting medium on the slide (up to four coverslips can be mounted per slide).
19. Take the coverslips with tweezers, remove the excess medium by touching a Kleenex tissue with the edge of the coverslip and place the coverslips face-down onto the drops of mounting medium.
20. With a long white tip connected to the vacuum, remove the excess of mounting medium trying not to move the coverslips.
21. Put some nail polish around the coverslips.
22. Let the nail polish dry a few hours (typically o/n).
23. Gently remove the dried PBS on the coverslips with a wet piece of Kleenex tissue.
24. The coverslips can now be analyzed with the appropriate imaging system.

Author: Alessandro Annibaldi

Introduction.

In molecular biology, reverse transcription polymerase chain reaction (RT-PCR) is a laboratory technique for amplifying a defined piece of a ribonucleic acid (RNA) molecule. The RNA strand is first reverse transcribed into its DNA complement or complementary DNA, followed by amplification of the resulting DNA using polymerase chain reaction. This can either be a 1 or 2 step process.

Polymerase chain reaction itself is the process used to amplify specific parts of a DNA molecule, via the temperature-mediated enzyme DNA polymerase.

Reverse transcription PCR is not to be confused with real-time polymerase chain reaction which is also marketed as RT-PCR.

The present SOP only describes the reverse transcription part of the procedure.

RNA isolation.

Day 0

1. Add 500 μ l of TRI reagent (for 10^5 to 3×10^7 cells) to the cells and scrape them. Incubate at room temperature for 5 minutes.
2. Add 200 μ l of Chloroform, vortex and incubate 5 minutes at room temperature.
3. Spin 15 minutes at maximum speed (13'000 rpm in the Eppendorf centrifuge 5415R; $16'100 \times g$).
4. Transfer the aqueous phase into a new tube, add 500 μ l of isopropanol, mix by inverting the tube a few times and put at -20°C o/n.

Day 1

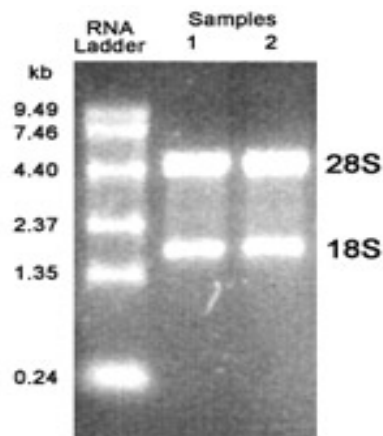
1. Spin 20 minutes at high speed (13'000 rpm in the Eppendorf centrifuge 5415R; $16'100 \times g$). At this stage if you do not see the pellet, add 40 μ l of NaCl 5 M, mix by inverting the tube a few times and spin down again 15 minutes.
2. Aspirate the isopropanol.
3. Wash with 800 μ l of ethanol 70%.
4. Place the tubes in the thermomixer (Eppendorf Thermomixer Comfort, it is located in the lab) at 60°C for 10 minutes without shaking to let them dry.
5. Resuspend the pellet in 50 μ l of high quality water.
6. Quantitate the RNA using the Eppendorf Biophotometer located in the lab. Push button n°9 to select the program to quantitate RNA, take the quartz cuvette QS 1.000 (usually located next to the Biophotometer), fill the cuvette with 200 μ l of TE pH 8.0 and add 2 μ l of your RNA. Mix. Click on the button labelled "Dilution" and enter the dilution (2:200). Proceed with the quantitation. Do not forget to do first the blank by filling the same cuvette with 200 μ l of TE and subsequently clicking on the button labelled 'Blank'. You will get 260 nm values. An A260 reading of 1.0 is equivalent to $\sim 40 \mu\text{g/ml}$ single-stranded RNA.

Note that measuring the 260 nm/280 nm absorbance ratio of your samples is not a very informative method to monitor the purity of your preparation (despite what is written in some protocols) (Glaser, 1995). Note also that this ratio is influenced by the pH and ionic strength of the solution. As pH increases, the A280 decreases while the A260 is unaffected. This results in an increasing A260/A280 ratio (Wilfinger *et al.*, 1997). Because water often has an acidic pH, it can lower the A260/A280 ratio. It is recommended to use a buffered solution with a slightly alkaline pH, such

as TE (pH 8.0), as a diluent (and as a blank) to assure accurate and reproducible readings. An example of the variation in A260/A280 ratio at different pH values is shown below

BLANK/DILUENT	A260/A280 ratio
DEPC-treated water (pH 5-6)	1.60
Nuclease-free water (pH 6-7)	1.85
TE (pH 8.0)	2.14

7. To have a better idea of the quality of your RNA, run it on an agarose-formaldehyde gel as follows:
- Melt 0.5 g of agarose in 37 ml of H₂O, cool down a little bit, add 5 ml of 10x MOPS buffer and 8.75 ml of formaldehyde 36.5 %.
 - RNA loading: prepare a mix composed of a few micro litres of your RNA (corresponding more or less to 500 ng), one fifth of the final volume with 5X RNA denaturing buffer, and water (usually up to a final volume of 10 µl).
 - Perform electrophoresis in 1x MOPS.
 - If your RNA preparation is good, you should see 2 bands, the highest one corresponds to the 28S RNA, the lowest one to the 18S RNA.



Reverse Transcription

0.5-1.0 µg total RNA

1.0 µl of a 500 ng/µl oligo dT solution in water.

The Oligo dT primer is purchased from Microsynth; you have to send an e-mail to the following address:

administration@microsynth.ch asking for Random Hexamer D(N)₆. Once you receive the tube (the quantity received is indicated on the datasheet), dissolve the oligo dT in water to get a concentration of 500 ng/µl. The oligo dT solution can be stored at -80 °C (alternatively, if you use them quite often, you can store some aliquots at -20 °C). For the delivery you can write in the e-mail your customer number, like that they automatically know your delivery address).

Add water to 11 µl.

3 minutes at 70°C and then keep on ice

Prepare the mix according to the table below. The buffer 5x, the DTT, the dNTPs, the RNAsin, and the reverse transcriptase come from the Superscript II Reverse Transcriptase Kit.

Reagent	μ l
dNTPs 10 mM each	5
RNAsin	0.5
Buffer 5x	5
DTT	2
Superscript reverse transcriptase	0.5
H2O	1
Total	14

Add the RNA to the mix and perform an incubation at 39°C for 1 hour followed by 15 minutes at 70°C. Your cDNA is now ready to be amplified by PCR.

Materials and reagents	Source/Company	Code
Agarose	Eurogenetec	EP-0010-10
β -mercaptoethanol	Sigma	M6250
Bromophenol blue	Fluka	18030
EDTA	Fluka	03620
Ethidium Bromide	Acros	170960010
Formamide (25 M)	Fluka	47670
Formaldehyde 36.5% (13.2 M)	Fluka	47629
Ficoll	Pharmacia Biotech	17-0400-01
Guanidinium Thiocyanate	AppliChem	593-84-0
MOPS (morpholinopropanesulphonic acid)	Sigma	M3183
N-Lauryl Sarcosyl sodium	Sigma	L9150
NaOH	Fluka	71690
Phenol (water saturated)	EUROBIO	GEXPHE01-0U
RNA sin	Promega	N211A
SDS	Sigma	L4390
Sodium Acetate	Sigma	S288
Sodium Citrate	Sigma	C8532
dATP	Promega	U120D
dGTP	Promega	U121D
dCTP	Promega	U122D
dTTP	Promega	U123D
Superscript II Reverse Transcriptase Kit (Buffer 5x, DTT and Superscript reverse transcriptase)	Invitrogen	18064-014

TRI solution (1.7 M guanidinium thiocyanate, 0.1 M sodium citrate, 0.25% sarcosyl, 0.05 M β -mercaptoethanol, 0.1M sodium acetate)

Mix 10 ml guanidinium thiocyanate 4 M, 352 µl sodium citrate 0.75 M (pH 7), 528 µl sarcosyl 10% and 76 µl β-mercaptoethanol 14.3 M for a total volume of 10.9 ml.

Place 10 ml of this mixture in a new tube, add 1 ml 2 M sodium acetate pH 4 and 10 ml of water-saturated phenol. This is the final TRI solution that is good for at least 2 month at 4°C.

10x MOPS buffer (0.2 M MOPS, 50 mM sodium acetate and 5 mM EDTA)

200 ml of MOPS 1M

25 ml of sodium acetate 2M pH 4

5 ml of EDTA 1 M

Up to 1 liter with water

The buffer is adjusted to pH 7.0 with 1 M NaOH and sterilised by autoclaving. Keep at 4 ° C protected from light.

Ethidium bromide 1mg/ml solution.

Ethidium bromide is prepared under the chemical hood (wear gloves, protection glasses and mask) by dissolving the appropriate amount of powder in water; the solution is then stored at 4 ° C. After preparing the solution wrap the tube with aluminium paper because EtBr is sensitive to light.

FESB solution (Ficoll 10%, EDTA 10 mM, SDS 0.5% and bromophenol blue 0.02%) x 10 ml

5 ml of Ficoll 20%

100 µl of EDTA 1 M

250 µl of SDS 20%

2 mg of bromophenol blue.

RNA denaturing buffer 5x (Formaldehyde 2.6 M, Formamide 12.5 M, 2% Ficoll, 2mM EDTA, 0.1%SDS, 0.004% bromophenol blu , ethidium bromide 40 µg/ml, in MOPS 1x)

For ~1 ml

200 µl of formaldehyde 36.5 %.

500 µl of formamide.

100 µl of MOPS 10x buffer.

40 µl of ethidium bromide 1 mg/ml

200 µl of FESB solution.

Store at -20 °C.

Tris-EDTA (TE) buffer (10 mM Tris; 1 mM EDTA; pH 8.0)

1 M Tris pH 8.0	1 ml
-----------------	------

0.5 M EDTA pH 8.0	0.2 ml
-------------------	--------

H ₂ O	98.8 ml
------------------	---------

Autoclave

Reference List

Glaser, J.A. (1995). Validity of nucleic acid purities monitored by 260nm/280nm absorbance ratios. *BioTechniques* 18, 62-63.

Wilfinger, W.W., Mackey, K., and Chomczynski, P. (1997). Effect of pH and ionic strength on the spectrophotometric assessment of nucleic acid purity. *BioTechniques* 22, 474-481.

Author : Alessandro Annibaldi

Introduction.

In molecular biology Cell Fractioning is a laboratory technique used to break cells and separate their molecular and structural components. Cell Fractioning can be divided in two steps: Homogenization and Fractionation. The Homogenization phase, whose purpose is to break the cell, is obtained either by the osmotic alteration of the media where cells are broken open through the utilization of an hypotonic buffer or by mechanical disruption. The Fractionation phase relies on the utilization of centrifugations at different speeds and times to separate cellular components on the basis of their size.

Cell Fractioning (Nuclei/Cytoplasm).

Day 0

Spread at least $2 \cdot 10^6$ in a 10 cm plate. If you want to look at the localization of one or more exogenous protein transfect your cells according to either SOP 1.0 or SOP 3.0, depending on the cell type with which you are working.

Day 1

1. Wash your 10 cm plate with PBS.
2. Add 400 μ l of lysis buffer 0.5% Triton X-100.
3. Scrape cells and incubate on ice for 20 minutes.
4. Centrifugate at 13.000 rpm (16'100 x g) in the Eppendorf centrifuge 5415R located in the lab.
5. Transfer the supernatant (membrane/cytoplasm fraction) into a new Eppendorf tube and keep the pellet.
6. Quantitate the protein concentrations of your samples using the Eppendorf Biophotometer located in the lab (see SOP 13.0 [Bradford]).
7. After completing the quantitation, add the loading buffer according to the amount of protein you want to load. At this point your **Cytoplasmic fraction** is ready to be loaded or alternatively you can store it at -20 °C.
8. Rinse the pellet representing the nuclear/mitochondrial fraction with the lysis buffer once and resuspend in the lysis buffer containing 0.5% SDS. Shear the released genomic DNA by sonication. The sonicator (Heischer DmbH) is now located downstairs, in a room that is in front of Peter Clark's group cell culture room. The settings you have to use are the followings:
Cycle (representing the number of cycles per second): 0.8-0.9.
Amplitude: 80%
9. Once there you have to insert the metallic tip of the sonicator inside your Eppendorf tube and press the black button located on the top of the sonicator for 10 seconds. Two sonications are enough to completely break the DNA. After each sonication place the sample back on ice for a few seconds. Before processing the next sample, wash the metallic tip of the sonicator first with ethanol 70% and then with water. Dry the tip with a clean tissue.
10. After sonication, centrifuge at 13.000 rpm (16'100 x g) in the Eppendorf centrifuge 5415R and transfer the supernatant in a new Eppendorf.

11. Quantitate the protein concentrations of your samples using the Eppendorf Biophotometer located in the lab (see SOP 13.0 [Bradford]).
12. After completing the quantitation, add the loading buffer according to the amount of protein you want to load. At this point your **Nuclear fraction** is ready to be loaded or alternatively you can store it at -20 °C.

Cell Fractioning (Nuclei, Mitochondria, Cytoplasm and Membrane)

Day 0

Start from at least $10 \cdot 10^6$ using 10 cm plates. If you want to look at the localization of one or more exogenous protein transfect your cells according to either SOP 1.0 or SOP 3.0, depending on the cell type with which you are working.

Day 1

1. Wash your 10 cm plate with PBS.
2. Add 300 µl of hypotonic lysis buffer.
3. Scrape cells and incubate on ice for 20 minutes.
4. Break mechanically the cells with a Dounce homogenizer.
5. Centrifugate at 300 x g 5 minutes at 4 °C in the Eppendorf centrifuge 5415R to pellet nuclei.
6. Transfer the supernatant in a new eppendorf and wash the pellet twice with the hypotonic lysis buffer. For each wash add 250 µl of hypotonic lysis buffer, centrifugate at 300 x g and discard the supernatant.
7. Resuspend the pellet in 200 µl of hypotonic lysis buffer + Triton X100 1%.
8. Sonicate as described above.
9. Centrifugate 10 minutes at 13.000 rpm (16'100 x g).
10. Discard the supernatant, resuspend the pellet, that represents the nuclear fraction, in 250 µl of lysis buffer 0.5% Triton X-100 containing 0.5% SDS and pass through a 26 gauge needle several times to break.
11. Sonicate 5 times 15 seconds.
12. Centrifugate 10 minutes at 13.000 rpm (16'100 x g).
13. Quantitate the protein concentrations of your samples using the Eppendorf Biophotometer located in the lab (see SOP 13.0 [Bradford]).
14. After completing the quantitation, add the loading buffer according to the amount of protein you want to load. At this point your **Nuclear fraction** is ready to be loaded or alternatively you can store it at -20 °C.
15. For the mitochondrial fraction start from point number 5. After transferring the supernatant in a new Eppendorf tube, centrifugate at 10'000 x g in the Eppendorf centrifuge 5415R located in the lab for 10 minutes at 4 °C to pellet mitochondria.
16. Transfer the supernatant in a new Eppendorf tube and resuspend the pellet in 200 µl of hypotonic lysis buffer + Triton X-100 1%.

17. Sonicate as described above.
18. Quantitate the protein concentrations of your samples using the Eppendorf Biophotometer located in the lab (see SOP 13.0 [Bradford]).
19. After completing the quantitation, add the loading buffer according to the amount of protein you want to load. At this point your **Mitochondrial fraction** is ready to be loaded or alternatively you can store it at -20 °C.
20. Take the supernatant you transferred in a new Eppendorf tube (point number 10) and centrifugate at 100'000 x g 1.5 hours at 4 °C. For this centrifugation, you have to use the ultra-centrifuge named Centrikon T-108 located in the P2 lab. The rotor, 'Kontron 18425', is located in the fridge in front of Romano Regazzi's lab. Tubes that suit the rotor are provided from Beckman and the maximum volume you can put in the tubes is 1 ml. After the centrifugation (as well as before using it) clean it with ethanol 70% and water. Do not forget to put the rotor back to its storage place.
21. Transfer the supernatant in a new Eppendorf tube.
22. Quantitate the protein concentrations of your samples using the Eppendorf Biophotometer located in the lab (see SOP 13.0 [Bradford]).
23. After completing the quantitation, add the loading buffer according to the amount of protein you want to load. At this point your **Cytoplasmic fraction** is ready to be loaded or alternatively you can store it at -20 °C.
24. Resuspend the pellet in 150 µl of hypotonic lysis buffer + Triton X100 1%.
25. Sonicate as described above.
26. Quantitate the protein concentrations of your samples using the Eppendorf Biophotometer located in the lab (see SOP 13.0 [Bradford]).
27. After completing the quantitation, add the loading buffer according to the amount of protein you want to load. At this point your **Membrane fraction** is ready to be loaded or alternatively you can store it at -20 °C.

Materials and reagents	Source/Company	Code
TRIS (Trizma base)	Sigma	T1503
Triton X-100	Fluka	93426
NaCl	Acros	207790050
Glycerol	Fluka	49780
MgCl ₂	MERCK	TA 808932
KCl	Fluka	60130
SDS (sodium dodecyl sulphate)	Sigma	L4390
HEPES	AppliChem	A3724
Centrifuge tubes 11 x 34 mm	Beckman	343778

Lysis buffer 0.5% Triton X-100 (0.5% Triton X-100, 50 mM Tris-HCl pH 7.5, 137 mM NaCl, 10% glycerol, 0.5% Triton X-100)

For 10 ml

5 ml of Tris-HCl pH 7.5 1M

274 μ l of NaCl 5M

1 ml of glycerol 100%

50 μ l of Triton X-100

Up to 10 ml with water

Hypotonic lysis buffer (10 mM HEPES pH 7.4, 10 mM MgCl₂, 42 mM KCl)

For 10 ml

200 µl of HEPES pH 7.4 500 mM

100 µl of MgCl₂ 1 M

420 µl of KCl 1 M

Up to 10 ml with water

Immunoprecipitation (IP) is the technique to precipitate a protein antigen out of solution using an antibody that specifically binds to that particular protein. It is useful when an interaction between two or more proteins has to be detected.

Immunoprecipitation is not a difficult technique to carry out, it only requires the choice of a suitable lysis buffer and appropriate beads.

The choice of the lysis buffer is critical because it should allow a proper cell membrane solubilisation without denaturing protein, when an interaction between two proteins is the ultimate purpose of the immunoprecipitation. Indeed denaturation might alter protein native three-dimensional structure thereby affecting the interaction occurring between the proteins of interest.

The choice of beads depends on the isotype of the chosen antibody.

Experimental protocol

Lysis buffer preparation:

IP lysis buffer should always contain:

- One agent that buffers the pH change induced by lysed cells. Two buffer agents are commonly used:

Tris-HCl pH 7.4 or HEPES-KOH pH 7.4

- NaCl at concentration between 0 and 1 M to ensure osmotic shock for cell breaking.

- Detergent to solubilise proteins. Detergents can be classified into two groups: Ionic and non-ionic. Ionic detergents include sodium dodecyl sulphate (SDS) and deoxycholate, they are strong detergent but they also are denaturing agent that might affect the native structure of the protein and binding with other proteins. When it is important to retain native protein:protein interaction it is better to use non-ionic detergents such as NP-40 or Triton X-100. Non-ionic detergents are less efficient for protein solubilisation. Non-ionic detergents should be used at concentrations ranging from 0.1 up to 2% whereas ionic detergents should be used at concentration ranging from 0.01 to 0.5%. The final choice of detergent and concentration as well as of salt concentration is quite empirical. Researchers may have to test different conditions before succeeding in co-immunoprecipitating proteins of interest.

For example a protein complex may require ionic detergents to be solubilised, but an excess of detergent might denature the native protein structures disrupting in this way the specific protein-protein interaction. In this case the co-immunoprecipitation of the proteins of interest would not be possible anymore.

In the tables below are shown some physical and chemical properties of commonly used detergents.

TABLE 1 PHYSICAL PROPERTIES OF COMMONLY USED DETERGENTS

Detergent	Monomer, Da mw	Micelle, Da mw	CMC % (w/v)	CMC Molarity
<i>Anionic</i>				
SDS	288	18,000	0.23	8.0×10^{-3}
Cholate	430	4,300	0.60	1.4×10^{-2}
Deoxycholate	432	4,200	0.21	5.0×10^{-3}
<i>Cationic</i>				
C ₁₆ TAB	365	62,000	0.04	1×10^{-3}
<i>Amphoteric</i>				
LysoPC	495	92,000	0.0004	7×10^{-6}
CHAPS	615	6,150	0.49	1.4×10^{-3}
Zwittergent 3-14	364	30,000	0.011	3.0×10^{-4}
<i>Nonionic</i>				
Octylglucoside	292	8,000	0.73	2.3×10^{-2}
Digitonin	1,229	70,000	-----	-----
C ₁₂ E ₈	542	65,000	0.005	8.7×10^{-5}
Lubrol	582	64,000	0.006	1.0×10^{-4}
Triton X-100	650	90,000	0.021	3.0×10^{-4}
Nonidet P-40	650	90,000	0.017	3.0×10^{-4}
Tween 80	1,310	76,000	0.002	1.2×10^{-5}

TABLE 2 CHEMICAL PROPERTIES OF COMMONLY USED DETERGENTS

Property	Ionic Detergents							Nonionic Detergents						
	SDS	CHO	DOC	C ₁₆	LYS	CHA	ZWI	OGL	DIG	C ₁₂	LUB	TNX	NP40	T80
Strongly denaturing	+	-	-	+	+/-	-	+/-	-	-	-	-	-	-	-
Dialyzable	+	+	+	+	-	+	+/-	+	-	-	-	-	-	-
Ion exchangeable	+	+	+	-	-	-	-	-	-	-	-	-	-	-
Complexes ions	-	-	-	-	-	-	-	-	-	-	-	+	+	-
Strong A ₂₈₀	-	-	-	-	-	-	-	-	-	-	+/-	+/-	+/-	+/-
Assay Interference	+	-	+	+	-	-	-	-	-	-	-	-	-	-
Cold Precipitates	-	-	-	-	+	+	+	+	+	+	-	-	-	-
High Cost	+	+	+	+	+	+	+/-	+	+	+/-	+	+	+	+
Availability	-	-	-	-	-	-	-	-	-	-	-	-	-	-
Toxicity	+	+	+	+	+/-	+	+	-	+	-	-	-	-	-
Ease of Purification	+	+	+	-	+	-	-	+	-	+	+	+	+	+
Radiolabeled														
Defined Composition	+	+	+	+	+	+	+	+	-	-	-	-	-	-
Auto-oxidation	-	-	-	-	-	-	-	-		+	+	+	+	+

Three commonly used lysis buffer for immuno/co-immunoprecipitation are now described.

‘RIPA-like’ lysis buffer

150 mM NaCl

50 mM Tris-HCl pH 7.4

0.25% Sodium Deoxycholate

1 mM EGTA (Protease inhibitor)

1 mM Na₃VO₄ (Phosphatase inhibitor)

1 mM NaF (Phosphatase inhibitor)

Supplemented with protease inhibitor cocktail

Lysis buffer 1% NP-40

50 mM Tris-HCl pH 7.4

150 mM NaCl

1% NP-40

1 mM EGTA

1 mM Na₃VO₄

1 mM NaF

1 mM MgCl₂

Supplemented with protease inhibitor cocktail.

Lysis buffer 1% Triton X-100

See lysis buffer 1% NP-40 and replace the NP-40 with Triton X-100.

Choice of beads

The commonly so-called beads for immunoprecipitation are composed of protein A or G coupled to a matrix. The most used matrices are sepharose and agarose. Protein G and A are bacterial proteins from Group G *Streptococci* and *Staphylococcus aureus*, respectively. When coupled to a matrix, protein G and protein A create useful, easy to-use media for routine purification of antibodies; in other words they are able to bind the Fc region of an immunoglobulin. This is the reason why they are largely employed for immunoprecipitation. In the table below are indicated the affinities of the different immunoglobulin classes for protein G and A.

Species	Antibody Class	Protein A	Protein G	Protein A/G	Protein L*
Human	Total IgG	S	S	S	S*
	IgG ₁	S	S	S	S*
	IgG ₂	S	S	S	S*
	IgG ₃	W	S	S	S*
	IgG ₄	S	S	S	S*
	IgM	W	NB	W	S*
	IgD	NB	NB	NB	S*
	IgA	W	NB	W	S*
	Fab	W	W	W	S*
	ScFv	W	NB	W	S*
Mouse	Total IgG	S	S	S	S*
	IgM	NB	NB	NB	S*
	IgG ₁	W	M	M	S*
	IgG _{2a}	S	S	S	S*
	IgG _{2b}	S	S	S	S*
	IgG ₃	S	S	S	S*
Rat	Total IgG	W	M	M	S*
	IgG ₁	W	M	M	S*
	IgG _{2a}	NB	S	S	S*
	IgG _{2b}	NB	W	W	S*
	IgG _{2c}	S	S	S	S*
Cow	Total IgG	W	S	S	NB
	IgG1	W	S	S	NB
	IgG2	S	S	S	NB
Goat	Total IgG	W	S	S	NB
	IgG ₁	W	S	S	NB
	IgG ₂	S	S	S	NB
Sheep	Total IgG	W	S	S	NB
	IgG ₁	W	S	S	NB
	IgG ₂	S	S	S	NB
Horse	Total IgG	W	S	S	?
	IgG(ab)	W	NB	W	?
	IgG(c)	W	NB	W	?
	IgG(T)	NB	S	S	?
Rabbit	Total IgG	S	S	S	W*
Guinea Pig	Total IgG	S	W	S	?
Pig	Total IgG	S	W	S	S*
Dog	Total IgG	S	W	S	?
Cat	Total IgG	S	W	S	?
Chicken	Total IgY	NB	NB	NB	NB

Legend:	W = weak binding	M = medium binding	NB = no binding
		S = strong binding	? = information not available
*Binding to Protein L will occur only if the immunoglobulin has the appropriate kappa light chains. The stated binding affinity refers only to species and subtypes with appropriate kappa light chains. Lambda light chains and some kappa light chains will not bind. For more information, see instructions for Protein L (Product No. 21189).			

Immunoprecipitation

- 1) 20 µl of beads (G or A according to the isotype and the antibody type) per immunoprecipitation are transferred to an eppendorf tube and washed 3 times with washing buffer (20 mM Tris-HCl pH 7.4, 150 mM NaCl, 1% NP-40). For each wash, 1 ml of washing buffer is added to the eppendorf tube, which is then centrifuged at maximum speed in the Eppendorf centrifuge (5415R) located in the lab and previously cooled down to 4°C.
- 2) After the last wash, the beads are resuspended in 500 µl of washing buffer and 1 to 2 µg of antibody is added.
- 3) Samples are incubate 2 hours at 4°C with rotation.
- 4) Beads are washed 3 times with washing buffer and after the last wash 500 µg to 1 mg of cellular lysate is loaded onto the beads.
- 5) Sample is incubated 2 hours at 4 °C with rotation.
- 6) Immunocomplexes are washed 3 times with washing buffer and resuspended in 2X sample buffer. The samples can be kept at -20 °C until further use.

7) Optional: samples are boiled 10 minutes at 95 °C. Boiling is not always useful and may even sometimes alter migration of given proteins.

Reagents

Materials and reagents	Source/Company	Code
Deoxycholic acid	Acros	218590250
Tris	Sigma	T1503
NaCl	Acros	207790050
NaF	Acros	409910250
EGTA	Acros	201295000
NP-40	Acros	205330500
Protein G sepharose	Amersham	17-0618-01
Protein A agarose	Roche	1134515
Protease inhibitor cocktail tablets	Roche	04693132001
NP-40 (IGEPAL)	Sigma	I3021